

GEOLOGIC ANALYSIS OF PRIMARY AND
SECONDARY TIGHT GAS
SAND OBJECTIVES

Phase A: Selective Investigation of Six
Stratigraphic Units

Phase B: Initial Studies

Annual Report

Prepared by

Robert J. Finley, Chester M. Garrett, Jong H. Han, Zsay-Shing Lin,
Steven J. Seni, Alva E. Saucier, and Noel Tyler

Assisted by

William A. Ambrose, Mark J. Berlinger, and
Gay Nell T. Gutierrez

with contributions by Alan J. VerPloeg and Rodney H. de Bruin,
Geological Survey of Wyoming, by CBW Services, Inc.,
and by Lewis R. Ladwig, Colorado Geological Survey

Bureau of Economic Geology
W. L. Fisher, Director
The University of Texas at Austin
Austin, Texas 78712

Prepared for

The Gas Research Institute
Contract No. 5082-211-0708
October 31, 1983

DISCLAIMER

LEGAL NOTICE This report was prepared by the Bureau of Economic Geology as an account of work sponsored by the Gas Research Institute (GRI). Neither GRI, members of GRI, nor any person acting on behalf of either:

- a. Makes any warranty or representation, express or implied, with respect to the accuracy, completeness, or usefulness of the information contained in this report, or that the use of any apparatus, method, or process disclosed in this report may not infringe privately owned rights; or
- b. Assumes any liability with respect to the use of, or for damages resulting from the use of, any information, apparatus, method, or process disclosed in this report.

RESEARCH SUMMARY

Title Geologic Analysis of Primary and Secondary Tight Gas Sand Objectives, Phase A: Selective Investigation of Six Stratigraphic Units
Phase B: Initial Studies

Contractor Bureau of Economic Geology, The University of Texas at Austin, GRI Contract No. 5082-211-0708

Principal Investigator R. J. Finley

Report Period November 1, 1982-October 31, 1983

Objective To expand and verify interpretation of the depositional systems and other geologic and engineering characteristics of six blanket-geometry tight gas sandstones, to recommend two formations for major research emphasis, and to begin initial geologic framework studies of these two formations.

Technical Perspective Finley (1982) listed geologic and engineering characteristics of over 30 blanket-geometry tight gas sandstones in a survey of 16 sedimentary basins. Emphasis was placed on defining clastic depositional systems and on using constituent facies as a method of evaluating the common features of stratigraphic units of different ages in diverse sedimentary and structural settings. Blanket-geometry tight gas sandstones considered suitable for future research by the Gas Research Institute were found to occur primarily within deltaic and barrier-strandplain depositional systems. An assessment of expected transferability of research results (extrapolation potential) was made between stratigraphic units, and more detailed study of six formations was recommended.

Results The Corcoran and Cozzette Sandstones of the Piceance Creek Basin and the Travis Peak Formation of the East Texas Basin and North Louisiana Salt Basin were recommended for research by the Gas Research Institute on blanket-geometry tight gas sandstones, and initial studies of depositional systems were begun. The Corcoran and Cozzette represent the barrier-strandplain system and contain barrier, offshore bar, and associated marginal-marine facies. Detailed studies of the Corcoran-Cozzette in Shire Gulch and Plateau Fields show shoreface sequences common to the lower parts of both units, and bay-lagoon and deltaic facies occur in the upper parts. The Travis Peak Formation represents a deltaic system, having a lower subdivision of progradational deltaic facies, a thick middle subdivision of braided alluvial deposits, and an upper subdivision of marginal marine deposits influenced by marine transgression. Sands greater than 50 ft thick are prominent in the middle subdivision in areas on the west flank of the Sabine Uplift. The Frontier Formation and the upper Almond Formation of the Greater Green River Basin and the Olmos Formation of the Maverick Basin are not recommended for further research, but should be considered when the need arises to test barrier, offshore bar, and possibly deltaic facies outside the two main research areas. The estimated gas resources associated with the Corcoran-

Cozzette and the Travis Peak in Texas are 3.7 and 17.3 Tcf, respectively. The Mancos "B" of the Piceance Creek Basin is not recommended for any additional research because its unique distribution of lithologies limits its extrapolation to a small group of shelf deposits, some of which have already been investigated. The extrapolation potential of the Travis Peak is largely to itself over a wide area of East Texas and North Louisiana. Extrapolation potential of the Corcoran and Cozzette extends to a large number of stratigraphic units, mostly within the Upper Cretaceous of the Rocky Mountain Region.

Technical
Approach

Base maps and a selected number of well logs were acquired in order to prepare new cross sections and maps illustrating the stratigraphic characteristics of each unit. Depositional systems and constituent facies were defined from cross sections and maps in conjunction with published and unpublished information compiled by Finley (1982). No major differences were noted between results reported here and the previous data compilation, but a better understanding of the genetic stratigraphy of each unit was gained. For formations included in previous studies of tight gas resources, new resource estimates for particular formations were made by separating published data that had been combined for multiple formations. A completely new resource estimate was prepared for the Travis Peak Formation. Once the Corcoran-Cozzette Sandstones and Travis Peak Formation were selected, expanded data acquisition was begun, with particular emphasis on porosity logs in the Piceance Creek Basin. Opportunities for cooperative coring and logging with operators were evaluated within the Corcoran-Cozzette producing trend. Within the East Texas Basin, emphasis was placed on study of a six-county area where operator activity was most active, and in North Louisiana regional structure and isopach maps necessary to facies studies were completed.

Project
Implications

This analysis represents a two-part study by the Bureau of Economic Geology (The University of Texas at Austin). Phase A of the study analyzed the depositional systems and other geologic and engineering characteristics of six blanket-geometry tight gas sandstones. As a result of Phase A, two candidates appeared to offer higher impacts for GRI's Tight Gas Sands Program. GRI concurred with the recommendations of the Bureau to select the Travis Peak Formation of the East Texas Basin and Northern Louisiana Salt Basin, and the Corcoran and Cozzette Sandstones of the Piceance Creek Basin as the principal formations of study for GRI's applied research program. Phase B of the study represents the initial geologic framework studies of these formations. In addition, GRI plans to launch a comprehensive core, log and well test program in these formations aimed at developing the technological base needed for industry to economically develop tight reservoirs.

GRI Project Manager
Patrick O'Shea
Manager, Tight Gas Reservoirs

CONTENTS

PHASE A: SELECTIVE INVESTIGATION OF SIX STRATIGRAPHIC UNITS	xx
SUMMARY AND RECOMMENDATIONS: PHASE A.	1
INTRODUCTION: PHASE A	4
Gas Research Institute Objectives	4
Background	4
Approach to Geologic Aspects of Resource Characterization	10
Organization of The Phase A Report	11
METHODOLOGY	12
TRAVIS PEAK FORMATION, EAST TEXAS BASIN AND NORTH LOUISIANA SALT BASIN by Jong H. Han	13
Introduction	13
Structure	15
Stratigraphy and Depositional Systems	19
Stratigraphy	19
Salt Tectonics	21
Depositional Systems	26
East Texas Basin	26
North Louisiana Salt Basin	35
Summary of Selected Parameters and Production Data	40
OLMOS FORMATION, MAVERICK BASIN by Noel Tyler	47
Introduction	47
Structure	51
Stratigraphy and Depositional Systems	52
Overview and Methodology	52
The Western Subbasin	55

Sandstone A	55
Sandstone B	59
Sandstone C	59
Sandstones D and E	59
The Eastern Subbasin	67
Summary of Selected Parameters and Conventional Hydrocarbon and Tight Gas Production	67
COZZETTE AND CORCORAN SANDSTONES, PICEANCE CREEK BASIN	
by Robert J. Finley	74
Introduction	74
Structure	78
Stratigraphy	79
Depositional Systems	79
Overview	79
Regional Depositional Relationships	81
Genetic Depositional Units	83
Formation Thickness	97
Corcoran-Cozzette Paleogeography	100
Clays and Cementing Agents in Corcoran and Cozzette Reservoirs	102
Corcoran Sandstone	102
Cozzette Sandstone	102
Cementing Agents	103
Summary of Selected Parameters and Production Data	103
A Note on the Sego and Castlegate Sandstones	108
MANCOS "B", PICEANCE CREEK BASIN by Robert J. Finley	
Introduction	113
Structure	113
Stratigraphy	114

Depositional Systems	119
Summary of Selected Parameters and Production Data	122
UPPER ALMOND FORMATION, GREATER GREEN RIVER BASIN	
by Robert J. Finley	124
Introduction	124
Structure	127
Stratigraphy	127
Depositional Systems	130
Overview	130
Regional Stratigraphic Relationships	131
Genetic Depositional Units	132
Formation Thickness	137
Upper Almond Paleogeography	137
Summary of Selected Parameters and Production Data	139
FRONTIER FORMATION, GREATER GREEN RIVER BASIN	
by Alva E. Saucier	145
Introduction	145
Structure	147
Structural Setting	147
Structural History	151
Stratigraphy	151
Depositional Environments	157
Delta System	157
Barrier-Offshore Bar System	162
Paleogeographic Reconstruction	164
Summary	169
Production	172
Exploration Potential and Summary of Selected Parameters	173

RESOURCE ESTIMATES by Zsay-Shing Lin	175
Introduction	175
Methodology	175
Volumetric Method	175
Proportioning Method	176
Areal Proportioning	176
Volumetric Proportioning	177
Results	177
Travis Peak Formation, East Texas Basin	177
Frontier Formation, Corcoran and Cozzette Sandstones, and Upper Almond Formation	179
Uncertainty in Gas Resource Estimates	183
EXTENT OF NATURAL FRACTURING AND DISTRIBUTION OF CLAY MINERALS by Chester M. Garrett	189
Introduction	189
Discussion	189
Natural Fractures	189
Clay Minerals	192
Summary	194
DISCUSSION: PHASE A	197
Refinement of Depositional Systems Interpretations	197
Travis Peak Formation	198
Olmos Formation	199
Corcoran and Cozzette Sandstones	199
Upper Almond Formation	200
Frontier Formation	201
Extrapolation Potential	202
CONCLUSIONS: PHASE A	204

PHASE B: INITIAL STUDIES	207
INTRODUCTION: PHASE B	208
TRAVIS PEAK FORMATION: EAST TEXAS by Steven J. Seni	208
Depositional Systems	209
Whelan Field Area	210
Rusk and Panola Counties Area	214
Thickness Variations.	214
Lower Progradational Sequence	220
Middle Fluvial Facies	220
Upper Transitional Facies	221
Travis Peak Fields and Structure	221
Recent Exploration Activity in the East Texas Basin	223
HOSSTON (TRAVIS PEAK) FORMATION, SOUTH ARKANSAS AND NORTH LOUISIANA by Alva E. Saucier	229
Introduction	229
Stratigraphy	229
Hosston (Travis Peak) Formation	230
Sligo-Hosston Isopach Map	234
Structure	237
Sligo Structure Map	237
Summary	240
CORCORAN AND COZZETTE SANDSTONES, PICEANCE CREEK BASIN	242
by Robert J. Finley	
Introduction	242
Methodology	242
Analysis of Potential Piggyback Locations	243
Regional Depositional Patterns	244
Corcoran Sandstone	246

Permeability Determinations	288
Methodology	295
Working Equations	295
Solution Technique	297
Computations of Real Gas Pseudo-Pressure	297
Input Data	297
Results and Discussion	301
DISCUSSION AND CONCLUSIONS: PHASE B	306
ACKNOWLEDGMENTS	307
REFERENCES	309

Figures

1. Stratigraphic nomenclature, East Texas and North Louisiana	14
2. Well location map, East Texas Basin	16
3. Well location map, North Louisiana Salt Basin	17
4. Tectonic map, East Texas Basin	18
5. Structure-contour map, Travis Peak Formation.	20
6. Cross section D1-D1', East Texas Basin	22
7. Cross section D2-D2', East Texas Basin	23
8. Cross section D3-D3', East Texas Basin	24
9. Isopach map, Travis Peak Formation, East Texas Basin	25
10. Facies tracts, Travis Peak Formation	27
11. Cross section S1-S1', East Texas Basin	28
12. Cross section S2-S2', East Texas Basin	30
13. Well locations in areas of detailed study	31
14. Cross section DA-DA', East Texas Basin.	32
15. Cross section DB-DB', East Texas Basin	33

16. Cross section DC-DC', East Texas Basin.	34
17. Cross section D1-D1', North Louisiana Salt Basin	36
18. Cross section D2-D2', North Louisiana Salt Basin	37
19. Cross section S1-S1', North Louisiana Salt Basin	38
20. Cross section S2-S2', North Louisiana Salt Basin	39
21. Travis Peak gas fields, East Texas Basin.	41
22. Perforated intervals in Travis Peak gas fields	46
23. Stratigraphic column, Maverick Basin	48
24. Structure contour map, Olmos Formation	49
25. Structural framework, Maverick Basin	50
26. Schematic dip section, Maverick Basin	53
27. Well location map, Maverick Basin	54
28. Cross section a-a', Maverick Basin	56
29. Cross section b-b', Maverick Basin	58
30. Cross section A-A', Maverick Basin	60
31. Cross section B-B', Maverick Basin	62
32. Detailed cross section, D-D', Maverick Basin	64
33. Isopach map, Olmos Formation	65
34. Typical logs, Olmos Formation	66
35. Olmos oil and gas fields	68
36. Histogram of oil production from the Olmos	69
37. Stratigraphic column, Piceance Creek Basin	75
38. Generalized structure, Piceance Creek Basin	76
39. Tight gas sand application areas, Piceance Creek and Uinta Basins	77
40. Structure-contour map, Cozzette Sandstone	80
41. Cross section index, Piceance Creek Basin	82
42. Cross section A-A', Piceance Creek Basin	84

43. Cross section B-B', Piceance Creek Basin	86
44. Cross section G-G', Piceance Creek Basin	88
45. Cross section F-F', Piceance Creek Basin	89
46. Structural cross section A-A', Piceance Creek Basin	90
47. Structural cross section F-F', Piceance Creek Basin	92
48. Cross section A ₁ -A ₁ ', Piceance Creek Basin	94
49. Cross section I-I', Piceance Creek Basin.	96
50. Isopach map, Corcoran Sandstone	98
51. Isopach map, Cozzette Sandstone	99
52. Generalized paleogeography of the Corcoran and Cozzette Sandstones	101
53. Distribution of gas fields, Piceance Creek Basin	105
54. Cross section A ₂ -A ₂ ', Piceance Creek Basin	106
55. Cross section C-C', Piceance Creek Basin	109
56. Cross section D-D', Piceance Creek Basin	110
57. Structure-contour map, Mancos "B"	115
58. Isopach map, Mancos "B"	116
59. Cross section H-H', Piceance Creek Basin	117
60. Cross section E-E', Piceance Creek Basin	118
61. Log detail of the Mancos "B"	120
62. Isopach thin compared to structure, Mancos "B"	121
63. Stratigraphic column, Greater Green River Basin	125
64. Tight gas sand application areas, Greater Green River Basin	126
65. Tectonic elements, Greater Green River Basin	128
66. Structure-contour map, upper Almond Formation	129
67. Log character, upper Almond Formation	133
68. Location map, cross section E-E'.	135
69. Cross section E-E', Sand Wash Basin	136

70. Isopach map, upper Almond Formation	138
71. Index map, Greater Green River Basin	146
72. Structural features and Frontier outcrop, Greater Green River Basin	149
73. Cross section A-A', Moxa Arch	150
74. Cross section B-B', Rock Springs Uplift	152
75. Stratigraphic chart, Frontier Formation	154
76. Isopach map, Frontier Formation	155
77. Type logs, Frontier Formation	156
78. Isopach map, fluvial-deltaic facies, Frontier Formation	159
79. Northwest to southeast cross section, Greater Green River Basin	160
80. Cross section C-C', Wind River and Washakie Basins	161
81. Isopach map, barrier-offshore bar sand	163
82. Cross section E-E', Greater Green River Basin	165
83. Isopach map, post-Cloverly to pre-uppermost Frontier	167
84. Age distribution, uppermost Frontier sandstones	168
85. Paleogeographic reconstruction, Frontier Formation	170
86. Schematic distribution of deltaic and barrier-offshore bar depositional systems	171
87. Cumulative frequency versus in situ permeability in the Travis Peak Formation.	178
88. Gas porosity versus in situ permeability in the Travis Peak Formation.	178
89. Net pay versus in situ permeability in the Travis Peak Formation.	180
90. Distribution of in situ permeability in the Travis Peak Formation.	180
91. Proportions of Frontier Formation combined with other formations, by area	184
92. Cross section of Travis Peak Formation at Whelan Field	211
93. Dip-oriented cross section A-A' of Travis Peak showing distribution of sandstone and mudstone	215

94. Dip-oriented cross section A-A' of Travis Peak showing depositional facies	216
95. Strike-oriented cross section B-B' of Travis Peak showing distribution of sandstone and mudstone	217
96. Strike-oriented cross section B-B' of Travis Peak showing depositional facies	218
97. Location map of cross sections	219
98. Map of Travis Peak fields and structural highs	222
99. Map of Travis Peak fields showing recent drilling locations	224
100. Number of wells drilled in 1981, 1982, and in first half of 1983	226
101. Number of new fields for Pettet, Travis Peak, Cotton Valley, Smackover, and Eagle Mills stratigraphic units	227
102. Map showing the major facies tracts of the Hosston (Travis Peak) Formation	231
103. Stratigraphic section A-A' showing the various facies within the Hosston (Travis Peak) Formation	232
104. Isopach map of the combined Sligo and Hosston (Travis Peak) Formations	235
105. Index map of north Louisiana and southwest Arkansas	236
106. Structure-contour map drawn on the top of the Sligo Formation	238
107. Logs, perforation, and production data for two wells in Plateau Field	245
108. Total net sand in the Corcoran Sandstone	247
109. Generalized coal isoliths for the Corcoran and Cozzette Sandstones.	249
110. Index to cross sections through Shire Gulch and Plateau Fields	251
111. Explanation of log facies and producing interval codes	252
112. Cross section A-A', Shire Gulch and Plateau Fields	255
113. Cross section B-B', Shire Gulch and Plateau Fields.	256
114. Cross section C-C', Shire Gulch and Plateau Fields	257
115. Cross section D-D', Plateau Field	258
116. Cross section E-E', Plateau Field.	259
117. Net sandstone in the lower Corcoran Sandstone, Shire Gulch and Plateau Fields	260

18. Net sandstone in the upper Corcoran Sandstone, Shire Gulch and Plateau Fields	262
19. Net sandstone in the lower Cozzette Sandstone, Shire Gulch and Plateau Fields	264
20. Net sandstone in the upper Cozzette Sandstone, Shire Gulch and Plateau Fields	265
21. Procedures to determine porosity from well log analysis	272
22. Porosity and lithology determination from density and compensated neutron logs	275
23. Correlation between core porosity and cross-plot porosity for the Cozzette Sandstone	284
24. Correlation between core porosity and neutron-density porosity for the Cozzette Sandstone	285
25. Correlation between core water saturation and calculated water saturation for the Cozzette Sandstone	293
26. Correlation between core water saturation and calculated water saturation for the Cozzette Sandstone	294
27. Sensitivity of calculated permeability to varying gas porosity	300
28. Permeability distribution in the Travis Peak Formation at Lansing North Field	304

Tables

1. Summary of characteristics of tight gas sands	6
2. Gas production, Travis Peak Formation	42
3. Gas production, Olmos Formation	70
4. Gas production, Corcoran and Cozzette Sandstones	104
5. Gas production, Castlegate Sandstone	112
6. Gas production, Mancos "B"	123
7. Gas production, Almond Formation	141
8. Summary of gas production by Almond Formation subdivision	143
9. Fields producing in the Almond and other formations	144

10. Sample resource calculation, Travis Peak Formation	181
11. Gas resource estimates, Travis Peak Formation	182
12. Gas resource estimates, Frontier Formation, Corcoran-Cozzette Sandstones, and upper Almond Formation	185
13. Areal proportioning data, Frontier Formation	186
14. Volumetric proportioning data, combined Frontier Formation	187
15. Volumetric proportioning data, uncombined Frontier Formation	188
16. Natural fracture distribution	190
17. Clay mineral distribution	191
18. List of wells used in cross section A-A', Travis Peak, East Texas	212
19. List of wells used in cross section B-B', Travis Peak, East Texas	213
20. List of wells used in cross sections A-A' through E-E', Corcoran and Cozzette Sandstones	253
21. Porosities from log analysis and from core measurements for the Cozzette Sandstone in Koch Exploration, Horseshoe Canyon no. 1-21	277
22. Water saturations from log analysis and from core measurements for the Cozzette Sandstone in Koch Exploration, Horseshoe Canyon no. 1-21	289
23. Reservoir properties and flow test data in the Cotton Valley Formation	299
24. Comparison of permeabilities calculated from transient-pressure analysis and from back pressure tests	302
25. Well names and numbers shown on figure 128	305

PHASE A: SELECTIVE INVESTIGATION OF
SIX STRATIGRAPHIC UNITS

SUMMARY AND RECOMMENDATIONS: PHASE A

Six blanket-geometry tight gas sandstones were reviewed to assist the Gas Research Institute (GRI) in selecting two areas for further research. Base maps, selected well logs, and well completion data were acquired to verify and expand the information on depositional systems and the evaluations of extrapolation potential compiled by Finley (1982). Extrapolation potential, or the expected transferability of research results, is herein related to the facies contained within each stratigraphic unit rather than to the overall depositional system. Resource estimates were prepared either by refinement of existing information or by use of raw data to prepare an entirely new estimate.

The Mancos "B" interval of the Mancos Shale (Piceance Creek Basin) is not recommended for any further research. This intracratonic shelf deposit differs from other blanket-geometry sandstones under consideration by GRI in its distribution of lithologies and its thinly bedded character.

The Frontier Formation (Greater Green River Basin), Olmos Formation (Maverick Basin), and the upper Almond Formation (Greater Green River Basin) are recommended for possible future evaluation of a specific depositional facies or for testing of a particular engineering application as may arise during future research programs. The Frontier Formation contains continental deltaic to barrier and offshore bar facies; the latter form blanket to near-blanket geometry tight gas reservoirs over relatively wide areas. Depth to the top of the Frontier increases rapidly off-structure. The Olmos Formation offers the opportunity to test deltaic and barrier facies at depths shallower than those of the Frontier. The upper Almond is a thin interval, often consisting of a single barrier or offshore bar sandstone, and depth to the top of the upper Almond increases rapidly off-structure.

The Corcoran-Cozzette Sandstones and the Travis Peak Formation are recommended as suitable for a major research program by GRI. Selection of these units does not imply

extrapolation potential between them; in fact, differences exceed similarities, but each has properties that are important in the GRI program.

The Corcoran and Cozzette contain barrier and offshore bar sands expected to have extrapolation potential to similar facies in other progradational stratigraphic units of the Upper Cretaceous in the Rocky Mountain Region. These facies include other units in the Mesaverde Group, the Fox Hills Sandstone, the Lewis Shale, the Frontier Formation, and the upper marginal marine part of the Dakota Sandstone. Associated with study of the Corcoran and Cozzette would be a secondary emphasis on the Rollins Sandstone; these three stratigraphic units, each approximately 200 ft thick, constitute a related package of marginal marine sandstones. Estimated maximum recoverable gas-in-place in the Corcoran-Cozzette is 3.7 Tcf. Significant topographic constraints exist within parts of the Piceance Creek Basin where elevations of 8,000 to 10,000 ft or more are encountered, roads are lacking, and winter weather conditions may affect exploration and production activities.

The Travis Peak Formation contains progradational, marginal marine facies at the base, a middle braided alluvial facies, and an upper facies related to marine transgression. The Travis Peak is widespread in the East Texas Basin and North Louisiana Salt Basin, is 500 to 2,500 ft thick, and is sand-rich. The extrapolation potential of the Travis Peak is limited to similar facies occurring in a wide geographic area, and both its area and thickness contribute to a resource estimate of 17.3 Tcf (in Texas alone) if 15 percent of the basin area is ultimately proven productive. Thus, the Travis Peak is a significant potential resource to be developed in an area where physical constraints (topography and climate) do not restrict exploration and production activities. The portion of the Travis Peak that contains blanket-geometry sandstones rather than broadly lenticular sandstones remains to be fully evaluated. Continuity of the braided alluvial facies is expected to be better than that of lenticular sandstones deposited by meandering streams. Correlation problems may be encountered, however, because of the sand-rich character of the unit.

Selection of the Corcoran-Cozzette and the Travis Peak as priority research areas is consistent with GRI criteria that include industry interest, potential for development of reserves, and consideration of technology transfer (extrapolation potential) based on the genetic stratigraphy of each formation. Testing of extrapolation potential of the Corcoran-Cozzette will require selection of a stratigraphic unit outside the Piceance Creek Basin; appropriate facies of the Frontier, Olmos, or upper Almond units may be selected, or another unit may be evaluated and selected after initial experience is gained with the Corcoran-Cozzette. At this time it appears most appropriate to remain within the Rocky Mountain Region to seek an area for testing the extrapolation of technology related to exploitation of the barrier and offshore bar facies of the Corcoran and Cozzette Sandstones.

The Travis Peak, on the other hand, will likely be tested in one of the same basins included in the original study of the formation. Distribution of source areas and the proportion of different genetic facies over the basins of interest may control placement of a well designed to test extrapolation potential.

INTRODUCTION: PHASE A

Gas Research Institute Objectives

The Gas Research Institute (GRI) has designated as one of its goals the increased understanding and ultimate utilization of unconventional gas resources. One such resource is gas contained within low-permeability, or tight, sandstone reservoirs. Estimates of maximum recoverable natural gas in tight formations in the continental United States vary from 192 to 574 Tcf, depending upon price and the state of technology (National Petroleum Council, 1980a, 1980b). GRI (1982) has recognized the "need for a coordinated and cost-effective research program that will advance unconventional gas exploitation technology, thereby increasing the commercialization of the resource." In response to this need, GRI has set out to "develop the information and tools necessary to stimulate near term development at competitive prices of blanket tight gas sands that are not exploitable using current gas recovery methods and stimulation techniques" (P. O'Shea, personal communication, 1983). Six major project areas are included in this research and development effort: resource characterization, formation evaluation, stimulation design, fracture diagnostics, real-time analysis development, and staged field tests. Resource characterization includes geologic analysis; the first step in this analysis has been to evaluate blanket-geometry tight gas sandstones suitable for the GRI research program.

Background

Previous exploitation of tight gas formations has been related to two simplified categories of external reservoir geometry controlled by the depositional setting of the sands. "Blanket" and "lenticular" sandstone reservoirs are consistently differentiated (Lewin and Associates, 1978). Research sponsored by the U.S. Department of Energy as part of the Western Gas Sands Project includes studies of the predominantly lenticular tight gas sand reservoirs of the Piceance Creek, Uinta, and Greater Green River Basins (Spencer and others, 1977; Spencer, 1983).

The Gas Research Institute has focused on the exploitation of gas in tight, blanket-geometry sandstones rather than that in lenticular sandstones. Finley (1982) surveyed the geology and engineering characteristics of over 30 blanket-geometry sandstones in 16 sedimentary basins to provide the basis for selection of a smaller number of stratigraphic units suitable for additional study. Finley (1982) emphasized the environment of deposition as a key factor controlling internal and external geometry of sandstone reservoirs. In contrast to predominantly fluvial sandstones of lenticular geometry, blanket-geometry sandstones were deposited as barrier-strandplain and deltaic systems and, to lesser extent, as shelf systems. Table 1 lists the most important parameters of selected blanket-geometry tight gas sandstones included in the survey. Excluded from this group are the "J" Sandstone (Denver Basin) and the Cotton Valley Sandstone (East Texas Basin/North Louisiana Salt Basin), which are already highly commercialized and are not considered suitable candidates for future research efforts where degree of commercialization is a limiting criterion.

Six stratigraphic units were recommended for additional study based on data assembled by Finley (1982): the Travis Peak Formation (East Texas Basin/North Louisiana Salt Basin), the Olmos Formation (Maverick Basin), the Corcoran and Cozzette Sandstones and Mancos "B" interval of the Mancos Shale (Piceance Creek Basin), and the Frontier Formation and upper Almond Formation (Greater Green River Basin). Important differences exist in thickness, depth distribution, and depositional systems among this group. These factors have been evaluated in the present study, and have been compared to GRI preferences in the selection of stratigraphic units suitable for a research and development program.

Study of the latter group of six formations was initiated in the period August 1 - October 31, 1982, under a GRI subcontract through CER Corporation. The primary effort during that period involved acquisition of a data base (maps and geophysical well logs) from which to expand knowledge of each formation (Finley and Han, 1982). During the period November 1, 1982 - March 31, 1983, interpretation of these data, of completion and production information,

Table 1. Summary of major characteristics of selected blanket-geometry low-permeability gas sands.

Formation	Depositional System	Depth	Thickness
Areally Extensive Fan Delta and Deltaic Systems			
Travis Peak (Hosston) Formation, East Texas Basin (North Louisiana Salt Basin)	Fan delta, with braided alluvial surface and marine-influenced fan delta margins	Ranges from 3,100-10,900 ft. Generally 7,000-9,000 ft.	500-2,500 ft
Frontier Formation, Moxa Arch, Greater Green River Basin	Wave-dominated deltaic system with prodelta through delta plain and associated barrier-strandplain facies	Ranges from 6,700-11,900 ft. Generally 6,700-8,300 ft.	300-1,200 ft
Frontier Formation, Rock Springs Uplift and Washakie - Red Desert Basins, Greater Green River Basin	(as above, for Moxa Arch area)	Averages 11,700 ft along Rock Springs Uplift. Averages 7,100 ft in Washakie - Red Desert Basins	250-600 ft
Frontier Formation, Wind River Basin	(as above, for Moxa Arch area)	Ranges from outcrop to over 25,000 ft. Generally 2,000-4,200 ft.	600-1,000 ft
Deltaic Systems and Deltas Reworked by Transgression			
Carter Sandstone, Black Warrior Basin	Deltaic or barrier and offshore bar facies in association with deltaic Parkwood Formation. Limited data.	No data in tight areas	No data in tight areas
Davis Sandstone, Fort Worth Basin	Deltaic and barrier-strandplain in a wave-dominated environment	4,800-5,200 ft.	20-400 ft
Olmos Formation, Maverick Basin	Deltaic and deltaic reworked by transgression, with multiple depocenters, wave-dominated	4,500-7,200 ft	400-1,200 ft
Blair Formation, Greater Green River Basin	Deltaic (prodelta to delta front?). Limited data.	Ranges from outcrop to 15,000 ft. Approx. 8,200 ft in one producing area.	1,400-1,900 ft
Barrier Strandplain Systems			
Oriskany Sandstone, Western Basin and Low Plateau Provinces of Appalachian Basin	Transgressive shallow marine or shoreline deposit	In Western Basin, ranges from 1,600-5,300 ft. In Low Plateau, ranges from 1,700-8,000 ft.	0-200 ft
Oriskany Sandstone, High Plateau and Eastern Overthrust Belt Provinces of Appalachian Basin	Transgressive shallow marine or shoreline deposit	Ranges from outcrop to greater than 12,000 ft. Generally 7,000-9,000 ft.	0-300 ft
Hartselle Sandstone, Black Warrior Basin	Barrier island with associated nearshore bars	1,000-3,400 ft.	0-150 ft
Pictured Cliffs Sandstone, San Juan Basin	Barrier-strandplain with associated nearshore bars	2,300-3,500 ft	50-400 ft

Table 1 (continued)

Net Pay	Post-Stimulation Flow	Operator Interest	Extrapolation Potential
30-86 ft	500-1,500 Mcfd	High. Five tight gas applications.	Good. Areally extensive across basins in Texas and Louisiana. Expected similarity to "Clinton"-Medina sands of the Appalachian Basin.
10-90 ft	0-2,500 Mcfd	High. Four tight gas applications.	Good. Areally extensive across several basins in Wyoming and a good example of a wave-dominated deltaic system. Probably, in part, similar to deltaic elements of the Davis, Olmos, and Fox Hills, and to barrier-strandplain elements of several units of the Mesaverde Group.
10-65 ft	0-1,500 Mcfd	High. Two tight gas applications.	Good, as above for Moxa Arch area
10-45 ft	No data from tight gas areas	Potentially moderate. No tight gas applications.	Good, as above for Moxa Arch area
No data in tight areas	No data from tight areas	Unknown. No tight gas applications.	Poor to fair. Limited data. Deltaic facies may be similar to parts of Fox Hills. Barrier/bars form conventional reservoirs.
No data	No data from tight gas areas	Low. No tight gas applications.	Poor to fair. Limited data. Expected similarities to the Olmos Formation, part of the Fox Hills, and part of the Frontier.
12-85 ft	Averages 86 Mcfd	Moderate. Two tight gas applications.	Fair to good. Expected similarity to parts of the Fox Hills and Frontier Formations, the Davis Sandstone, and possibly to deltaic sediments at the base of the Cleveland.
No data	No data	Low to moderate. One tight gas application.	Poor to fair. Limited data. Possible analogies to Davis and Olmos Formations. Data inadequate to make comparisons.
10-20 ft	No data from tight gas areas	Low. No tight gas applications.	Cannot be evaluated due to inadequate available data on depositional systems.
150-265 ft	No data from tight gas areas	Low. No tight gas applications.	Cannot be evaluated due to inadequate available data on depositional systems.
No data	50-100 Mcfd	Low to moderate. One tight gas application.	Fair to good. Limited data. Expected similarity to barrier and offshore bar facies of formations within the Mesaverde Group, parts of the Fox Hills, and possibly the upper part of the Dakota Sandstone.
20-30 ft	300-1,600 Mcfd	Moderate. Two tight gas applications.	Good. Expected similarity to barrier-strandplain facies of the Mesaverde Group in the San Juan and other Rocky Mountain basins. Also, similarity expected to the upper part of the Dakota Sandstone and to part of the Fox Hills.

Table 1 (continued)

Formation	Depositional System	Depth	Thickness
Cliff House Sandstone, Mesaverde Group, San Juan Basin	Reworked barrier-strandplain, transgressive, probably preserving mostly subaqueous facies such as upper shoreface	4,000-6,300 ft	50-100 ft
Point Lookout Sandstone, Mesaverde Group, San Juan Basin	Barrier-strandplain, regressive, including minor lagoonal and estuarine channel facies	4,400-6,700 ft	100-200 ft
Dakota Sandstone, (upper part), San Juan Basin	Barrier-strandplain, dominantly transgressive, including offshore bar facies and associated lagoonal, estuarine, and wash-over facies	6,000-8,700 ft	200-350 ft
Cozzette Sandstone, Piceance Creek Basin	Barrier-strandplain, regressive, possibly including offshore bar facies. Limited data.	2,400-7,200 ft	Averages 175 ft
Corcoran Sandstone, Piceance Creek Basin	Barrier-strandplain, regressive, possibly including offshore bar facies. Limited data.	2,700-7,600 ft	150-200 ft
Sego and Castlegate Sandstones, Uinta Basin	Probably nearshore marine to barrier-strandplain. Regressive. Limited data.	8,000-9,500 ft (Castlegate)	
Fox Hills Formation, Washakie Basin, Greater Green River Basin	Predominantly barrier-strandplain but includes deltaic and estuarine facies	Averages 7,300 ft	150-600 ft
Almond Formation (upper part), eastern Greater Green River Basin	Shallow marine and offshore bar to barrier strandplain, possibly including tidal flat, tidal inlet channel, and tidal delta facies.	6,200-15,450 ft. Averages 10,200 ft.	100 ft (upper Almond only)
Shelf Systems			
Cleveland Formation, Anadarko Basin	Possible thin deltaic deposit at base of the unit. Major part is a marine shelf deposit.	6,000-9,400 ft. Generally less than 8,000 ft.	80-170 ft
Mancos "B" interval, Piceance Creek Basin	Marine shelf deposit	3,400-3,600 ft	400-700 ft
Mancos "B" interval, Uinta Basin	Marine shelf deposit	Averages 5,000 ft	450-1,000 ft

Table 1 (continued)

Net Pay	Post-Stimulation Flow	Operator Interest	Extrapolation Potential
10-70 ft	500-3,600 Mcfd	Moderate. Three Mesaverde tight gas applications.	Fair to good. Expected similarity to transgressive Dakota Sandstone (upper part) and to parts of the Point Lookout Sandstone. Probably also similar to other Mesaverde Group sandstones, and possibly parts of the Pictured Cliffs and Fox Hills.
10-80 ft	500-3,600 Mcfd	Moderate. Three Mesaverde tight gas applications.	Good. Expected similarity to other barrier-strandplain facies of Mesaverde Group, Hartselle, Pictured Cliffs, Fox Hills (in part), and Dakota (upper part) stratigraphic units.
10-70 ft	200-300 Mcfd	High. Six tight gas applications.	Good. Expected similarity to transgressive Cliff House Sandstone, to parts of the Mesaverde Group in the San Juan Basin and other Rocky Mountain basins, and to parts of the Fox Hills and Pictured Cliffs stratigraphic units.
60-70 ft	Averages 1,229 Mcfd	High. Two tight gas applications.	Good. Expected similarity to other barrier-strandplain facies of Mesaverde Group, Hartselle, Pictured Cliffs, Fox Hills (in part), and Dakota (upper part) stratigraphic units
10-70 ft	Averages 1,251 Mcfd	High. Two tight gas applications.	Good. Expected similarity to other barrier-strandplain facies of Mesaverde Group, Hartselle, Pictured Cliffs, Fox Hills (in part) and Dakota (upper part) stratigraphic units.
25-60 ft	No data	Unknown. One tight gas application.	Fair. Limited data. Expected similarity to Cozzette and Corcoran Sandstones and other Mesaverde Group sandstones in Rocky Mountain basins.
25 ft	Averages 775 Mcfd	Low to moderate. One tight gas application.	Good. The deltaic facies is expected to be similar to parts of the Frontier and Olmos Formations. Barrier-strandplain facies have analogies in the Dakota Sandstone (upper part), the Mesaverde Group, the Pictured Cliffs and possibly the Hartselle.
14-18 ft	1,500-1,700 Mcfd	Moderate. One tight gas application.	Good. Expected similarity to barrier-strandplain and possible offshore bar facies of other Mesaverde Group sandstones. In part possibly similar to the Dakota (upper part), Pictured Cliffs and Hartselle.
10-75 ft	Averages 220 Mcfd	Moderate. Two tight gas applications.	Fair. Thin deltaic deposit at base has no good analogy. Marine shelf deposit has expected similarities to the Mancos "B" in the Piceance Creek and Uinta Basins.
90-120 ft	260-350 Mcfd	High. Four tight gas applications.	Fair. Part of a trend across two basins. Also expected similarity to upper part of the Cleveland Formation.
38-98 ft	260-350 Mcfd	Moderate. One tight gas application.	Fair. Part of a trend across two basins. Also expected similarity to upper part of the Cleveland Formation.

and of engineering parameters, has resulted in additional understanding of the depositional systems and the gas resource associated with each formation, as reported herein.

Approach to Geologic Aspects of Resource Characterization

Guiding basin analysis research at the Bureau of Economic Geology has been the concept that sandstone bodies are the product of a suite of processes operating within major depositional systems that are active during infilling of a basin. Typically these systems include several major environments of sand deposition; resultant sand bodies are the genetic facies such as meanderbelt, coastal barrier, or crevasse splay facies. Each of these facies has consistent physical attributes within an individual system or major depositional element where processes and available sediment types were relatively uniform. Consequently, interpretive description and mapping of the depositional systems and their component facies are basic steps in the geologic characterization of a tight gas sand or any hydrocarbon reservoir (Galloway and others, 1982, for example).

Such factors as initial permeability, proximity to source or sealing lithologies, and interconnection with other permeable units are inherent attributes of genetic facies that control or affect migration and distribution of hydrocarbons. Thus, facies analysis may identify preferred reservoir types and provide the basis for improved resource estimation and geographic extrapolation or prediction of tight gas trends. The significance of these attributes is indicated by the fact that typically only limited zones that constitute a small percent of the total sand-bearing interval contain producible gas.

Delineation of the depositional framework has greatest application in providing the basis for characterization of tight gas reservoirs, both regionally and locally. Delineation of depositional systems outlines the principal building blocks of the basin fill that may produce gas. Within each of these building blocks, sand bodies of component facies will have similar dimensions, orientation, interconnectedness, and internal permeability variations or compartmentalization. Internal heterogeneity of sand bodies results from the style of sediment

accumulation, which may include aggradation, progradation, and lateral accretion. Though similar in geometry, progradation and lateral accretion are characterized by coarsening-upward and fining-upward textures that are typically reflected in permeability trends. Quantification of sand-body geometry in a complex depositional system necessitates initial recognition of differing external and internal geometric elements. Further, extrapolation of detailed sand body studies based on limited areas of dense data is guided by the regional interpretation.

Composition of reservoir sandstones reflects depositional processes, influences certain petrophysical parameters, and affects the extent and mineralogy of diagenetic mineral phases that occlude pore space and affect reservoir quality. For example, quartzo-feldspathic sands with siliceous or carbonate cement will respond differently to thermal and mechanical stress at depth than will a sandstone rich in relatively plastic clay and rock fragments. In effect, mineralogic facies are mappable and reflect initial sediment mineralogy and subsequent burial history. Facies recognition can guide development to areas or intervals of most favorable reservoir properties and will improve selection of appropriate reservoir stimulation techniques.

Organization of The Phase A Report

The order of data presentation in this report follows the sequence of Finley (1982), which is east to west across Texas and south to north through the Rocky Mountain Province. A review of trapping mechanisms and other engineering aspects of the Corcoran and Cozzette Sandstones was completed by CBW Services, Arvada, Colorado. A study of the Frontier and upper Almond Formations, with emphasis on local detail and production characteristics in designated tight areas, was completed by the Geological Survey of Wyoming (GSW), Laramie, Wyoming.

METHODOLOGY

Finley (1982) relied primarily on published information and information available from state oil and gas commissions to complete a preliminary survey of blanket-geometry tight gas sandstones. Much of the available data on porosity, permeability, water saturation, net pay, and production rates were derived from operator applications for tight formation designations under Section 107 of the Natural Gas Policy Act (NGPA) and associated rules of the Federal Energy Regulatory Commission (FERC). These data are therefore most representative of tight areas of operator interest through March 1982. The number of new applications for tight formation status under NGPA Section 107 in the period March 1982 to February 1983 has been low relative to the preceding 12-month period; large quantities of new data have not become available through Section 107 applications.

This report presents a more complete description of the depositional systems of six stratigraphic units than was included in Finley (1982). Interpretation of geophysical well logs and drilling and completion reports, and consultation with subcontractors in Wyoming and Colorado form the basis of this report. Further details on expected extrapolation potential are presented. New resource estimates are included, based in part on assistance from Lewin and Associates, Inc., in separating National Petroleum Council (1980a, 1980b) data into component parts, and on new estimates of recoverable gas made by the Bureau of Economic Geology.

The time period cited above allowed the use of only selected well logs and placed limitations on the level of detail presented. This was especially true for formations as areally extensive as the Travis Peak Formation, and, to a lesser extent, the Frontier Formation. Acquisition of logs from development wells was restricted to few specific areas and a limited number of porosity logs (neutron-density and sonic) were obtained. Additional data acquisition will be required to continue depositional systems analysis of any of the formations described herein.

TRAVIS PEAK FORMATION, EAST TEXAS BASIN AND NORTH LOUISIANA SALT BASIN

Introduction

The Lower Cretaceous Travis Peak Formation in the East Texas Basin and North Louisiana Salt Basin is characterized by thick, low-permeability, terrigenous clastic deposits that extend east from Texas across southern Arkansas and northernmost Louisiana. The term Travis Peak was introduced by Hill (1890) to designate the type locality of the formation in Central Texas; the same unit is also termed the Hosston Formation, primarily in Arkansas and Louisiana. The Travis Peak Formation conformably overlies a thin sequence of limestone and sandy shale termed the Knowles Limestone over almost the entire area except where it directly overlies the Cotton Valley Sandstone (Schuler) on the eastern margin of the East Texas Basin. The Travis Peak Formation is, in turn, overlain by Pettet (Sligo) Limestone of the Lower Glen Rose Formation (Nuevo Leon Group) throughout the East Texas Basin and North Louisiana Salt Basin (fig. 1).

Data from several different sources have been used in this study, including base maps from Geomap, Inc., reference maps showing production and field names for East Texas and North Louisiana, yearbooks of the Railroad Commission of Texas (RRC), and tight gas production data in RRC districts 5 and 6 from Petroleum Information Corporation. Operator applications for tight formation designation of the Travis Peak in Texas and one in Louisiana were also essential to this regional and detailed study. As of November 1982, seven applications had been filed for the Travis Peak in different parts of the East Texas Basin. However, only two have been approved by the Federal Energy Regulatory Commission (FERC), and an application for approval of a 47-county area remains pending with FERC. In Louisiana, an application was approved for the Hosston Formation by the Louisiana Office of Conservation (1981) on December 24, 1981, and has more recently been approved by FERC.

SYSTEM	SERIES	GROUP	FORMATION
CRETACEOUS	COAHUILAN	NUEVO LEON	SLIGO / PETTET
			TRAVIS PEAK / HOSSTON
JURASSIC	UPPER JURASSIC	COTTON VALLEY	COTTON VALLEY SANDSTONE (UPPER COTTON VALLEY/SCHULER)
			BOSSIER SHALE
			COTTON VALLEY LIME (GILMER / HAYNESVILLE)
	LOUJARK	BUCKNER	
		SMACKOVER	

Figure 1. Stratigraphic nomenclature showing parts of the Jurassic and Cretaceous systems in the East Texas Basin and North Louisiana Salt Basin (from Finley, 1982).

A total of 531 electric logs (430 from East Texas and 101 from North Louisiana, figs. 2 and 3) which penetrate the base of the Travis Peak Formation was acquired from well-log files of the Bureau of Economic Geology and through commercial sources. A structure-contour map of the top of the Travis Peak Formation, derived from an operator application, was combined with a structure-contour map drawn as part of this study for the North Louisiana Salt Basin.

Structure

Regional tectonic history of the East Texas Basin and North Louisiana Salt Basin was initiated by tilting of rift-margin crustal blocks toward the incipient Gulf of Mexico Basin following the breakup of Pangaea and separation of North and South America during the Triassic (Kehle, 1971; Burke and Dewey, 1973; Wood and Walper, 1974, Walper, 1980). Cooling-induced subsidence following initial uplift and rift volcanism dominated the East Texas Basin, allowing thick shallow-marine and continental deposits to prograde toward the Gulf Coast Basin by Early Cretaceous time (Jackson, 1981).

The mobility of the Louann Salt and the development of peripheral graben systems (fig. 4) and the Sabine Uplift greatly affected the structure of the Travis Peak Formation in East Texas and North Louisiana. A number of salt domes developed simultaneously with Travis Peak sedimentation in the area bounded updip by the Mexia-Talco fault system and to the east by the Sabine Uplift. In the North Louisiana Salt Basin, the salt domes are scattered to the east of the Sabine Uplift and significantly complicate the structure of the central part of the basin. Syndepositional salt-related structures in East Texas and North Louisiana include a peripheral graben system, low to intermediate amplitude salt structures, and salt anticlines and salt domes (McGowen and Harris, in press). Development of salt domes was most active during Late Jurassic and Early Cretaceous time in the East Texas Basin (Seni and Kreitler, 1981).

Turtle structures, anticlines of clastic sediment developed during continuous salt withdrawal, are salt-related structures characteristic of a region of salt mobility, and are formed within the Travis Peak Formation (Trusheim, 1960). Turtle structures are not shown on the

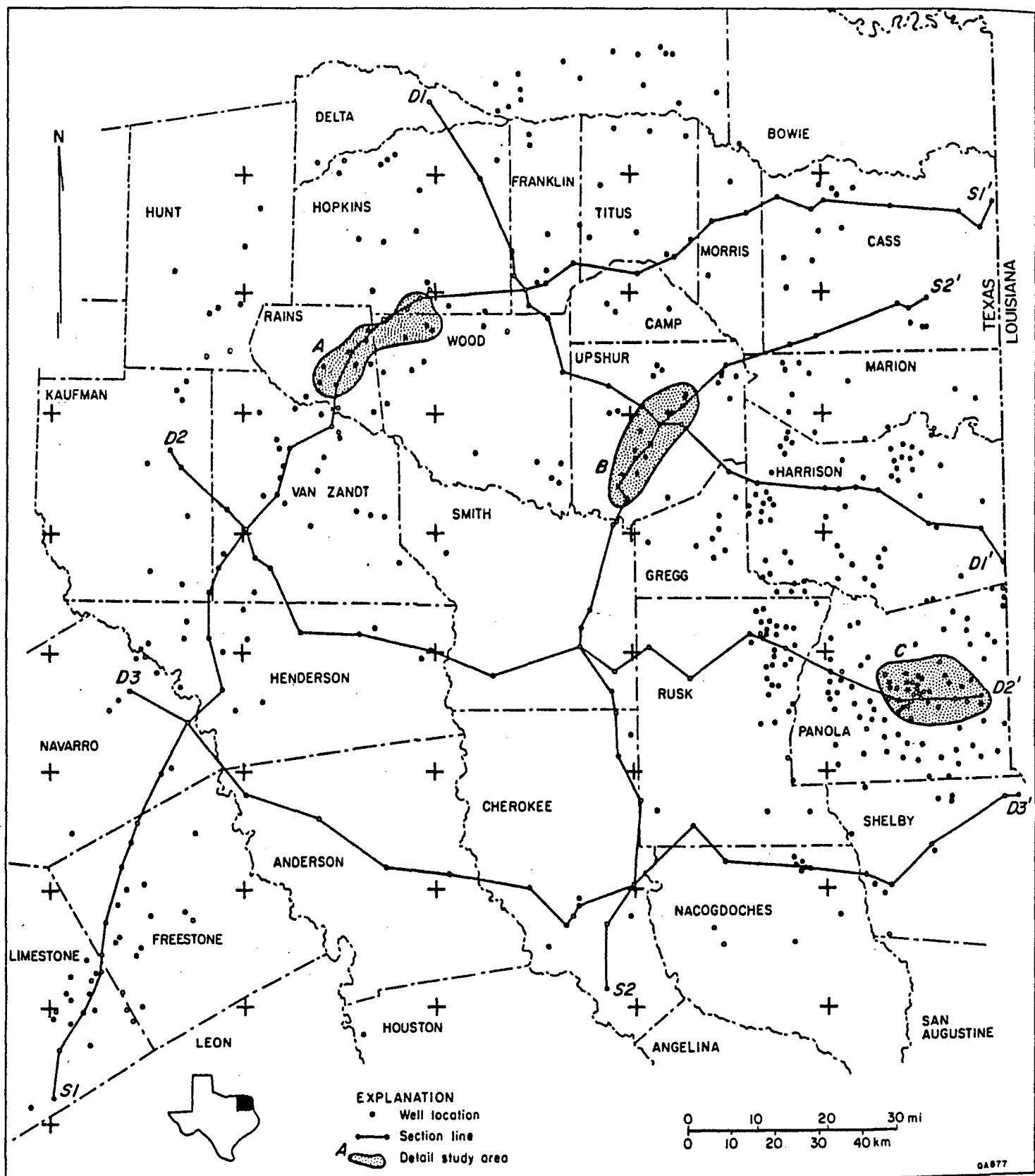


Figure 2. Location map of wells, cross-sections, and areas of detailed study in the East Texas Basin.

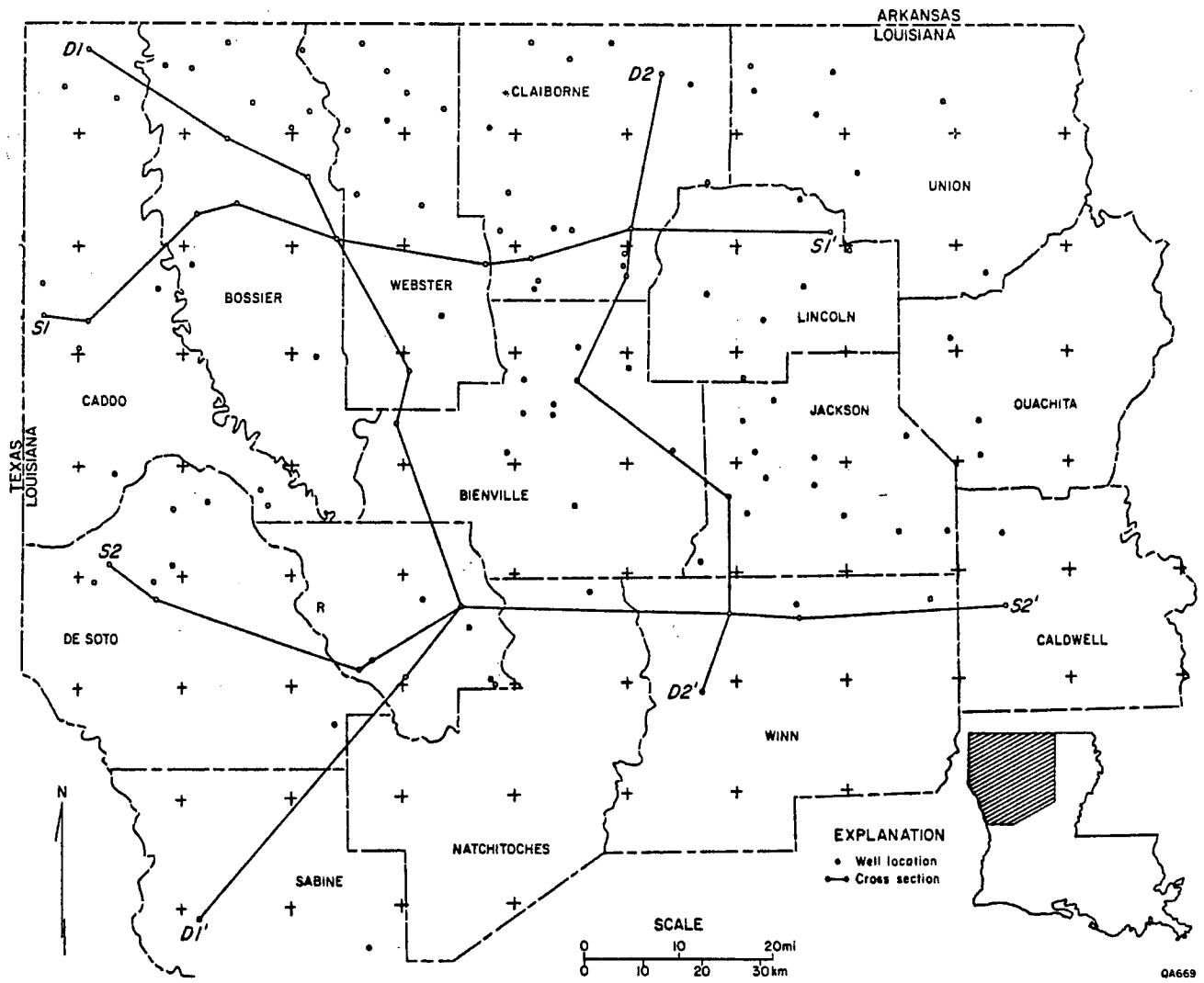


Figure 3. Location map showing wells and cross sections in the North Louisiana Salt Basin.

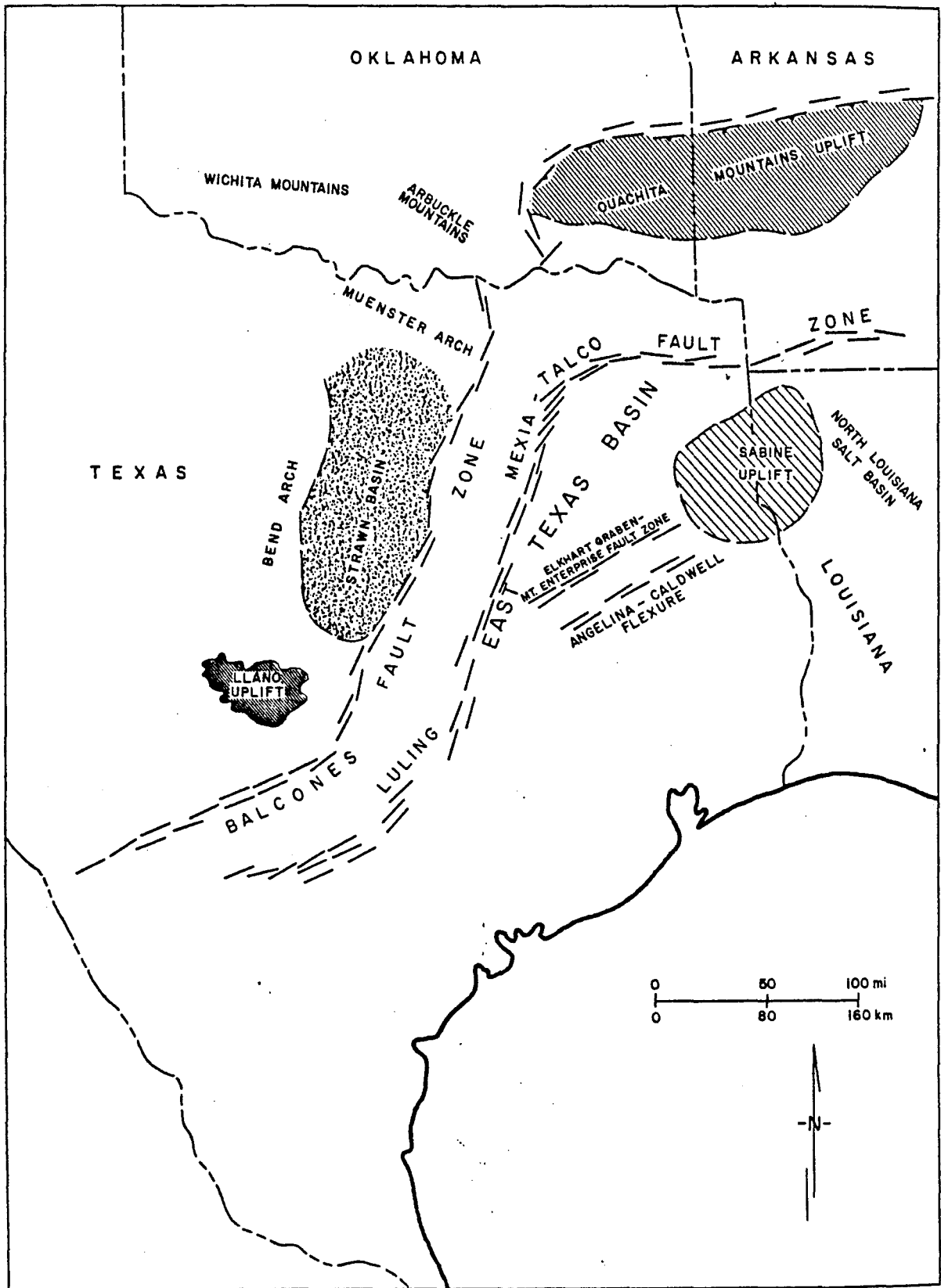


Figure 4. Tectonic map of the East Texas Basin and adjacent areas (from McGowen and Harris, in press).

regional structure map (fig. 5) because the contour interval of the map is far greater than the range of thickness variation resulting from the turtle structures.

The Mexia-Talco fault system is a significant zone of structural relief forming the north and west margins of the East Texas Basin (fig. 4). The fault zone consists of a series of en echelon normal faults and grabens, and is believed to be due to the combination of downdip flow of Louann salt and subsequent basinward creep of clastic overburden (Jackson, 1982; McGowen and Harris, in press). The Elkhart Graben - Mt. Enterprise fault system and the Angelina-Caldwell flexure mark the southern limit of the salt dome area in the East Texas Basin (fig. 4).

The Sabine Uplift divides the East Texas Basin and North Louisiana Salt Basin near the Texas-Louisiana border (fig. 5). The Sabine Uplift postdates Travis Peak deposition and thus had no relationship to the depositional history of the formation. In general, the top horizon of the Travis Peak Formation in the East Texas Basin ranges in depth from 4,000 ft to more than 11,000 ft subsea. Saddle-shaped structural lows extend from the central basin to deeper southern parts of the basins. In the North Louisiana Salt Basin, a structural depression recognized in Claiborne and Union Parishes (fig. 5) is inferred to be a fault-controlled graben system. The overall structure of the East Texas Basin and the North Louisiana Salt Basin shows some degree of symmetry in that both are bounded by fault systems, contain syngenetic salt structures, and have been influenced by basement uplift.

Stratigraphy and Depositional Systems

Stratigraphy

The Travis Peak (Hosston) Formation in the East Texas Basin and North Louisiana Salt Basin contains a thick, alluvial facies which is probably composed of extensive braided stream deposits, and a shallow marine deltaic facies. The thickness of the formation ranges from 800 ft to more than 2,800 ft in the East Texas Basin, and 1,800 ft to more than 3,200 ft in the North Louisiana Salt Basin.

In general, the top of the Travis Peak is placed at the base of the lowest Pettet (Sligo) Limestone bed, which intertongues with Travis Peak sandstone. The base of the Travis Peak can be determined easily by recognition of the Knowles Limestone in the eastern part of East Texas and in all of North Louisiana. The Knowles Limestone, considered as the upper formation of the Cotton Valley Group in North Louisiana (Thomas and Mann, 1966), consists of alternating units of dark gray, argillaceous limestone, gray shale, and locally thin sandstone lenses. In the East Texas Basin, the carbonate sediments are well developed in the counties bordering the Texas-Louisiana boundary (figs. 6 and 7), but tend to be gradationally interbedded with terrigenous clays and sandy clays toward the central basin area. Shaly sediments of the Knowles die out in the updip part of the basin where sandstones of the Travis Peak and Cotton Valley Group are superposed.

Salt Tectonics

Salt tectonism greatly influenced the thickness of the Travis Peak Formation. In Anderson and Cherokee Counties (fig. 8), salt movement generated turtle structures and resulted in the formation of locally thickened sedimentary sections. These thick depocenters later formed the cores of the turtle-shaped anticlines that are present in areas of salt withdrawal surrounded by salt-domes. In cross-section (fig. 8), thicker intervals of the Travis Peak (wells 119-121) represent sand packages now part of turtle structures. Their appearance on the cross-section is attributable to using the top of the formation as stratigraphic datum. Thickness changes of the Travis Peak, caused by salt-movement, can be seen on the isopach map of the formation (fig. 9). Major turtle-shaped thickness anomalies, which are typical of those found within unstable salt-withdrawal areas, are well developed in Anderson, Henderson, Smith, and Wood Counties. Isopachs generally parallel structure contours in the marginal and deeper part of the East Texas Basin (fig. 9), but do not conform to the structural configuration of the Sabine Uplift. This indicates that Travis Peak deposition was not genetically associated with basement tectonic movement in the border area between East Texas and North Louisiana. Consequently, the Sabine Uplift is a post-Travis Peak structure.

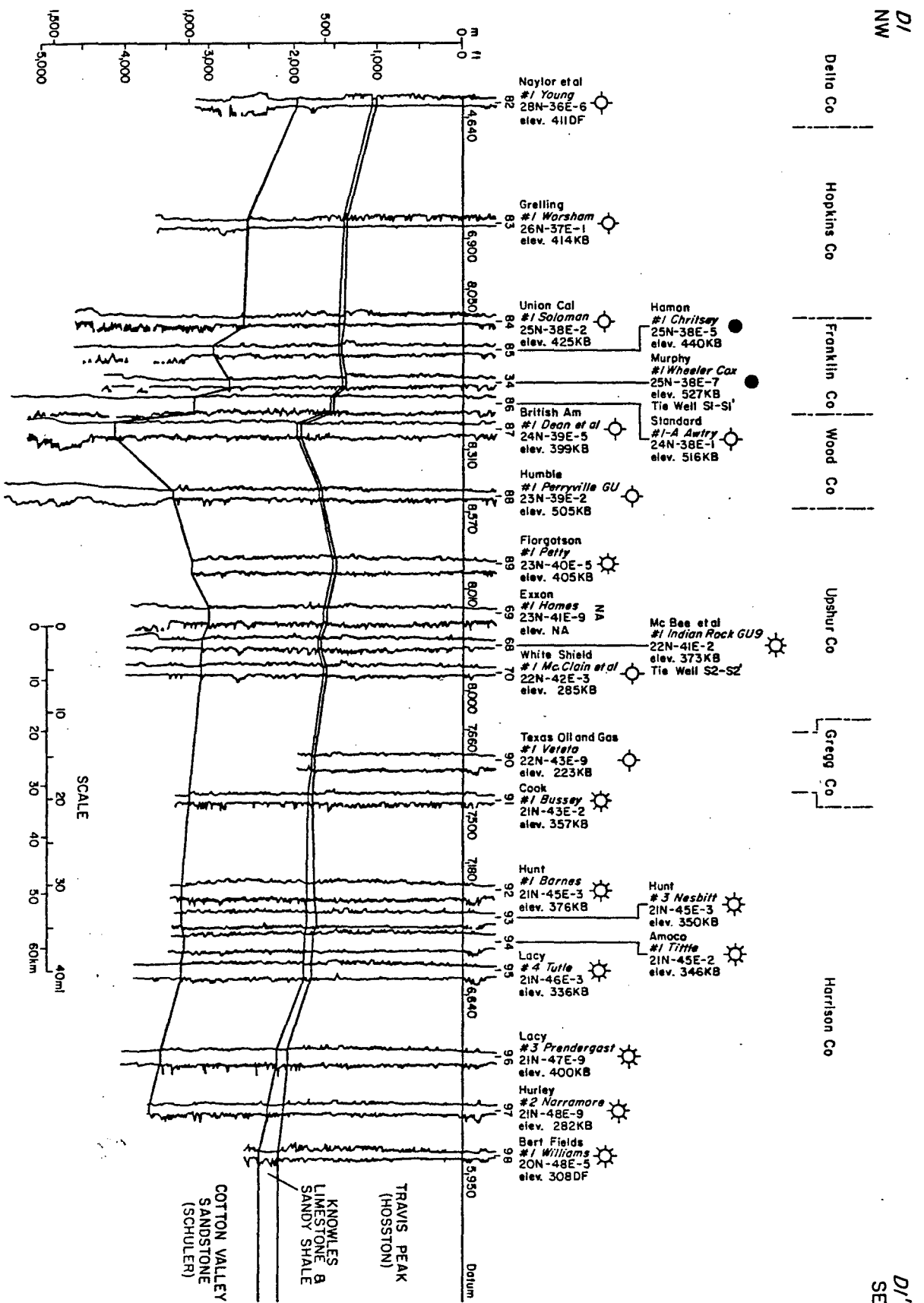


Figure 6. Dip-oriented stratigraphic cross section D1-D1' in the East Texas Basin. Location shown on figure 2.

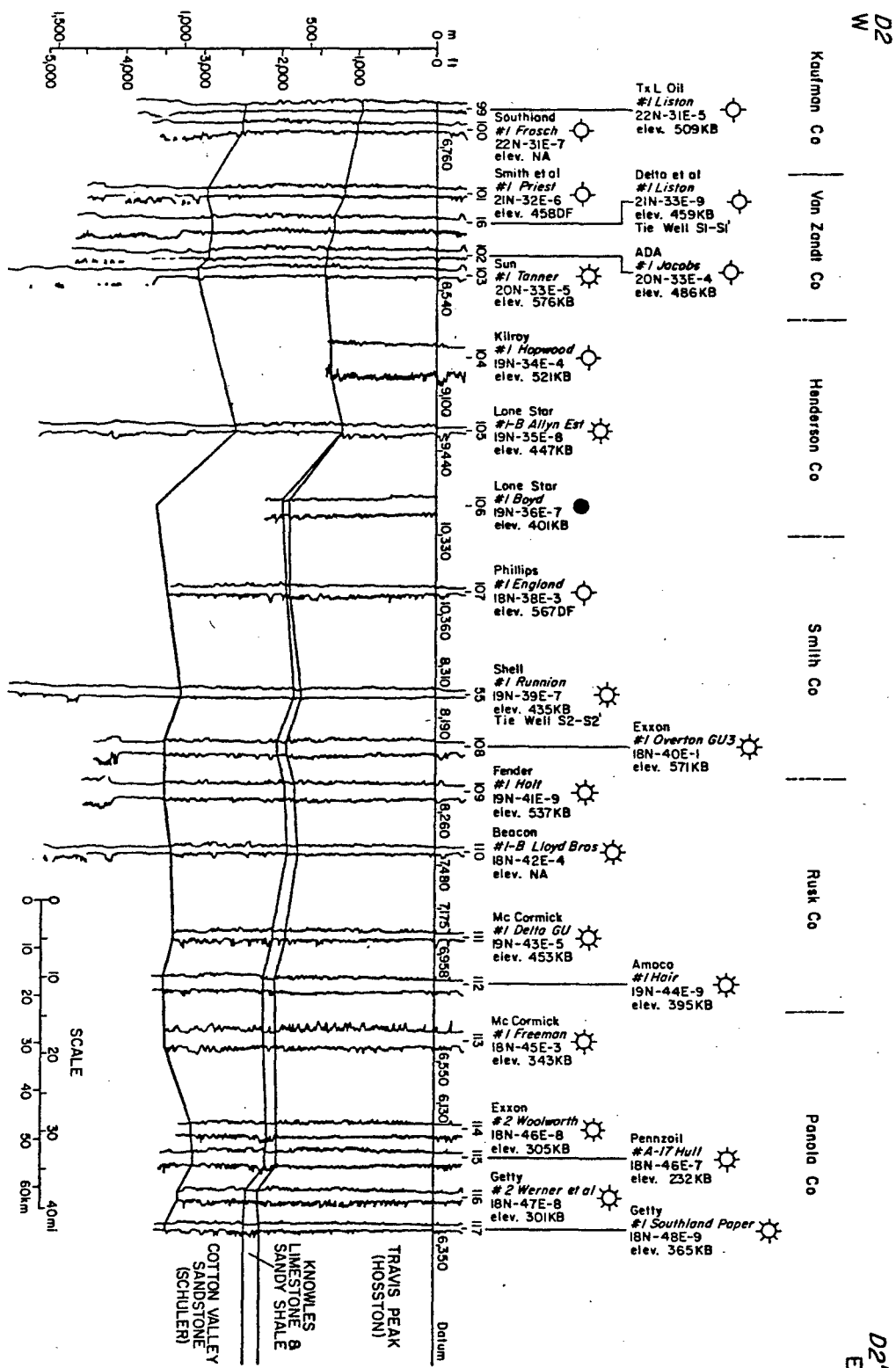


Figure 7. Dip-oriented stratigraphic cross section D2-D2' in the East Texas Basin. Location shown on figure 2.

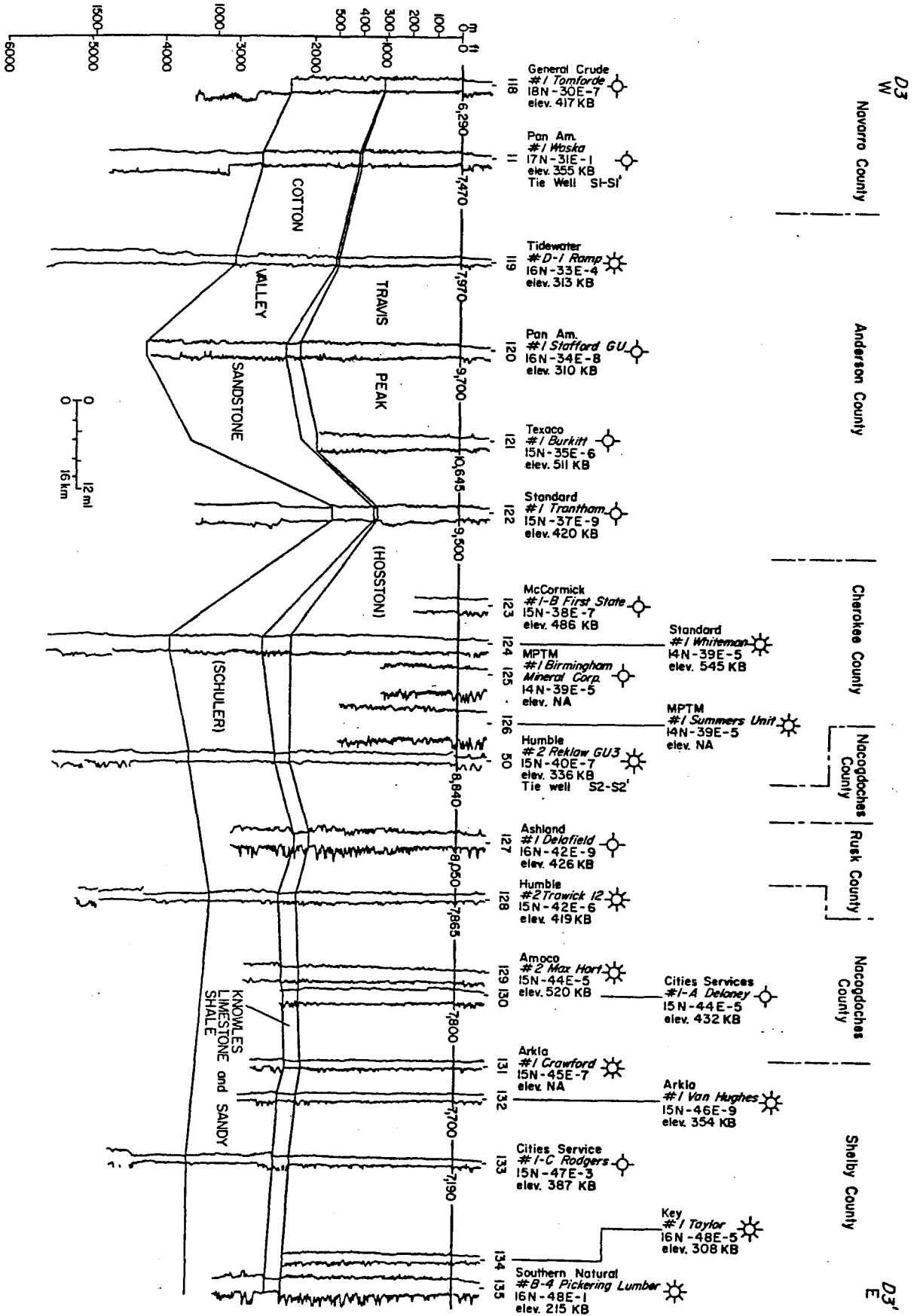


Figure 8. Dip-oriented stratigraphic cross section D3-D31 in the East Texas Basin. Location shown on figure 2.

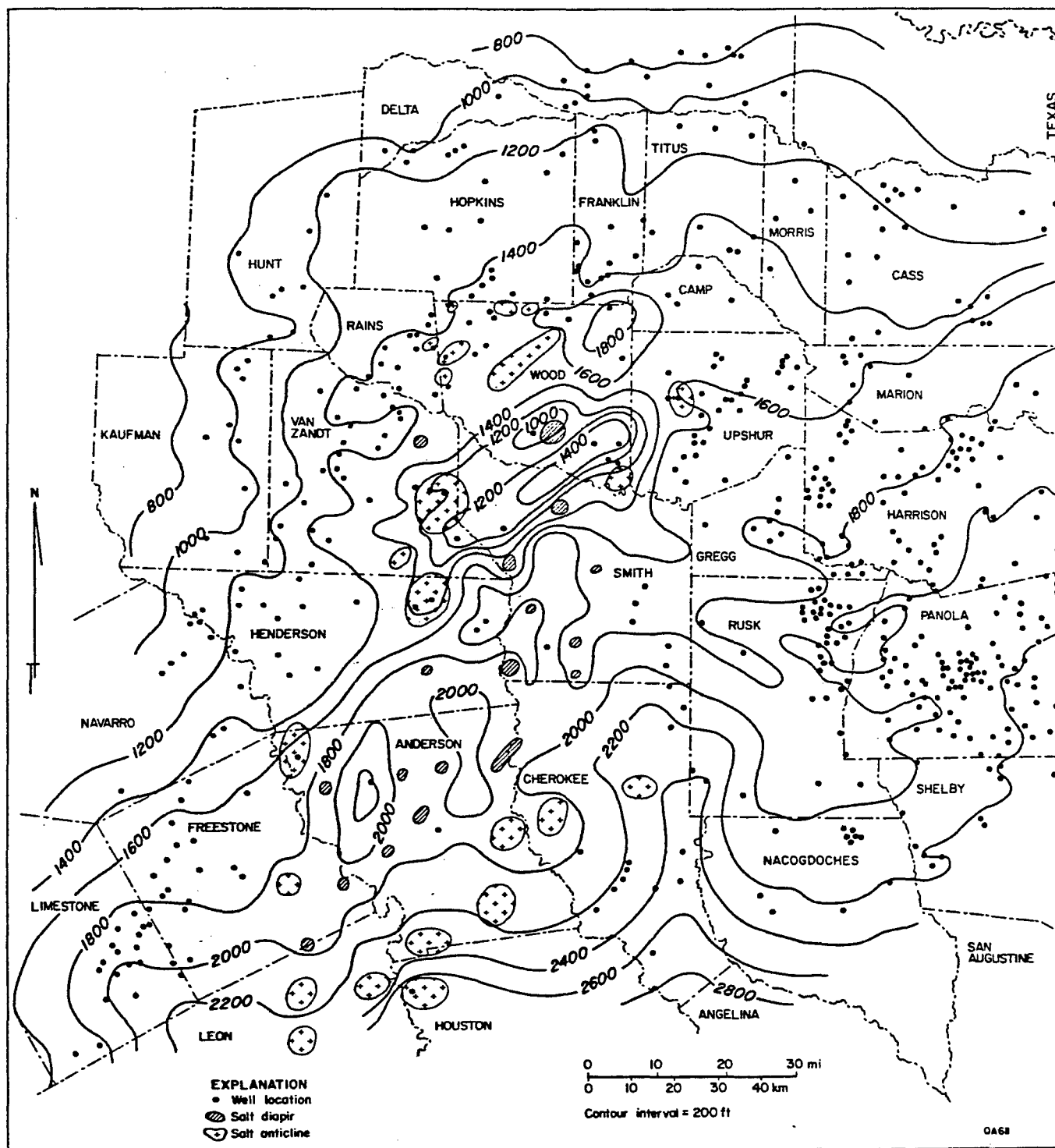


Figure 9. Isopach map of the Travis Peak Formation in the East Texas Basin. Information on salt structures from Wood (1981).

Depositional Systems

East Texas Basin.--Regional depositional systems of the Travis Peak Formation over the East Texas Basin were delineated by Bushaw (1968, fig. 10). McGowen and Harris (in press) carried out an areally limited but detailed subsurface study in the updip part of the basin. Using the above studies, we interpret the Travis Peak Formation as a system of coalescing fan deltas that prograded from the west, northwest, and north. In the proximal part of the basin, the Travis Peak Formation is represented by thick and occasionally coarse-grained sandstone (fig. 11) (McGowen and Harris, in press).

In the updip basin-margin area, the Knowles Limestone and associated thin sandy shale were not deposited, so that the lower Travis Peak sandstones are in direct contact with the uppermost sandstones of the underlying Cotton Valley Group. The absence of a thin shale section between the Travis Peak Formation and the Cotton Valley Sandstone in the updip area and their similar log character caused difficulty in distinguishing between these sandstone packages. In a north-south stratigraphic cross section (fig. 12), the Travis Peak Formation has a thick, wedge-like geometry and consists predominantly of laterally extensive, stacked braided stream deposits (Railroad Commission of Texas, 1981b).

Three Travis Peak fields (Yantis, Gilmer and Stamps, and Carthage Fields, fig. 13) were chosen for a detailed study of facies, and the Travis Peak Formation was tentatively subdivided into three subunits. Log patterns of the lower unit show repetitive progradational sequences, which are interpreted as distal deltaic facies. In a small area, the cyclic sequences seem to be fairly continuous (fig. 14). However, in Upshur and Panola Counties, the coarsening-upward sandstone sequences are not persistent in every direction, which indicates that multiple lobes of delta-front sediments were stacked laterally and vertically and also prograded basinward (figs. 15 and 16). Several fining-upward sequences in the lower unit indicate abandonment of deltaic lobes.

The lower sandstone unit is overlain by an exceptionally thick middle unit composed of stacked, coarse-grained braided stream deposits (Bushaw, 1968) forming an alluvial plain over

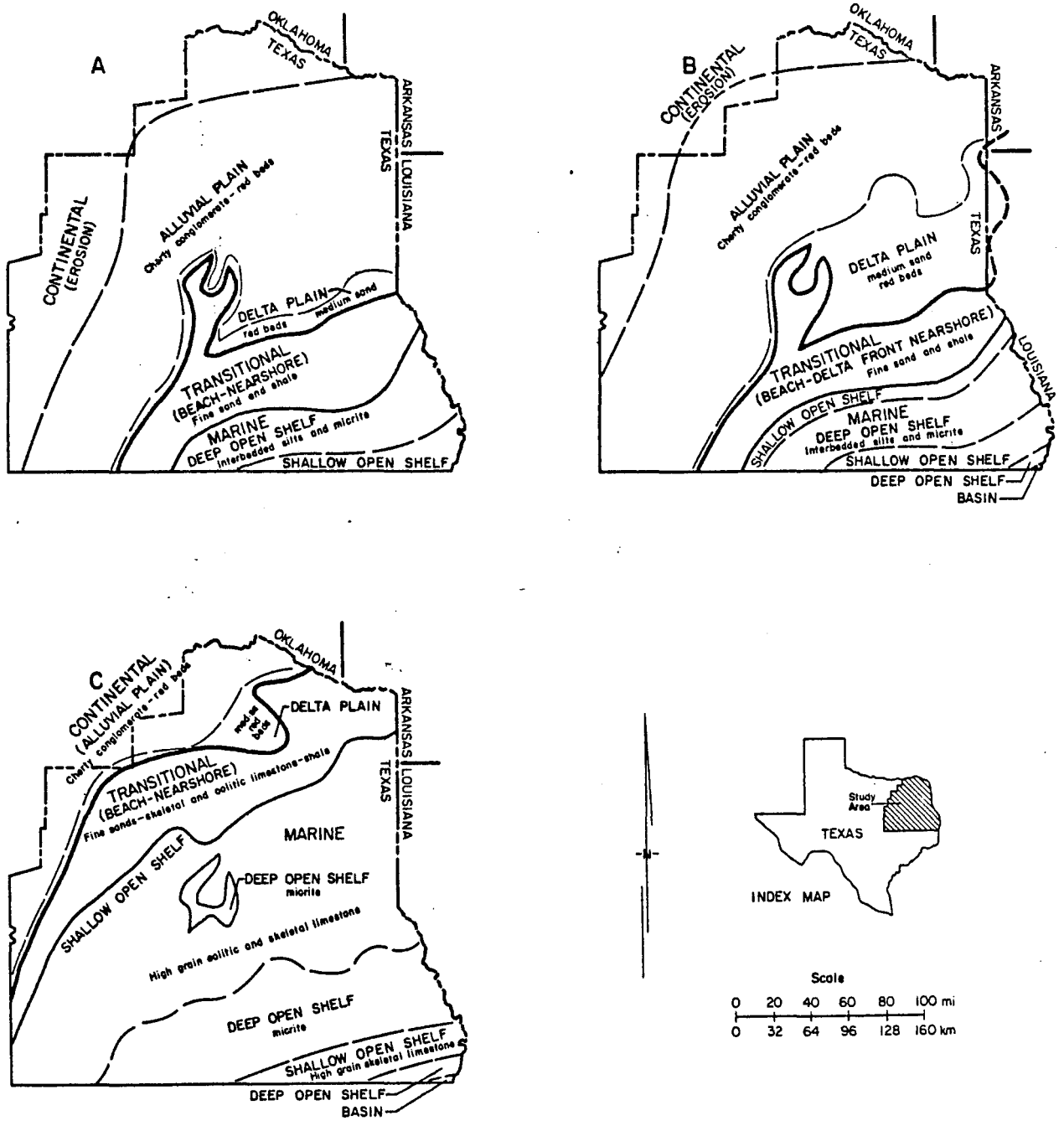


Figure 10. Facies tract maps of three subdivisions in the Travis Peak Formation, East Texas Basin: (A) lower; (B) middle; and (C) upper units (after Bushaw, 1968).

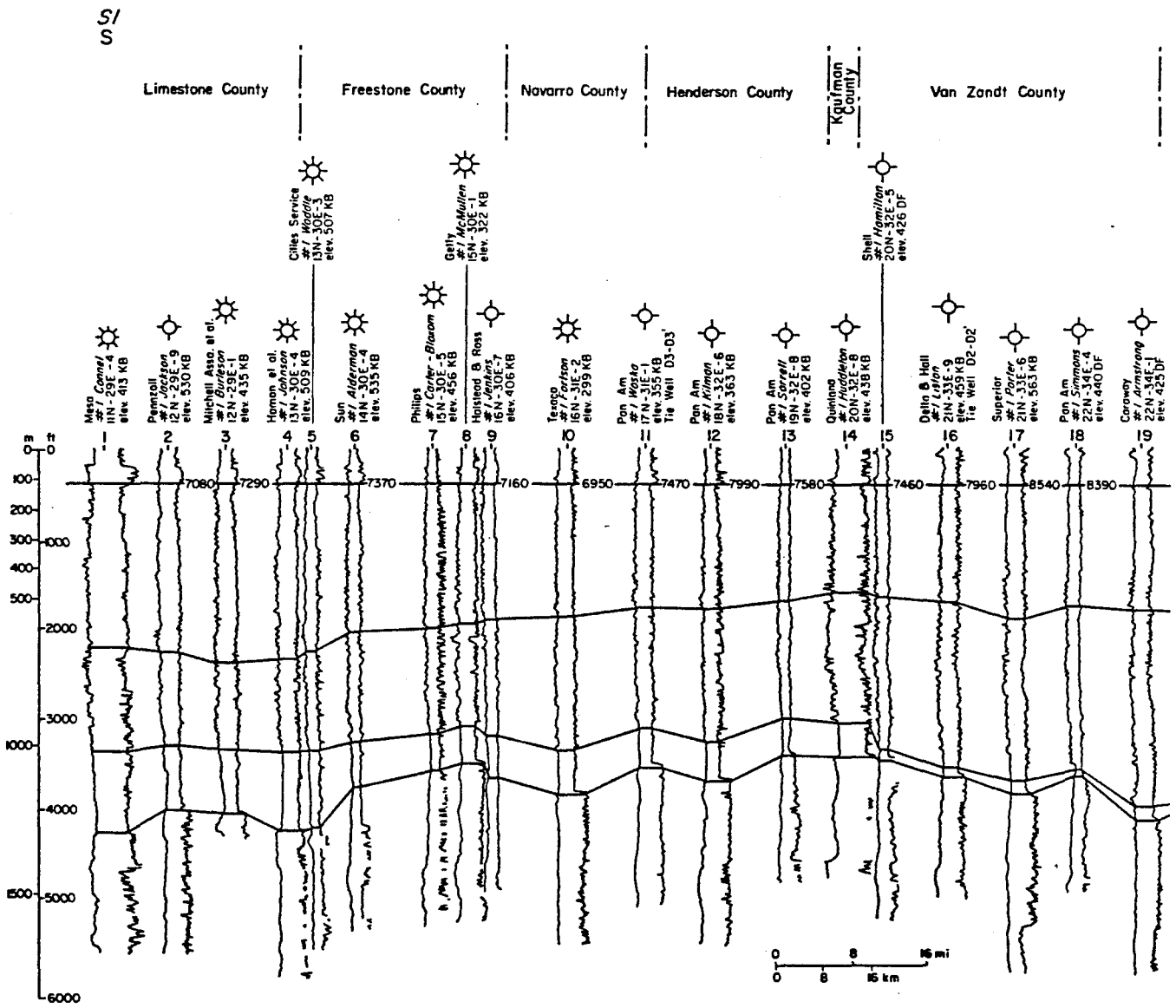


Figure 11. Strike-oriented stratigraphic cross section S1-S1' in the East Texas Basin. Location shown on figure 2. SP curve is on left; resistivity curve is on right.

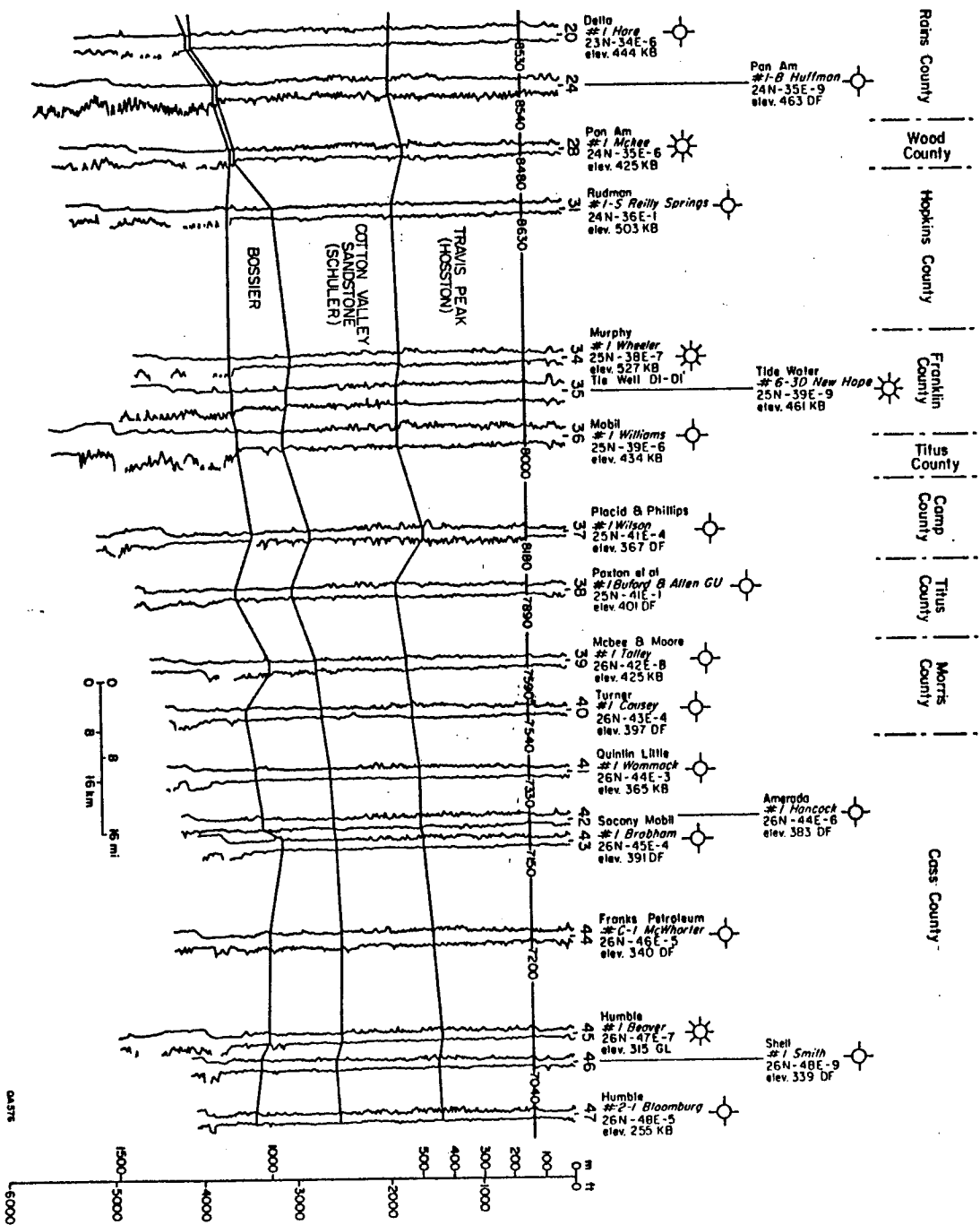


Figure 11 (cont.)

S/N

S2
S

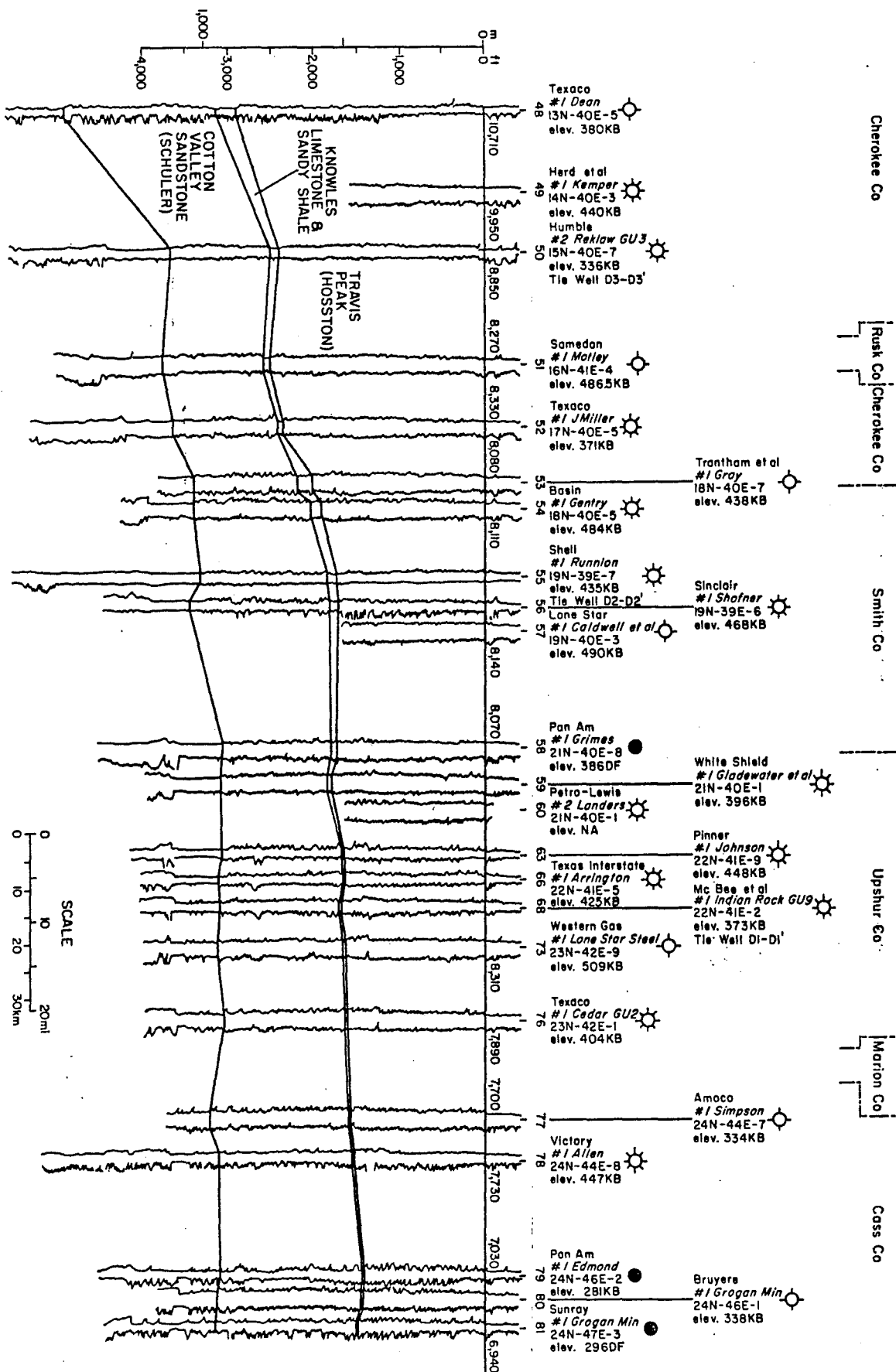


Figure 12. Strike-oriented stratigraphic cross section S2-S2' in the East Texas Basin. Location shown on figure 2.

S2'
N

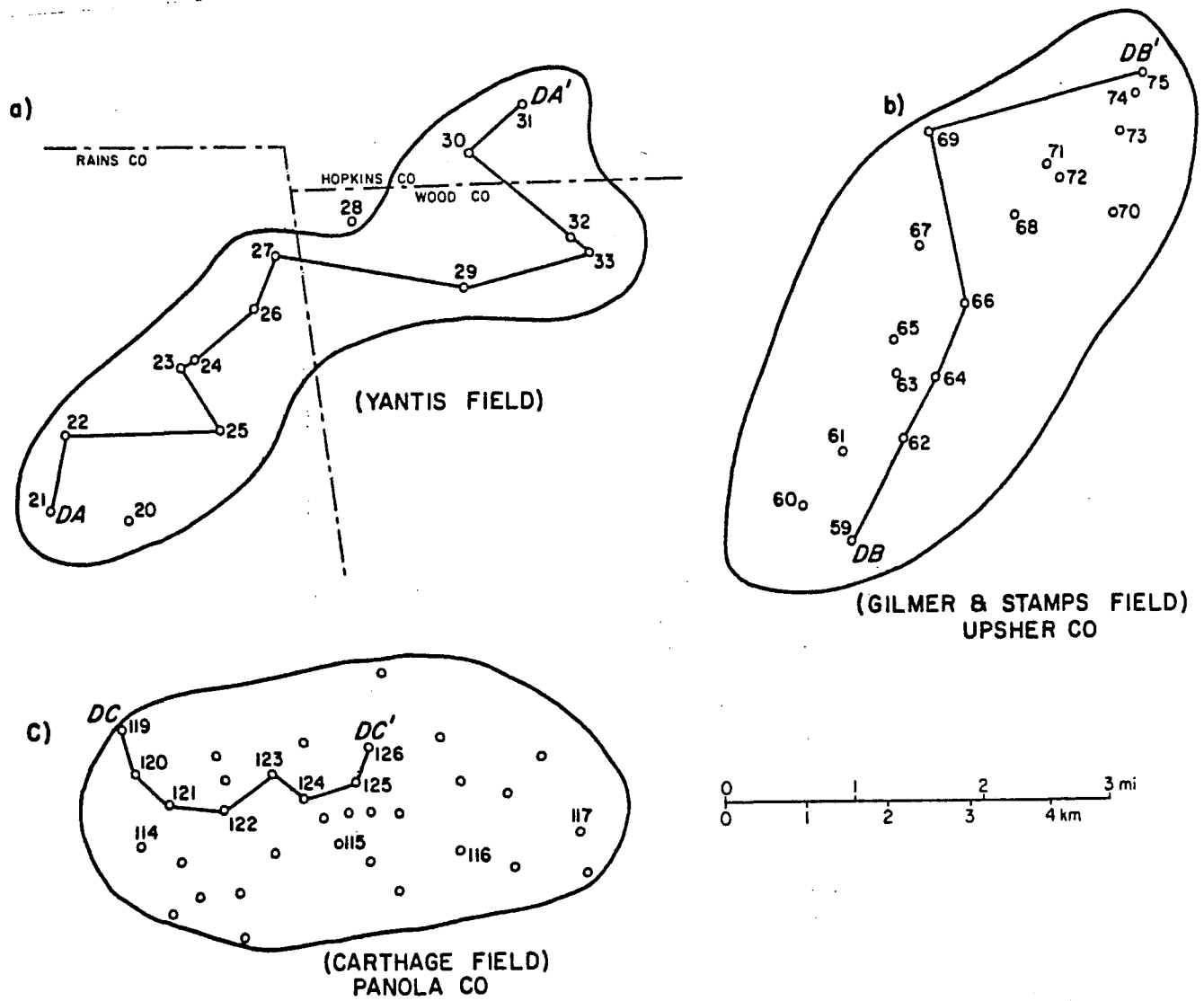


Figure 13. Location of wells in three areas of detailed study in the East Texas Basin.

DA
S

DA'
N

32

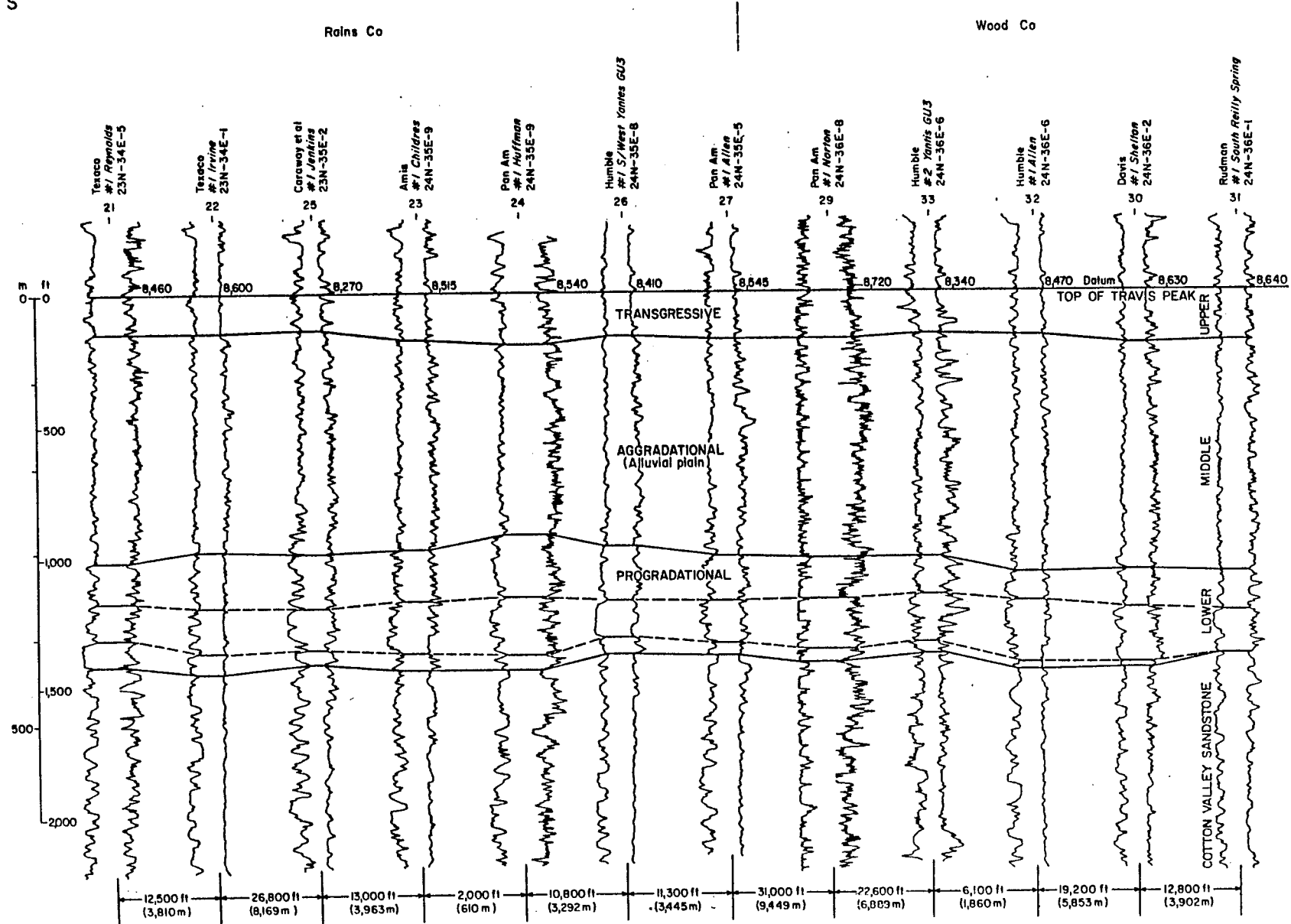


Figure 14. Detailed stratigraphic cross section DA-DA' in Rains and Wood Counties, East Texas Basin, showing three subdivisions of the Travis Peak Formation. Location shown on figure 13.

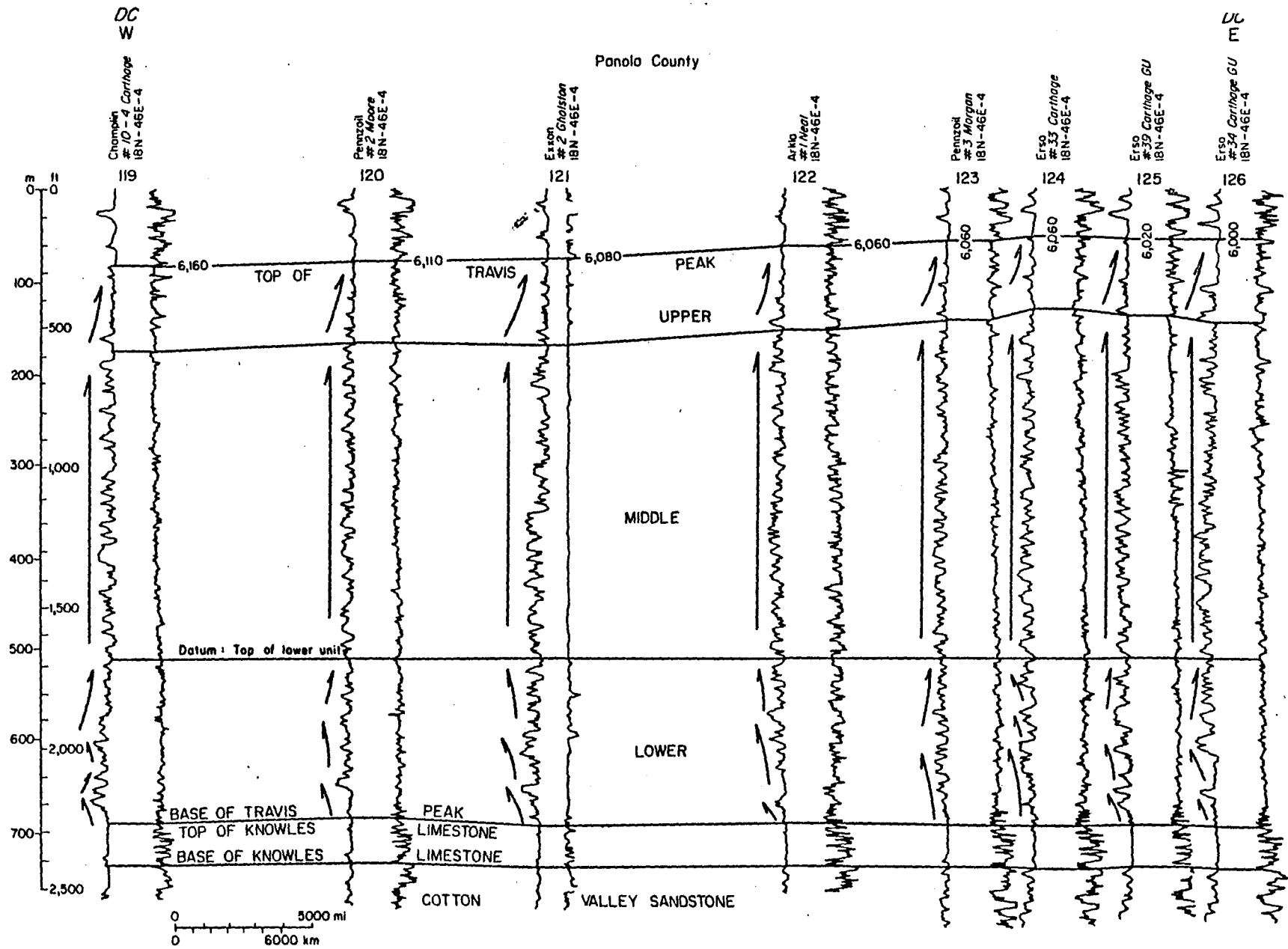


Figure 16. Detailed stratigraphic cross sections DC-DC' in Panola County, East Texas Basin, showing three subdivisions of the Travis Peak Formation. Location shown on figure 13.

much of the basin. These alluvial-plain sandstones accumulated during a stage of fairly continuous aggradation in the East Texas Basin and the central part of the North Louisiana Basin. In the middle unit, individual sandstones cannot be readily correlated between nearby wells; this unit has a comparatively uniform thickness, ranging from 700 to 1,000 ft over the study area.

The thick, sand-rich middle unit grades upward into a facies of interbedded shale and sandstone. In Panola Field, the upper unit shows fining-upward sequences deposited during a transgressive phase which ended Travis Peak sedimentation. These three facies recognized in the detailed study areas appear consistent with Bushaw's (1968) interpretations.

North Louisiana Salt Basin.--In the North Louisiana Salt Basin, the thickness of the Hosston (Travis Peak) Formation is greater than that in the East Texas Basin. Near the Texas-Louisiana border area, in the vicinity of the Sabine Uplift, the formation has a thickness of only 1,800 ft (fig. 17). Basinward, the thickness increases (fig. 18), toward a maximum in the center of the basin. Salt tectonism appears to have affected the overall thickness of the Hosston Formation as in Claiborne Parish (well 1, fig. 19). The Knowles Limestone is fairly well developed in the entire North Louisiana Salt Basin and is more than 500 ft thick in Winn Parish (fig. 20).

In Claiborne Parish, the Hosston Formation has been described as nearshore mixed facies, and deltaic channel sandstones and siltstones (Shreveport Geological Society, 1980). The middle Hosston sandstones in Jackson Parish represent alternating sequences of fluvial and littoral sands with marine shales and some thin-bedded limestone. In general, depositional systems of the Hosston Formation in the North Louisiana Salt Basin are similar to those of the East Texas Basin; they consist of complex assemblages of alluvial and shallow marine clastics and thin marine limestone beds. However, the Hosston Formation in North Louisiana contains more carbonate sediments, including oolitic limestone and thin micritic limestone beds.

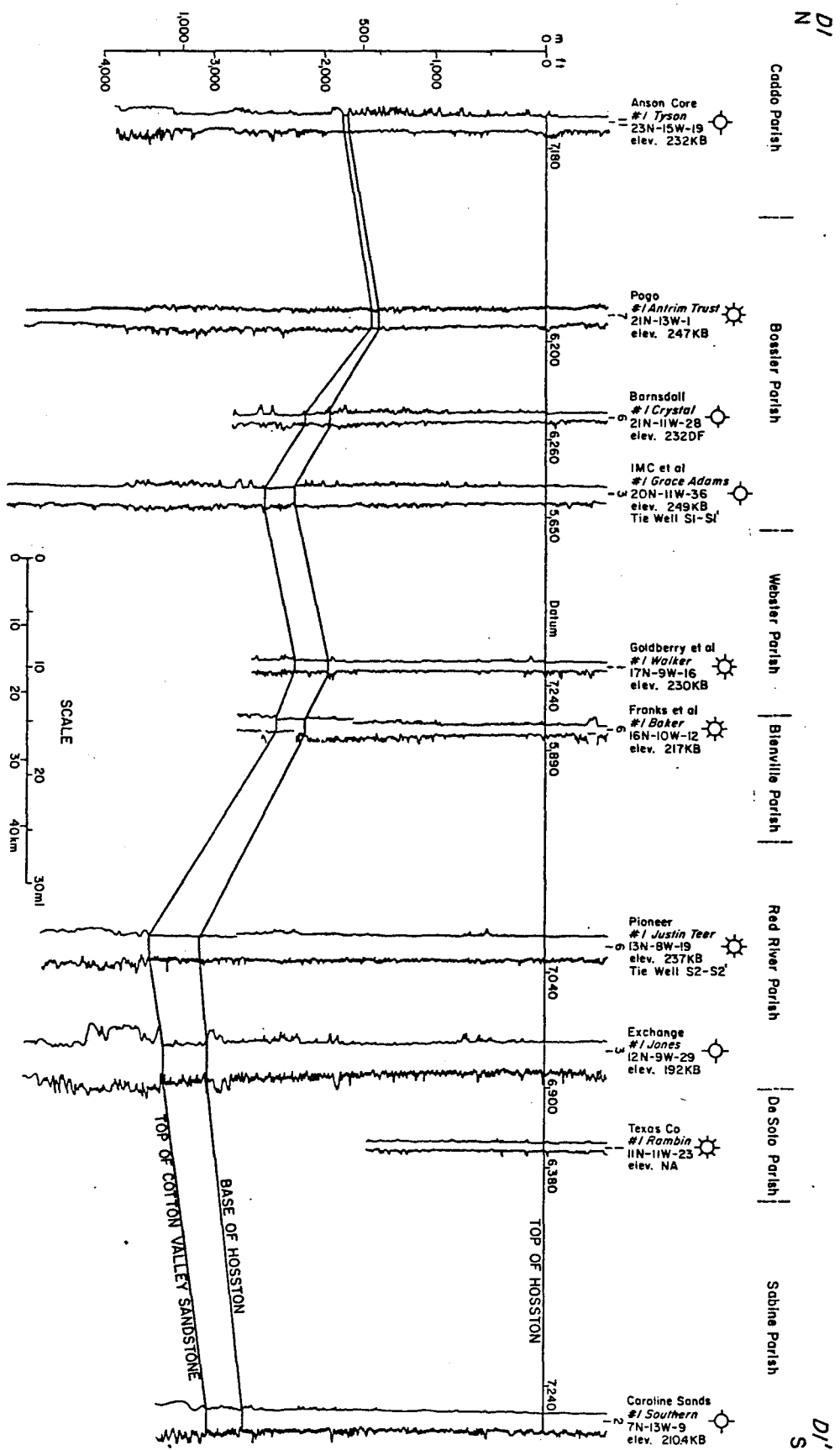


Figure 17. Dip-oriented stratigraphic cross section D1-D1' in the North Louisiana Salt Basin. Location shown on figure 3.

D2
N

D2'
S

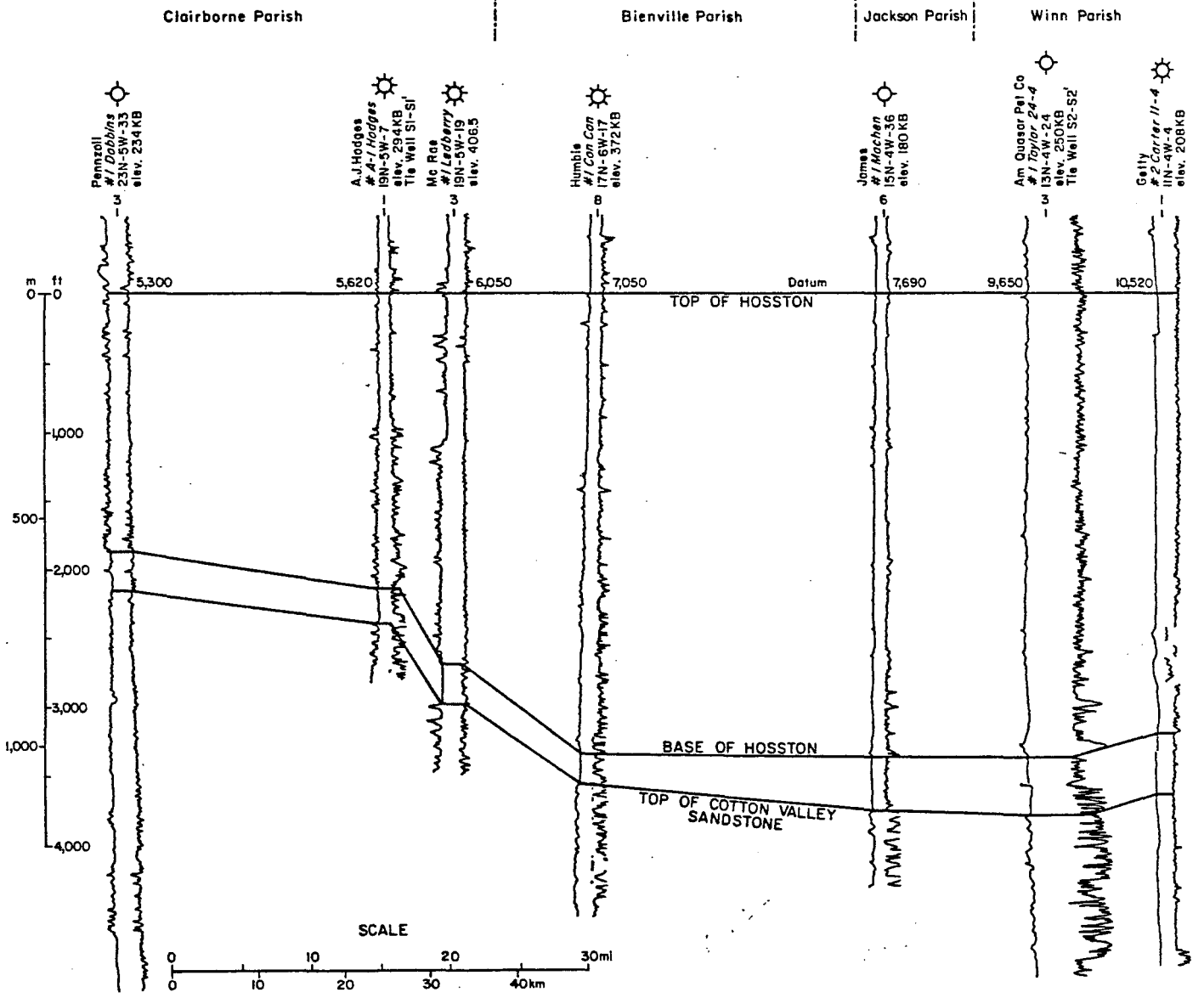


Figure 18. Dip-oriented stratigraphic cross section D2-D2' in the North Louisiana Salt Basin. Location shown on figure 3. SP curve is on left; resistivity curve is on right.

S2' E

Caldwell Parish

Winn Parish

Red River Parish

De Soto Parish

S2' W

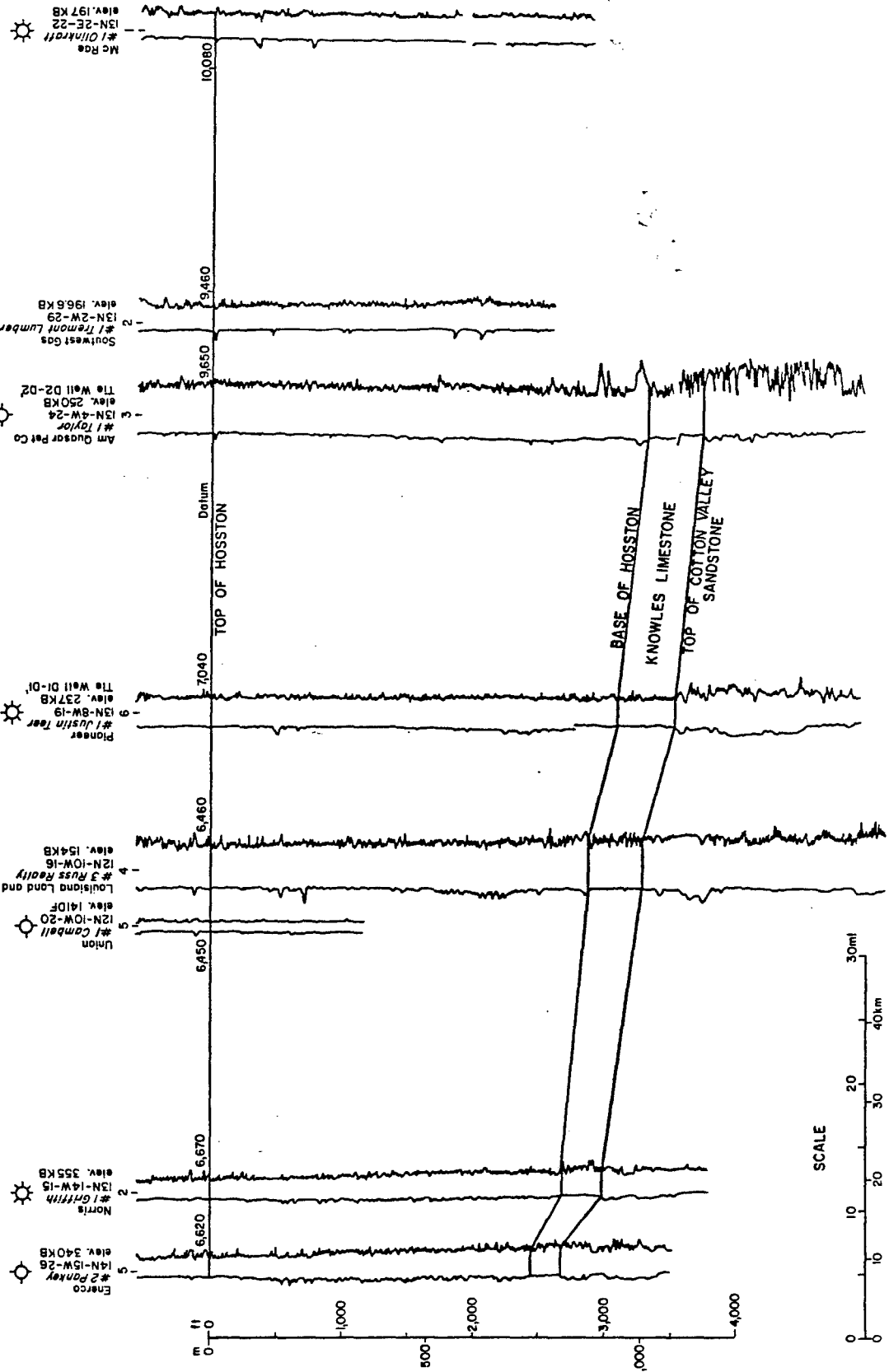


Figure 20. Strike-oriented stratigraphic cross section S2-S2' in the North Louisiana Salt Basin.

Summary of Selected Parameters and Production Data

Tables summarizing the general attributes, geologic and engineering characteristics, and the extrapolation potential of the Travis Peak Formation were given by Finley (1982).

During 1981, more than 106 Bcf of gas was produced from 115 Travis Peak fields in the East Texas Basin (31 fields in Railroad Commission District 5 and 84 fields in District 6, fig. 21). This figure includes both pre- and post-stimulation gas production. Sixteen fields, including Bear Grass, Bethany, Opelika, and Tri-Cities Fields, each produced more than 1 Bcf annually during 1980 and 1981. The Travis Peak is not tight, however, in Opelika Field (R. E. Jenkins, personal communication, 1983). Travis Peak gas production records in the East Texas Basin show that 615 wells produced 106 Bcf of gas in 1981 (Table 2). Cumulative production is not tabulated in the Railroad Commission of Texas Annual Report.

Perforated intervals were plotted against depth in 11 major fields in the East Texas Basin (fig. 22). It is notable that perforated intervals in Bethany and Carthage Fields were limited in the upper unit, ranging in depth from -6,000 to -7,000 ft msl, in which the sandstones show transgressive, fining-upward sequences. In Trawick Field, perforations were tested in the upper portion of the middle unit of the Travis Peak Formation. In these fields the sand-rich middle and lower units of the Travis Peak Formation remain, therefore, as unexplored areas and as possible exploration targets with unknown potential for gas production from tight sandstones. In the other fields, perforations were made throughout the Travis Peak Formation with large spacings between uppermost and lowermost perforations. The factors controlling the distribution of sandstones selected by operators for testing and production will be investigated should the Travis Peak be selected for additional research by GRI.

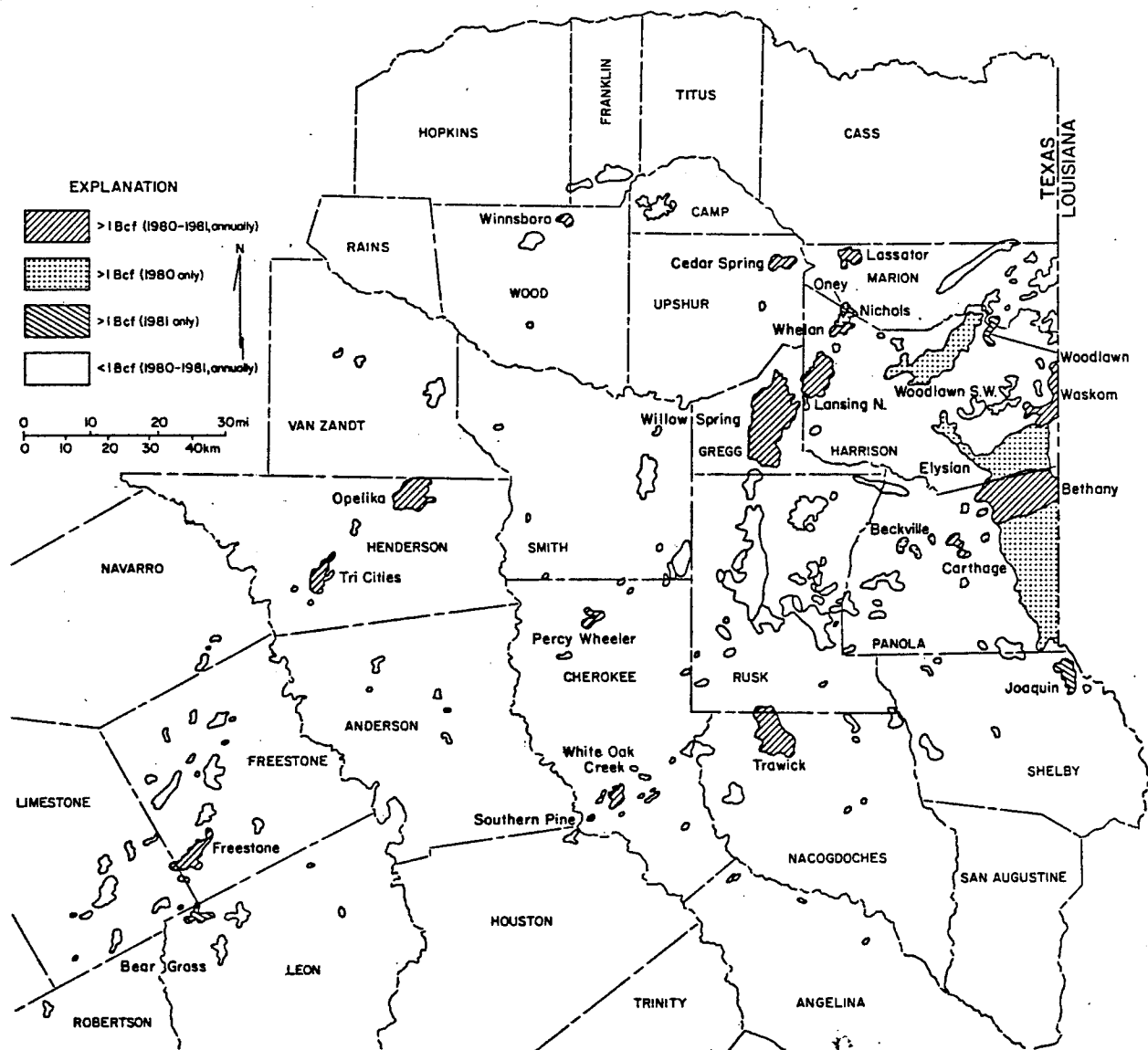


Figure 21. Field map showing Travis Peak gas production in the East Texas Basin. Compiled from executive reference map from Geomap, Inc., producing oil and gas fields map from Citizens First National Bank of Tyler, and Railroad Commission of Texas (1981 and 1982).

Table 2. Travis Peak gas production in 1981 in the East Texas Basin
(Railroad Commission of Texas, 1981b).

Field	Producing Wells* (at end of yr)	Gross Gas Prod. (Mcf)	Hydrocarbon Liquids (bbl)
Railroad Commission District 5			
Bear Grass	8	1,213,693	5,681
Box Church	0	0	0
Buffalo East	1	23,979	0
Burleson Hill	4	124,003	0
Cheneyboro	0	0	0
Cotton Gin	0	0	0
Fairfree	1	22,575	142
Fallon	1	1,698	0
Farrar	0	0	0
Freestone	6	1,036,639	592
Harold D. Orr	0	0	0
Jewett	4	237,709	426
Keechi-Hamill	1	111,059	0
Kirvin	1	166,943	1,926
La Rue	0	675	29
Malakoff	9	459,336	1,307
McBee	1	6,789	0
Oaks	0	0	0
Oletha	1	86,843	785
Opelika	29	11,257,202	0
Personville	1	78,859	115
Pokey	4	365,185	750
Reed	7	500,443	6,516
Reka	0	0	0
Rischers Store	3	134,744	2,279

*Producing well number is taken as highest number of wells in one horizon. If different numbers of wells are listed as producing for various horizons, it is assumed that dual completions make this difference.

Table 2. (continued)

Field	Producing Wells (at end of yr)	Gross Gas Prod. (Mcf)	Hydrocarbon Liquids (bbl)
Roundhouse	2	707,863	1,091
Stewards Mill	1	10,667	149
Teague	6	1,048,875	2,810
Tillmon	0	0	0
Tri-Cities	36	10,130,828	2,967
Van, West	0	0	0
Railroad Commission District 6			
Alpine	7	333,434	1,569
Alto	4	173,472	534
Appleby North	1	216,536	4,083
Barnhardt Creek	1	8,274	583
Beckville	1	55,450	1,006
Belle Bower	6	426,672	2,328
Bethany	57	10,526,319	39,494
Big Barnett	0	2,591	211
Big Shorty	2	37,772	676
Caddo Lake	0	0	0
Caney Creek	0	0	0
Carthage	75	11,030,854	33,839
Cedar Springs	9	1,135,385	21,514
Centennial	1	34,728	0
Center, West	0	22,485	125
Chapel Hill	2	134,413	3,990
Chapman	3	239,069	3,747
Church Hill	4	354,707	8,066
Clinton Lake	0	0	0
Cyril	5	349,364	9,981
Danville	4	227,827	3,860
Diamond-Mag	0	0	0

Table 2. (continued)

Field	Producing Wells (at end of yr)	Gross Gas Prod. (Mcf)	Hydrocarbon Liquids (bbl)
Douglas, West	7	328,054	140
Elysian	3	292,762	5,995
Excelsior	0	0	0
Fairplay	1	96,981	1,552
Garrison	9	248,334	5,682
Girlie Caldwell	1	30,289	2,438
Gooch	6	320,386	4,086
Green Fox	0	0	0
Hamlet	0	0	0
Harleton, East	0	0	0
Henderson, South	8	280,284	4,892
J.G.S.	2	238,212	2,586
Jarrell Creek	0	0	0
Joaquin	13	1,385,269	2,034
Kendrick	1	201,257	1,317
Laneville	2	284,297	3,025
Lansing	11	4,441,878	52,203
Lassater	19	2,949,343	12,899
Leigh	0	0	0
Lets	1	48,015	0
Longview	1	47,939	1,272
Longwood	0	0	0
Manziel	3	111,097	1,682
Minden	6	849,855	15,443
Mt. Enterprise	0	0	0
Nacogdoches	0	0	0
Naconiche Creek	0	0	0
North Timpson	0	0	0
Oak Hill	1	49,100	935
Overton	0	0	0
P.L.	0	0	0

Table 2. (continued)

Field	Producing Wells (at end of yr)	Gross Gas Prod. (Mcf)	Hydrocarbon Liquids (bbl)
Paxton	0	0	0
Penn - Griffith	0	0	0
Percy-Wheeler	8	1,979,677	47,361
Pine Hill	2	376,265	5,444
Pone	4	331,081	6,527
Rayburn Lake	0	4,280	0
Red Land	1	309,004	9,573
Redwine	3	410,959	6,882
Reklaw	2	308,801	0
Rodessa	5	337,587	3,637
Rufus	1	25,548	259
Scoober Creek	0	2,404	0
Scottsville, North	2	138,207	890
Shiloh	3	236,591	7,132
Smithland	0	0	0
Southern Pine	11	1,489,378	195
Stamps	0	0	0
Stockman	6	255,820	7,232
Swanson	0	0	0
Sym-Jac	1	11,193	285
Tenaha	1	9,649	1
Trawick	53	12,945,802	1,253
Troup	1	18,614	243
Waskom	32	3,160,427	6,992
Whelan	30	6,329,767	7,351
White Oak Creek	23	3,918,248	3,170
William Wise, Southeast	0	0	0
Willow Springs	39	5,380,408	76,887
Winnsboro	7	1,370,644	28,639
Woodlawn	3	1,913,526	1,013
Woods	0	0	0

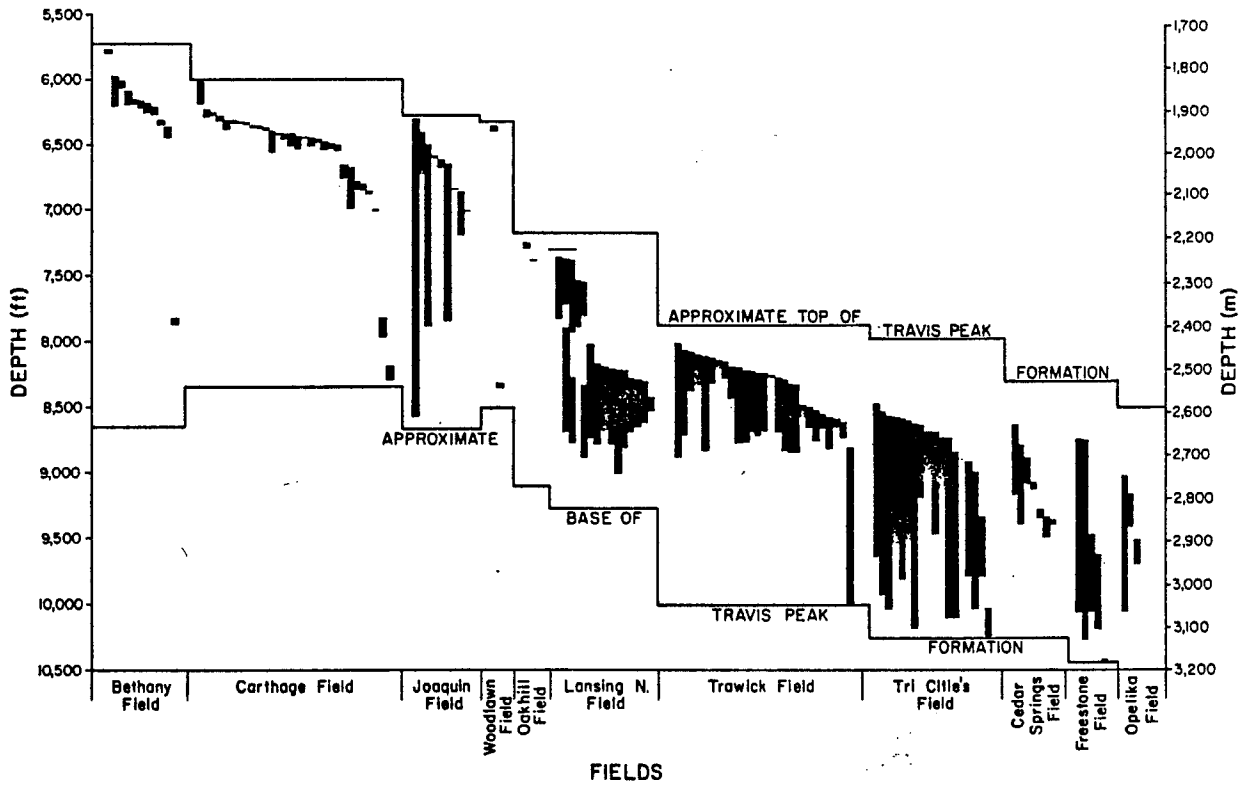


Figure 22. Distribution of perforated intervals in selected major Travis Peak gas fields in the East Texas Basin. Data abstracted from unpublished compilation by Petroleum Information, Inc.

OLMOS FORMATION, MAVERICK BASIN

Introduction

The Olmos Formation (Gulfian) is one of three terrigenous clastic formations deposited during the Late Cretaceous in the Maverick Basin of the Rio Grande Embayment. It rests on deltaic deposits of the San Miguel Formation (Weise, 1980) and is overlain by the Escondido Formation (fig. 23) which contains a spectrum of wave-dominated delta types similar to those in the San Miguel (Pisasale, 1980). The Olmos Formation crops out in Maverick County, Texas, over the Chittim anticline, and further west along a southwest trending exposure-belt (fig. 24). The subsurface extent of the Olmos is primarily within eight counties of South Texas and part of adjacent Mexico (fig. 25). The Olmos Formation consists of fine to very fine grained silty sand interbedded with massive shales (Glover, 1955). Locally developed lignite beds have been recognized on the electric logs.

There have been no up-to-date regional syntheses of the depositional framework of the Olmos Formation in South Texas. Published data specifically on the Olmos dealt primarily with oil and associated gas production and do not include recent information (Dunham, 1954; Glover, 1955; Glover, 1956). A recently published study focused only on Webb and southwest LaSalle Counties (Snedden and Kersey, 1982). The regional study of depositional patterns in the Olmos Formation described in this report covers eight counties and utilizes 350 electric logs.

Three applications for tight gas formation designations regarding the Olmos Formation have been received by the Railroad Commission of Texas. As of July 1983, two are still pending decision at the Railroad Commission and one application has been approved by the Commission and by FERC (Petro-Lewis Corporation; TRRC Docket No. 4-77, 136; approved by FERC 9-30-82).

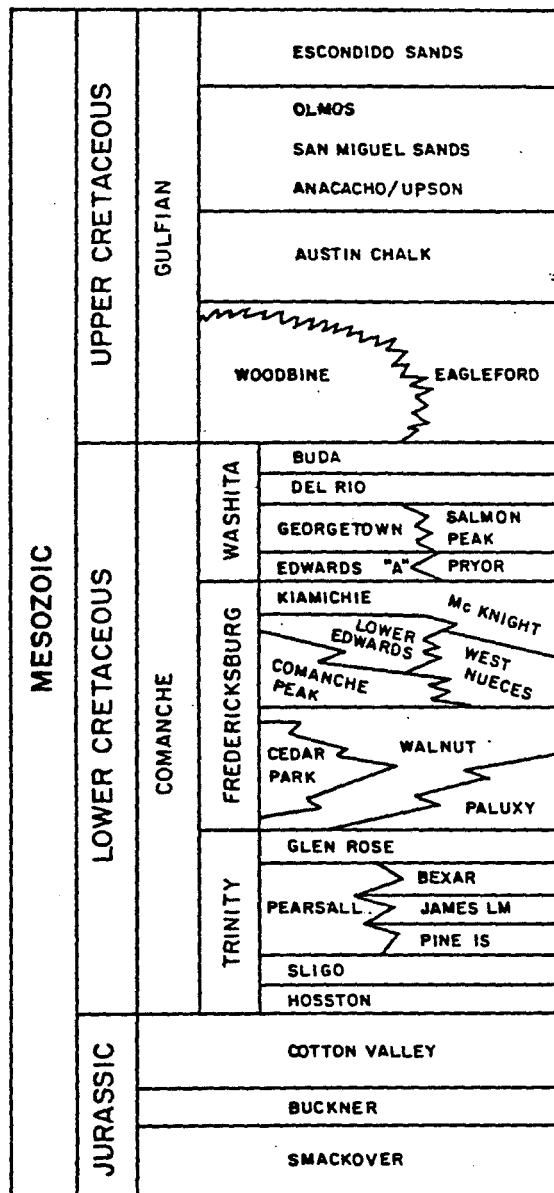


Figure 23. Stratigraphic column for part of the Jurassic and Cretaceous Systems in the Maverick Basin (from Finley, 1982).

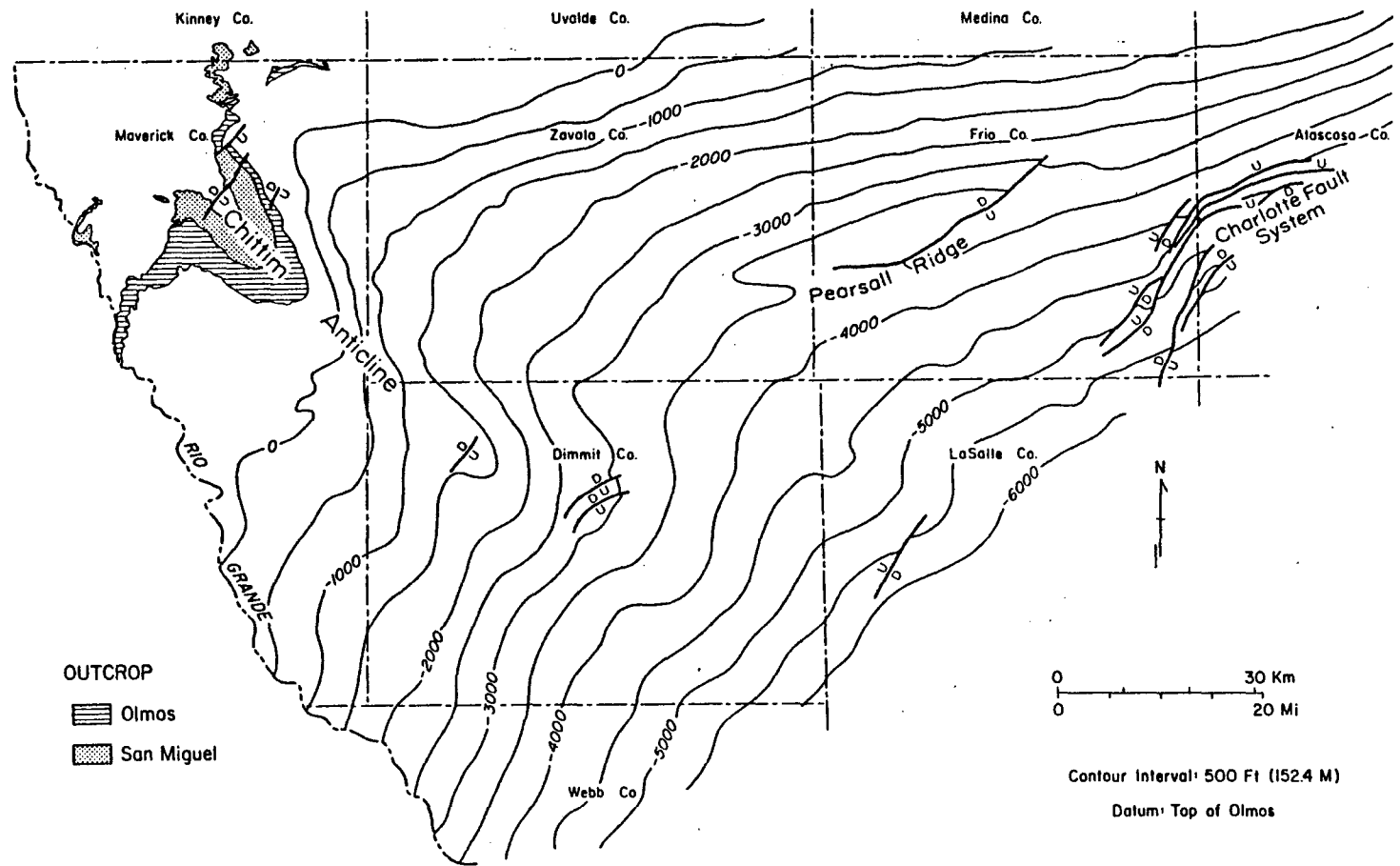


Figure 24. Structure map of the Maverick Basin contoured on top of the Olmos Formation (from Weise, 1980).

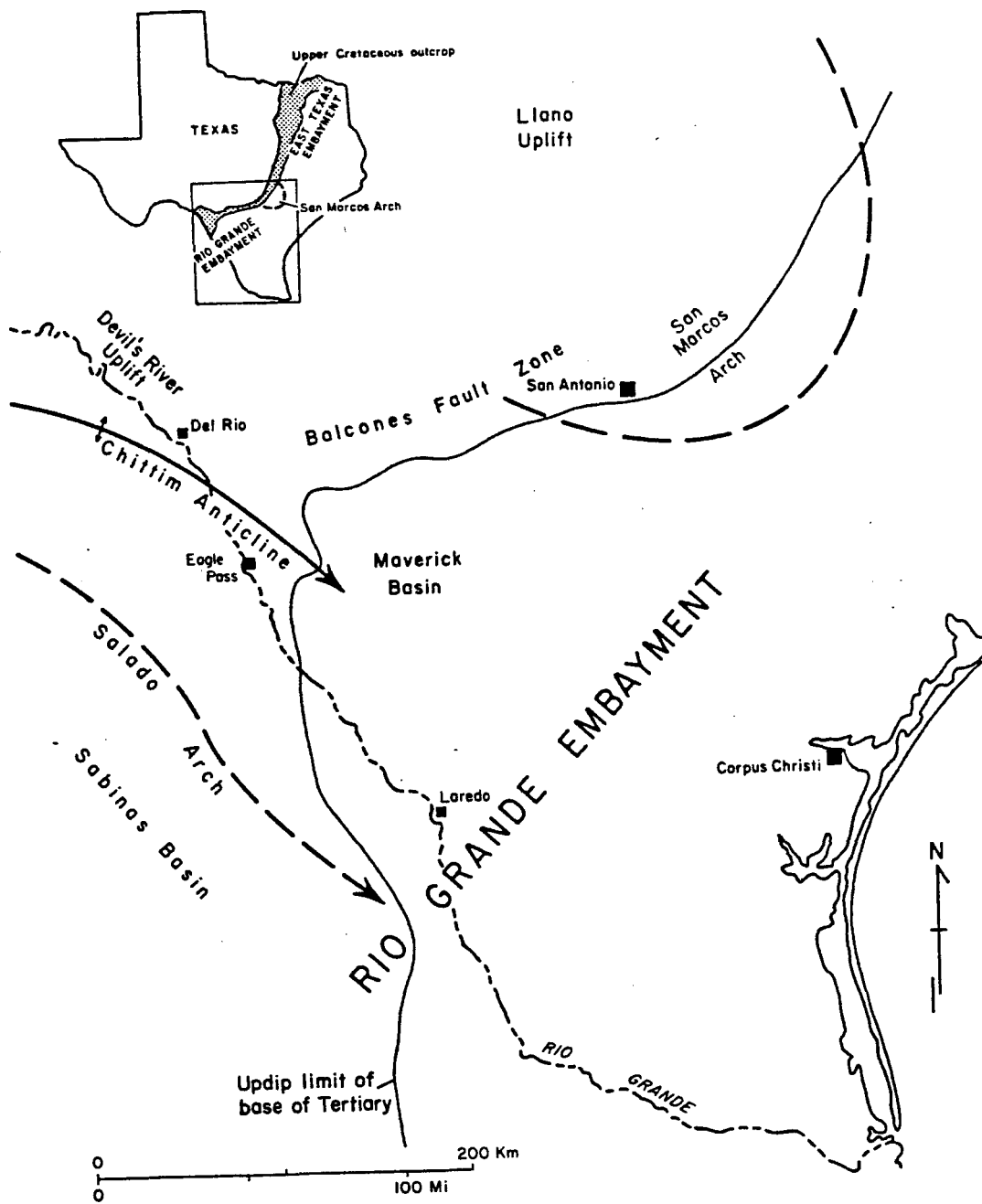


Figure 25. Structural framework of the Maverick Basin (from Weise, 1980).

Structure

The Upper Cretaceous Olmos Formation of southwest Texas and eastern Mexico was deposited in a restricted depression (the Maverick Basin) in the Rio Grande Embayment (fig. 25). This embayment contains a thickened Upper Cretaceous clastic sequence (Murray, 1957) and is considered to have formed as an aulacogen resulting from the breakup of Pangaea during the Triassic (Walper, 1977). Subsidence of the embayment resulted in a structurally negative area receiving sediment from adjacent areas. Carbonate deposition dominated sedimentation during the Early Cretaceous until renewed tectonism in western and northwestern source areas caused an influx of clastics into the Maverick Basin (Weise, 1980).

The structure of the Maverick Basin is uncomplicated. It is bounded to the east by the San Marcos Arch, which acted as a mildly positive structure that subsided at a lower rate than did adjacent basins during Cretaceous sedimentation. To the west, the Salado Arch separates the Maverick Basin from other basins in the Rio Grande Embayment (fig. 25). The Devils River Uplift and Balcones Fault Zone comprise the northwestern and northern limits of the basin, respectively. Structure contours on the Olmos Formation (fig. 24) indicate a regional southeast to east-southeast gulfward dip. Post-sedimentation second-order structures affecting the Olmos are the Chittim anticline, which plunges southeastward parallel to dip and is well defined by the outcrop of the Olmos Formation, and several fault systems including the Charlotte faults (fig. 24). Minor faults not distinguishable at this scale of mapping are also present in the downdip parts of the Olmos. These faults, which act as traps for Olmos gas accumulation, result from displacement along the Stuart City shelf margin (Snedden and Kersey, 1982).

Numerous basaltic volcanic plugs occur in the northern Maverick Basin, especially in Zavala County. Differential compaction and small tensional structures occur over the plugs. The significance of volcanic plugs to tight gas production is not known; none are mentioned in operator applications for tight formation designations.

Stratigraphy and Depositional Systems

The Olmos Formation comprises the uppermost component of the Taylor Group (fig. 26). It conformably overlies the deltaic San Miguel Formation. Uplift following deposition of the Olmos resulted in truncation of the updip deposits and the unconformable superposition of the Escondido over progressively older units of the eroded Olmos and San Miguel Formations. The lowest interval in the Taylor Group is composed of updip shallow-water carbonates of the Anacacho Formation and downdip shelf muds of the Upson Formation. Luttrell (1977) suggested that the Anacacho carbonates were deposited around basaltic volcanic plugs that were active during deposition of the Austin and lower Taylor Groups (fig. 26).

The Olmos has been interpreted as non-marine in outcrop, grading downdip to shallow marine deposits (Glover, 1955). Snedden and Kersey (1982) described the downdip sandstones in Webb County as a series of overlapping lobate deltas offshore of which are thin sheet sands that were deposited on the shelf. The Olmos updip in the Rio Escondido Basin of Mexico has been interpreted to be of delta-plain origin (Caffey, 1978).

Overview and Methodology

Four regional stratigraphic cross sections (two strike and two dip sections) were prepared (figs. 28-31; section locations shown on fig. 27). An additional section utilizing closely spaced wells from the Catarina Southwest Field in Dimmit County (D-D', fig. 27) was constructed to allow examination of local continuity of the sandstones in the area designated as tight gas productive (fig. 32). A preliminary isopach map of the Olmos Formation was compiled (fig. 33). From this basic framework additional infill cross sections were prepared and adjacent wells not on section lines were correlated.

The Olmos is subdivided into seven depositional packages arbitrarily numbered A through G (figs. 30 and 31). Five of the sandstone sequences are located in the western part of the study area and two in the east. From the strike sections it is evident that Olmos sedimentation

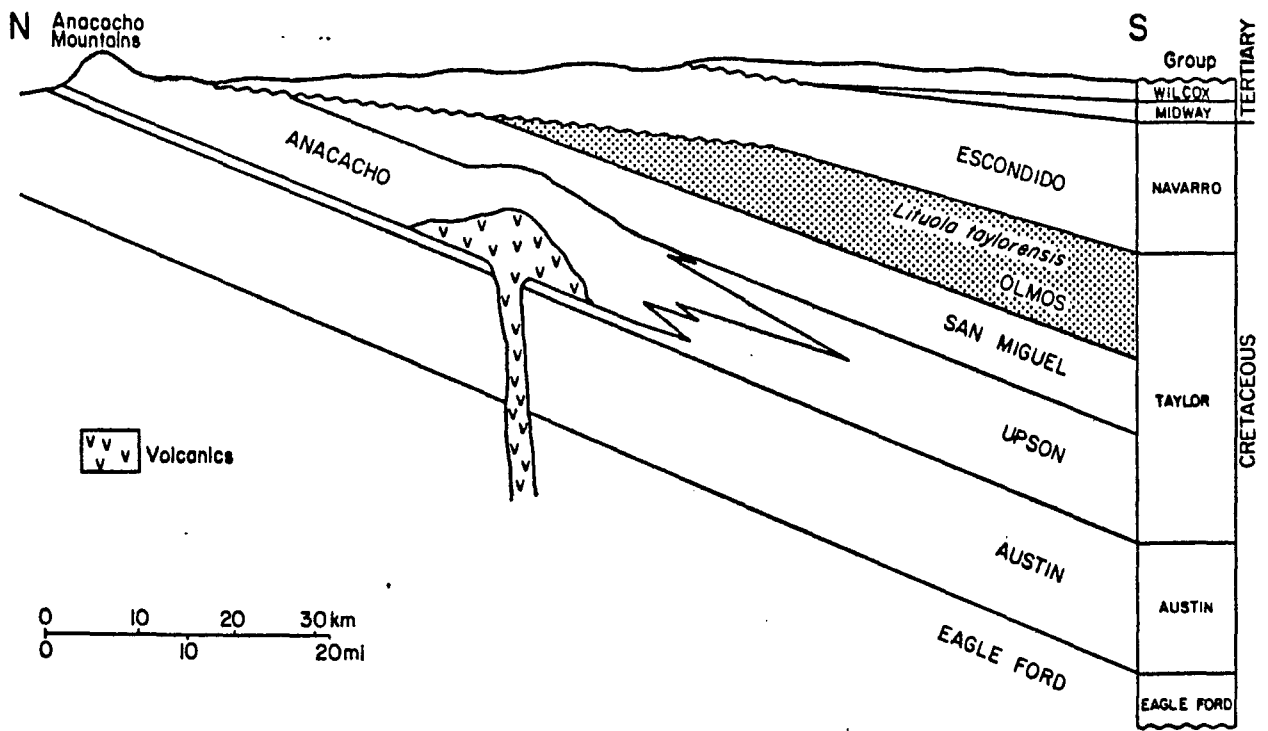


Figure 26. Schematic dip section through the Maverick Basin (modified from Weise, 1980; after Spencer, 1965).

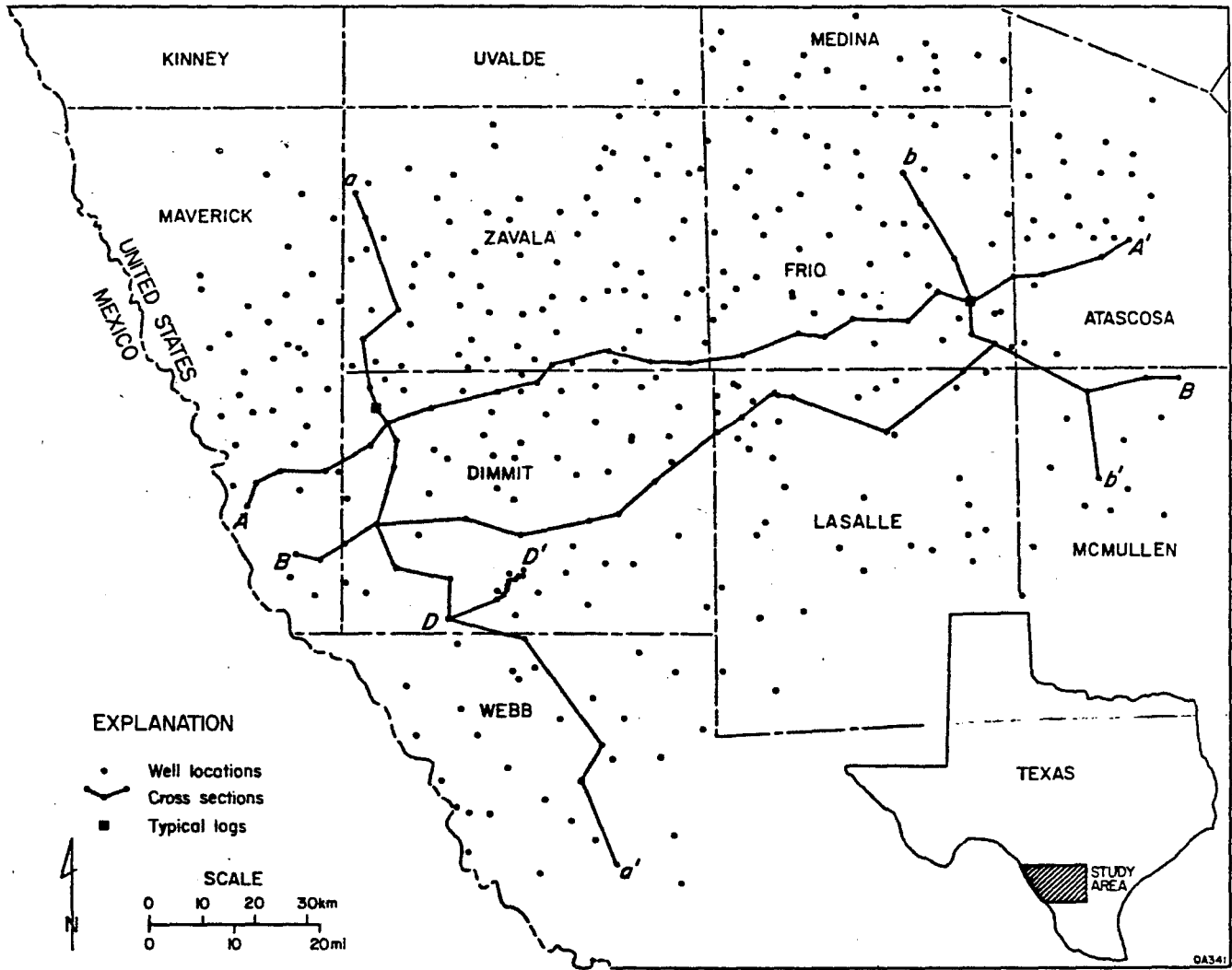


Figure 27. Well control and locations of cross sections, Olmos Formation, Maverick Basin.

had two principal depocenters. The eastern subbasin containing the F and G sandstone packages is characterized by less subsidence than is the western subbasin. Sediment input was from the north and possibly northeast in the eastern subbasin whereas the western depocenter was fed by rivers that entered the basin from the northwest. An isopach map of the Olmos Formation (fig. 33) illustrates thickening of the formation toward the south and southwest.

Typical log traces from the two subbasins differ greatly (fig. 34). The upward-coarsening sand packages in the eastern subbasin are thicker and more persistent than those to the west, which are comparatively thin and commonly have serrate SP log patterns. Preliminary interpretations indicate that sedimentation in the Olmos was predominantly deltaic. Early sedimentation took place in the western subbasin, then shifted eastward where the F and G sands were deposited. Lateral to the thick deltaic deposits of the eastern subbasin, clastic sedimentation took place in a barrier/strandplain system (the D and E sands), possibly in an interdeltic embayment.

The Western Subbasin

Intervals C and E are the most persistent in the downdip direction of the five sandstone depositional sequences in this subbasin (fig. 28). All of the sandstone sequences pinch out toward the east but are still thickening at the western limit of well control (figs. 30 and 31).

Sandstone A.--This sandstone is developed at the base of the Olmos in the western subbasin (figs. 28, 30 and 31), and probably predates the sands of the eastern subbasin. The package is laterally extensive, having an areal distribution of more than 2,500 mi² in Texas (downdip extent of 50 mi). It has an average thickness of 30 ft in Texas and thickens into Mexico. The sandstone is 100 ft thick at the Rio Grande.

Log patterns are characteristically serrate and upward coarsening, with little variation in log character throughout the subbasin. The sands are inferred to have been deposited in a wave-dominated delta system. Wave-reworked deltas of this nature are characteristic of the underlying San Miguel Formation (Weise, 1980).

North
a

ZAVALA CO

DIMITT CO

TIE WELL |A-A'

TIE WELL |B-B'

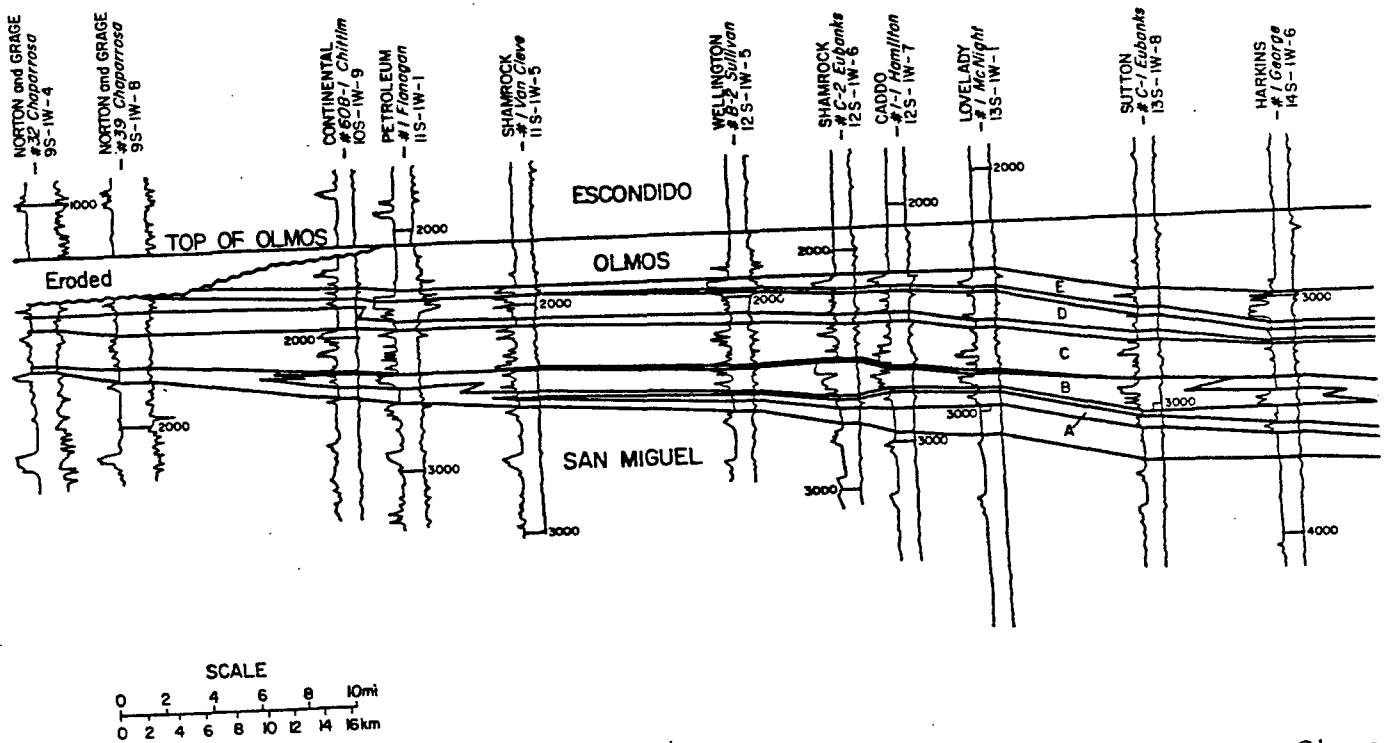


Figure 28. Stratigraphic dip cross section a-a' through the western subbasin of the Olmos Formation. All electric logs on this and succeeding cross sections dealing with the Olmos Formation are SP (left trace) and resistivity (right trace).

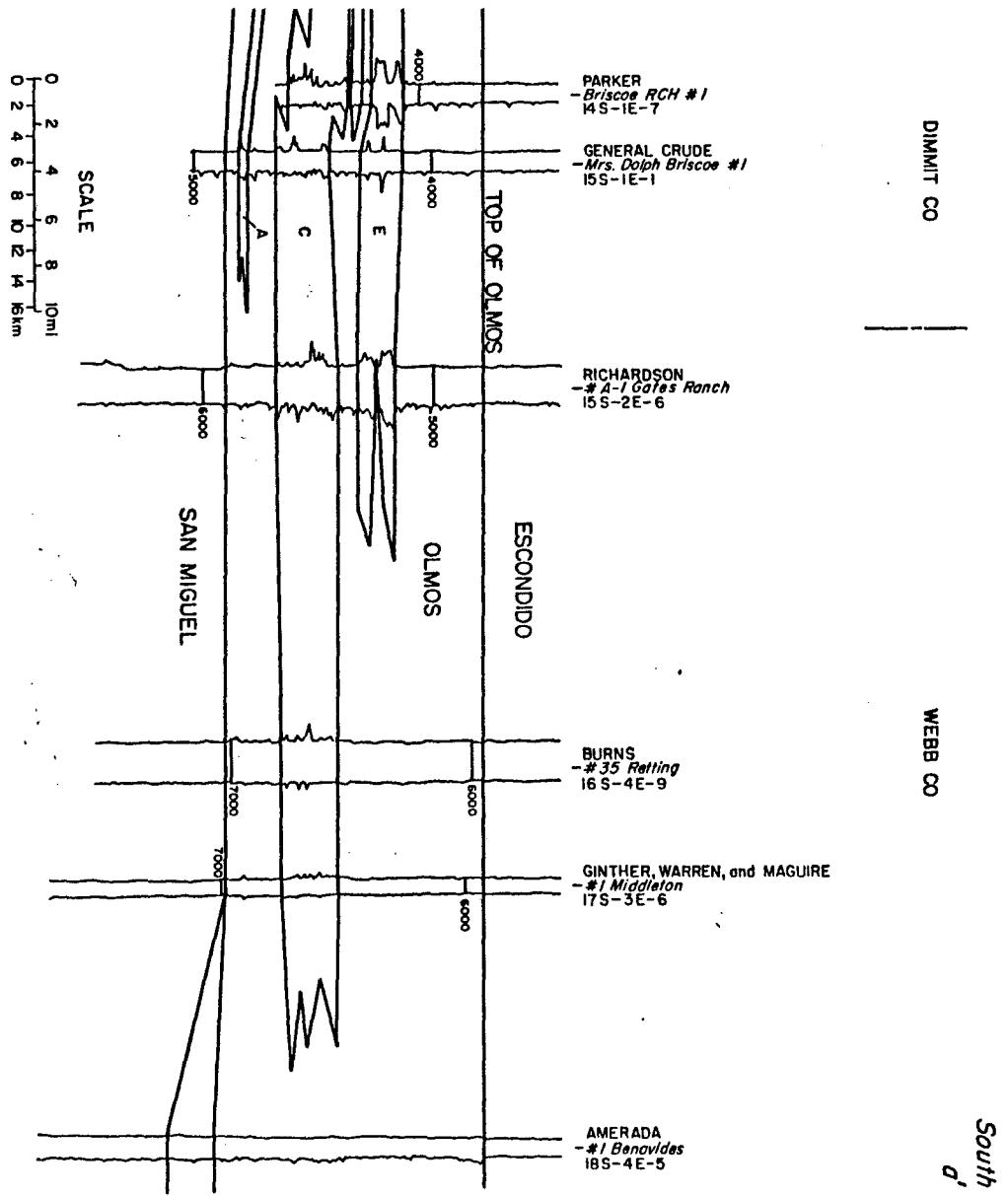


Figure 28 (cont.)

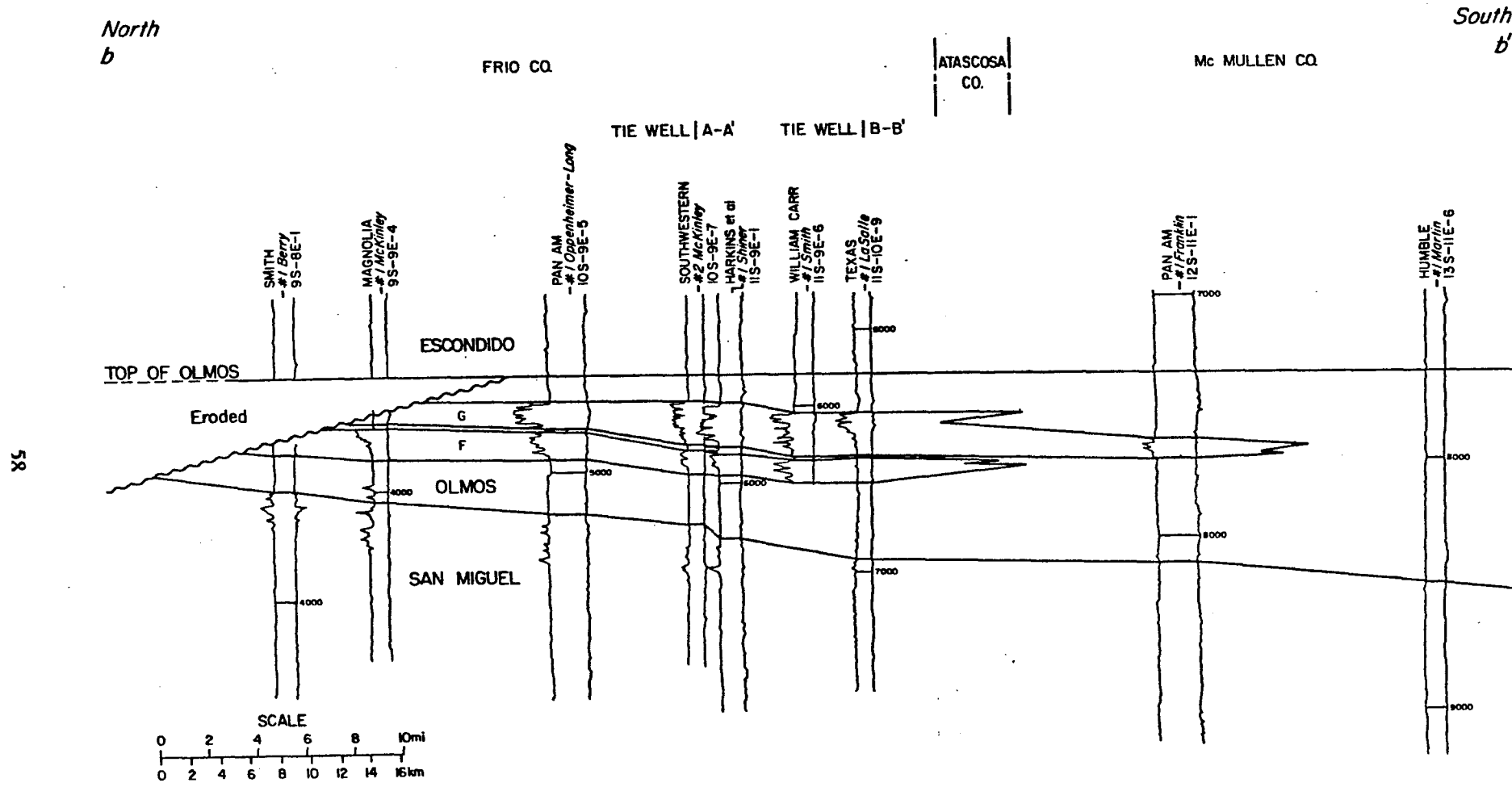


Figure 29. Stratigraphic dip cross section b-b' through the eastern subbasin of the Olmos Formation.

Sandstone B.--Sandstone B is characterized by diverse log patterns. In the central parts of the sand package a well-defined, upward-coarsening cycle is prevalent (see fig. 30, Tobin grid numbers 12S-1W and 11S-3E and 4E); however, this changes rapidly both in strike and dip directions to serrate but still coarsening upward, or to mixed (coarsening and/or fining upward) serrate log patterns. The B sand thins toward the Rio Grande, as well as toward the east. Average thicknesses are approximately 100 to 500 ft.

This sand probably was deposited by a high constructive delta. The variation in log character is a response to sedimentation under differing hydrologic conditions on the delta platform. On the central delta platform where the river entered the receiving basin, progradation was at a maximum, resulting in thick, upward-coarsening, delta-front sands. On the delta flanks, progradation alternated with aggradation; consequently SP patterns are serrate and varied.

Sandstone C.--Sandstone package C is composed of laterally impersistent sandstones of highly variable thickness and electric log character. In the updip part of the sequence, upward-fining aggradational cycles are the most common electric log pattern, although upward-coarsening cycles are present (figs. 30 and 31). This sand package overlaps the underlying deltaic B sand both along strike and, more importantly, downdip (fig. 28). The C sand interval thickens as it transgresses the B sand and log character changes to upward-coarsening units overlain by a serrate, upward-fining sequence. This sand is the most extensive of all of the sands in the western subbasin extending more than 100 mi into the basin.

The C sand is interpreted as a composite fluvial-deltaic progradational sequence. The lenticular, highly variable, updip sands represent fluvial and delta-plain facies that grade downdip into more persistent delta front (distributary-mouth bar and frontal splay) facies.

Sandstones D and E.--The D and E sandstones have similar electric log characters. They have serrate SP patterns and are variable in number and thickness. The SP response of the D sands is generally more subdued than that of the E sands, which are commonly thicker and show some evidence of downdip continuity (fig. 28). A laterally-continuous mudstone separates the

West
A

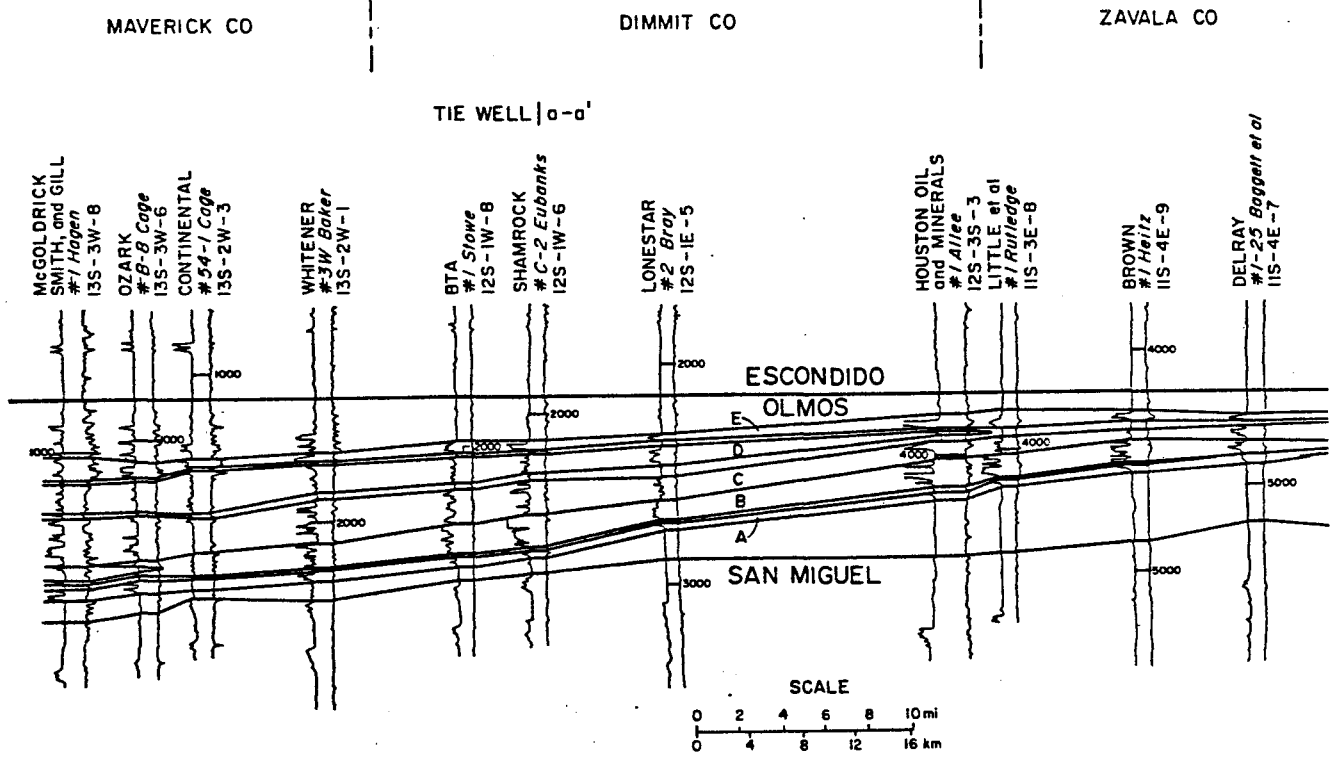
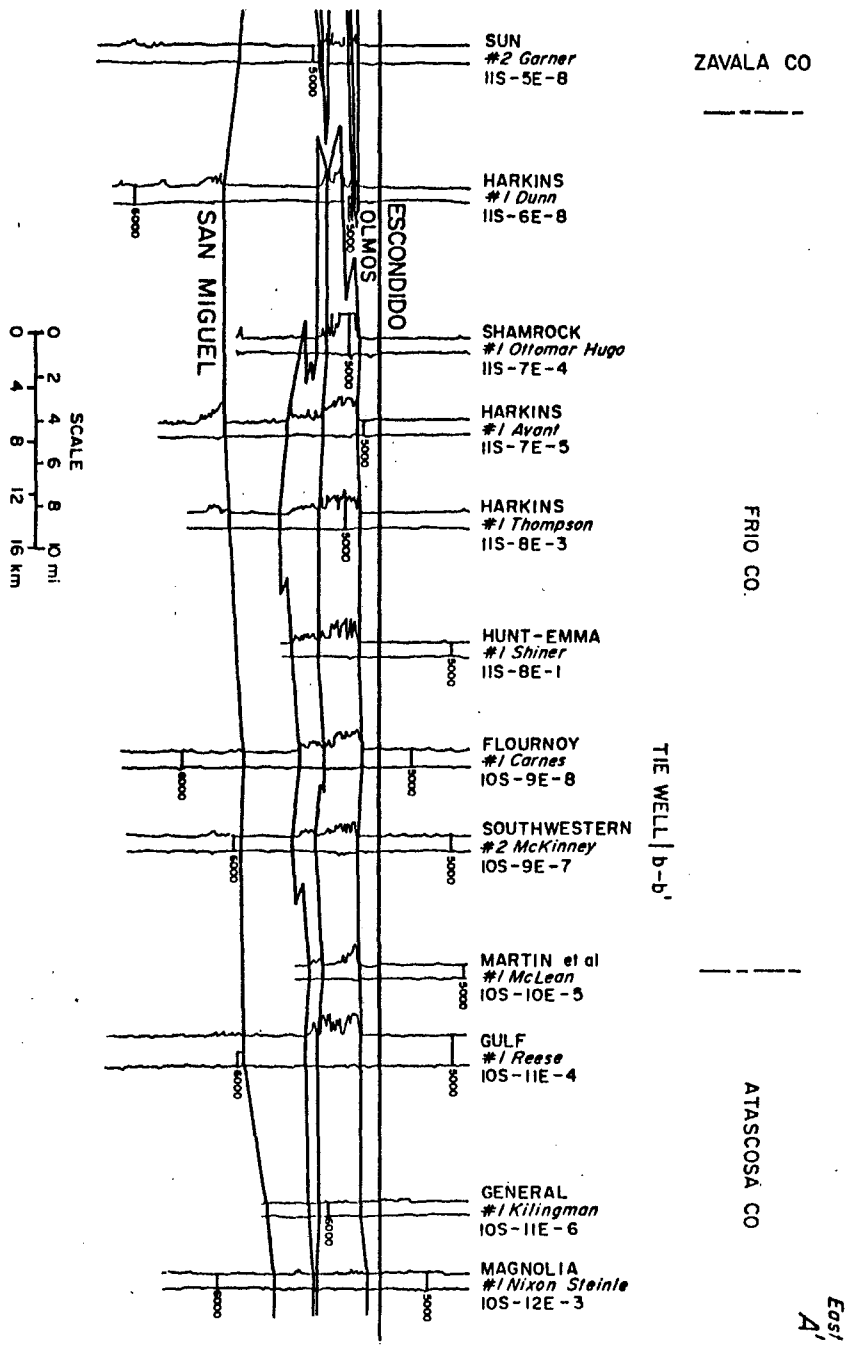


Figure 30. Stratigraphic strike cross section A-A' through the updip part of the Olmos Formation.

Figure 30 (cont.)



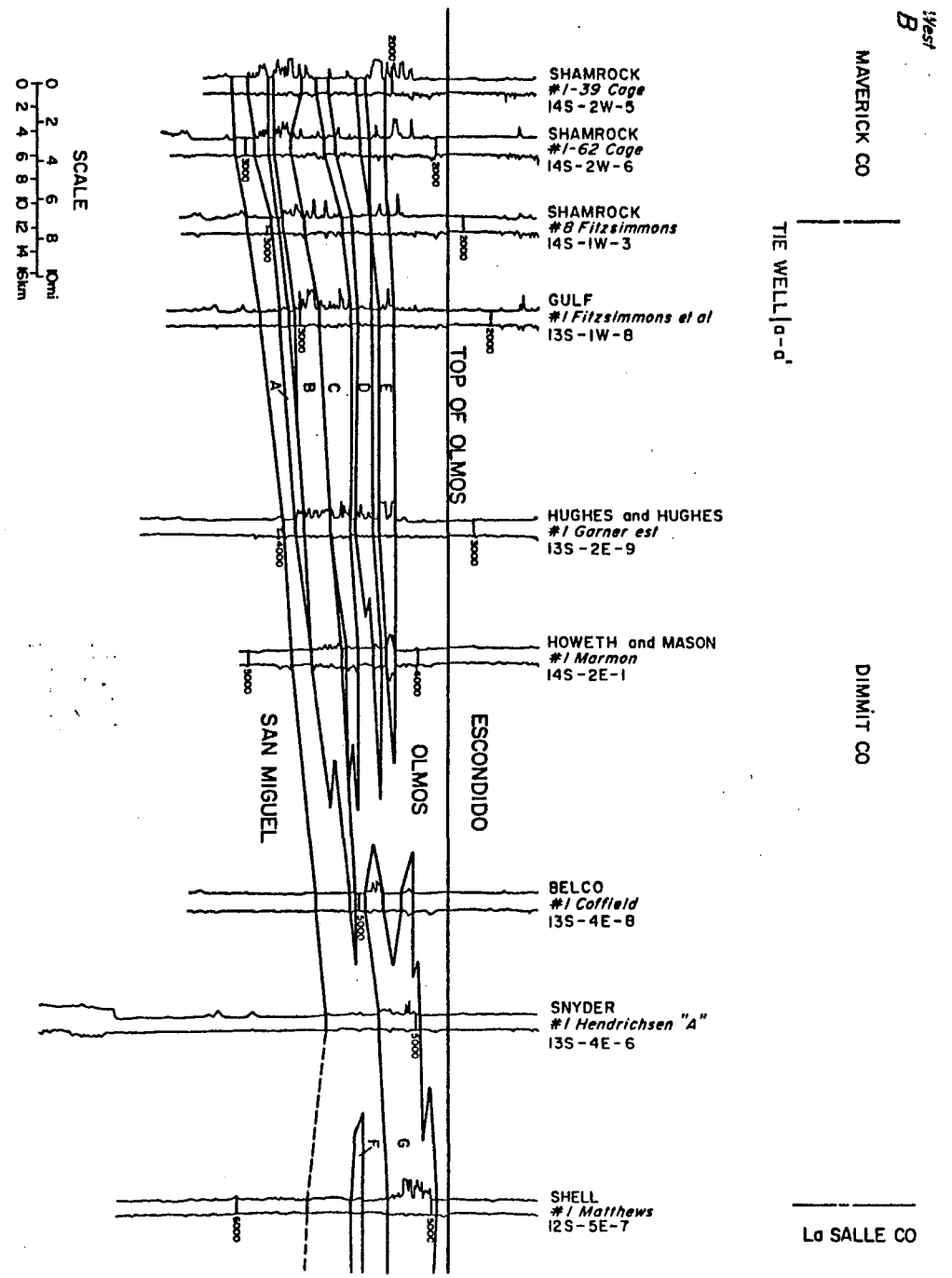


Figure 31. Strike cross section B-B', Olmos Formation.

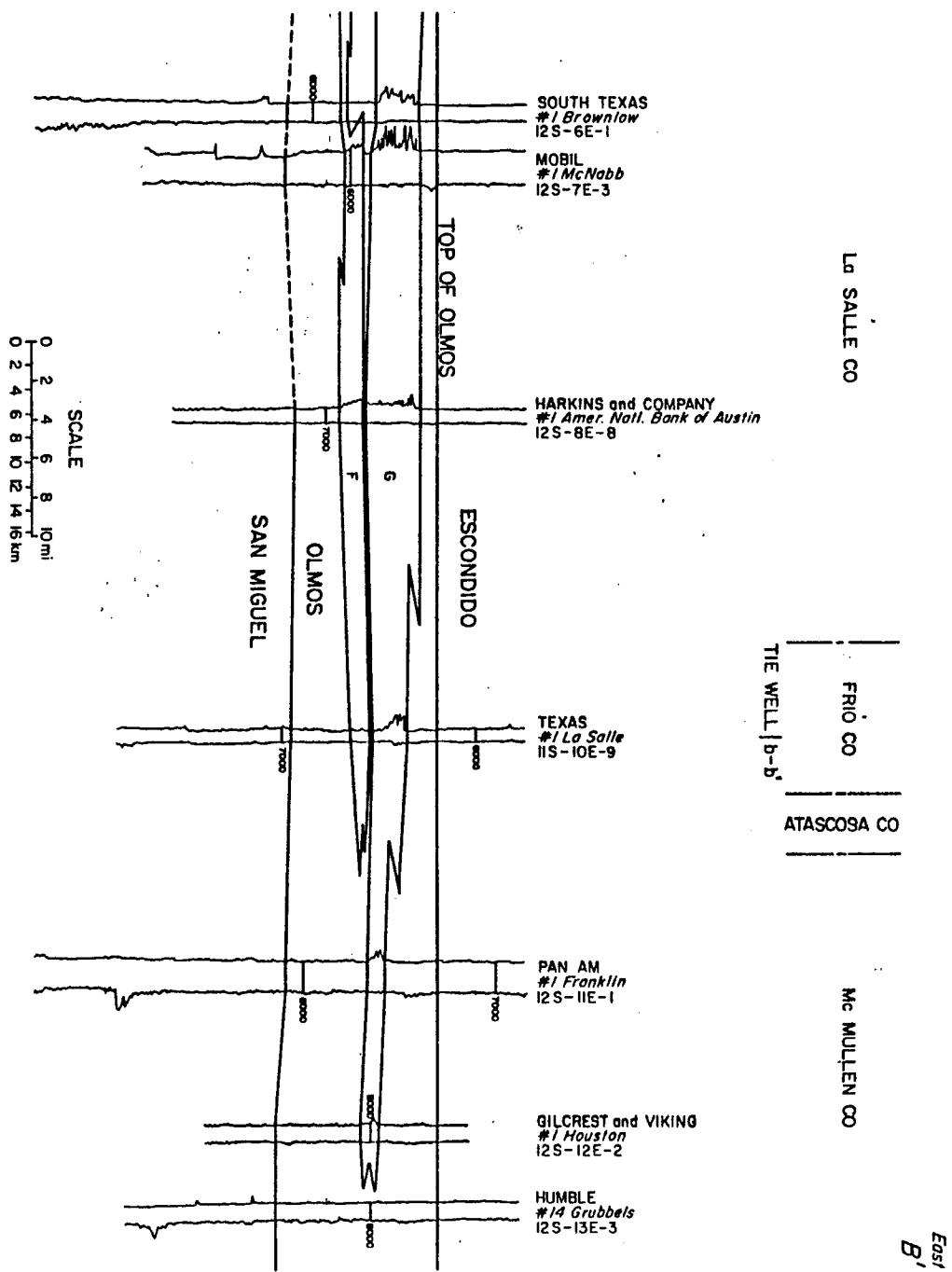


Figure 31 (cont.)

Southwest
D
TIE WELL |a-a'

DIMITT CO
Catarina Southwest field

Northeast
D'

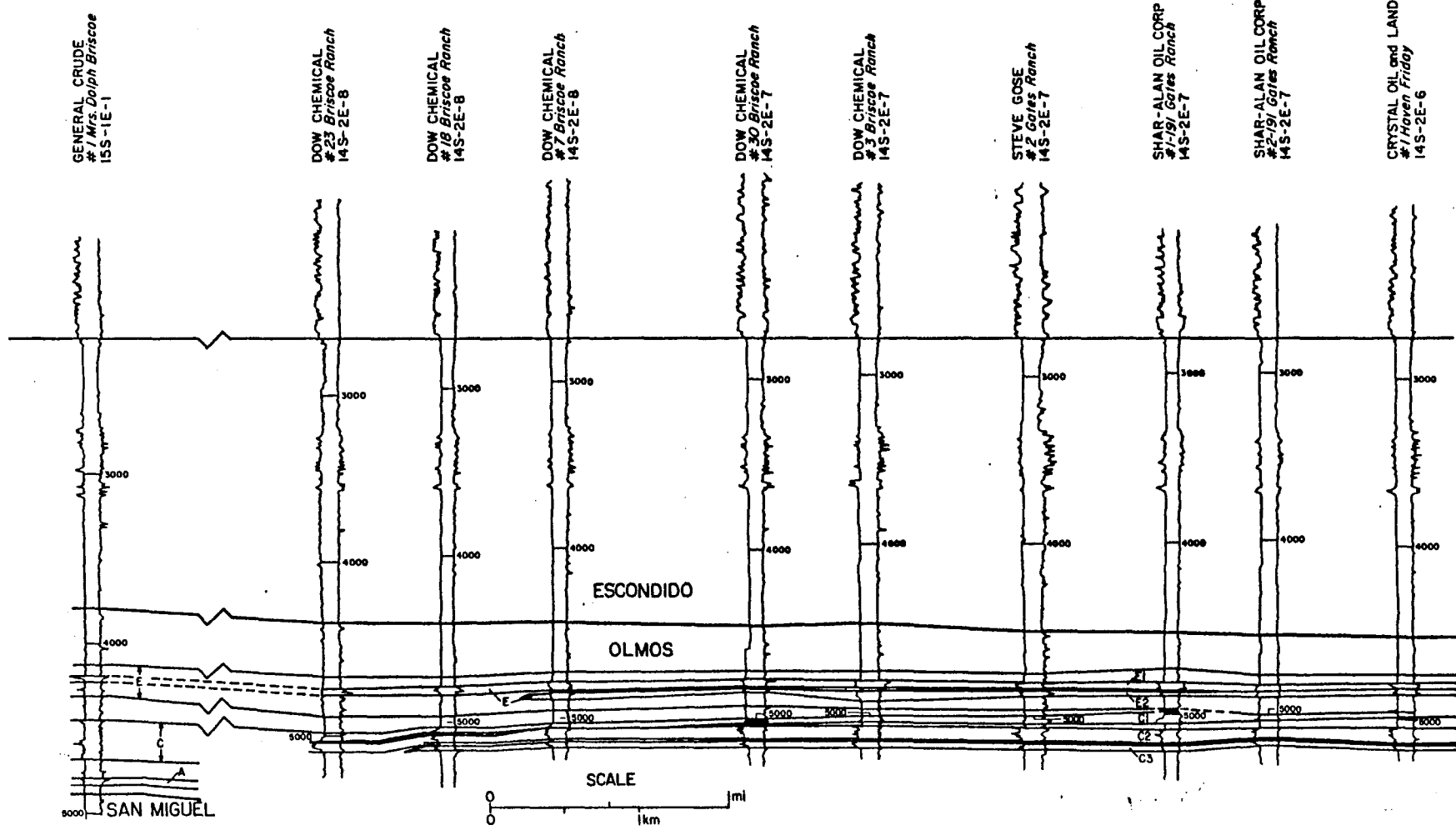


Figure 32. Detailed section D-D' oriented obliquely to strike in the Catarina Southwest Field. Sheet sandstones E-1 and C-2 are sandwiched between more lenticular sandstones.

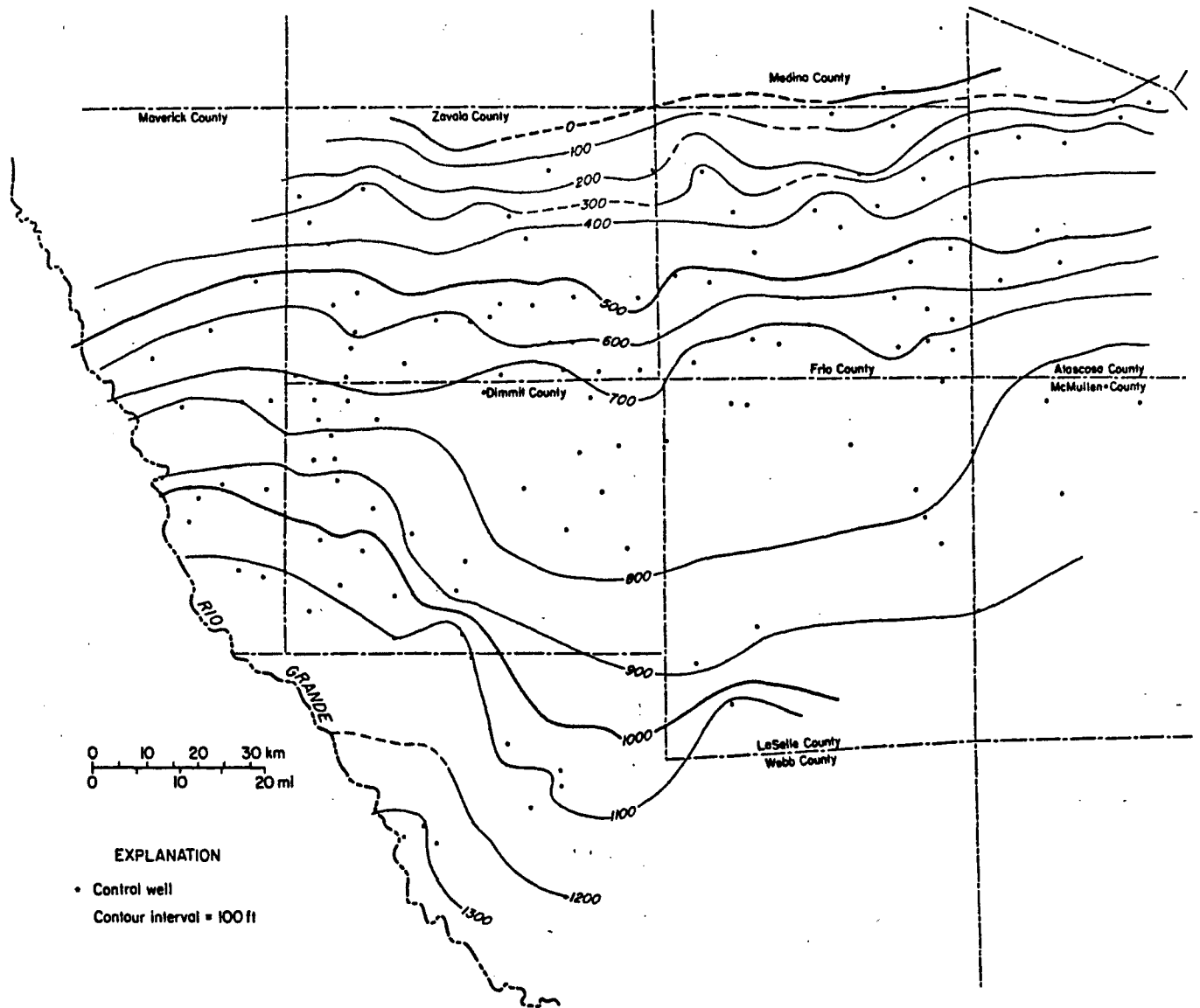


Figure 33. Isopach map of the Olmos Formation. A central thinned area separates the eastern subbasin from the western subbasin which thickens rapidly towards the west.

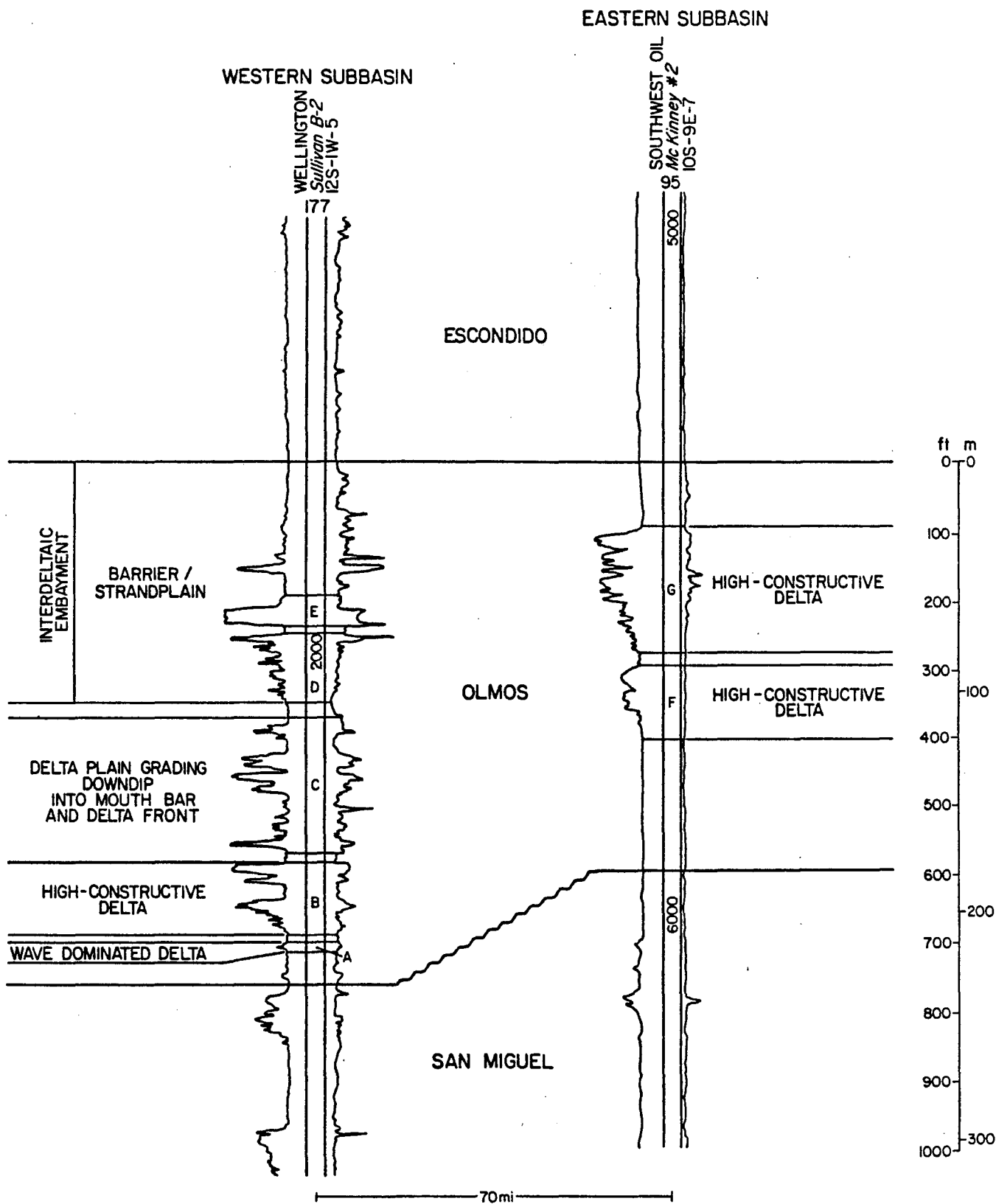


Figure 34. Typical logs of the Olmos Formation. Sandstone sequences in the western subbasin are highly variable and characteristically exhibit serrate SP patterns. Because of their variable nature the sands are difficult to correlate even on a local scale. The F and G sandstone packages of the eastern subbasin generally coarsen upward and exhibit serrate, funnel-shaped SP patterns. Locations illustrated on figure 27.

D interval from the E interval, the D being less extensive. Both thicken toward Mexico and pinch out toward the east (figs. 30 and 31). Common SP patterns of the E sands are upward-coarsening to blocky; the D sands also coarsen upward but SP patterns are serrate.

Preliminary interpretation of the depositional environments of these sands is that they are barrier island or strandplain. The serrate and thinner D sands represent barrier-front facies whereas the blocky nature of the E sands indicate that these are barrier-core deposits. Net-sand maps of the intervals will further assist in interpreting the sands.

The Eastern Subbasin

The character of the sands in the eastern subbasin differs remarkably from those sands of the western subbasin. The F and G sands coarsen upward and are thicker than the western sands (figs. 29, 30, and 31). The G sand is the thicker and more extensive of the two sand bodies. It overlaps the underlying F sand both along strike and downdip. Both sands feather-edge out toward the east and west but remain upward-coarsening. The F sand has an average thickness of 110 ft; the G depositional unit has a maximum thickness of 300 ft (fig. 31) and an average thickness of 200 ft. Both sand intervals are interpreted to have been deposited by high constructive deltas.

Summary of Selected Parameters and Conventional Hydrocarbon and Tight Gas Production

Tables summarizing the general attributes, geology, engineering characteristics, and extrapolation potential of the Olmos Formation are included in Finley (1982). There are 102 conventional gas fields producing from the Olmos, the majority of which are located in Dimmit (53 fields), Zavala (18 fields), and Webb (17 fields) Counties (fig. 35). Of these gas fields only one has produced more than 100 Bcf of gas (Big Foot, West; Table 3), four have produced more than 10 Bcf, and 15 more than 1 Bcf up to 1980 (Table 3). A histogram of cumulative production per reservoir for 79 Olmos oil fields illustrates that most of the fields are small; 49

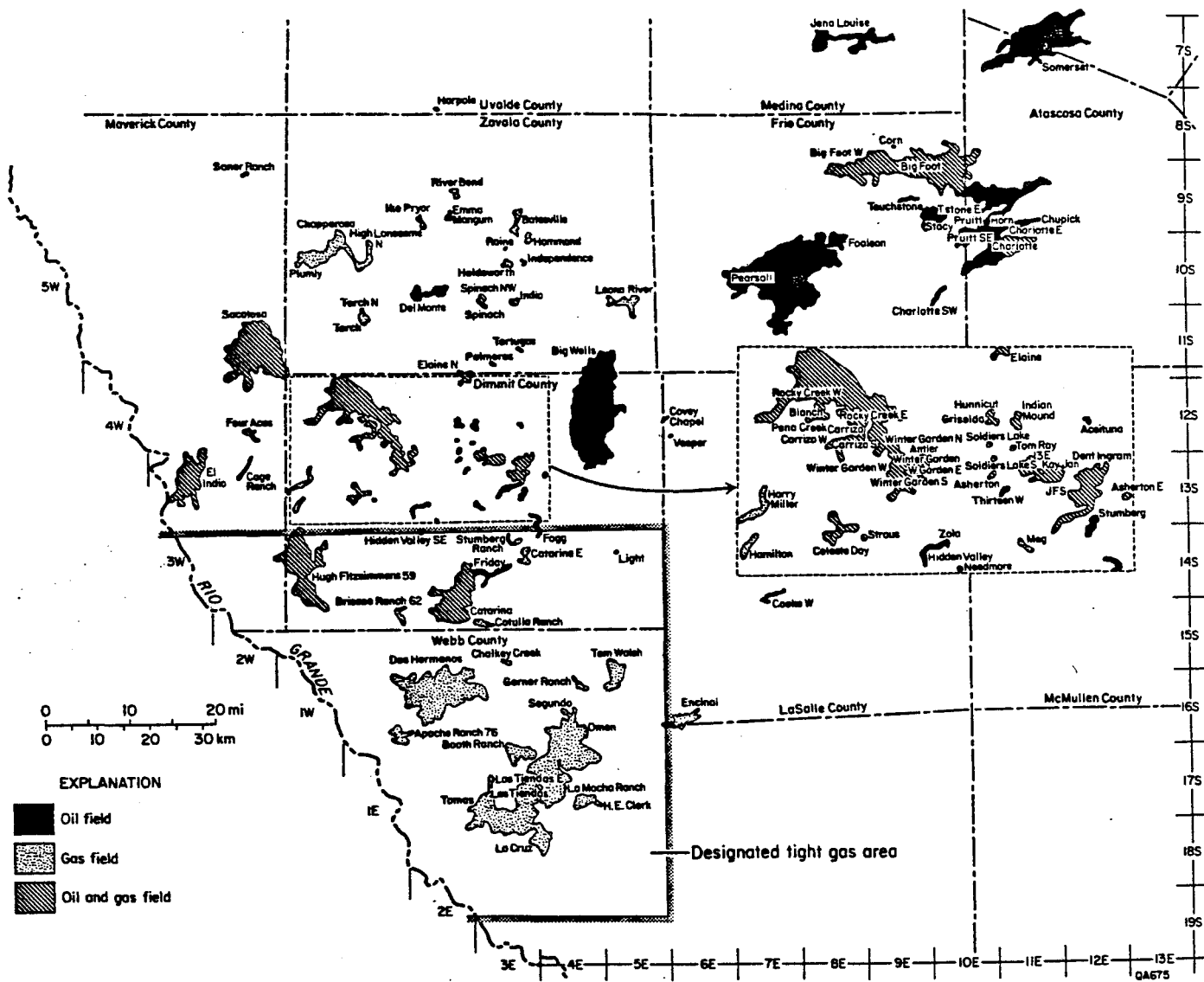


Figure 35. Oil and gas fields in South Texas that produce from the Olmos Formation. Parts of northwestern Webb and southern Dimmit Counties have been designated as tight gas productive by the RRC.

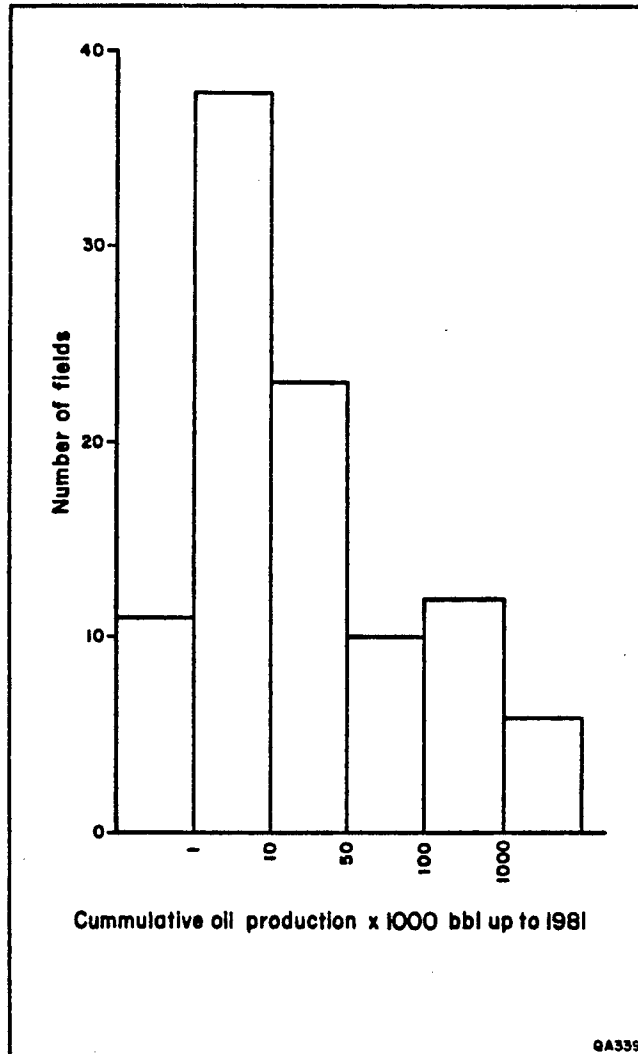


Figure 36. Histogram of oil production from the Olmos Formation. More than half of the fields have cumulative productions of less than 10,000 barrels of oil. Information was obtained from RRC Annual Report for 1981.

Table 3. Cumulative gas production up to 1980 from Olmos gas fields, Maverick Basin.

<u>Field Name</u>	<u>Avg. Net Pay (ft.)</u>	<u>Cumulative Condensate, 1980 (bbls)</u>	<u>Associated Cumulative Gas, 1980 (Mcf) x 1000</u>	<u>Non-Associated Cumulative Gas, 1980 (Mcf) x 1000</u>
Apache Ranch				92
Asherton	5	943		242
Asherton, East	17	767		76
Batesville	6			1,633
Big Foot, West	20			103,304
Blanch	10		74	
Booth Ranch		6,076		5,972
Carrizo				3
Carrizo, South	10			625
Carrizo, West				326
Catarina, East	15	24,398		1,797
Catarina, East	6	1,816		144
Catarina, Southwest	32	192,179		20,636
Celeste-Fay				16
Celeste-Fay	12			64
Chapparosa	14			233
Dent Ingram	9	15,548		2,015
Dos Hermanos		340,430		50,335
Dos Hermanos, East		23,316		5,275
Dos Hermanos, West		35,471		4,820
El Indio				1
El Indio				326
El Indio				1
Emma Mangum	22			5,848
Encinal	15	3,916		361
Garner Ranch		2,248		351
H. E. Clark		1,068		330
Hamilton Ranch	10			262
Hammond	4	491	2,636	

Table 3. (continued)

<u>Field Name</u>	<u>Avg. Net Pay (ft.)</u>	<u>Cumulative Condensate, 1980 (bbls)</u>	<u>Associated Cumulative Gas, 1980 (Mcf) x 1000</u>	<u>Non-Associated Cumulative Gas, 1980 (Mcf) x 1000</u>
Harry Miller	7			18
High Lonesome	4			325
Holdsworth	6			237
Horn	10		57	
Hugh Fitzsimons	9		1,023	823
Hunnicut	22	444		522
Hunnicut	4	182		103
Ike Pryor	10			6,330
Indian Mound	5	195		142
Indio				596
John High	6	1,725		543
Kay-Jan	10	6,031		600
La Cruz				1,633
La Moca Ranch		9,031		1,757
Las Tiendas		6,202		5,172
Las Tiendas, East		3,335		5,310
Owen		138,348		22,852
Pena Creek	7			137
Pena Creek	10			48
Pena Creek	15			
Pena Creek				6
Pendencia	5			972
Plumly	10			3,817
Raine	4			92
River Bend	5			468
Rocky Creek, East	3			3
Rocky Creek, East	17			327
Rocky Creek, East	10		13	
Sacatosa	12			1

Table 3. (continued)

<u>Field Name</u>	<u>Avg. Net Pay (ft.)</u>	<u>Cumulative Condensate, 1980 (bbls)</u>	<u>Associated Cumulative Gas, 1980 (Mcf) x 1000</u>	<u>Non-Associated Cumulative Gas, 1980 (Mcf) x 1000</u>
Segundo		61,120		11,489
Soldiers Lake				37
Soldiers Lake, South	6	290		257
Spinach, Northwest				37
St. Anthony	7	46		74
Straus	5	270		382
Stumberg Ranch	12	7,873		941
Tom Walsh		70,393		7,318
Tom-Ray		1,343		370
Tomas				238
Torch	5			307
Winter Garden, East	6		76	
Winter Garden, East		1,936		452
Winter Garden, South				410
Winter Garden, South	10	8,537		2,560
Winter Garden, South	6			201
Winter Garden, South	12			68
Winter Garden, West		<u>2,386</u>		<u>345</u>
Total		<u>968,354</u>	<u>3,879</u>	<u>283,406</u>

have cumulative production of less than 10,000 barrels of oil (fig. 36) (Railroad Commission of Texas, 1981a).

Oil and gas accumulation in the Olmos results primarily from entrapment by strike faults, permeability barriers, and truncation of the sandstones at the pre-Escondido unconformity (fig. 26) (Glover, 1956). Smaller hydrocarbon accumulations occur around and over volcanic centers. Snedden and Kersey (1982) differentiated between "updip" and "downdip" fields in Webb County on the basis of reservoir genesis and gas production trends. The updip fields (Dos Hermanos and adjacent fields, fig. 35) produce from deltaic distributary channel sandstones (Sandstone C of this report), whereas the downdip reservoirs (Las Tiendas and others nearby) produce from shelfal sands, probably delta-front splays. Updip fields are roughly twice as productive, averaging 51.7 MMcfg/well in 1980, compared with average production of 32.5 MMcfg/well in the downdip fields (Snedden and Kersey, 1982).

In addition to the shelfal sheet sandstones in Webb County described by Snedden and Kersey, other sheet sandstones that may be potential tight gas producers are considered to be present in the barrier-strandplain sequences of sandstones D and E, delta-front sandstones of delta sequences B, C, F, and G, and strandplain sandstones of the wave-dominated delta sequence A. The continuity of sandstones in the downdip parts of intervals C and E is illustrated in figure 32. Prospective sheet sandstones E-1 and C-2 are interbedded with more lenticular sandstone facies.

COZZETTE AND CORCORAN SANDSTONES, PICEANCE CREEK BASIN

Introduction

The Cozzette and Corcoran Sandstones are part of the Upper Cretaceous Mesaverde Group (fig. 37) and occur in the subsurface of the southern Piceance Creek Basin. These units and the Rollins Sandstone, which overlies the Cozzette and is separated from it by a tongue of the Mancos Shale, are Campanian in age. The Rollins, Cozzette, and Corcoran Sandstones are stratigraphically equivalent to lower parts of the Iles and Mount Garfield Formations as defined by Johnson and Keighin (1981). The Piceance Creek Basin is located in northwestern Colorado (fig. 38). The areas of interest for Rollins-Cozzette-Corcoran gas production are primarily in Mesa and Garfield Counties in the southern half of the basin.

Five operator applications for tight formation designations for the Cozzette and Corcoran have been approved by FERC (fig. 39) (Colorado Oil and Gas Conservation Commission, 1980c, Cause NG-7; 1980d, Cause NG-12; 1980g, Cause NG-17; 1981b, Cause NG-21, and 1981c, Cause NG-26). The Cozzette and Corcoran Sandstones may not be specifically mentioned in all these applications, but are included where applications refer to the "Mesaverde" (Formation or Group) and to the "Upper Mancos" (Shale). The Cozzette and Corcoran Sandstones have been designated tight formations in virtually all of the southern Piceance Creek Basin where they exist as stratigraphically definable units. An exception to this generalization may exist in Garfield County immediately east and southeast of the southern end of the Douglas Creek Arch. However, in this area a transition is evident from the marginal marine facies of the Cozzette and Corcoran to continental and fluvial facies of the Mesaverde Group, and the Cozzette and Corcoran cannot be consistently identified.

Since mid-1982, there have been few operator applications for tight formation designations in the Piceance Creek Basin. An application for the non-marine Mesaverde Group in Rio Blanco County (Colorado Oil and Gas Conservation Commission, 1982b, Cause NG-35) was

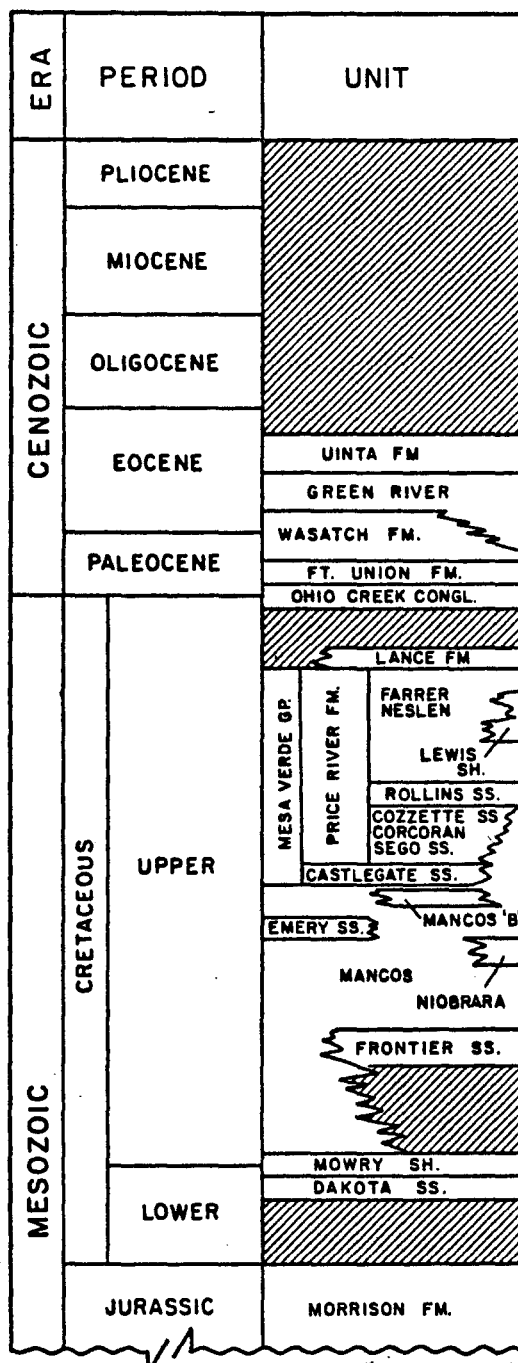
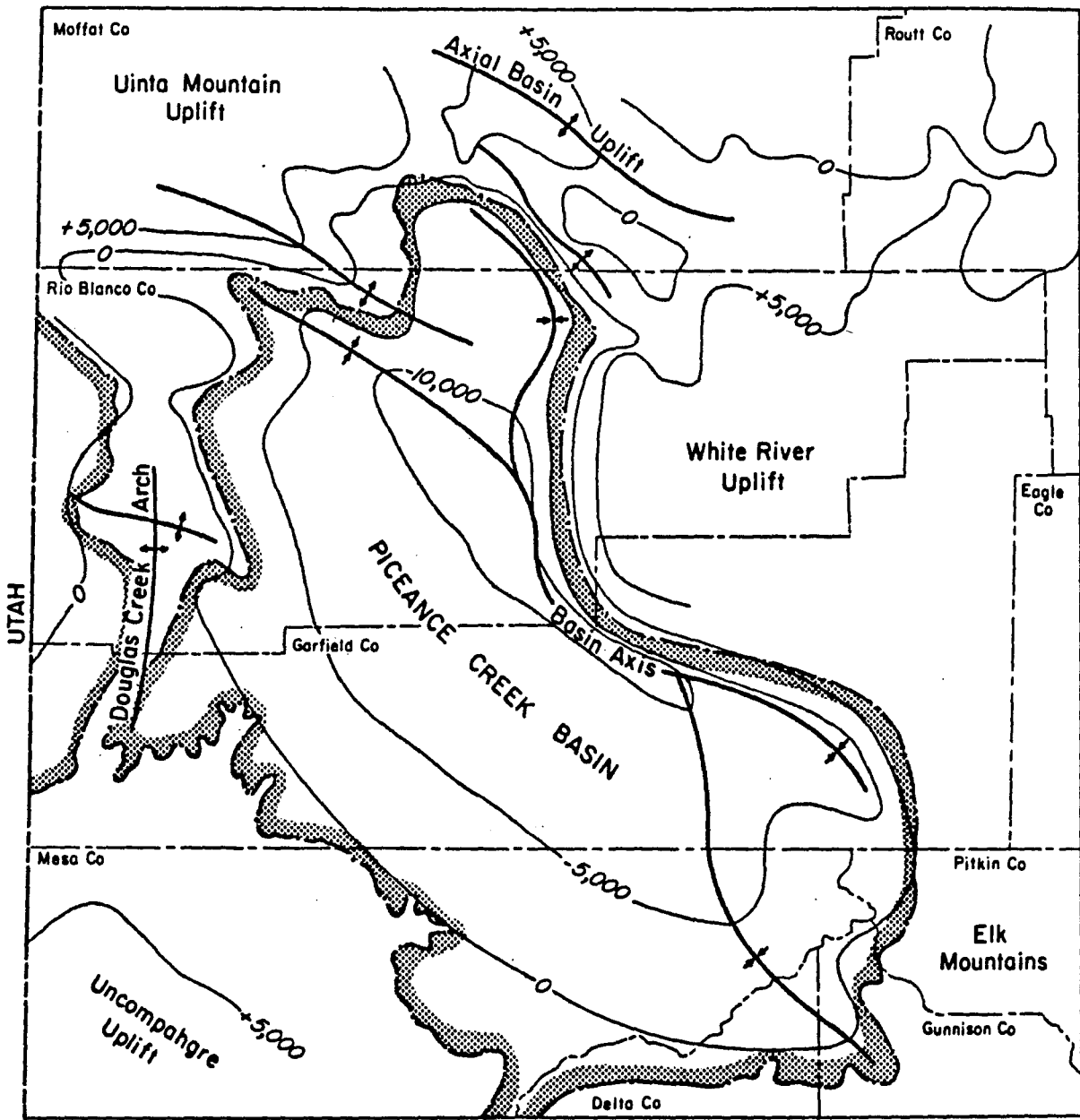


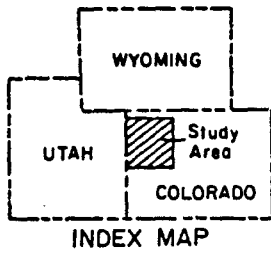
Figure 37. Stratigraphic column from the Jurassic Morrison Formation through the Pliocene Series, Piceance Creek Basin (after Rocky Mountain Association of Geologists, 1977).



EXPLANATION

—○— Structure contour on top of the Dakota Fm.

▨ Tertiary outcrop



INDEX MAP

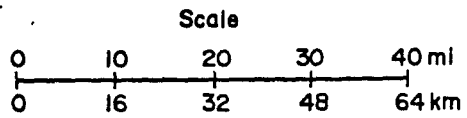
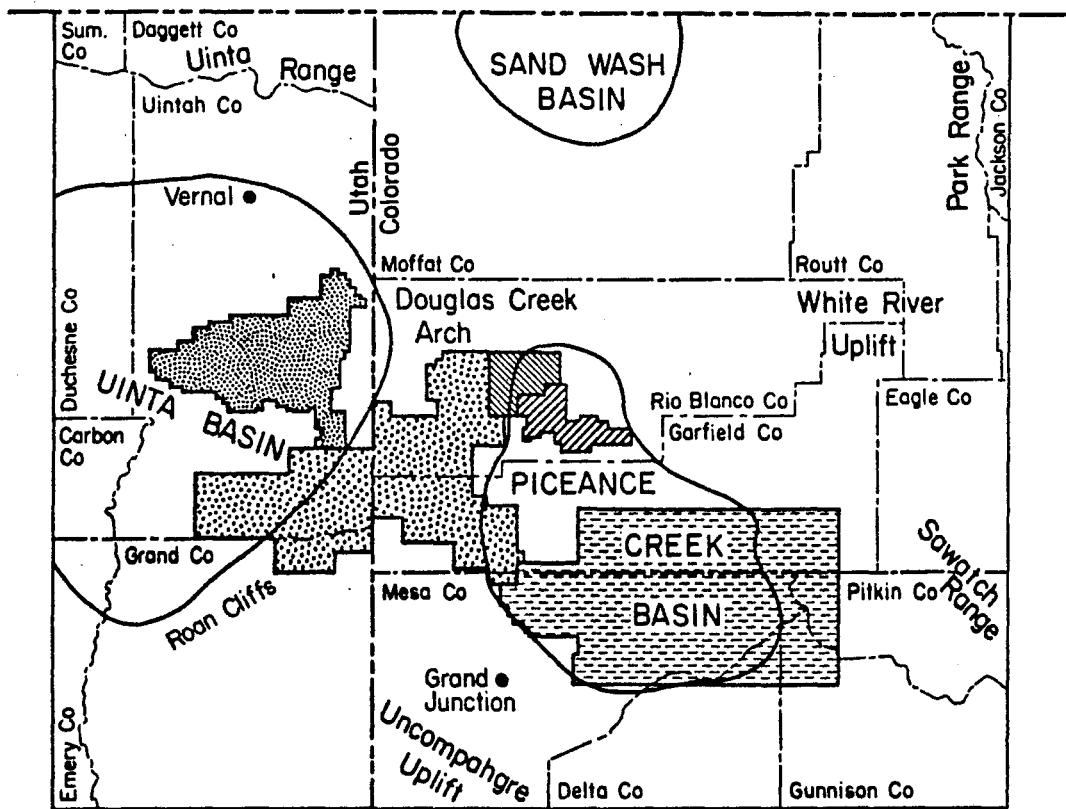


Figure 38. Location and generalized structure map of the Piceance Creek Basin (after Dunn, 1974).



EXPLANATION

-  Wasatch Formation and Mesaverde Group (undifferentiated) tight gas sand area (Utah Cause No. TGF-100)
-  Mancos "B" tight gas sand areas (in Utah, Cause TGF-100; in Colorado Cause Nos. NG-5, NG-6, NG-15)
-  Mancos "B" and Mesaverde Group (undifferentiated) (Colorado Cause No. NG-27)
-  Corcoran and Cozzette Sandstones (in part includes Rollins) tight gas sand area (Colorado Cause Nos. NG-7, NG-17, NG-21, NG-26, NG-12)
-  Mancos "B" to base Douglas Creek Sand (includes Mesaverde Group) (Colorado Cause No. NG-9)

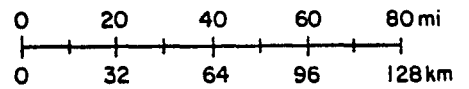
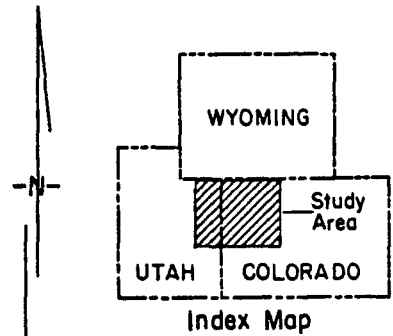


Figure 39. Areas of tight gas sand applications, Piceance Creek and Uinta Basins, through March 1982. Through February 1983, no additional applications were filed for any remaining parts of the southern Piceance Creek Basin where the Corcoran, Cozzette, and Rollins Sandstones are developed.

approved by the State of Colorado after a hearing on June 21, 1982, but has not been approved by FERC as of February 1, 1983. The only recent application activity in the southern Piceance Creek Basin concerns the Dakota Sandstone and the Morrison Formation (F. Piro, personal communication, 1983) (fig. 37).

Data from approximately 100 wells were used in this study of the Cozzette and Corcoran Sandstones; a few additional wells penetrated the Rollins or the Rollins and Cozzette only. Some wells did not penetrate all of the Corcoran Sandstone; therefore there were fewer data available for the Corcoran isopach map than for the Cozzette map. Completion and production information were purchased from Petroleum Information, Inc., and an analysis of engineering and production characteristics of the Cozzette and Corcoran was performed by CBW Services, Inc. (1983).

Structure

The Piceance Creek Basin is a Late Cretaceous to early Tertiary sedimentary basin defined by a series of Laramide uplifts. The basin is bounded on the southeast by the Sawatch Uplift, on the east by the White River Uplift, on the southwest by the Uncompahgre Uplift, and on the west by the Douglas Creek Arch. The Douglas Creek Arch is a mildly positive feature that separates the Piceance Creek Basin from the Uinta Basin in Utah (fig. 38). There is little evidence of uplift on the Douglas Creek Arch and the Uncompahgre Uplift at the time of Mesaverde Group deposition, and Laramide structural elements in general had little influence on Cretaceous depositional patterns (Johnson and Keighin, 1981; Murray and Haun, 1974). Part of the Douglas Creek Arch may, however, have been slightly positive during Mancos time and influenced deposition of the Mancos "B."

The asymmetrical Piceance Creek Basin has a gentle western flank and a steeply dipping eastern flank; the deep axis of the basin lies along its eastern margin (fig. 38). Nearly vertical beds cropping out along the Grand Hogback north of Rifle, Colorado, when compared to the gentle basinward dips of strata in the Book Cliffs northeast of Grand Junction, Colorado, are

indicative of the contrasting structural configurations of the opposite basin flanks. Structure contours on top of the Cozzette Sandstone show relatively uniform northeast to north dip from central Garfield County to northeast Delta County over most of the southern Piceance Creek Basin (fig. 40). The area east of R93W and north of T10S is structurally complex and likely contains faulting in addition to the single major fault shown. The structural boundary of the basin is well marked by the Mancos Shale-Mesaverde Group outcrop contact (fig. 40, as modified from Tweto, 1979).

Stratigraphy

In eastern Garfield County, the sedimentary sequence between the top of the Dakota Sandstone and the Precambrian surface is approximately 8,000 ft thick. The Dakota and younger Cretaceous sediments (fig. 37) constitute the thickest sequence in northwestern Colorado, including thick marine shales and dominantly regressive sequences (Murray and Haun, 1974). The Mesaverde Group is such a regressive sequence, having a source area west of the present basin. The thickness of the Mesaverde Group from the top of the Rollins Sandstone (or equivalent) to the Cretaceous-Tertiary unconformity varies from less than 2,500 ft to more than 4,000 ft from west to east and east-northeast across the Piceance Creek Basin (Johnson and Keighin, 1981). A series of Late Cretaceous transgressions and regressions affected overall Mesaverde deposition. The overall Mancos-Corcoran-Cozzette-Rollins-Mesaverde sequence represents a major regressive episode across the southern Piceance Creek Basin. Most of the Mesaverde Group is non-marine.

Depositional Systems

Overview

The Rollins, Cozzette, and Corcoran Sandstones in the lower part of the Mesaverde Group are generally considered marginal marine and of "beach and bar origin" (Dunn, 1974). Lorenz (1982), who studied outcrops at Rifle Gap, Colorado, described these sandstones as blanket,

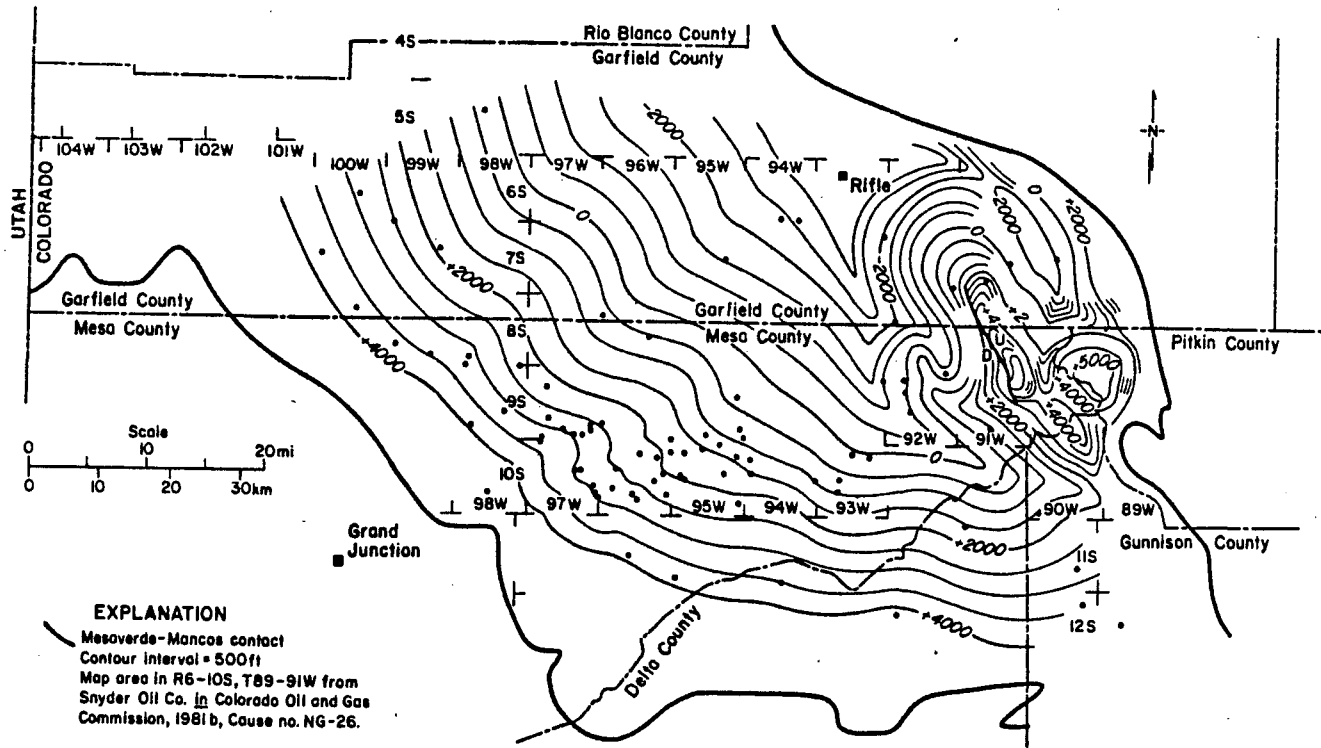


Figure 40. Structure contour map on the Cozzette Sandstone in the southern Piceance Creek Basin. Mesaverde-Mancos contact from Tweto (1979).

wave-dominated, shoreline deposits. The presence of an oyster bed overlying the Cozzette Sandstone at Rifle Gap suggests that seaward of that location the Cozzette may have built upward to form a barrier island backed by a brackish lagoon (Lorenz, 1982). Hummocky cross stratification is developed in parts of the Cozzette and Corcoran Sandstones and is another indication of their marginal marine origin where parts of each unit were influenced by waves and wind-driven currents.

Warner (1964) also considered the Cozzette and Corcoran to be regressive marginal marine deposits and inferred general east-northeast to northeast shoreline trends in the southern Piceance Creek Basin. These trends were indirectly defined on the basis of downdip limits of "nonmarine deposits" (presumably coal) and updip limits of marine shales. Results reported in this study suggest that shoreline positions can be further defined on the basis of an aggradational log-facies pattern and isopach maps of the Cozzette and Corcoran Sandstones.

Regional Stratigraphic Relationships

Regional cross sections were prepared using shoreline orientations from Warner (1964) as an initial guide to depositional dip and strike directions (fig. 41). The Mancos Shale tongue between the Rollins and the Cozzette thickens toward the southeast and the sand content of the Cozzette and the Corcoran decreases in the same direction (fig. 42 and 43). Cross sections aligned approximately north-south are slightly oblique to depositional strike and show greater sand content updip and, contrary to Quigley (1965), do not show major north-eastward thickening of the Mancos Shale tongue (figs. 44 and 45).

Drilling depth to the top of the Rollins-Cozzette-Corcoran sequence is a function of both basin structure and surface topography. Well 11, cross section A-A' (fig. 42) and well 36, cross section F-F' (fig. 45) cut the top of the Rollins at 7,660 ft and 7,920 ft, respectively. Structural cross sections hung on a +4,000 msl datum (figs. 46 and 47) show that these wells either penetrate a structurally low part of the basin or are downthrown relative to a major fault. Surface topographic profiles along the cross section lines show that these wells are also

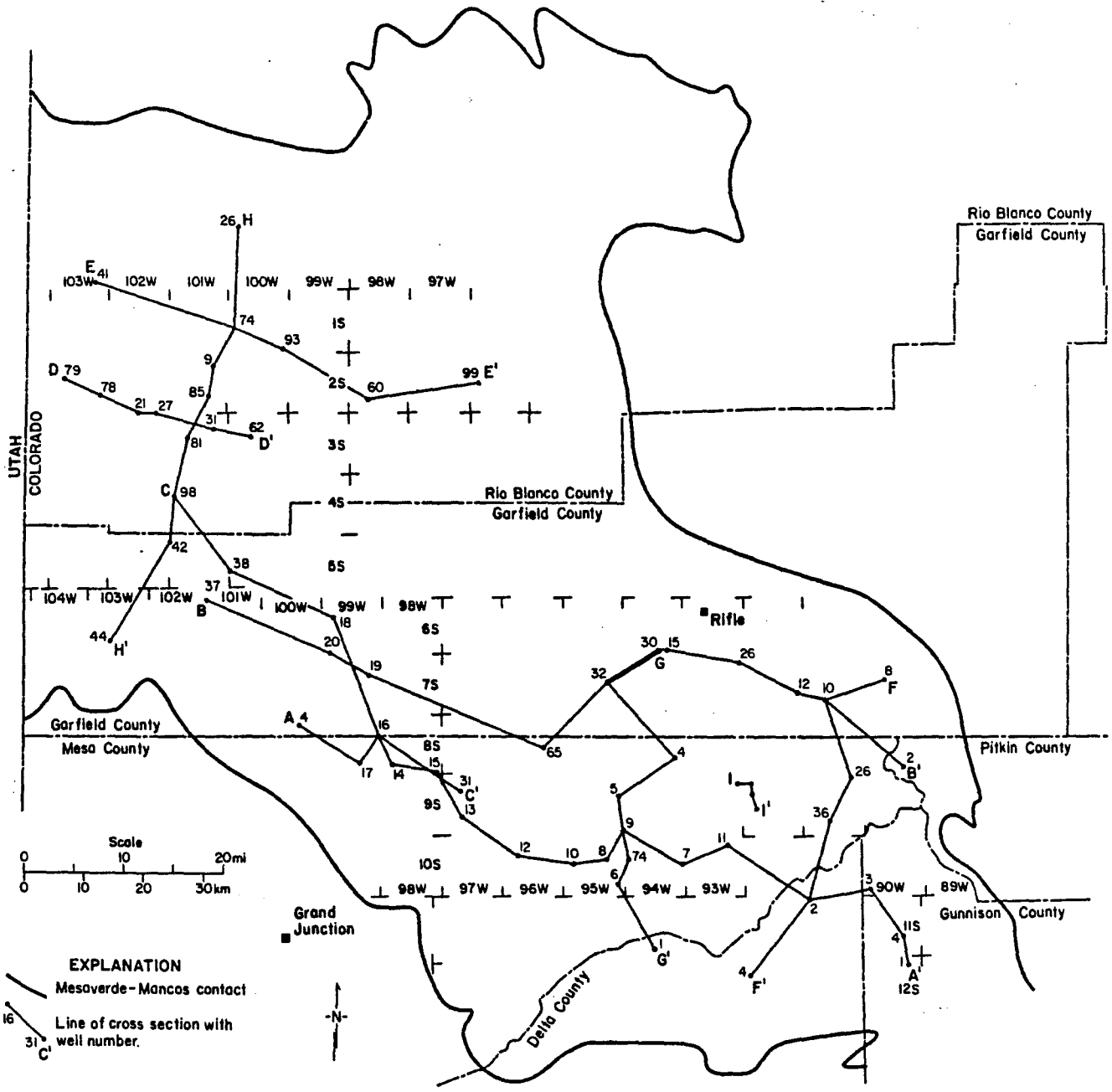


Figure 41. Index map for cross sections in the Piceance Creek Basin. Mesaverde-Mancos contact from Tweto (1979).

1,000 to 3,000 ft topographically higher than other wells along the cross sections. Thus, topography and structure can act in concert in certain areas to maximize drilling depths to the Rollins-Corcoran-Cozzette sequence. The topographic low between wells 12 and 8, cross section A-A', represents the valley of the Colorado River (fig. 46).

Genetic Depositional Units

Six depositional units can be identified within the Cozzette and Corcoran Sandstones using wells selected from cross section A-A' and incorporated into cross section A₁-A₁' (fig. 48). All well logs utilized incorporated gamma-ray (GR) traces on which the thickness and the contact relationships of the sandstones were distinctive. Many spontaneous potential (SP) logs in the Piceance Creek Basin, as elsewhere in the Rocky Mountain Province, have poor character because of the lack of resistivity contrast between borehole and formation fluids. Geologic interpretation of the resistivity curve on the GR trace is therefore preferred over use of the SP in many instances.

Unit A within the Corcoran Sandstone occurs only in updip wells; it has a blocky, aggradational log pattern in well 16 (fig. 48) that changes downdip into an upward-coarsening pattern (well 15) (fig. 48). Further downdip this unit grades into a pattern of individual sand spikes with loss of the unit's identity (wells 13 and 12). This unit forms the initial regressive sedimentary package of the Corcoran and probably represents a foreshore to lower shoreface sequence.

Units B and C form a pair of sandstone "benches" with blocky log character in the positionally updip Corcoran, changing downdip to upward-coarsening or highly serrate log character. The blocky sandstones are 25 to 50 ft thick and may represent part of a barrier core. The upward-coarsening sequence with slightly serrate log character (Unit B, well 12, fig. 48) is interpreted as a shoreface sequence. Southeast of well 12, Unit B breaks into multiple, poorly defined, upward-coarsening sequences (well 8) or into individual, thin sandstone beds, resulting in a highly serrate log character. Such sandstones may be storm-reworked shelf

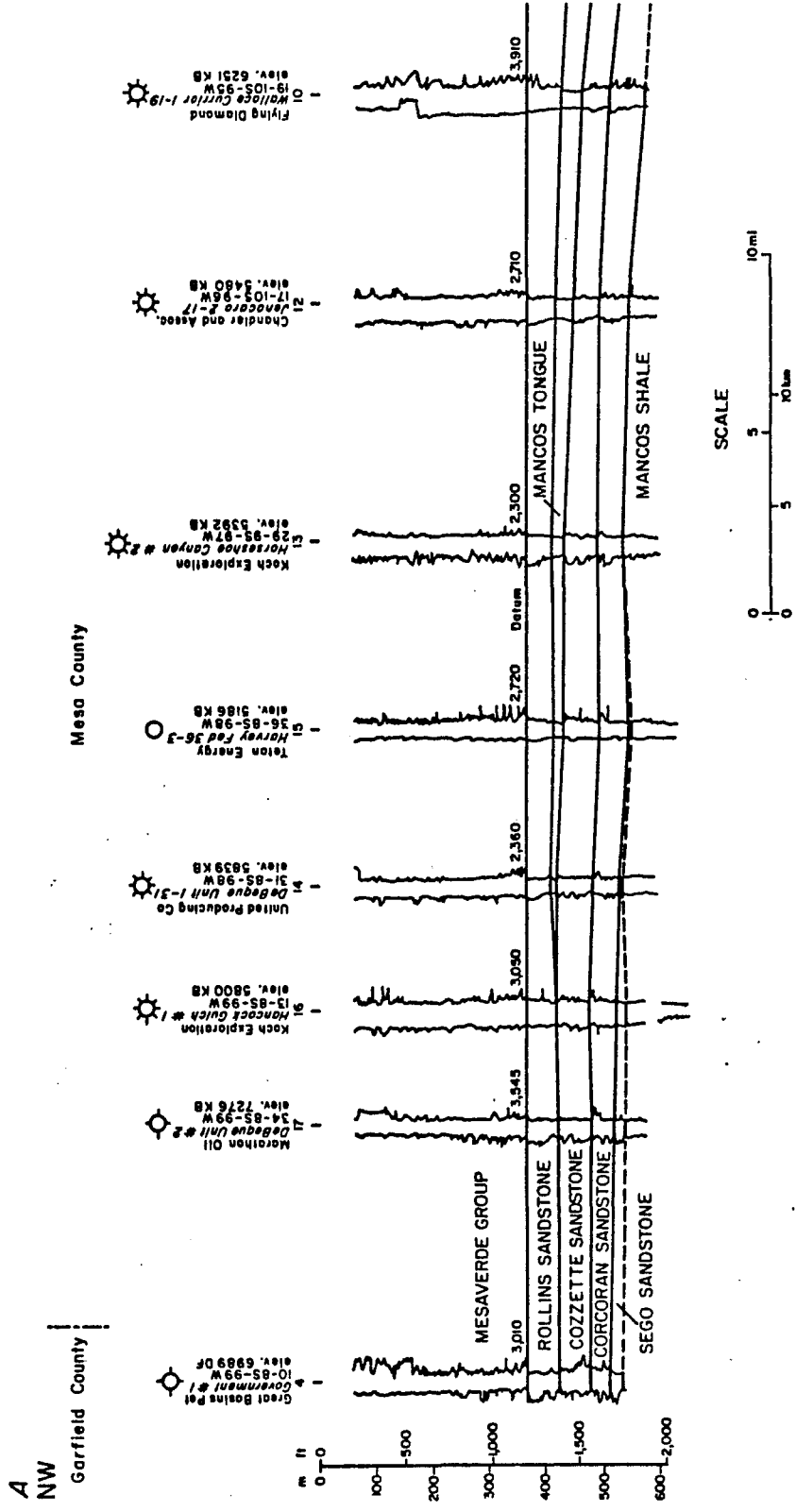


Figure 42. Stratigraphic cross section A-A'. See figure 41 for location.

A' SE

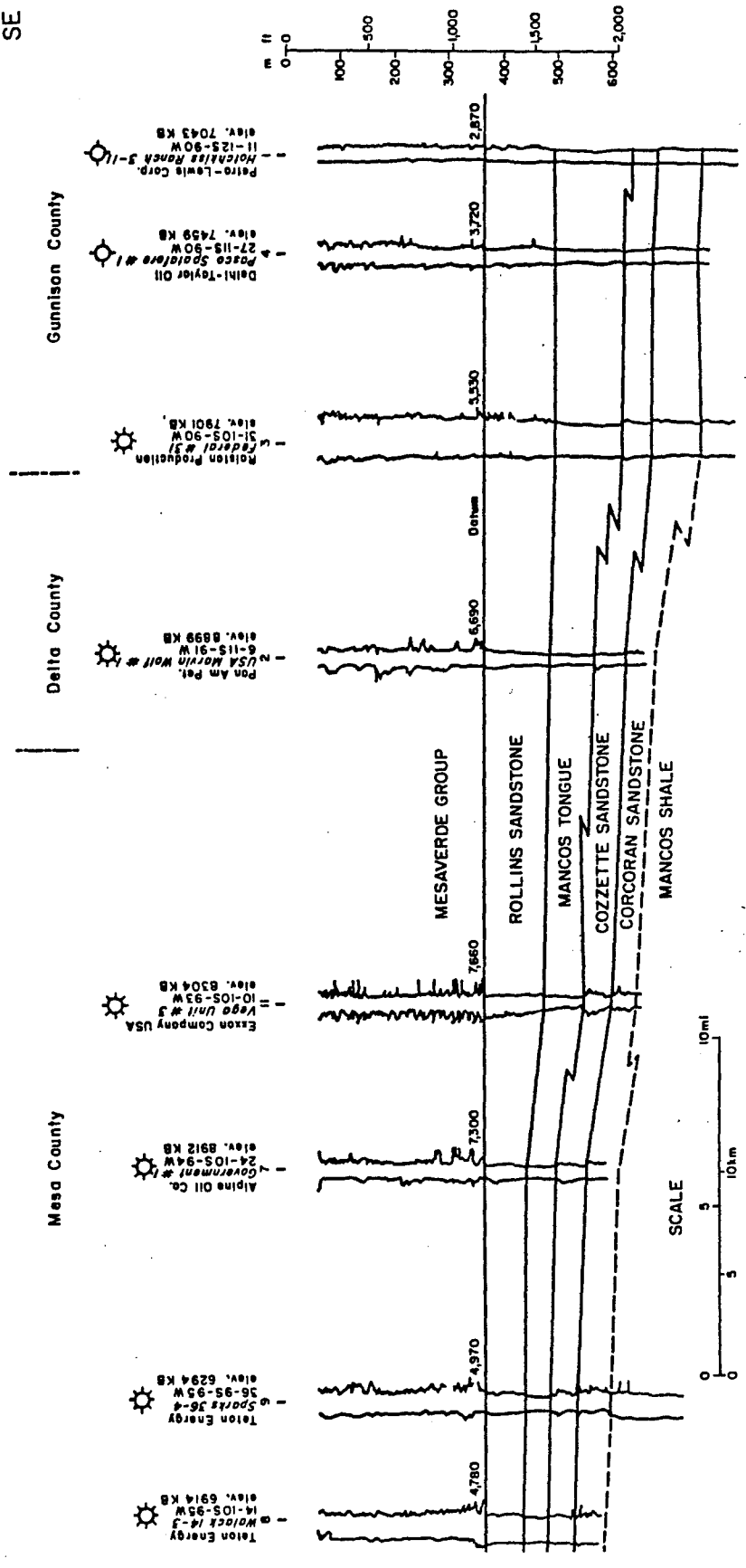


Figure 42 (cont.)

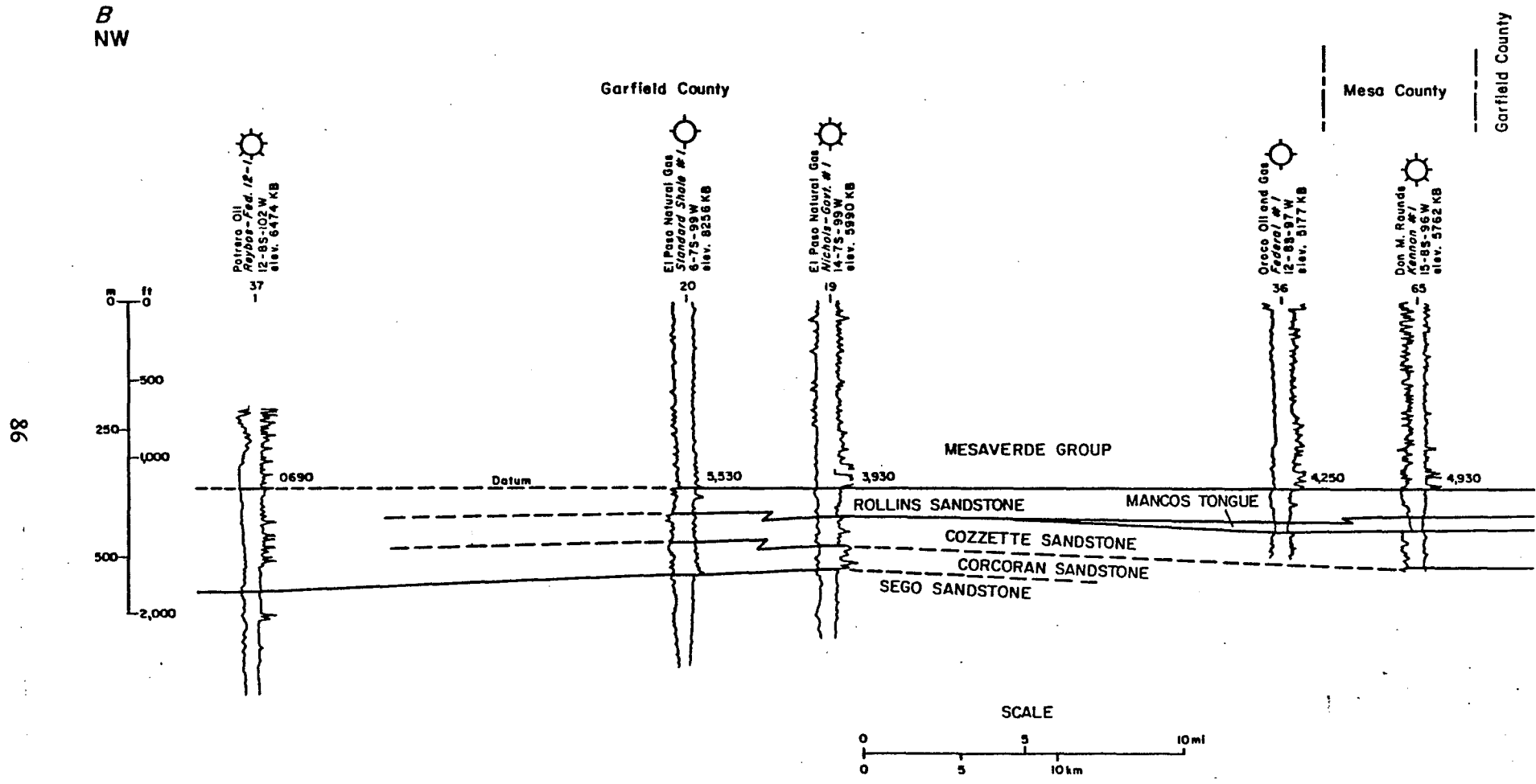


Figure 43. Stratigraphic cross section B-B'. See figure 41 for location.

B' SE

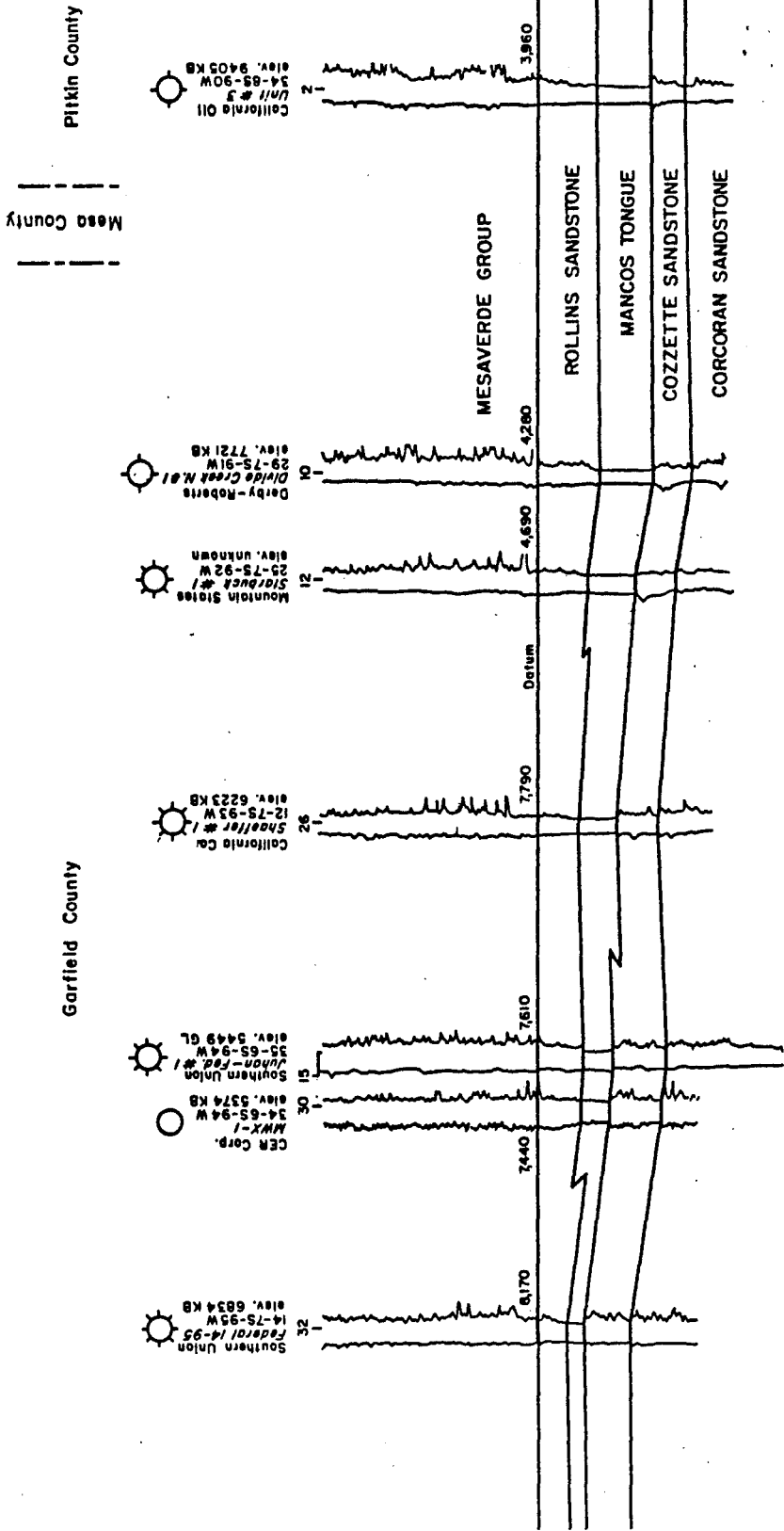


Figure 43 (cont.)

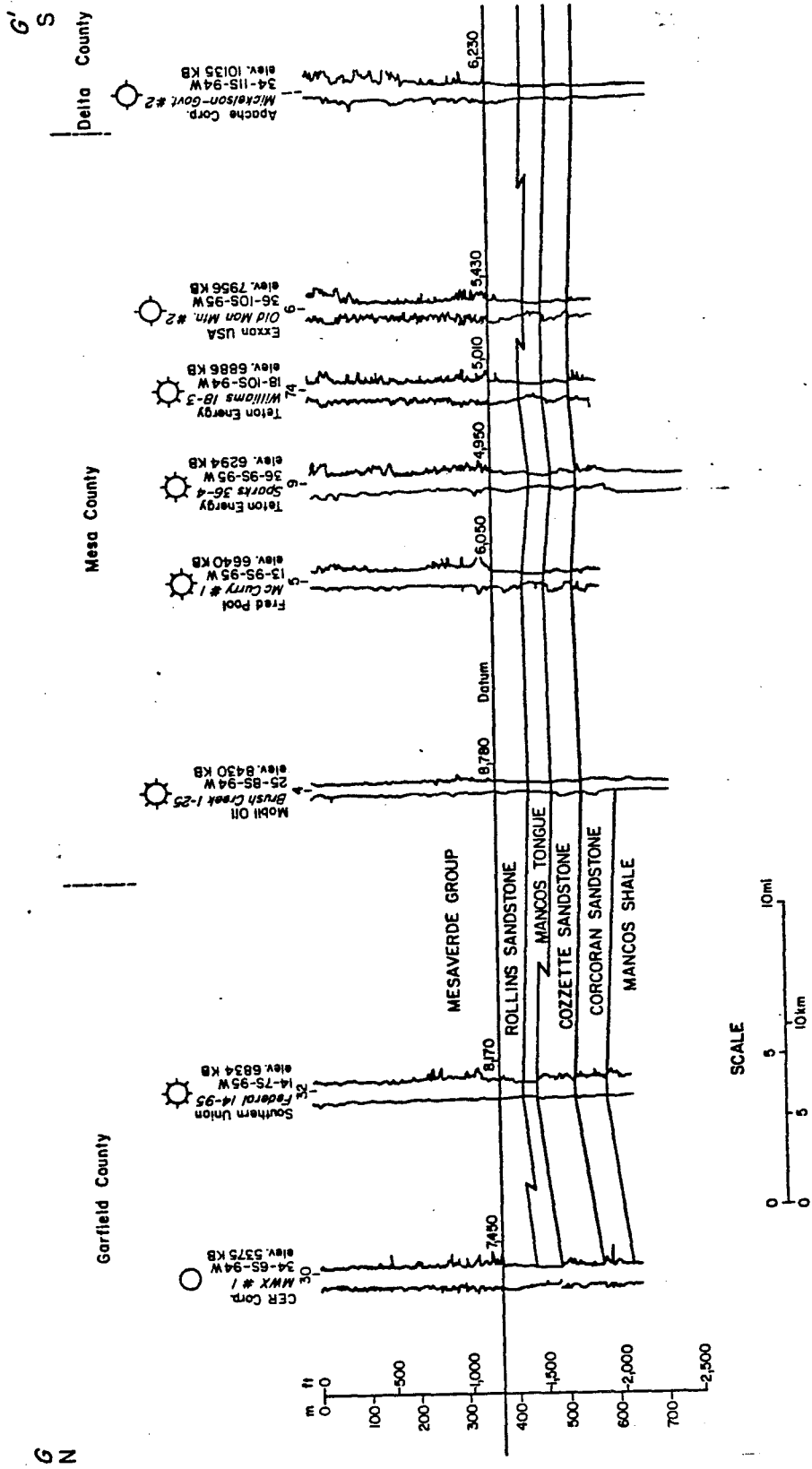


Figure 44. Stratigraphic cross section G-G'. See figure 41 for location.

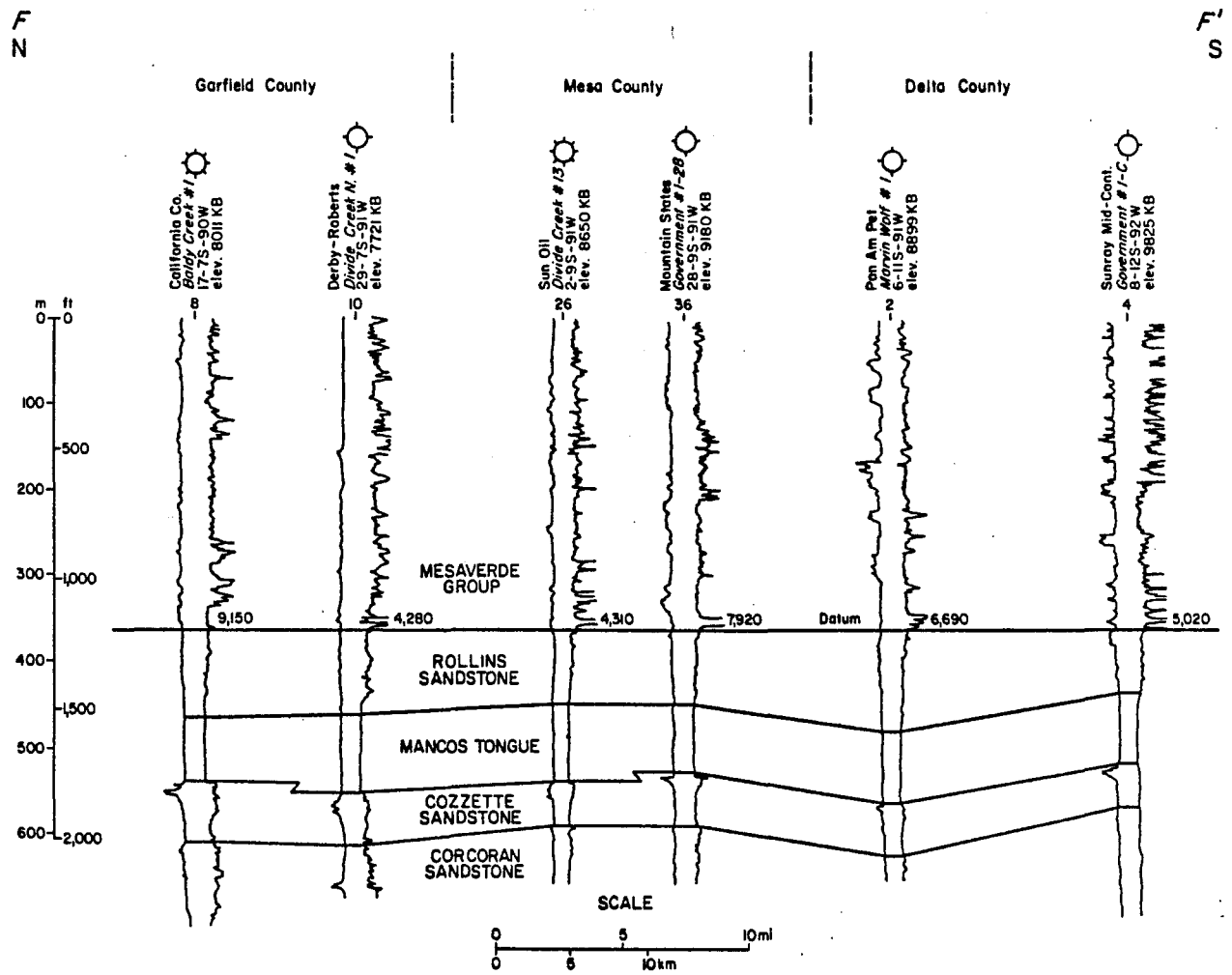


Figure 45. Stratigraphic cross section F-F'. See figure 41 for location.

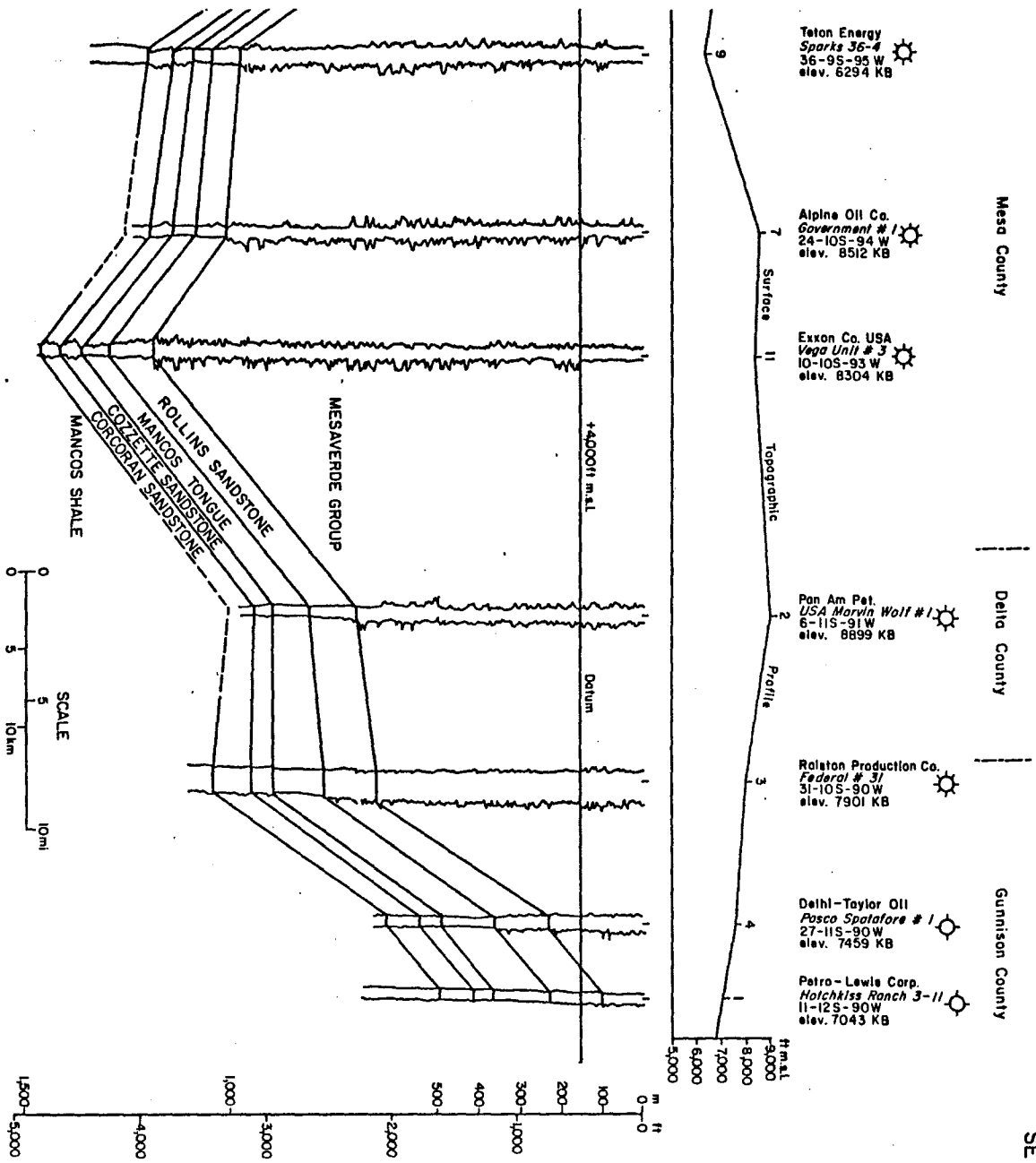


Figure 46 (cont.)

A' SE

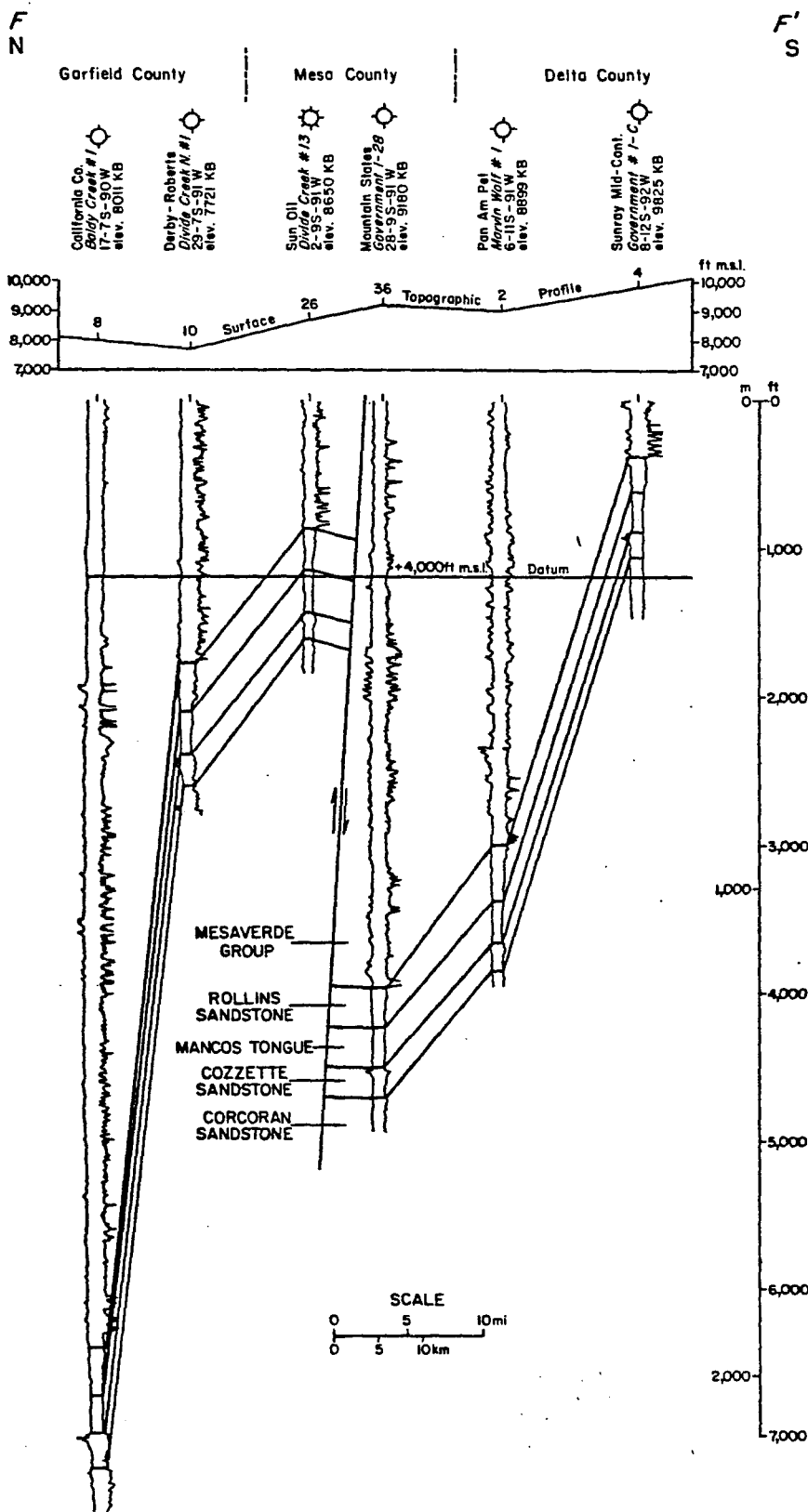


Figure 47. Structural cross section F-F' along the same line as stratigraphic cross section F-F'. Exact fault position and sense of throw are poorly controlled. See figure 41 for location.

sands. In well 11 (fig. 48) an apparently isolated, coarsening-upward sand package within Unit B may represent a shelf bar similar to offshore bars described by Boyles and Scott (1982) and by Porter and Weimer (1982). Further seaward, relatively little sand is present in well 4 in what is predominantly a shelf deposit.

Where exposed at Rifle Gap, Colorado, the lower Corcoran Sandstone includes shale and interbedded sandstone, some of which contains hummocky cross stratification, shale drapes on poorly developed ripple bedding, and carbonaceous debris on bedding surfaces. The upper sandstone in the Corcoran is trough crossbedded at the base and massive to possibly planar bedded at the top. These observations are consistent with the interpretations from subsurface data and would probably place the Rifle Gap section at or just seaward of the Corcoran shoreline position.

Unit D, the lower sandstone "bench" in the Cozzette Sandstone (fig. 48), is very similar to Units B and C of the Corcoran Sandstone. The blocky log character of the unit in a proximal position (wells 15 and 13) changes distally to one or two coarsening-upward sequences with a highly serrate log character (wells 70 and 11). In the most distal position little sandstone is present (well 4, fig. 48). As with units B and C in the Corcoran, Unit D in the Cozzette may represent a barrier core proximally, grading distally (southeast) into shoreface and offshore bar sandstones.

In parts of the Buzzard Creek (well 34) and Sheep Creek Fields (wells 22, 20, and 24), the Cozzette Sandstone is inconsistently gas productive in Unit D (fig. 49). A tendency toward two superposed coarsening-upward depositional cycles is present in Unit D in these wells; the Cozzette was tested but not completed in wells 22 and 24. The wells on section I-I' are 4.5 to 7 mi north-northeast of well 11, cross section A₁-A₂' (fig. 48), and the facies appear similar across this distance.

Unit E, the upper sandstone "bench" in the Cozzette Sandstone, does not extend down depositional dip beyond well 8; its distal equivalents are shales and offshore bars. The

A/
Northwest

Mesa County

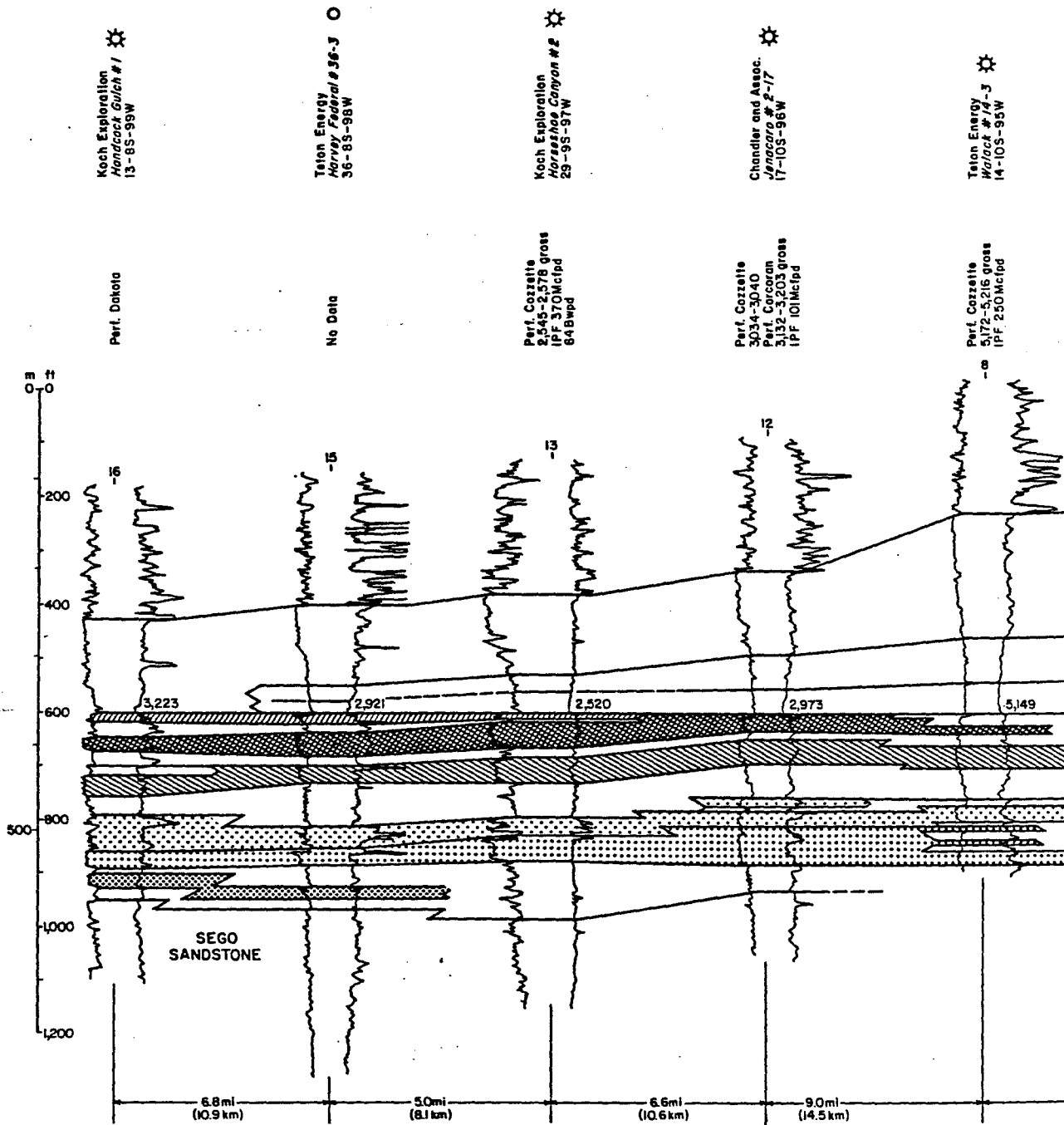


Figure 48. Stratigraphic cross section A₁-A₁', consisting of selected wells from cross section A-A'. Wells can be located by number on figure 41. All logs are gamma-ray resistivity.

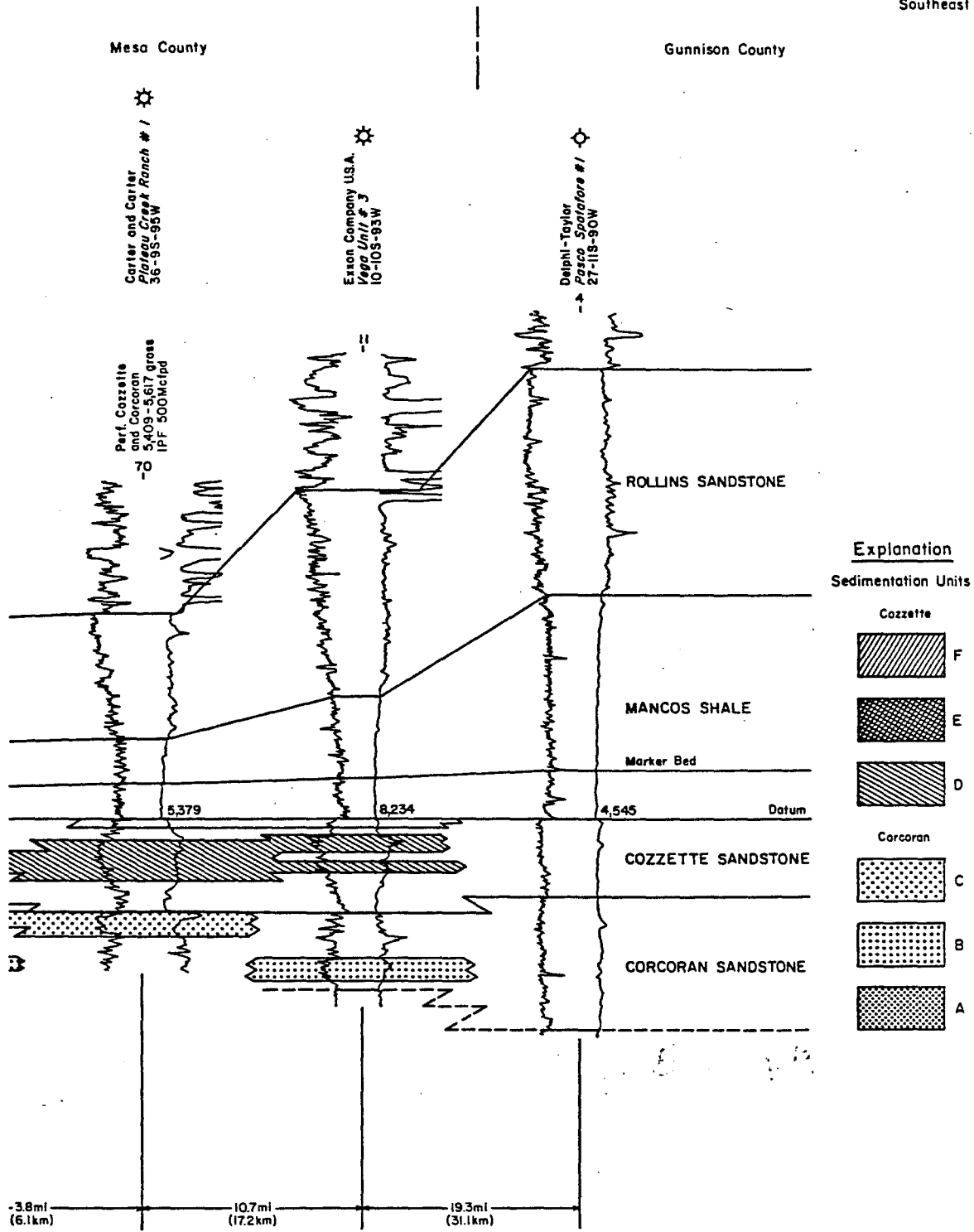


Figure 48 (cont.)

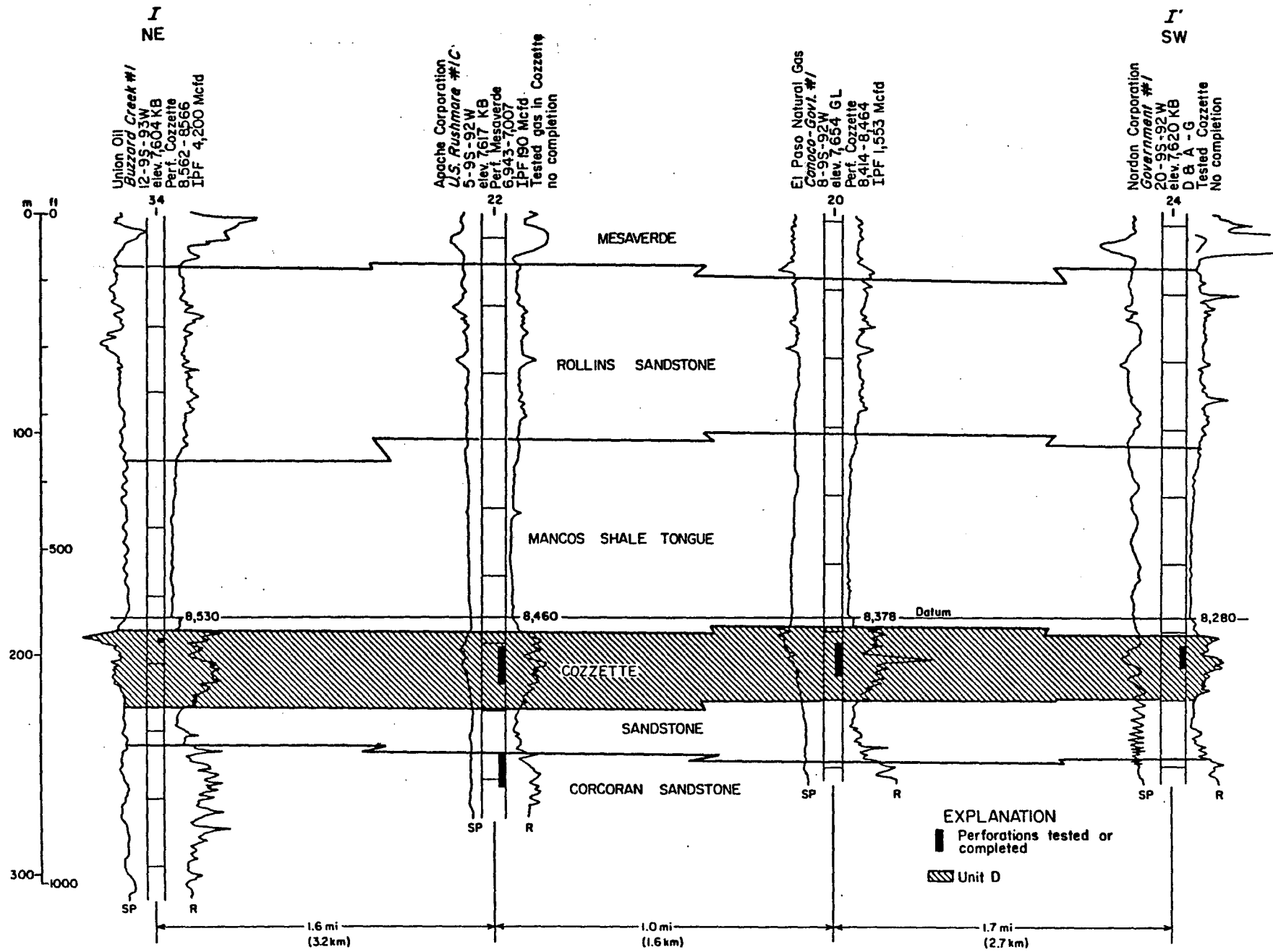


Figure 49. Stratigraphic cross section I-I' in the Buzzard Creek/Sheep Creek Field area showing variation in sedimentation unit D of the Cozzette Sandstone. See figure 41 for location.

coarsening-upward bar sequences in well 11 (fig. 48) built up through the equivalent of the thin shaly interval separating Units D and E to the northwest.

The uppermost sandstone in the Cozzette, Unit F, is approximately 20 ft thick and occurs in a proximal position only (wells 16, 15, and 13; fig. 48). Distally, its equivalents probably represent a shelf or offshore bar sand prior to the transgression of the tongue of the Mancos Shale separating the Cozzette from the Rollins. Proximally, in well 16, it may be part of a lagoonal to fluvial sequence overlying Unit E. A few feet of marine shale may still be present between the Rollins and the Cozzette in well 16.

The above unit descriptions relate to two cross sections that are believed to be representative of a wider sampling of the Corcoran and Cozzette Sandstones based on a log correlation network across the southern Piceance Creek Basin. Further detail on the strike variation of each unit must await any additional studies in this basin.

Formation Thickness

Total-interval isopach maps of the Cozzette and Corcoran Sandstones show northeast-trending maxima across the southern Piceance Creek Basin (figs. 50 and 51). Maximum thickness of the Corcoran extends from T10S R96W in the vicinity of Plateau Field to T6S R92W southeast of Rifle, Colorado. The greatest total thickness values in T7S R91W (fig. 50) may, in part, be an artifact of steep dip on the northeast side of the Divide Creek structure and on the margin of the basin. An isopach thick also occurs in T6S R90W in an area where steep dip does not occur (fig. 40). The base of the Corcoran is not drilled in many wells or may be difficult to define where total depth logged is at or very near the base of the Corcoran. Consequently, the data base for the Corcoran isopach map is significantly smaller than that for the Cozzette isopach map.

Maximum thickness of the Cozzette Sandstone extends from T10S R97W in the vicinity of Shire Gulch Field to T6S R93W near Rifle, Colorado, where well control ends. Again, greater formation thickness in and east of T6-9S R91W may be related to steep structural dip on the

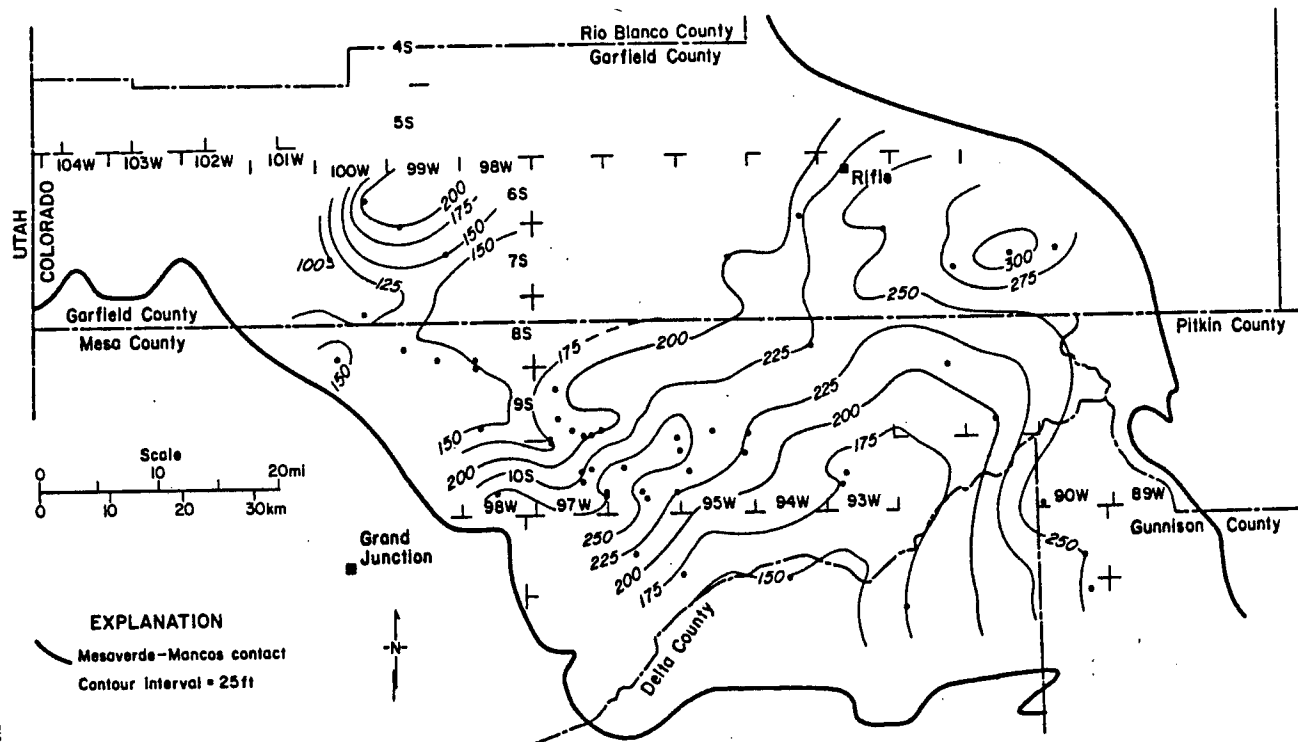


Figure 50. Isopach map of the Corcoran Sandstone, southern Piceance Creek Basin. Mesa-verde-Mancos contact from Tweto (1979).

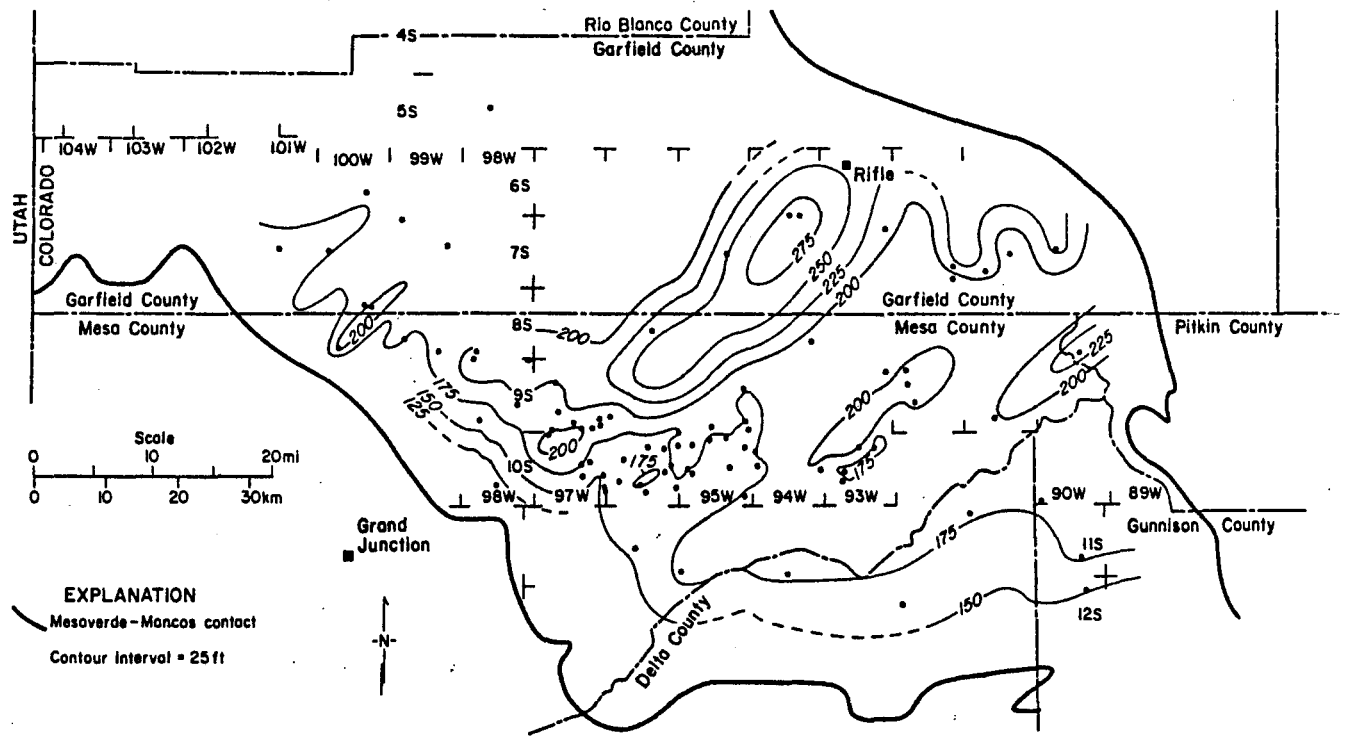


Figure 51. Isopach map of the Cozzette Sandstone, southern Piceance Creek Basin. Mesaverde-Mancos contact from Tweto (1979).

northeast flank of the basin. A minor isopach thick in T9-10S R92-93W is probably not structurally influenced but parallels the depositional trend of maximum thickness 15 mi to the northwest.

Trends of maximum thickness of the Cozzette and Corcoran Sandstones are generally parallel to shoreline positions described by Warner (1964). Warner's (1964) interpretations were based on integration of outcrop and some subsurface data. The shoreline positions were based on the seaward limits of coal and carbonaceous shales, and appear to be substantiated by additional well control which has since become available. Warner (1964) placed the Corcoran shoreline seaward of that of the Cozzette, which is the same relationship shown by the Cozzette and Corcoran isopach maxima. The Cozzette and Corcoran strandlines suggested by CBW Services, Inc. (1983) appear to be too far updip by one or two townships.

Cozzette-Corcoran Paleogeography

Mapping trends of maximum formation thickness and defining genetic depositional units based on geophysical log patterns permits reconstruction of generalized paleogeography of the southern Piceance Creek Basin (fig. 52). As basal units of the prograding Mesaverde Group, a change from non-marine through marginal marine barrier or strandplain to marine shelf deposits is expected from west and northwest to east and southeast in Cozzette-Corcoran time. The blocky, aggradational GR and SP log patterns associated with the proximal parts of Units B and C (Corcoran) and D and E (Cozzette) (fig. 48) are best developed along the trends of greatest thickness in each unit. Seaward (southeastward) of the major isopach thicks is an offshore bar trend in the Cozzette illustrated by log patterns in wells 20 and 22 in Sheep Creek Field (fig. 49), and by the isopach data (figs. 50 and 51). Other, thinner, coarsening-upward sequences within the marine shelf environment may represent more limited bar development.

Paleogeographic interpretation of the study interval would be enhanced by completion of net-sand maps for the Cozzette, Corcoran, and Rollins Sandstones. However, for this study emphasis was placed on acquisition of resistivity logs to establish a basic correlation network.

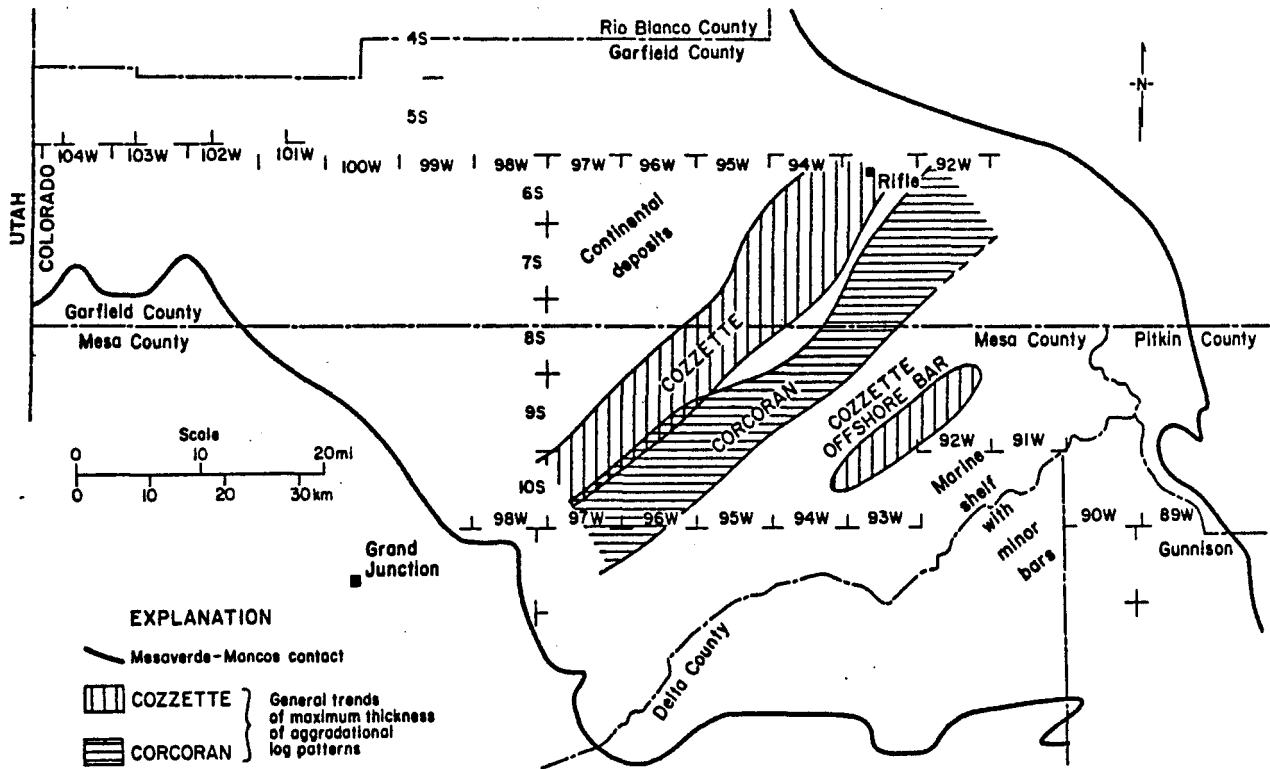


Figure 52. Generalized paleogeography of the Corcoran and Cozzette Sandstones in the southern Piceance Creek Basin. Trends of aggradational log patterns represent barrier or major offshore bar development.

Most of these logs contain SP traces of only poor to fair quality for the purpose of defining lithology. Sonic or neutron-density porosity logs most often contain a GR trace that is more consistent in its response to lithology than the SP. Should GRI continue studies of the Cozzette and Corcoran Sandstones, the completion of net-sand maps using GR traces would be accomplished using an expanded data base of porosity logs. Poor calibration of GR tools can be expected, however, and use of absolute values from GR traces is likely to be unsatisfactory.

Clays and Cementing Agents in Corcoran and Cozzette Reservoirs

The clay fraction of any tight gas reservoir is of concern during drilling, fracturing, and subsequent production. Clays may be sensitive to drilling and completion fluids, potentially leading to formation damage and decreased gas production. The following review of clay distribution and cementing agents in the Corcoran-Cozzette was provided by CBW Services, Inc. (1983).

Corcoran Sandstone

Clays in the Corcoran are primarily mixed layer smectite-illite and illite. Much of the clay is detrital, but examination by scanning electron microscope (SEM) shows the presence of some authigenic illite. Total clay fraction of the samples examined by CBW Services (1983) ranged from 6 to 17 percent. Of that fraction, 0 to 48 percent was mixed-layer smectite-illite, 20 to 88 percent was illite, and 0 to 25 percent was chlorite. Kaolinite was noted in one of five wells.

Cozzette Sandstone

Mixed-layer smectite-illite and illite are also dominant in the Cozzette wherein total clay content is 3 to 19 percent. However, one of six wells examined contained only 1 percent clay. The clay fraction in the Cozzette samples examined by CBW Services (1983) included 14 to 80 percent illite, 0 to 55 percent mixed-layer smectite-illite, and 10 to 32 percent chlorite. One well contained 57 percent kaolinite, which otherwise was not a major constituent.

Cementing Agents

Cementation of both the Corcoran and Cozzette is dominantly by quartz overgrowths. Some calcite (up to 7 percent) and minor siderite and ankerite are present. Moderate amounts of ankerite (14 percent) occurred in core from one of five wells investigated (CBW Services, 1983).

Summary of Selected Parameters and Production Data

Tables summarizing the general attributes, geologic and engineering characteristics, and extrapolation potential of the Cozzette and Corcoran Sandstones are included in Finley (1982). Gas production listed as from the Cozzette and Corcoran singly, in combination with each other, or in combination with other units, totaled 2.2 Bcf from 87 wells in 1981 (table 4). Plateau and Shire Gulch Fields are the largest fields producing from the Cozzette and Corcoran Sandstones, and also from the Rollins Sandstone (fig. 53). Table 4 includes wells carried by the Colorado Oil and Gas Conservation Commission as simply completed in the Mesaverde but which are shown by other data sources to be producing from either the Rollins (3 wells), Cozzette (10 wells), or Corcoran (9 wells).

A cross section through Shire Gulch and Plateau Fields shows that production is primarily from depositional Units D and E in the Cozzette and B and C in the Corcoran (fig. 54). Water and condensate are also produced with gas during the tests of initial potential. Note that section A₂-A₂' (fig. 54) is contained entirely between wells 13 and 8, which in turn appear on cross sections A-A' and A₁-A₁' (figs. 42 and 48). The continuity of depositional units within the Cozzette and Corcoran Sandstones suggested by cross section A₂-A₂' can be substantiated when additional wells are examined within field areas.

Much of the existing Corcoran-Cozzette gas production is from fields located in the valleys of the Colorado River and of Plateau Creek. The Roan Cliffs north of the Colorado River and Battlement Mesa south of the Colorado River reach elevations of over 8,000 ft and 10,000 ft, respectively, which hampers access and makes winter operations more difficult.

in a north-northeasterly direction. The Frontier Formation represents the first major regression of the western shoreline. Migration of the coastline to the east took place mainly in Cenomanian and Turonian time, according to the European stages (fig. 76). In the Big Horn and western Wind River Basins, the Frontier consists of one major regressive-transgressive cycle, whereas in the overthrust belt of southwest Wyoming the major regression was interrupted by a minor marine transgression in upper Frontier time. The source of the Frontier clastics was dominantly Paleozoic sedimentary rocks thrust up into mountain ranges in northern Utah and southeast Idaho.

Broad structural sags trending almost normal to the shoreline captured the major streams and became the major depocenters. One such downwarp, which possibly became the site of the largest delta complex in Frontier time, is indicated on a post-Cloverly to pre-uppermost Frontier isopach map in the Wind River Basin (Keefer, 1969). This map, which has been extended into the Greater Green River Basin in this study (fig. 83), shows the thickness of all the Cretaceous units from the top of the "Dakota Sandstone" to near the top of the Frontier Formation. It serves as a paleo-structure map that indicates a pronounced synclinal axis located over the crest of the present Wind River Mountain Range. Along this northwesterly plunging axis the large Wind River Delta developed and here it persisted longest, as indicated by the young ages that have been assigned to the upper-most Frontier sandstones in this area. The western Owl Creek Mountains may also have been a negative structure at this time (figs. 83 and 84), and the distribution of coarse andesite pebbles and coals reported around the Big Horn Mountains indicate that it too was possibly the site of a large delta that fed sand to offshore bars in the area of the present Powder River Basin. The Uinta Mountains in northeast Utah, which formed a subsiding trough at various times in the past (Hansen, 1965), apparently began to rise after the Mowry regression and were a low uplifted area in Frontier time (Reeside, 1955; Weimer, 1962; Young, 1975). South of this early Uinta Uplift was another large Frontier delta called the Ferron Delta, which spread eastward across the Uinta Basin (Hale and Van de Graaff, 1964).

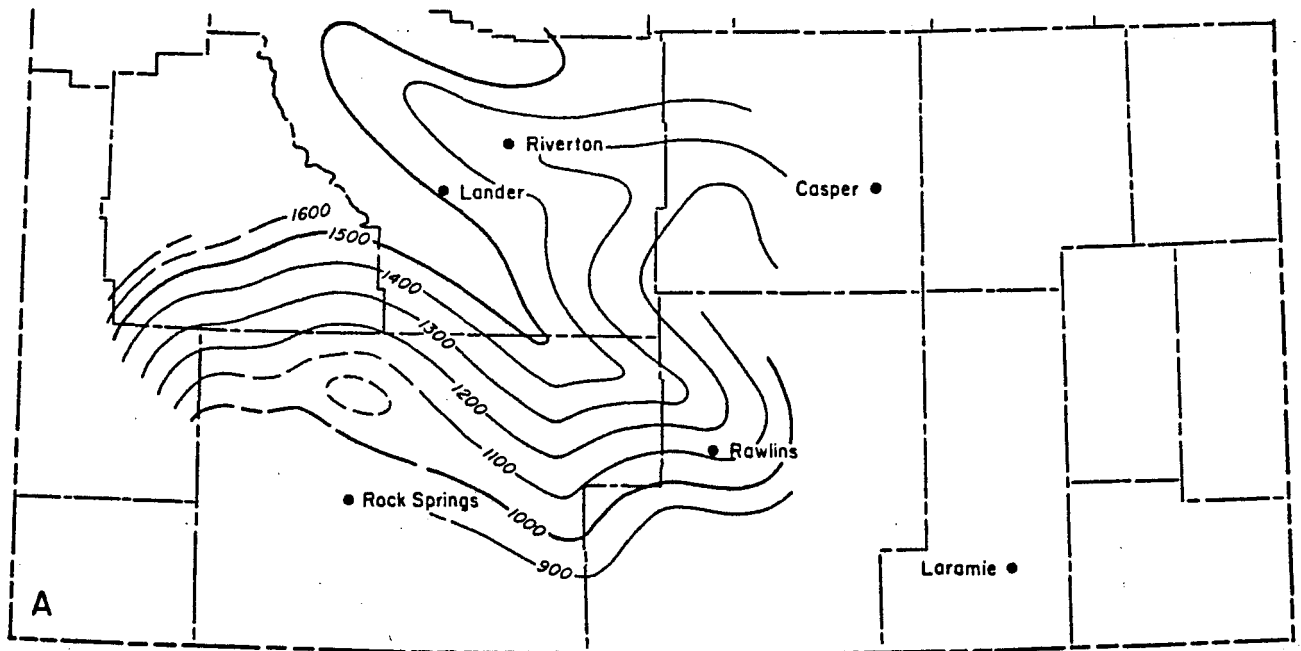


Figure 83. Isopach map of post-Cloverly to pre-uppermost Frontier strata in the Wind River and Greater Green River Basins. Based on data from Anderman (1956), Gudim (1956), and Keefer (1969).

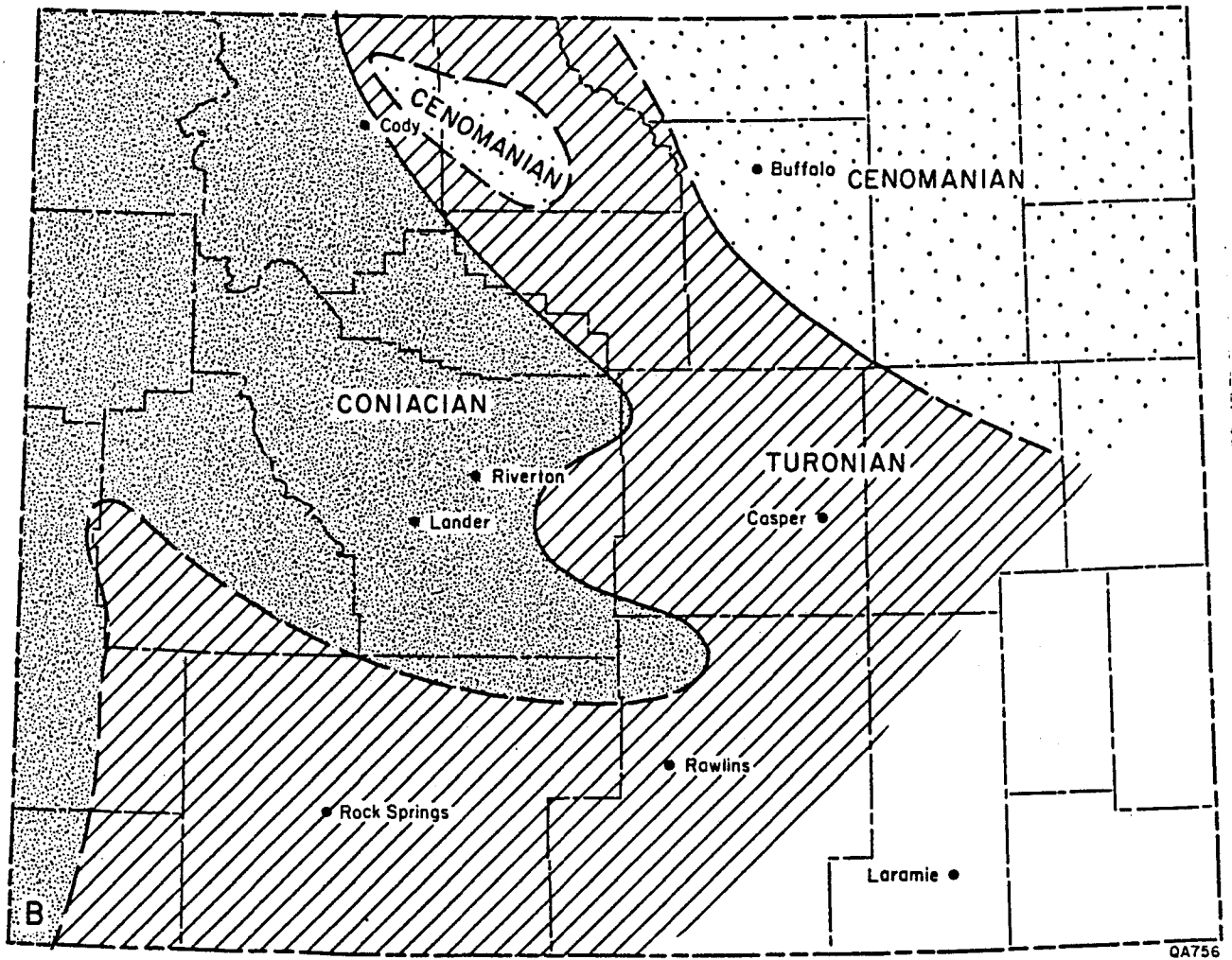


Figure 84. Map showing the age distribution of the uppermost sandstones in the Frontier Formation. Based on data from Cobban and Reeside (1952), Hansen (1965), Haun (1958), Hunter (1952), Merewether and others (1975), Tillman and Almon (1979), and Van Houten (1962).

A composite reconstruction of these paleogeographic elements (fig. 85) shows all the postulated deltas at their maximum development, irrespective of age; it also shows the orientation of bar sands mapped during this study and described in the literature. The numerous barrier and offshore bars in the Big Horn and Wind River Basins are expected to have the same northerly trend as those shown, because the longshore drift was from north to south along the west shore of the seaway (Kent, 1968). Frontier deposition ended with a major marine transgression that shifted the western coastline farther to the west and resulted in deposition of at least 3,000 ft of marine shale over the Frontier Formation in the La Barge area.

Summary

Three main depositional systems have been distinguished in this subsurface study. These are the delta system, the barrier-offshore bar system, and the marine shelf system. Only the first two are blanket-geometry sand depositional systems, and these result in sand bodies of contrasting characteristics. The delta system contains coarse, lenticular sandstones with high initial porosities and permeabilities which diagenetic changes failed to completely obliterate. The bar system produces finer-grained, quartz-rich sheet sandstones that retain little of the initial porosity and permeability.

Three paleogeographic maps illustrate the evolution of the two depositional systems. Average strandline positions of the Frontier Formation in the Wind River Basin were taken mostly from Burgess (1970). The Wind River Delta (Fifth through Third Frontier) rapidly prograded into the southern Wind River Basin in early Frontier time (fig. 86A). By middle Frontier time (fig. 86B), equivalent to the top of the Second Frontier, the La Barge Delta had prograded as far as the Rock Springs Uplift at approximately the same time that the small Uinta Delta was forming to the south. These two deltas were abandoned and transgressed before the Wind River Delta could prograde into the area of the northern Great Divide Basin (fig. 86B). In latest Frontier time the Wind River Delta withdrew to the west, but its regression

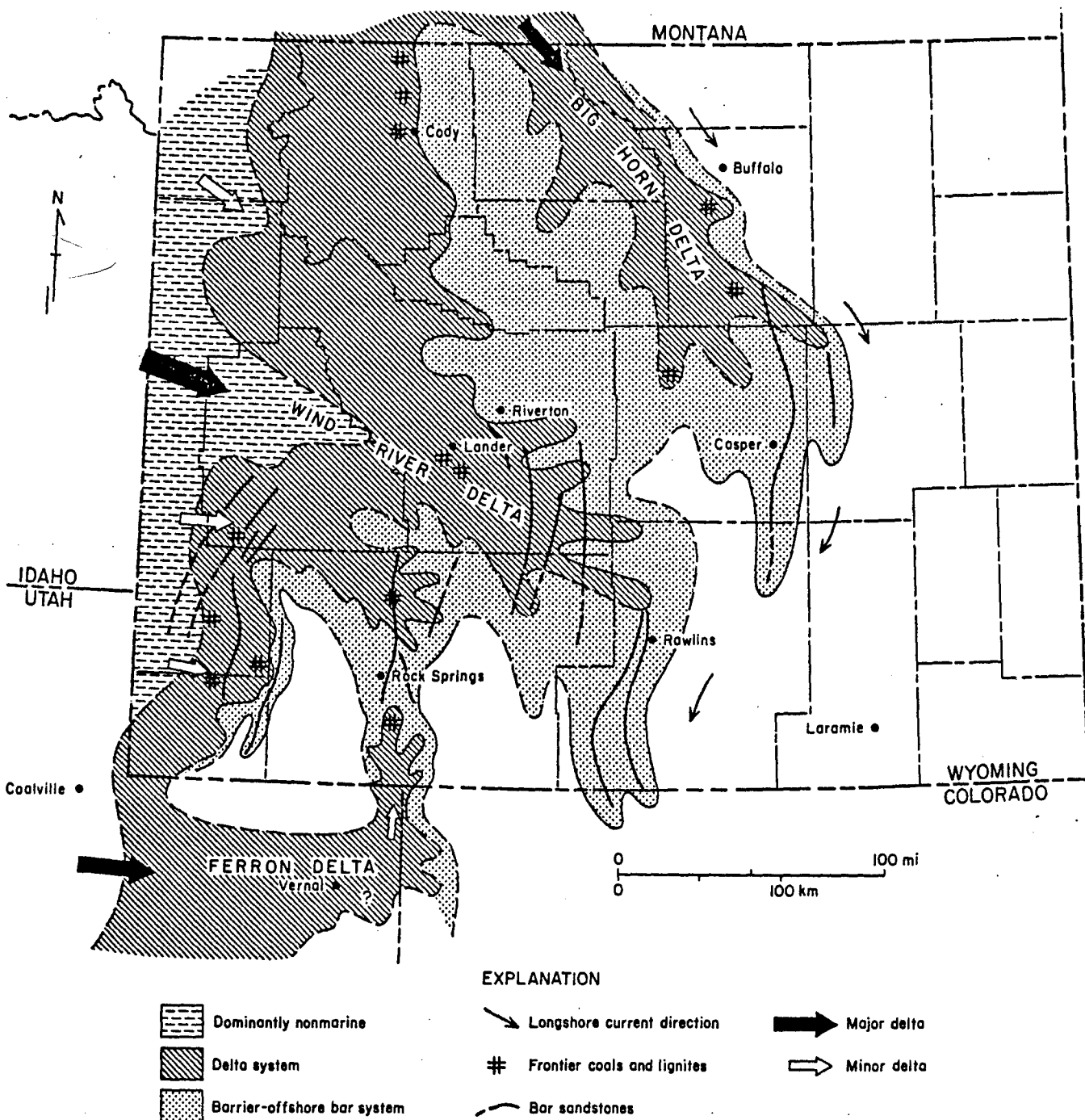
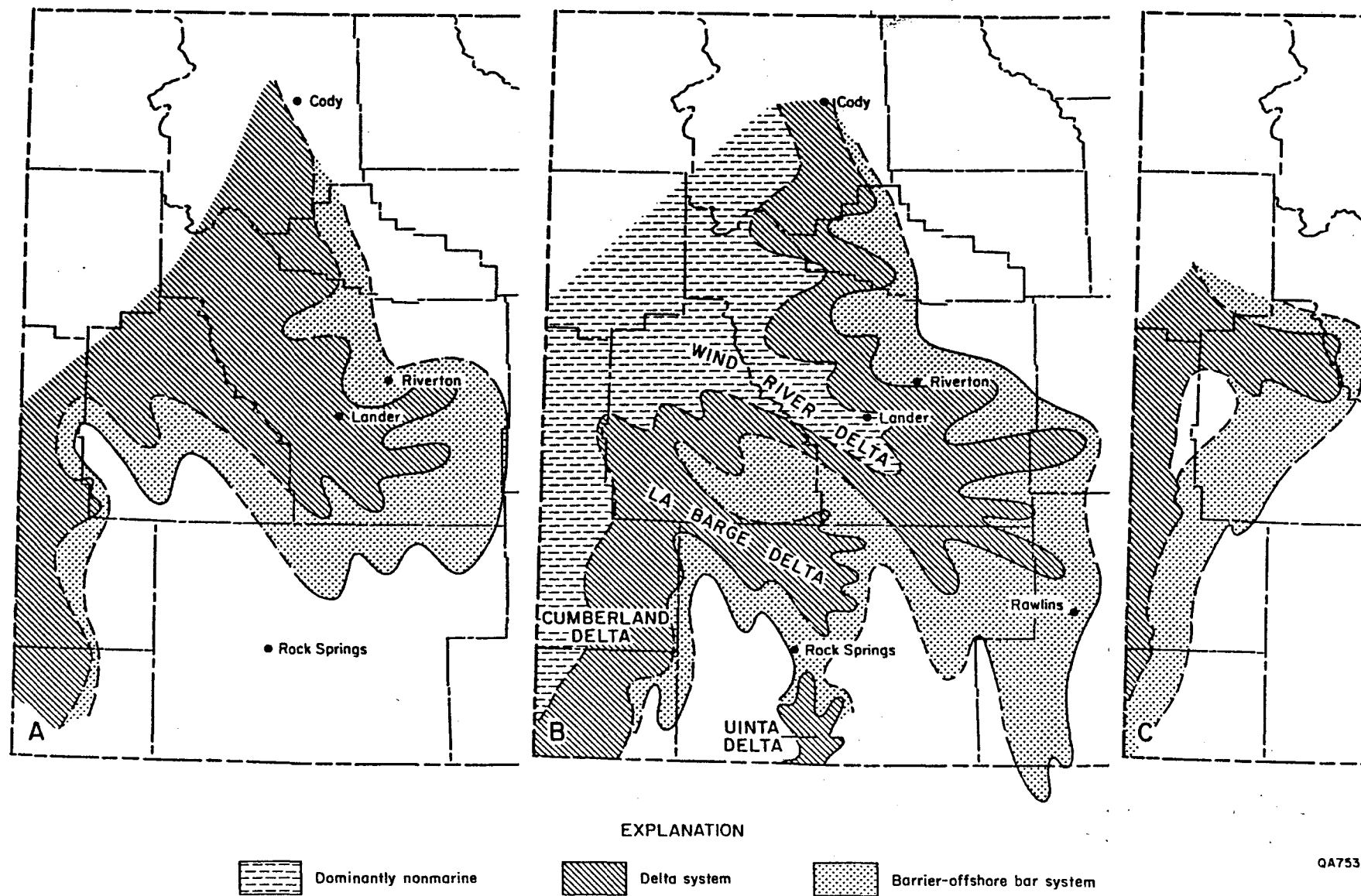


Figure 85. Paleogeographic reconstruction of the Frontier Formation showing the reported occurrences of coal and lignite, the orientation of bar sandstones, and the maximum extent of all the major Frontier deltas in Wyoming irrespective of age. Based on data from Barlow and Haun (1966), Burgess (1970), Hale and Van de Graaff (1964), Haun (1958), Hunter (1952), Masters (1952), Myers (1977), and Towse (1952).



QA753

Figure 86. Schematic distribution of deltaic and barrier-offshore bar depositional systems in early Frontier time (15A), middle, pre-bentonite marker bed time (15B), and late or First Frontier time (15C).

ceased long enough to develop a bar system which extended to the south-southwest across the La Barge platform. This bar system is the First Frontier Sandstone (fig. 86C).

Major Frontier deltas, such as the Big Horn and Wind River, and even the La Barge Delta, were elongate, highly constructive deltas that prograded rapidly over the shallow shelf that existed northeast and east of the Moxa Arch. The narrow, elongate geometry and generally southeast orientation may be due to the influence of earlier northwest trending folds. The possibility that some of the present mountain ranges may have been structural lows in Frontier time is a new concept that has not been previously considered. In fact, most previous workers have assumed that the uplifts had early stages of growth that influenced Frontier depositional patterns.

In summary, the Frontier Formation in the Greater Green River Basin contains facies and depositional patterns that resemble other Late Cretaceous deposits along the western side of the Cretaceous interior seaway. Similar conditions and depositional environments persisted throughout Late Cretaceous time, particularly in western Wyoming, until the ancient coastline was divided into separate basins during the Laramide orogeny.

Production

Wyoming produces about 410 Bcf of natural gas annually. According to Miller and Ver Ploeg (1980) about 60 percent of this production comes from Upper Cretaceous strata. In the Greater Green River Basin the Cretaceous and early Tertiary units contain an estimated 135 Tcf of gas in place, of which only 53 to 65 Tcf can be recovered by present technology (Miller and Ver Ploeg, 1980). Most of the potential gas reserves in the Upper Cretaceous, and in the Frontier Formation in particular, are in tight sands.

The Frontier Formation in Wyoming has been of economic importance for a long time, because it contains coal, bentonite, and petroleum. But it is primarily a gas-producer, and in fact, it is proving to be one of the largest reservoirs of natural gas in the Rocky Mountains. In the Greater Green River Basin the Frontier is famous for the giant Big Piney-La Barge gas field

which contains major reserves in the First and Second Frontier sandstones (McDonald, 1973). The Second Frontier is gas productive along most of the Moxa Arch in Wyoming and was an early producer of gas from the Baxter Basin on the axis of the Rock Springs Uplift. Around the northeast rim of the Great Divide Basin, the productive sandstones are best developed in the upper half of the Frontier Formation in such fields as the Bison Basin, Crooks Gap, and Lost Soldier. Nearly all the Frontier fields are a combination of structural and stratigraphic traps (Newman, 1981). Clean, well-sorted sandstones that accumulated on contemporaneous positive structures trapped hydrocarbons. The early oil and gas accumulations appear to have aided in preserving some of the original porosity and permeability.

Production is mostly from coarser-grained, lenticular, delta-distributary sandstones where artificial fracturing is most successful in boosting recoveries. In addition to being tight, the Frontier sandstones are usually overpressured at depths greater than 11,000 ft. Many of the tighter and more extensive barrier and offshore bar sands await further improvements in technology and gas price before their enormous potential can be realized.

Exploration Potential and Summary of Selected Parameters

The value of mapping the three main depositional systems, as done in this report, is that facies tracts can be projected across areas of little or no data, such as the deep basin centers and the existing mountain ranges. This was one of the main objectives of this study as originally outlined by Finley and Han (1982a, 1982b). There are essentially no prospects in the mountains, but the deeper portions of the basins hold the reserves of the future. This study suggests that sandy units will be poorly developed in the southern Green River Basin and the Washakie Basin, but that good to excellent sandstone development can be expected in the northern Green River Basin and in the Great Divide Basin.

To date, practically all the discovered reserves in the Frontier Formation in the Greater Green River Basin have been found in structural or combination structural-stratigraphic traps. There are few untested structures left, but one of the most obvious is the Pinedale Anticline in

the northern Green River Basin (fig. 72). There the Frontier has yet to be penetrated. It is possible that the First Frontier sandstone is present across the north half of this anticline and the Second Frontier should consist of a fluvial-deltaic complex similar to that found on the La Barge Platform. Drilling depths to test the Frontier Formation will be in the 25,000 ft range.

There are almost no purely stratigraphic traps that produce from the Frontier in the study area. One exception is the Marianne Field on the east flank of the Rock Springs Uplift, which produces gas from Frontier bar sandstones that lense out updip (Wellborn, 1981). More of these bars should be present down the flanks of the Rock Springs Uplift. The numerous barrier-offshore bars on the north rim of the Great Divide Basin extend an unknown distance southward into the basin. Some of these may reach reasonable drilling depths toward the Wamsutter Arch. There is also a good possibility that one or more lobes of the Wind River Delta prograded into the Great Divide Basin. These lobes will provide potentially large stratigraphic traps if hydrocarbon-bearing facies are present.

Numerous unconformities within the Frontier Formation (Cobban and Reeside, 1952; Love, 1956; Reeside, 1955; Hale, 1962; Merewether and others, 1975) may influence the accumulation of hydrocarbons. A stratigraphic accumulation of oil and gas in reworked Frontier sandstones at two small unconformities has been reported by Tillman and Almon (1979) in the Powder River Basin, and the thin producing zones in the Marianne Field may be of similar origin (Wellborn, 1981). Tracing unconformities in the Frontier could lead to the discovery of more accumulations of this type.

RESOURCE ESTIMATES

Introduction

For this study, gas resource estimates were made for four stratigraphic units, the Travis Peak Formation (East Texas Basin), the Corcoran and Cozzette Sandstones, the upper Almond Formation, and the Frontier Formation. Resource estimates presented here were calculated using either available published data or basic engineering and geological data available from state oil and gas commissions. The methodology of the National Petroleum Council (NPC) (1980a) or that suggested by Lewin and Associates, Inc. (M. Marchlik, personal communication, 1983), was used, depending upon the data available.

Methodology

Volumetric Method

Where basic engineering and geological data were available, the method of resource estimation used by the National Petroleum Council (1980a) was adopted. Basic data include permeability, net pay, gas porosity, productive area, formation pressure, and formation temperature. The procedures of the volumetric method for developing resource estimates can be summarized as follows:

- (1) Outline a boundary for the specific formation defined by the presence of reservoir sand;
- (2) Assign values for the following parameters for each zone:
 - (a) net pay thickness,
 - (b) permeability,
 - (c) gas porosity,
 - (d) formation pressure,
 - (e) formation temperature;
- (3) Estimate the areal extent of those reservoir characteristics for each zone;

- (4) Calculate gas-in-place (GIP),

$$\text{GIP} = (\text{area}) \times (\text{net pay}) \times (\text{gas porosity}) \times (\text{gas formation volume factor})$$

where gas formation volume factor is a function of formation pressure, formation temperature, and specific gas gravity. Specific gas gravity is assumed to be 0.65 (National Petroleum Council, 1980a);

- (5) Calculate technically recoverable gas-in-place (TRGIP),

$$\text{TRGIP} = (\text{technical recovery factor}) \times (\text{GIP})$$

where technical recovery factor is a function of formation pressure, formation temperature, wellbore pressure, and gas formation volume factor (National Petroleum Council, 1980a);

- (6) Calculate maximum recoverable gas-in-place (MRGIP),

$$\text{MRGIP} = (\text{recovery adjustment factor}) \times (\text{TRGIP})$$

where recovery adjustment factor is a function of permeability (National Petroleum Council, 1980a).

Proportioning Method

The gas resources of the Frontier, Corcoran-Cozzette, and upper Almond Formation were in part listed in combination (or in stacked form) with data from other formations when published by the National Petroleum Council (1980b). To estimate the gas resources of formations of interest from these data, Lewin and Associates, Inc. (M. Marchlik, personal communication, 1983) suggested the following two methods, both of which assume that the gas is distributed evenly over the area of the formation:

Areal Proportioning.--This method uses the known area of each portion of the formation in relation to the known gas-in-place (or the maximum recoverable gas-in-place) for some uncombined portion. The ratio of the total area (combined plus uncombined) to the uncombined area of the formation is multiplied by the gas-in-place (or the maximum recoverable gas-in-place) estimate for the uncombined area to calculate the gas-in-place (or the maximum recoverable gas-in-place) for the formation of interest. These statements can be expressed as the following equation:

Total gas resource for specific formation =

$$\left(\begin{array}{c} \text{gas resource} \\ \text{in uncombined} \\ \text{portion of} \\ \text{specific formation} \end{array} \right) \times \left(\frac{\text{total area of specific formation}}{\text{uncombined area of specific formation}} \right)$$

Volumetric Proportioning.--This method is equivalent to the areal proportioning method in that it uses the gas porosity, net pay, permeability, and gas formation volume factor from the uncombined portion of the formation along with the area of the combination to calculate the gas-in-place (or the maximum recoverable gas-in-place) for the area of the formation in the combination. Volumetric relationships outlined above were used.

Results

The volumetric method was used to estimate gas resources in the Travis Peak Formation, and the proportioning method was used for the Corcoran and Cozzette Sandstones, the upper Almond Formation, and the Frontier Formation.

Travis Peak Formation, East Texas Basin

The volumetric method was used to estimate the gas resource of the Travis Peak Formation in Texas but not in North Louisiana. The necessary data, such as permeability, net pay, gas porosity, productive area, formation pressure, and formation temperature, were extracted from applications by operators for tight formation designations submitted to the Railroad Commission of Texas.

Cumulative frequency versus permeability (fig. 87) was first plotted to show the distribution of in-situ gas permeability in the area of data availability. In the productive area permeabilities as high as 0.3 md are not likely (fig. 87); only 7.5 percent of the area attains this value. The minimum permeability is 0.0003 md, representing approximately 5.0 percent of data collected, and the median permeability, with 50 percent probability, is 0.012 md.

No strong correlation exists between permeability and porosity, but for the purposes of resource estimation, permeability versus porosity values from available information were

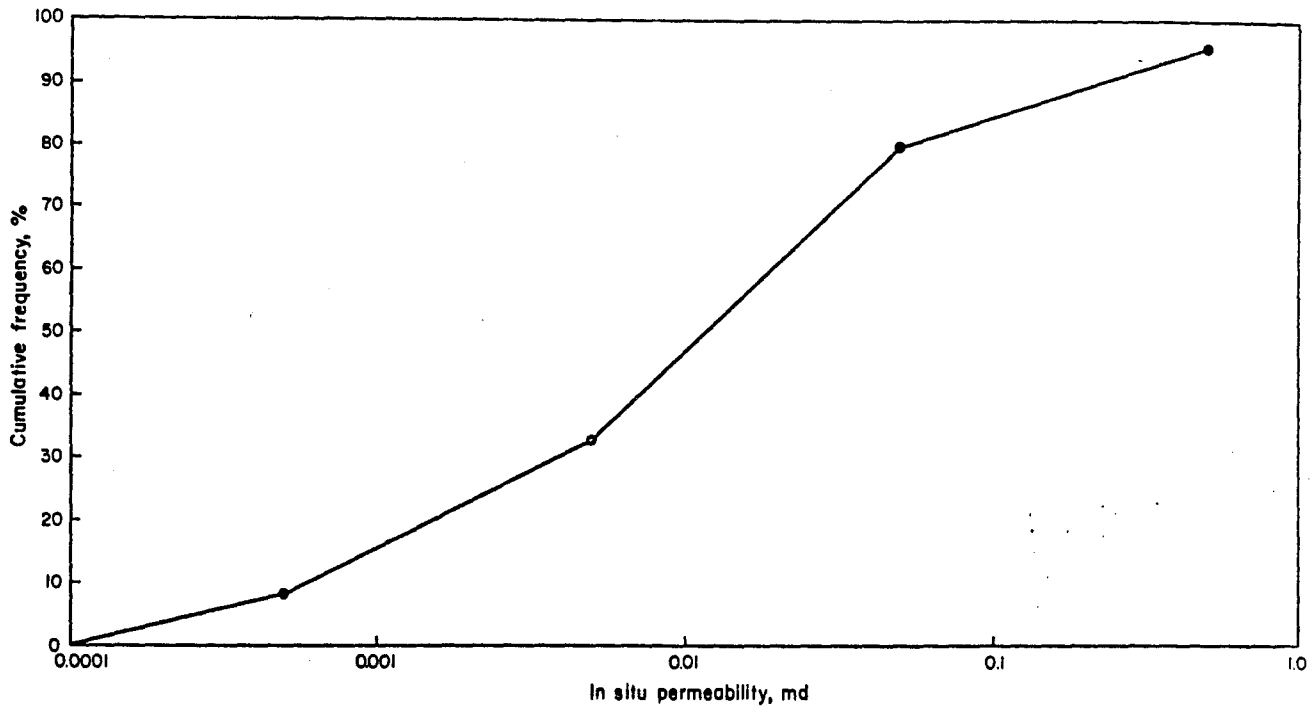


Figure 87. Cumulative frequency versus in situ permeability in the Travis Peak Formation, East Texas Basin.

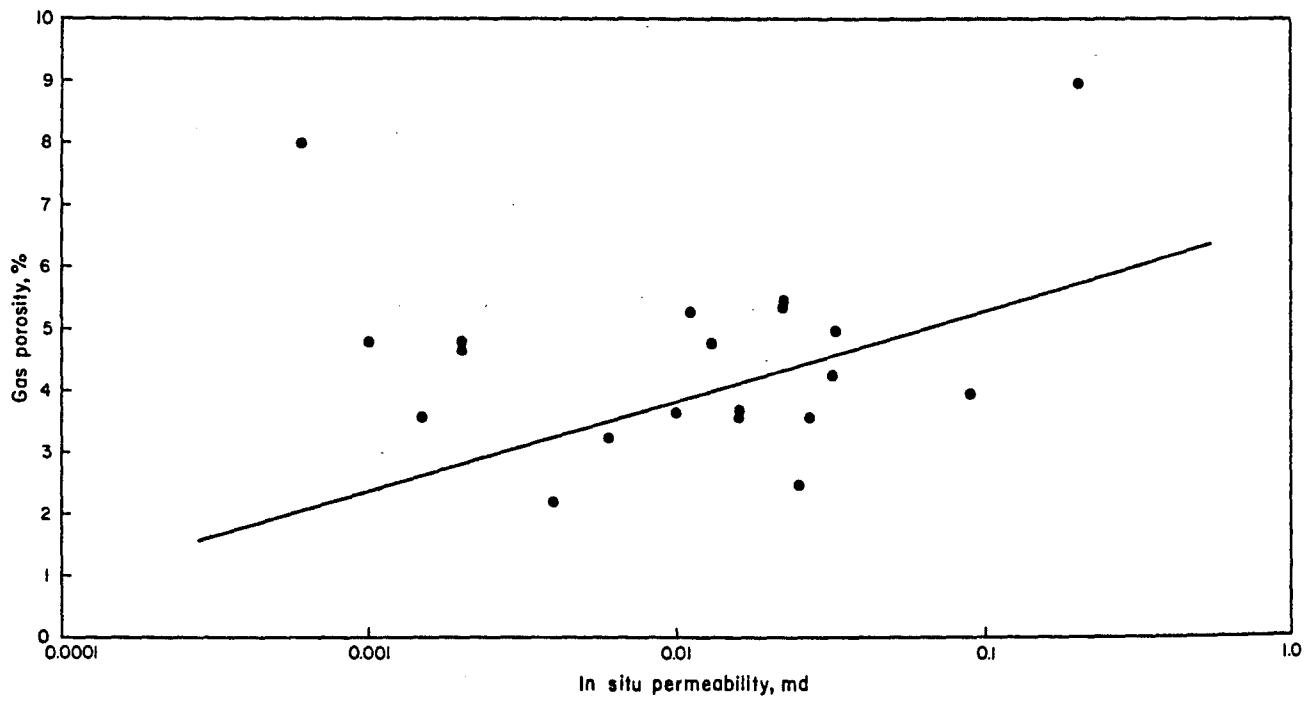


Figure 88. Gas porosity versus in situ permeability in the Travis Peak Formation, East Texas Basin.

displayed on a semi-logarithmic plot. A line through these data allows porosity and permeability values to be generally related (fig. 88) and used in the resource estimation. A similar plot is used to relate net pay and permeability (fig. 89) where no strong correlation exists. In addition, a line drawn to relate gas permeability and net pay is based on the assumption that when a well encounters a high permeability zone, the net pay tends to be small, whereas low-permeability zones will tend to be thicker. This relationship is not strong enough to warrant quantitative treatment but is commonly used in resource estimation.

A plot of area versus permeability (fig. 90) shows the distribution of in-situ gas permeability in the Travis Peak Formation. When the total productive area is known, each productive area with a given permeability can be estimated by using figure 90.

Values obtained from these plots were used to compute a resource estimate for the Travis Peak (table 10). It is assumed that data collected from hearing files of the Railroad Commission of Texas (approximately 40 wells with reasonably complete data) are generally representative of the engineering and geological characteristics of the whole basin. Using the assumption that 15 percent of the area of a tight gas basin may ultimately be productive (National Petroleum Council, 1980a), the estimated gas-in-place and maximum recoverable gas-in-place in the Travis Peak Formation in the East Texas Basin are 24.6 Tcf and 17.3 Tcf, respectively (table 10). In addition to the assumption that 15 percent of total basin area will be productive, gas resource estimates were also made for productive areas of 5 percent, 12 percent, and 20 percent of the total basin (table 11).

Frontier Formation, Corcoran-Cozzette Sandstones, and Upper Almond Formation

The gas resources of these formations, in part combined with those of other formations, have been estimated by the National Petroleum Council (1980b). In order to use these published data and to estimate the gas resource for each of these formations individually, a method of separating the combined resource estimates, the proportioning method, was used.

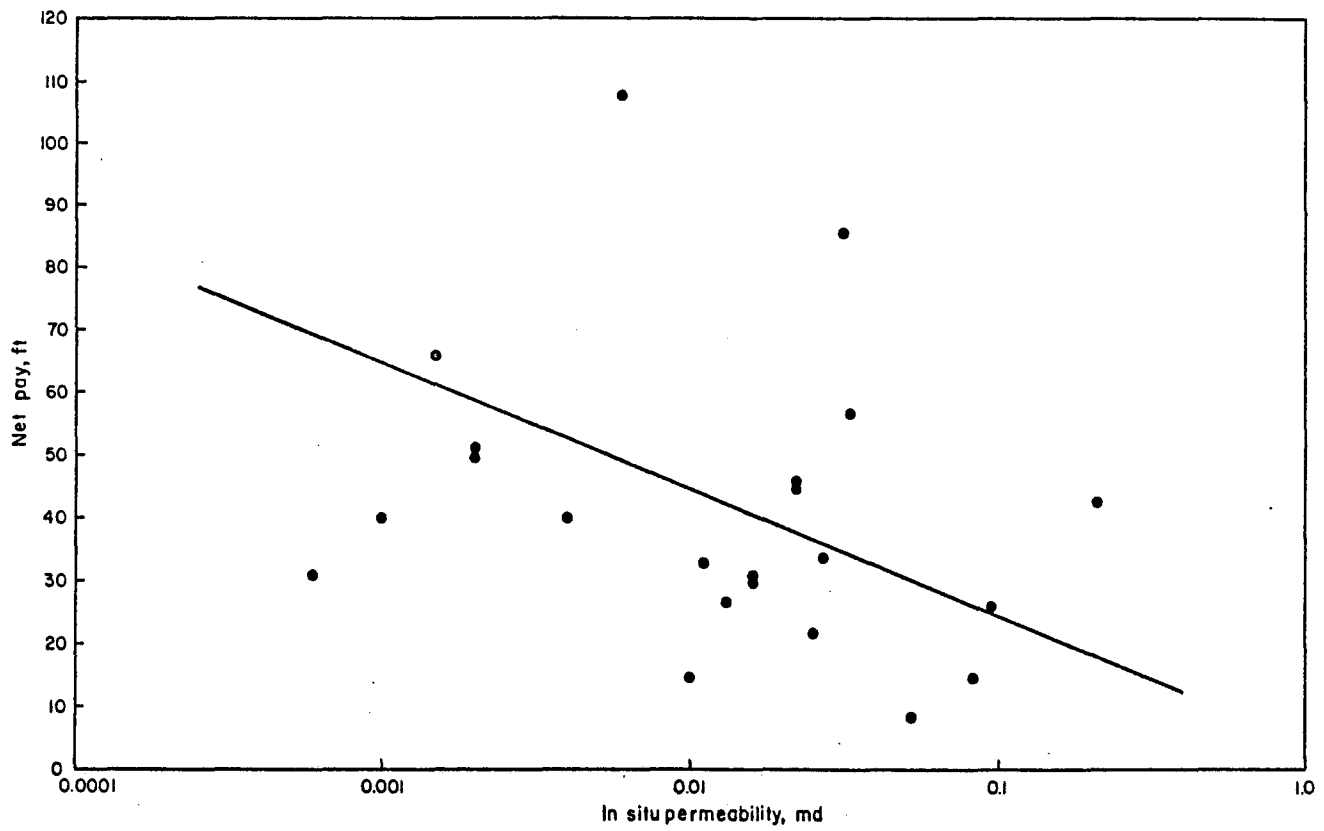


Figure 89. Net pay versus in situ permeability in the Travis Peak Formation, East Texas Basin.

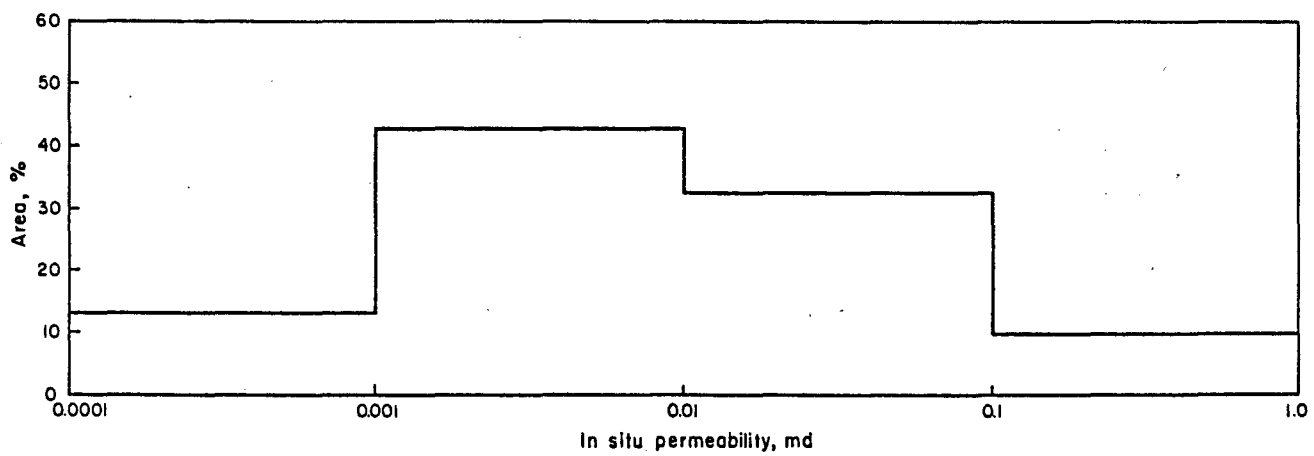


Figure 90. Distribution of in situ permeability in the Travis Peak Formation, East Texas Basin.

Table 10. Calculation of recoverable gas-in-place for the Travis Peak Formation in the East Texas Basin (assuming 15% of total area to be productive).

Permeability (md)	Net Pay (ft)	Gas Porosity (fraction)	Area (mi ²)	Gas-in-Place (Tcf)	Technical Recoverable GIP (Tcf)	Maximum Recovery Factor (fraction)	Maximum Recoverable GIP (Tcf)
0.1000	22.	0.052	135	1.08	0.96	0.90	0.86
0.0400	34.	0.048	515	5.86	5.24	0.85	4.49
0.0100	44.	0.038	704	8.22	7.33	0.80	5.87
0.0040	52.	0.032	352	4.09	3.65	0.76	2.76
0.0010	64.	0.022	352	3.46	3.09	0.70	2.16
0.0004	72.	0.018	216	<u>1.95</u>	1.74	0.66	<u>1.45</u>
				<u>24.67</u>			<u>17.29</u>

181

Initial formation pressure = 5,308 psi

Formation temperature = 258°F

Table 11. Gas resource estimates for the Travis Peak Formation in the East Texas Basin (assuming 5%, 12%, 15%, and 20% of total area to be productive).

<u>Percent of Total Area to be Productive</u>	<u>Gas-in-Place (Tcf)</u>	<u>Maximum Recoverable Gas-in-Place (Tcf)</u>
5	8.22	5.68
12	19.75	13.84
15	24.67	17.29
20	32.88	23.06

Gas resource estimates for the Frontier, Corcoran-Cozzette, and upper Almond are shown in table 12. Examples of detailed computations for the Frontier Formation, derived by the areal proportioning method, are illustrated in table 13(b) and figure 91. Examples of the volumetric proportioning method are given for the Frontier Formation in table 14 (combined with Mesaverde-Lance) and table 15 (uncombined portion). Table 12 shows that results from the areal proportioning method and from the volumetric proportioning method are very close; the areal proportioning method was arbitrarily chosen for preferred use in this study.

In the Frontier Formation, the estimated gas-in-place and maximum recoverable gas-in-place are 8.7 Tcf and 5.8 Tcf, respectively (table 12). The estimated gas-in-place and maximum recoverable gas-in-place for the Corcoran-Cozzette Sandstones are 5.2 Tcf and 3.7 Tcf, respectively (table 12). For the upper Almond Formation in Lewin areas 1, 2, and 3, the estimated gas-in-place and maximum recoverable gas-in-place are 4.9 Tcf and 3.4 Tcf, respectively (table 12). All areas for individual estimates are defined by National Petroleum Council (1980b).

Uncertainty in Gas Resources Estimates

Resource estimates are only as accurate as the available data and assumptions. Use of critical formation parameters from only a few wells to characterize the entire Travis Peak Formation in the East Texas Basin is a potential source of error which is difficult to quantify. Even with volumetric data, which confine the estimated gas resource within relatively narrow limits, there still exists a large, undefined uncertainty. The perfect resource estimate can only be made after well abandonment.

As this project proceeds, more data will become available to use in gas resource estimation and in quantification of the uncertainty associated with those estimates. Close coordination with, and support of, the work by Lewin and Associates will be maintained by the Bureau as part of the GRI focus on resource estimates.

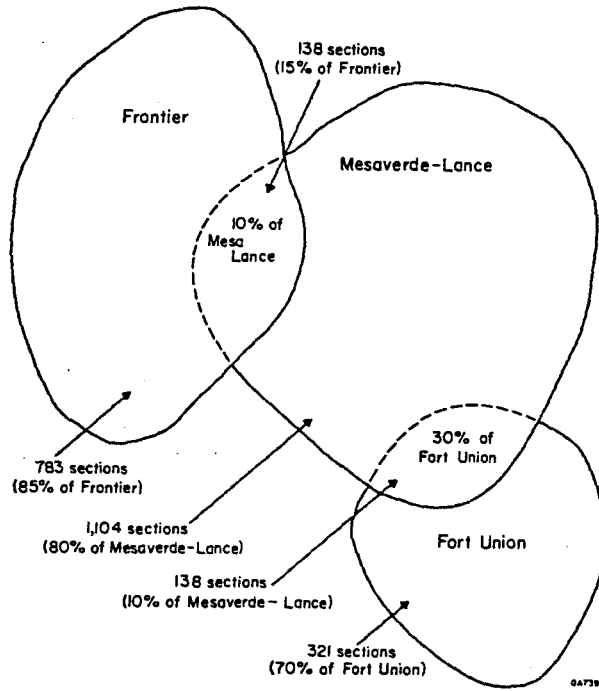


Figure 91. Proportions of Frontier Formation combined with other formations, by area.

Table 13. Data utilized and gas resource calculated for the Frontier Formation by the areal proportioning method.

(a) Published data from National Petroleum Council (1980b)

<u>After Combining Formations</u>	<u>Number of Sections</u>	<u>Maximum Recoverable GIP (Tcf)</u>	<u>GIP (Tcf)</u>
Fort Union (0.699)	321	2.87	4.75
Mesaverde-Lance (0.8)	1,104	7.54	12.87
Frontier (0.85)	783	4.92	7.39
Mesaverde-Lance (0.1) + Frontier (0.15)	138	1.80	2.73
Mesaverde-Lance (0.1) + Fort Union (0.301)	138	2.17	3.70

(b) Uncombined gas resource calculated by the areal proportioning method

<u>Before Combining Formations</u>	<u>Number of Sections</u>	<u>Maximum Recoverable GIP (Tcf)</u>	<u>GIP (Tcf)</u>
Fort Union	459	4.11	6.79
Mesaverde-Lance	1,380	9.43	16.09
Frontier	921	5.78	8.69

Table 14. Use of the volumetric proportioning method to calculate gas resource for Frontier Formation (portion combined with Mesaverde-Lance) in the Greater Green River Basin.

187

<u>Permeability (md)</u>	<u>Net Pay (ft)</u>	<u>Gas Porosity (fraction)</u>	<u>Area (mi²)</u>	<u>Gas-in-Place (Tcf)</u>	<u>Technical Recoverable GIP (Tcf)</u>	<u>Maximum Recovery Factor (fraction)</u>	<u>Maximum Recoverable GIP (Tcf)</u>
0.300	10.	0.064	1.38	0.01	0.01	0.95	0.01
0.100	14.	0.057	11.04	0.08	0.07	0.90	0.06
0.030	20.	0.050	32.12	0.28	0.25	0.85	0.21
0.010	25.	0.044	46.92	0.46	0.40	0.80	0.32
0.003	27.	0.039	26.22	0.24	0.21	0.75	0.16
0.001	29.	0.035	12.28	0.11	0.10	0.70	0.07
0.0003	30.	0.031	6.90	<u>0.05</u>	0.05	0.68	<u>0.04</u>
				<u>1.24</u>			<u>0.86</u>

Initial formation pressure = 7,700 psi

Formation temperature = 242°F

Table 15. Use of the volumetric proportioning method to calculate gas resource for Frontier Formation (uncombined portion) in the Greater Green River Basin.

<u>Permeability (md)</u>	<u>Net Pay (ft)</u>	<u>Gas Porosity (fraction)</u>	<u>Area (mi²)</u>	<u>Gas-in-Place (Tcf)</u>	<u>Technical Recoverable GIP (Tcf)</u>	<u>Maximum Recovery Factor (fraction)</u>	<u>Maximum Recoverable GIP (Tcf)</u>
0.300	10.	0.064	8	0.05	0.04	0.95	0.04
0.100	14.	0.057	63	0.44	0.39	0.90	0.35
0.030	20.	0.050	188	1.67	1.46	0.85	1.24
0.010	25.	0.044	266	2.60	2.27	0.80	1.82
0.003	27.	0.039	149	1.39	1.21	0.75	0.91
0.001	29.	0.035	70	0.63	0.55	0.70	0.38
0.0003	30.	0.031	39	<u>0.32</u>	0.28	0.67	<u>0.20</u>
				<u>7.11</u>			<u>4.95</u>

188

Initial formation pressure = 7,700 psi

Formation temperature = 242°F

EXTENT OF NATURAL FRACTURING AND THE DISTRIBUTION OF CLAY MINERALS

Introduction

A survey of industry personnel employed by operating and service companies was conducted to obtain data on natural fracturing and the distribution of clay minerals in six tight gas sandstones. Data are summarized in table 16, distribution of natural fracturing in six stratigraphic units, and table 17, distribution of clay minerals in six stratigraphic units. Industry personnel contacted were most cooperative and helpful and indicated interest in the tight gas sands project.

Discussion

Natural Fractures

Natural fractures noted in many oil and gas producing provinces are an aid to production when the fractures are interconnected and open to fluid flow. In tight gas sand provinces they may contribute to production; however, the typical case of near vertical fracturing may also prevent facies containment of a massive hydraulic fracturing (MHF) treatment by cutting across facies boundaries. This would certainly reduce the extrapolation potential of research results related to facies and depositional systems. Also, where natural fracturing is extensive, it is difficult to separate the respective contribution of fracture and matrix permeability to gas production, and short-term producibility of the fracture system may preclude the proper assessment of matrix characteristics.

The extent of natural fracturing in a given stratigraphic unit depends on (1) the degree of stress throughout the burial history and (2) the ductility of the rock. For those tight gas sand units investigated, a complete determination of the extent of natural fracturing was not possible due to lack of information. The most common procedure, that of examining cores from

Table 16. Distribution of natural fracturing in six stratigraphic units.

Tight Gas Sand Unit	Degree of Natural Fracturing in Cores	Other Evidence of Natural Fracturing	Effect on MHF Programs	Effect on Well Testing	Effect on Production	Comments
Travis Peak (Hosston)	Limited data.	Not common.	Limited effect on containment of MHF.	Buildup after production tests affected by presence or absence of natural fractures.	Not a limiting factor to production.	Natural fracturing not seen as restrictive factor in connection with selection as research area. Encouragement from industry as to value and need for additional research.
East Texas Basin	Not many cores taken but of those reported little or no fracturing noted.	Fracture finder logs not particularly helpful. Can be used under ideal conditions.				
North Louisiana Salt Basin						
Olmos Formation	Little evidence of natural fracturing, based on limited amount of core.	Minor degree of surface faulting; suggests less possibility for natural fracturing.	None apparent.	None apparent.	No particular effect.	Natural fracturing does not appear to be a major concern in connection with the tight gas sand resource.
Maverick Basin						
Corcoran/Cozzette	Several cores show fractures; degree of fracturing varies considerably.	Surface faulting and folding indicate that response to stress has produced natural fracturing in some areas.	Containment of MHF affected by degree of natural fracturing.	Buildup pattern after production test indicates degree of natural fracturing.	Moderate effect in specific areas.	Degree of fracturing varies with location in basin.
Piceance Basin						
Colorado						
Mancos "B"	Some fracturing noted in a limited number of cores.	Varies with position in basin. Surface faulting and folding suggest development of natural fractures; considerable variation in intensity is indicated.	Much higher than normal sand content used to compensate for natural fractures; higher injection rate also used.	Buildup pattern after production test (pre-MHF) determines degree of natural fracturing.	Seem to be able to compensate for natural fractures.	Extensive gross pay section and presence of natural fractures in some areas add to problems of containment for MHF.
Piceance Basin						
Colorado						
Upper Almond or Almond "A"	Less brittle, therefore less natural fracturing.	Stress conditions cause some natural fracturing; variable in degree.	Not considered a great problem, although natural fracturing does exist.	Buildup after pre-fracturing formation tests indicates extent of natural fracturing.	Moderate effect in specific areas.	Appears to be less susceptible to natural fracturing.
Greater Green River Basin						
Frontier Formation	More susceptible to fracturing; considerable variation depending on position in basin.	Several different logging techniques attempted, but not highly successful; sonic (micro seismogram), 4-arm dipmeter, and various cross plots tried. Techniques may detect presence of fractures but do not confirm permeability to fluid.	Difficulty in containment of MHF in zone of interest due (at times) to presence of pre-existent natural fractures. Problem varies in degree by area.	Extent of natural fracturing influences results of production tests and shape of buildup curves.	Alters rate of decline in some wells.	Varies from area to area but formation seen as susceptible to natural fracturing; presents some problems in resource evaluation as well as MHF containment.
Greater Green River Basin						

Table 17. Distribution of clay minerals in six stratigraphic units.

Tight Gas Sand Unit	Type and Quality of Clay Minerals Present	Effect on Drilling Programs	Effect on Completion Programs	Effects on Logging Programs	Effect on Well Testing, Buildup Tests, Production Tests (DST or others)	Comments
Travis Peak (Houston) East Texas Basin North Louisiana Salt Basin	Chlorite and illite present. Operators refer to sands as clean, fine to very fine grained and silty. Abundant calcite and silica cement. Clays present are mostly authigenic.	Some operators use KCl in drilling fluids. Not common practice.	Designed to prevent fresh or brackish water from contacting formation away from borehole in fractures. Reported use of kerosene, other chemicals, and limited use of CO ₂ in an attempt to limit migration of fines.	Special programs to assist in evaluation of clay types and amounts available, but not used extensively.	Pre-MHF testing is important in determining size of MHF to overcome damage.	Clays do not present excessive problem in evaluation or extraction of the resource; quartz overgrowths and calcite cement occlude most porosity.
Olmos Formation Maverick Basin	Abundant pore-filling clays. Illite, chlorite, kaolinite and some mixed layer smectite-illite present.	Presence of expandable clays requires foam drilling and other means to avoid excessive formation damage.	Use of kerosene and acid as fracture fluid reported; also, combination of CO ₂ and cross-linked methyl alcohol, or diesel oil and CO ₂ .	Neutron/density cross plots useful. Difficult to detect thin units, especially if KCl has been added to mud.	Pre-fracture testing; determine extent of damage and possibilities of successful MHF.	Use of pre-fracture injectivity survey important; significant clay problem exists.
Corcoran/Cozette Piceance Basin Colorado	Mixed-layer smectite-illite and authigenic illite, 3 to 19% of the rock unit.	Use of KCl in drilling fluid.	Use of small amount of KCl in fracture fluid.	Difficulties in interpretation of effective porosity and water saturation.	Mobility of clay particles presents problem for interpretation.	More detail presented in Corcoran/Cozette section of this report.
Mancos "B" Piceance Basin Colorado	Mixed layer smectite-illite. Abundant unstable clays.	Air drilled if possible; mist or KCl mud also used.	Use CO ₂ or nitrogen—also small amount of KCl in fracture fluid; chemical treatment for fines.	Type of fluid in hole at time of logging requires different interpretation techniques.	Very low matrix permeability presents difficulties in calculating reserves; problems in connection with rapid decline.	Thick section of gross pay invites concern that MHF may not reach all perforations; very rapid decline in rate of production may indicate degree of mobility of clay particles.
Upper Almond or Almond "A" Greater Green River Basin	Kaolinite, illite, montmorillonite; both authigenic and detrital clays common. Many feldspar grains that degrade readily to clays.	Many operators use small amount of KCl in drilling fluids, despite different opinions as to necessity.	Small amount of KCl used in completion fluids; chemical treatments used to reduce mobility of clay particles.	Comments range from no particular problem to use of special log interpretation formula. Washouts (borehole size compensation) present problems.	Use of pre-MHF formation tests (DST or other) common; buildup data critical in determining fracture size and probability of success.	Washouts common in producing trend and may be related to clay mineral problem.
Frontier Formation Greater Green River Basin	Mixed-layer smectite-illite; chlorite; montmorillonite (authigenic and detrital); feldspar grains that degrade readily to clays are present.	Many operators use small amount of KCl in mud. Necessity for this procedure is debated.	Small amount of KCl used in completion fluids; fracture fluids contain chemicals to reduce mobility of clay particles.	Washouts (borehole size compensation) seen as problem. Revised clean sand or shaly sand formula used for interpretation. Others dispute necessity for these special programs.	Pre-MHF testing determines degree of damage and possibility of success. Size of treatment also based on this evaluation plus core and logging information.	Swelling clays present; use of KCl fluids in drilling and completion.

the unit of interest, was inadequate in some areas because the number of cores available is very limited.

Fracture-finder logs, 4-arm dipmeter surveys, and microseismograms, among other logging programs, have been run in attempts to assess natural fracturing. Where there is some offset, these tools are able to detect fractures; however, their use is limited by an inability to determine the degree to which fractures are open. Under ideal well conditions significant improvement in determination of open fractures by logging methods can be obtained (Walter H. Fertl, personal communication, 1983). However, providing such ideal conditions in the well bore may not be cost-effective for the operator. Analysis of build-up curves from formation testing provides helpful information about the presence of open natural fractures; however, adequate build-up time in tight gas sand reservoirs is costly to the operator, and interpretation by this method is most often subject to a significant time constraint. Information was obtained and summarized (table 16) on: (1) degree of natural fracturing in cores; (2) other evidence of natural fracturing; (3) effect of natural fractures on MHF programs; (4) effect of natural fractures on well testing; and (5) effect of natural fractures on production.

Clay Minerals

One of the most common factors affecting the producibility of tight gas sandstones is the presence of clay minerals. Clays may be detrital and/or authigenic in origin and may include montmorillonite, chlorite, kaolinite, illite, and mixed layer smectite-illite. Certain transformations take place among these clay minerals due to changes in heat, pressure, pH, and Eh. Clays may either in part reduce, or be the primary cause of, the low permeability affecting production of the hydrocarbon resource. Pore lining, pore filling, and grain replacement by authigenic clays are of particular importance, as is the tendency of some clays to separate into loosely bound platelets upon contact with brackish or fresh water. These platelets, the "fines" of well treatment terminology, are highly mobile and frequently block the narrow pore throats connecting intergranular pore space.

Types and quantity of clay minerals present in the tight gas sandstones listed represent the consensus of those contacted in industry and is not intended as a complete listing of all minerals present or of all problems encountered. The Travis Peak (Hosston) and, to a lesser degree, the Frontier Formation, were consistently mentioned as units where clay minerals may not pose exceptional problems.

Drilling programs for the Olmos Formation in Texas, as well as for all of the Rocky Mountain units, have required modification due to the presence of clay minerals. The use of potassium chloride (KCl) in drilling fluid indicates concern for preventing contact of fresh water with expandable clays in the rocks drilled. The use of air and mist as drilling fluids is a response to the same concern.

Fluids used in the completion program were more important than fluids used in the drilling program. Mentioned were the use of kerosene, diesel oil, KCl, CO₂, nitrogen, and methyl alcohol, as well as other chemicals (various trade names) to reduce mobility of clay platelets.

The effect of clays on logging programs is discussed in detail by Kukal and others (1983). They found that conventional log analysis fails to adequately characterize tight gas sands, although significant emphasis is placed on log evaluation. Formation clay volume involved in correcting the responses of most logging tools is not accurately determined by current methods. Shale, shaly siltstones, and shaly sandstones are often treated similarly in log analysis but do not affect logging tool response in the same manner. Because shales typically contain approximately 60 percent clay minerals, these differences become important. The type of clay as well as its mode of distribution enters into the problem of log interpretation as different types cause different resistivity responses. Failure to recognize and correct the clay-related responses is seen as a significant detriment to resource evaluation.

The influence of clays on production testing is a subject requiring further investigation. Many of those responding remarked on the necessity of conducting pre-MHF testing, particularly pressure draw-down and build-up tests, but the relative importance of natural fracturing

and clay minerals in these tests remains unclear. Low rate of flow and the presence of water during test periods were also mentioned as problems in the interpretation of test results.

Table 17 summarizes information obtained in connection with clay minerals, including (1) type and quantity, (2) effect on drilling programs, (3) effect on completion programs, (4) effect on logging programs, and (5) effect on well testing (DST, production, etc.).

Summary

Many questions remain unanswered in connection with natural fracturing and the presence of clays in evaluation and development of the tight gas sand resource. The interest and cooperative attitude of industry personnel is indicative of the need for further research and is certainly an encouraging development.

The degree of natural fracturing, which bears a close relation to stress regimes, does not appear to pose too great a concern for the two Texas (and Louisiana) units. Even in the Rocky Mountain regions, care can be taken to avoid local areas where surface or other indicators suggest the presence of extensive fracturing that might affect the GRI research program. Structural studies should be used to complement stratigraphic studies when evaluating tight gas sand reservoirs.

Research into alleviating formation damage due to clay minerals has been extensive and fruitful, and yet most respondents agree that additional research is needed. This is true in nearly all domains: drilling, coring, testing, logging, fracturing, evaluation, and production. Drilling and coring programs to better evaluate tight gas sand reservoirs can be designed by careful consideration of all factors including that of cost. In some instances, casing set immediately above the zone of interest has allowed low-water loss muds or other drilling media to replace possible contaminating fluids with considerable improvement in hole conditions. Others have questioned the need or desirability of such programs; however, this latter viewpoint is definitely that of a minority.

Open-hole and/or cased-hole formation testing is an area receiving considerable attention. Difficulties in isolating potential reservoirs in tight gas sands in open hole have limited the use of formation testing, yet this period prior to casing and perforating is the time of minimum damage. Some experimentation with down-hole logging while drilling may improve reservoir determination and permit better open-hole testing. Further improvements are possible. Use of multiple-opening formation testing devices may also be practical under certain conditions. Cased-hole formation testing eliminates problems of packer seat selection, yet combined formation damage from drilling and running casing may prevent satisfactory testing. Better coordination of drilling and testing programs could lead to improvement in this area. The extensive time required for adequate pressure build-up in testing is a problem. Elimination or reduction in damage is seen as a key to this problem, although the very low permeabilities involved will still require considerable time for the disturbed pressure to reach equilibrium. Improved surface recording of pressure information in digital form might allow better projections of build-up data.

Research and development of natural gamma-ray spectral logging programs is seen as a possible solution to problems involving clay mineral types and volumes. Interpretation programs have been formulated, but the less than enthusiastic response to their use indicates further improvements may be necessary.

Research on fracturing (MHF) has proceeded rapidly, and many improvements have been reported, but failures and partial successes in fracture stimulation indicate the need for continued study. Fracture fluids as well as proppants have benefited from research on transporting large quantities of proppant at a high velocity over long distances. Fluids having high conductance and minimum density are the goal of these studies.

A principal concern in all these areas is that of cost-effectiveness. Particular conditions or treatments permit improvements in many of these areas, but cost considerations prevent their widespread acceptance. Additional or new research initiatives to resolve these concerns would be of great interest to operators and service companies and would be supported.

Although clay minerals are present in all the units investigated, current information indicates there would be fewer problems associated with clays in the relatively clean Travis Peak (Hosston) of the East Texas Basin and North Louisiana Salt Basin, parts of the Frontier Formation of the Greater Green River Basin, and the Corcoran-Cozzette of the Piceance Basin. Different opinions have been expressed as to the relative degree of clay problems even in these units, which suggests that further investigation is warranted.

DISCUSSION: PHASE A

Finley (1982) found that the deltaic and barrier-strandplain depositional systems included most of the blanket-geometry tight gas sandstones suitable for a major GRI research program. The Mancos "B" interval of the Mancos Shale is representative of a third depositional system, that of the intracratonic shelf; however, its extrapolation potential is limited when the shelf units already under study as part of the Western Gas Sands Project are excluded from further consideration. Analysis of the Mancos "B" for this report confirmed that its distribution of lithologies and other physical characteristics make it a tight gas reservoir very different from units with discrete sandstone beds bounded by shale and readily resolved on well logs. Extensive faulting and jointing on the Douglas Creek Arch, a primary area of Mancos "B" exploration, make it unsuitable as a research area focusing primarily on enhancement of production from matrix permeability. These characteristics were recognized early in this study as factors obviating further consideration of the Mancos "B"; our analysis of this unit is therefore limited.

The Olmos Formation of the Maverick Basin was not among the five formations originally recommended for additional study by Finley (1982), but it was described as representative of areally more restricted delta systems. Among the more than 30 stratigraphic units considered by Finley (1982), the Olmos Formation was the next leading candidate beyond the originally recommended five units. Because the Mancos "B" was not suitable for a major GRI program, the Olmos Formation was added to this study. Moderate drilling depths, operator interest, and appropriate depositional systems make the Olmos potentially attractive for further research.

Refinement of Depositional Systems Interpretations

The primary purpose of this study has been to verify and expand upon the information collected and conclusions drawn from a national survey of tight gas sandstones. The survey by Finley (1982) relied almost exclusively on published and unpublished interpretations by other researchers. Acquisition of base maps and well logs and the completion of selected cross

sections and maps included herein provide new data on depositional systems. No major differences were found between previous work and results reported here that would negate further consideration of any unit, except for the Mancos "B", as outlined above. For the Frontier Formation, differences between this work and numerous past studies are mostly related to different approaches to stratigraphic interpretation, to selection of formation boundaries, and to terminology used for subdivision of the Frontier and of adjacent units. New interpretations of depositional systems of the Travis Peak Formation, Olmos Formation, and Corcoran and Cozzette Sandstones were made where very limited previous studies were available. Interpretation of the upper Almond Formation was consistent with previous literature, and mapping of this unit defined the marginal marine part of the Almond over a wide area. Previously the upper Almond had been defined on only a few type logs and on maps and cross sections limited to specific fields.

Travis Peak Formation

Time available for this study permitted only a preliminary evaluation of the Travis Peak Formation in East Texas and a part of North Louisiana. Three generalized subdivisions of the Travis Peak were established, relating to progradation, aggradation, and ultimate transgression of the formation, followed by carbonate shelf deposition. The lower and upper units have the best continuity of individual sandstones between wells spaced a mile or less apart. These units are expected to include sandstones with the best continuity from the viewpoint of development geology and engineering. The middle unit is probably dominated by braided alluvial plain deposits. As such, the individual sandstones of the middle unit are likely to be broadly lenticular with greater potential for interconnection than in a mud-rich meandering fluvial system.

The Travis Peak as a formation probably has the best overall blanket-geometry of those stratigraphic units reported on by Finley (1982). It is a widespread, relatively thick, sand-rich unit; however, from the viewpoint of well stimulation and other engineering practices, some of

its contained sandstones appear to be broadly lenticular, primarily within the middle part of the formation. The sand-rich nature of the formation tends to reduce the certainty, in some instances, with which individual sandstones can be correlated between wells. Better continuity is associated with the more marine-influenced sandstones. Because of its sand-rich nature, thickness variations due to salt tectonics, and the lack of previous studies on the Travis Peak, future geological investigation of this unit will be challenging. The Travis Peak is expected to ultimately be a major tight gas producer in view of the resource estimates reported herein.

Olmos Formation

Examination of the wave-dominated deltaic deposits of the Olmos Formation included in this report represents the first up-to-date regional analysis of the depositional systems of the Olmos in the Maverick Basin. The tight, blanket-geometry sandstones that are gas-productive in the Olmos include delta front, barrier-strandplain, and deeper-water delta-front splays deposited on a shelf in front of prograding deltas. Gas is also produced from deltaic distributary channel sandstones that are lenticular. Thus the Olmos illustrates the expected juxtaposition of closely related depositional systems, such as deltaic and barrier-strandplain systems, as well as gas production from a variety of facies.

The Olmos is significantly more limited in areal extent than the Travis Peak, and its contained sandstones are better delimited by enclosing shale beds than in the latter formation. The presence of greater thicknesses of shale between sandstones relative to the Travis Peak is characteristic not only of the Olmos but also of the Frontier Formation. An estimate of the recoverable tight gas resource in the Olmos remains to be completed, but it appears that this resource will be smaller than that in the Frontier Formation and far smaller than that in the Travis Peak Formation in Texas alone.

Corcoran and Cozzette Sandstones

An improved understanding of the Corcoran and Cozzette Sandstones as marginal marine components of the Mesaverde Group has emerged from this investigation and from recent,

limited analysis of the Corcoran and Cozzette as part of the Western Gas Sands Project (Lorenz, 1982 and 1983). These units consist of barrier and shallow marine bar facies and are expected to be similar to Mesaverde regressive and transgressive shoreline deposits in several Rocky Mountain Basins. The correlation of subsurface log facies indicative of possible barrier trends and the strandline positions inferred from Warner (1964) and Gill and Hail (1975) suggests that back-barrier, barrier, and offshore marine bar facies will be important elements of study in any future investigations of the Corcoran and Cozzette Sandstones.

The Rollins Sandstone, which overlies the Cozzette but is separated from it by a tongue of the Mancos Shale, is expected to contain some facies similar to the Corcoran and Cozzette. The Rollins, however, prograded across the entire present area of the southern Piceance Creek Basin in advance of Mesaverde continental deposition, and shoreface to barrier deposition may be dominant in relation to the marine-bar facies component of the Corcoran and Cozzette. The development of the marine bar facies in the latter units is a function of the Corcoran-Cozzette progradation "stalling out" and not pushing the Mancos sea entirely beyond the southeastern limits of the present basin. The upward-coarsening to blocky log character of the Rollins is much more laterally persistent than any of the log character types of the Corcoran or Cozzette. The excellent blanket-geometry of the Rollins may be detrimental to its function as a reservoir, however, because its excellent continuity may maximize the potential for gas leakage to the surface without trapping (C. Brown, personal communication, 1982). In view of this consideration, and the relatively poor production record of the Rollins, the Rollins Sandstone will clearly be of secondary interest in any study of Corcoran and Cozzette tight gas potential.

Upper Almond Formation

The upper Almond Formation bears some similarity to the Corcoran and Cozzette Sandstones in that barrier and offshore bar facies are major constituents of the formation. However, the upper Almond is a much thinner unit than the Corcoran or Cozzette and

frequently consists of only one, or more rarely, two, major sandstone beds. The upper Almond is essentially the basal transgressive deposit of the Lewis sea, which deposited the overlying marine Lewis Shale. The upper Almond rises stratigraphically and becomes younger toward its western limit of deposition along the present Rock Springs Uplift.

Few wells appear to be drilled to only the upper Almond in the eastern Greater Green River Basin. Many wells targeted for the Mesaverde test all of the Almond and some test part of the underlying Ericson Formation. The lower Almond and the Ericson are expected to contain primarily lenticular sandstones as a product of fluvial channel and floodplain deposition (Newman, 1981). A large number of successful wells are completed in more than one interval of the Mesaverde, as is indicated by the few fields that uniquely produce gas from the blanket-geometry upper Almond (table 7). The upper Almond is therefore a very limited part of the Mesaverde tight gas sandstone target in the eastern Greater Green River Basin. The opportunity to stack the upper Almond with additional exploration targets of blanket geometry within the Mesaverde Group is limited except for some marginal marine deposits that may exist in the Blair Formation (fig. 63). Few Mesaverde wells are drilled as deep as the Blair Formation. The GRI research program may more suitably seek stacked blanket-sandstone targets that are more frequently penetrated by ongoing exploration programs.

Frontier Formation

Within the Greater Green River Basin the basal Upper Cretaceous Frontier Formation is a major regressive deposit with multiple deltaic depocenters. Minor transgressions and regressions alternated within the overall transgressive sequence, and the Frontier is bounded above and below by marine shales (Mowry and Baxter, respectively, and their equivalents). Much of the Frontier gas production can be related to fluvial channel and other proximal deltaic facies with limited lateral extent of sandstones. Of interest in this study is the barrier depositional system with associated offshore bars, which was fed by deltaic sediments redistributed by longshore currents. These bar sands are found on the Moxa Arch, the Rock Springs Uplift, and

the eastern margins of the Red Desert and Washakie Basins. Barrier and marine bar sandstones are also extensive in the Wind River Basin and are evidence of the potential for Frontier gas production outside the Greater Green River Basin (Finley, 1982). Numerous offshore bar sandstones on the Moxa Arch, on the Rawlins Uplift, and probably also on the Rock Springs Uplift, are associated with the postulated Wind River Delta. These are the Frontier sand bodies included within several tight gas sand applications, and the barrier and offshore bar facies may be encountered as more drilling takes place on deep basin flanks. The extrapolation potential of these facies, associated with a major deltaic system, to similar facies in other basins is not to be overlooked even though in other basins, such as the Piceance Creek Basin, the deltaic source facies may not be represented.

Extrapolation Potential

Extrapolation potential, or the expected transferability of geologic and engineering knowledge gained in the study of any given formation, was summarized briefly by Finley (1982) and is included herein in table 1. No substantial changes in these original assessments are required as a result of this investigation. Component facies have been better identified for the depositional systems making up each unit, and a clearer understanding of the distribution of these facies has been gained. For example, much of the tight gas potential in the Frontier Formation is from offshore bar and barrier sandstones transported along strike from deltaic depocenters. Similarly, portions of the Corcoran and Cozzette Sandstones seaward of the paleoshoreline trend are now considered likely to be offshore bar sandstones. These observations suggest increased extrapolation potential between the Corcoran and Cozzette Sandstones and parts of the Frontier Formation which was not envisioned when the latter unit was simply designated as a wave-dominated deltaic system (Finley, 1982).

Additional well log data from the Mancos "B" supported the interpretation that it is a marine shelf deposit, but also confirmed that its extrapolation potential was limited to few other units if formations in the Northern Great Plains Province of the Western Gas Sands

Project are excluded from further study. Thus, the Mancos "B" was only briefly treated in this study and the Olmos Formation was added to the group of stratigraphic units studied. With removal of the Mancos "B" from further consideration, all remaining units represent either deltaic or barrier-strandplain depositional systems. These depositional systems are not mutually exclusive, however, and the Frontier Formation is a good example of barrier (and marine bar) sandstone bodies closely associated with deltaic depocenters.

CONCLUSIONS: PHASE A

Blanket-geometry tight gas sandstones suitable for additional research by the Gas Research Institute are part of deltaic and/or barrier-strandplain depositional systems. Because previous work on shelf systems within the Western Gas Sands Project is extensive (Rice and Shurr, 1980), no additional intracratonic shelf systems meet GRI criteria for new work on significant, laterally extensive sandstones. Offshore bar sandstones, consisting of discrete sandstone bodies rather than siltstones and sandstones interbedded at spacings below the resolution of logging tools, are considered an integral part of the barrier-strandplain system. Such marine bars are often dependent on longshore currents or shelf currents for their sediment supply in the same way as a barrier-strandplain system. The Frontier Formation illustrates the relationship between the barrier-strandplain system, including offshore bars, and the updrift, deltaic depocenter acting as a sediment source.

No major differences were noted between the depositional systems generally outlined by Finley (1982) and the results of this study. Lateral and vertical facies variations within each stratigraphic unit have been better defined, and work reported here forms the basis for more detailed study of any of these blanket-geometry tight gas sandstones.

The Travis Peak Formation has been tentatively divided into three subunits with a braided alluvial facies dominating the middle unit and more marginal marine influence evident in the upper and lower units. The formation is present over a wide area, including the salt basins of East Texas and North Louisiana, and salt tectonics have caused variations in thickness of the Travis Peak. The potential resource of 17.3 Tcf in the Travis Peak in Texas alone makes this unit an attractive research candidate, and much of the desired extrapolation potential is within the Travis Peak itself because of its wide areal extent. The Travis Peak is therefore recommended for additional research.

The Olmos Formation contains deltaic and barrier-strandplain facies in two subbasins of the Maverick Basin; the better sand development occurs in the southern subbasin. Delta front

sandstones, shelf sandstones that probably represent delta front splays, and barrier sandstones are potential tight gas producers. A tight gas resource estimate for the Olmos Formation is in preparation. The Olmos occurs at relatively favorable drilling depths. It is recommended that further research on the Olmos not be considered at this time, but that (1) a resource estimate be completed, and (2) the Olmos be considered for testing of specific facies outside of any of the recommended formations if needed during further research.

The Corcoran and Cozzette Sandstones contain barrier core, shoreface, and offshore bar facies representative of marginal marine sandstones of the Mesaverde Group in several Rocky Mountain Basins. These sandstones occur at reasonable drilling depths, and together with a secondary emphasis on the Rollins Sandstone, offer the opportunity to investigate multiple formations with similar depositional environments. Major deltaic systems, such as occur within the Frontier Formation, include related development of barrier and offshore bar facies; therefore, the extrapolation potential of Corcoran and Cozzette studies extends to parts of the Frontier Formation and parts of other stratigraphic units considered to be dominantly deltaic. A resource estimate of 3.7 Tcf for the Corcoran-Cozzette represents a reasonable target for explorationists, but topographic constraints on surface access in parts of the Piceance Creek Basin mitigate against full recovery of this resource. It is recommended, however, that the Corcoran and Cozzette Sandstones be considered for additional research.

The Mancos "B" interval of the Mancos Shale is not recommended for any additional research on blanket-geometry sandstones. Its distribution of lithologies differs from all other units considered and from the larger group of units outside of the Northern Great Plains Province described by Finley (1982).

The upper Almond Formation is an informal designation for a blanket-geometry sandstone (or sandstones) at the top of the Almond Formation in the eastern Greater Green River Basin. This part of the Almond is described in the literature, based on both outcrop and subsurface field studies. This report, however, includes the first basinwide map of the upper Almond. The upper Almond is 25 to 75 ft thick over much of its area of deposition, and often consists of only

major barrier or offshore bar sandstone isolated between marine shale (Lewis Shale) and particular, continental sandstones making up the lower Almond. It is therefore a limited location target, generally is at greater depths than the Corcoran and Cozzette Sandstones, is overpressured in basin centers and on deep basin flanks. In view of these findings, the lower Almond Formation is not recommended for additional research. As in the case of the others, however, wells testing the upper Almond may be considered for tests of specific geologic or engineering applications where depth, thickness, and pressure gradients do not present constraints on extrapolation potential or research cost.

The Frontier Formation includes deltaic and barrier-strandplain depositional systems and extends over a wide area of western Wyoming. Much of the blanket-geometry tight gas sand potential is in barrier and offshore bar sands with sources in several different deltaic centers. These barrier and offshore bar sands are expected to be major future gas producers. The stratigraphy of the Frontier is complex; this study did not allow time to adequately examine many aspects of the Frontier, such as the distribution of unconformities. Well control for the Frontier is mostly limited to (subsurface) structural positives, but may even be sparse on these features where shallower hydrocarbon reservoirs are present. Much of the present and future potential development of the Frontier will be in areas with drilling depths in excess of 12,000 ft. The Frontier contains numerous blanket to near-blanket sandstones, but development of these sandstones will be constrained by the economics of moderate (around 10,000 ft) to deep (over 15,000 ft) drilling. This same factor also affects the economics of potential research and development programs in the Frontier. It is recommended that the Frontier be considered for testing of specific facies or of particular engineering practices where experience is required at greater depths, but it is not recommended that the Frontier be a primary candidate for additional research.

PHASE B: INITIAL STUDIES

INTRODUCTION: PHASE B

During Phase B of the contract period, work proceeded on geologic framework studies and on delineation of depositional systems of the Corcoran and Cozzette Sandstones in the Piceance Creek Basin and of the Travis Peak Formation in the East Texas Basin. The objective of this phase of work was to provide a foundation upon which detailed studies of reservoir geometry, diagenesis, and resource distribution may be based. Not all objectives of this phase of work were accomplished, however, because budget constraints imposed on the project limited staff time and precluded necessary expansion of the well-log data base over a 3.5-month period. Despite these restrictions, work proceeded on facies delineation in areas where well control was available. In the Piceance Creek Basin, this area centered on Shire Gulch and Plateau Fields, and in the East Texas Basin fields on the west flank of the Sabine Uplift in Harrison, Gregg, Rusk, Panola, and parts of Nacogdoches and Shelby Counties. These areas in both basins are the centers of the most recent operator activity, and, for the Shire Gulch - Plateau Field area, are the location of several potential cooperative coring and logging operations during the 1983 drilling season.

TRAVIS PEAK FORMATION, EAST TEXAS

During Phase B of the contract period, studies of the Travis Peak Formation in East Texas emphasized assembly of a regional subsurface data base, regional synthesis of depositional systems, and subregional or local detailed studies of depositional systems and facies in areas where the Travis Peak is productive. Detailed studies examined controls on gas production in Panola, Gregg, and Rusk Counties. Drilling activity in the Travis Peak was tabulated for the first half of 1983.

Depositional Systems

Systematic and repetitive well log patterns were used to divide the Travis Peak Formation into three major genetic packages:

- 1) a lower progradational delta system,
- 2) a middle aggradational fluvial system, and
- 3) an upper recessive facies tract including fluvial, strandplain-deltaic-tidal flat, and marine systems

The contacts between genetic packages are gradational. Also, the contact between the Travis Peak and the overlying Pettet Formation is transitional.

The Travis Peak Formation is underlain by the Jurassic Knowles Limestone or the Cotton Valley Sandstone and overlain by the Lower Cretaceous Pettet Limestone. Because the Travis Peak is conformably bounded above and below by marine limestones, it must comprise a single progradational and recessive facies tract.

The lower part of the Travis Peak is a progradational deltaic sequence. In the northern part of the Sabine Uplift area, the progradational sequence is only 100 to 300 ft thick. The lower part of the Travis Peak thickens southward and in southern Panola County the thickness exceeds 700 ft. According to hearing files of the Railroad Commission of Texas (1981b), the lower part of the Travis Peak consists of interbedded massive and lenticular sandstones, gray shales, and abundant lignite.

No gas in the Travis Peak is produced exclusively from the lower zone, although some wells in Joaquin, Tri Cities, and Freestone Fields are perforated there.

The middle part of the Travis Peak is sand rich. Sand bodies characteristically display a blocky spontaneous potential (SP) pattern. Individual sand body thickness ranges up to 250 ft, and thin mudstones separate sand bodies. Thin progradational packages 10 to 50 ft thick flank areas of thick net sand. The blocky SP patterns and paucity of matrix mudstone indicate that the fluvial systems were dominantly of the bed-load type. Braiding may have been common due to lack of mud for levee development.

No Travis Peak fields produce exclusively from the middle sequence. However, most of the producing wells in Lansing North and Tri Cities Fields produce from the central sand-rich sequence.

The upper part of the Travis Peak is a recessive facies tract that includes fluvial, strandplain-deltaic-tidal flat, and marine facies. Most of the production in the Travis Peak is from this recessive facies tract. Strandplain and shallow marine sandstone are the productive units in this facies tract. They were deposited during a period characterized by a relative rise in sea level.

Many Travis Peak fields produce gas almost exclusively from the upper recessive facies tract. Bethany, Carthage, and Trawick fields all produce from sandstones in the upper sequence. The perforated zones are much thinner and shallower in Bethany and Carthage fields than at Trawick field.

Relationships among the three major facies subdivisions in the Travis Peak Formation are illustrated in cross section in figures 92, 93, 94, 95, and 96. A list of the wells on cross sections A-A' and B-B' is given in Tables 18 and 19, respectively.

Whelan Field Area

Figure 92 shows the Travis Peak Formation at Whelan Field, Harrison County, where gross perforated intervals often include both the upper transitional facies and the middle fluvial facies. In the Whelan Field area fluvial facies are the thickest. Blocky SP patterns are common, indicating sand transport and deposition by bed-load or braided streams. Many of the sand bodies within this facies are greater than 50 ft thick. They show good lateral continuity between wells 1 to 3 mi apart. In the lower part of the fluvial facies, SP patterns include upward-fining sandstone packages with abrupt basal contacts. These sandstone packages are interpreted to be locally developed meandering fluvial channels. The lateral continuity of sandbodies deposited by meandering fluvial systems is less than the continuity of sandbodies deposited by the braided system.

WHELAN FIELD, HARRISON COUNTY, TEXAS

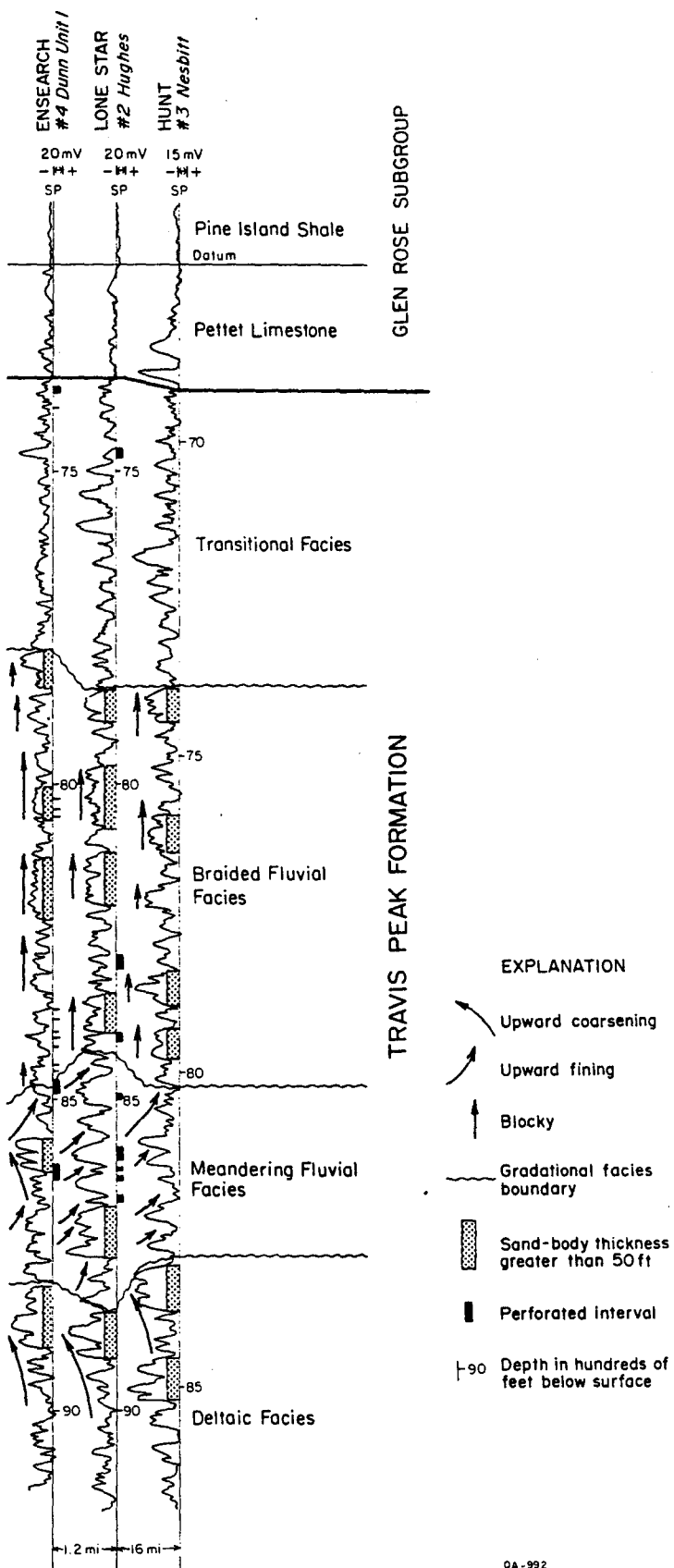


Figure 92. Cross section of Travis Peak Formation at Whelan Field showing depositional facies and perforated zones.

Table 18. List of wells used in cross section A-A',
Travis Peak Formation, East Texas.

Cross Section Well	BEG Number	County	Operator	Well Name
1	WR-35-60-799	Rusk	Goldsmith	2 Lawler
2	WR-35-60-498	Rusk	Seagull	1 Mauritzen-Cyphers
3	WR-37-01-499	Rusk	Samedan	1 Motley
4	WR-35-60-199	Rusk	Seagull	1 Smith
5	WR-35-59-399	Rusk	Arcadia	1 Bridges
6	WR-35-52-798	Rusk	Arkla	1 Duran
7	WR-35-52-799	Rusk	Arkla	2 Duran
8	WR-35-51-696	Rusk	Remuda	1 Prior GU
9	WR-35-51-697	Rusk	Remuda	1 Carter
10	WR-35-51-698	Rusk	Amoco	1 Strong A
11	WR-35-51-699	Rusk	Amoco	1 Strong B
12	WR-35-51-399	Rusk	Amoco	1 Swiley
13	WR-35-52-199	Rusk	Pioneer	1 Wilkins
14	WR-35-52-198	Rusk	Amoco	1 Kangera
15	WR-35-51-398	Rusk	Pioneer	1 Isaac
16	WR-35-44-798	Rusk	Amoco	1 Hair
17	WR-35-44-799	Rusk	Amoco	1 Wallace
18	WR-35-43-699	Rusk	McCormick	1 Longhorn GU
19	WR-35-44-498	Rusk	Forgotson	1 Williamson Heirs
20	WR-35-43-697	Rusk	McCormick	3 Rogers GU
21	WR-35-43-596	Rusk	McCormick	3 Thornton
22	WR-35-43-695	Rusk	McCormick	3 Gray GU
23	WR-35-43-299	Rusk	Cotton	1 Gandy
24	KU-35-35-999	Gregg	Tomlinson	2 Grissom
25	WR-35-36-897	Rusk	Tomlinson Interest	1 Bailey/Sheppard et al.
26	WR-35-36-898	Rusk	Champlin	5 Bailey/Sheppard

Table 19. List of wells used in cross section B-B',
Travis Peak Formation, East Texas.

Cross Section Well	BEG Number	County	Operator	Well Name
1	WR-35-43-597	Rusk	McCormick	1 Delta GU
2	WR-35-43-697	Rusk	McCormick	3 Rogers GU
3	WR-35-43-699	Rusk	McCormick	1 Longhorn GU
4	WR-35-44-798	Rusk	Amoco	1 Hair
5	WR-35-51-398	Rusk	Pioneer	1 Isaac
6	WR-35-52-199	Rusk	Pioneer	1 Wilkins
7	WR-35-52-198	Rusk	Amoco	1 Kangera
8	UL-35-52-501	Panola	Dallas Exploration	1 T.B. Waits
9	UL-35-53-498	Panola	Marshall	Pellham 1
10	UL-35-53-497	Panola	Getty	2 Spencer
11	UL-35-53-599	Panola	Champlin	4 Carthage GU 20
12	UL-35-53-601	Panola	Chicago	1 McNee
13	UL-35-53-602	Panola	Chicago	2 Carthage GU 3
14	UL-35-54-498	Panola	Pennzoil	2 Moore GU
15	UL-35-54-597	Panola	Exxon	2 Gholston
16	UL-35-54-596	Panola	Arkla	1 Neal
17	UL-35-54-696	Panola	Pennzoil	3 Morgan
18	UL-35-54-998	Panola	Pennzoil	21 Hull A
19	UL-35-55-798	Panola	Pennzoil	15 Hull A

Rusk and Panola Counties Area

Cross section A-A' (figs. 93 and 94) in Rusk County and B-B' (figs. 95 and 96) in Panola and Rusk Counties (location map is fig. 97) are an interesting contrast to the short cross section in Whelan Field. Cross sections are constructed from close-spaced wells penetrating the entire Travis Peak Formation. Most of these wells produce hydrocarbons from the Cotton Valley Group or were dry holes, thus there are no perforated intervals in the Travis Peak. Cross sections were made along each line of wells. Sandstone and mudstone were interpreted from SP logs (figs. 93 and 95). The sandstone-mudstone line was drawn at 25% of the deflection of the SP curve from shale baseline. Genetic interpretations within the Travis Peak include well-to-well correlations of upward-coarsening progradational sequences and aggradational sandstones in sand bodies greater than 50 ft thick. Permeable oolite shoals, characterized by strong negative SP deflection, within the Pettet Formation were also correlated. These shoals are inferred to be the best available time lines.

Cross section A-A' is oriented north-south along depositional dip, and cross section B-B' is oriented east-west along depositional strike. The effect of this orientation on thickness, lateral continuity of aggradational sandbodies, in offlapping character of progradational sequences at the base of the formation, and in onlapping character of oolite shoal sequences in the Pettet Limestone is easily compared on strike and dip sections. Each of these features will be discussed in turn.

Thickness Variations

On both cross section A-A' and B-B' (figs. 93 and 95), the Pettet and the Travis Peak Formations thicken to the south and to the east. The southward thickening is a part of the regional gulfward thickening that continues at least until the Angelina-Caldwell flexure. West of the area of cross section A-A', the Travis Peak Formation thickens into the axis of the East Texas Basin in Anderson, Cherokee, and Smith Counties. From Rusk County, the Travis Peak thickens toward the east and over the crest of the Sabine Uplift. These thickness variations

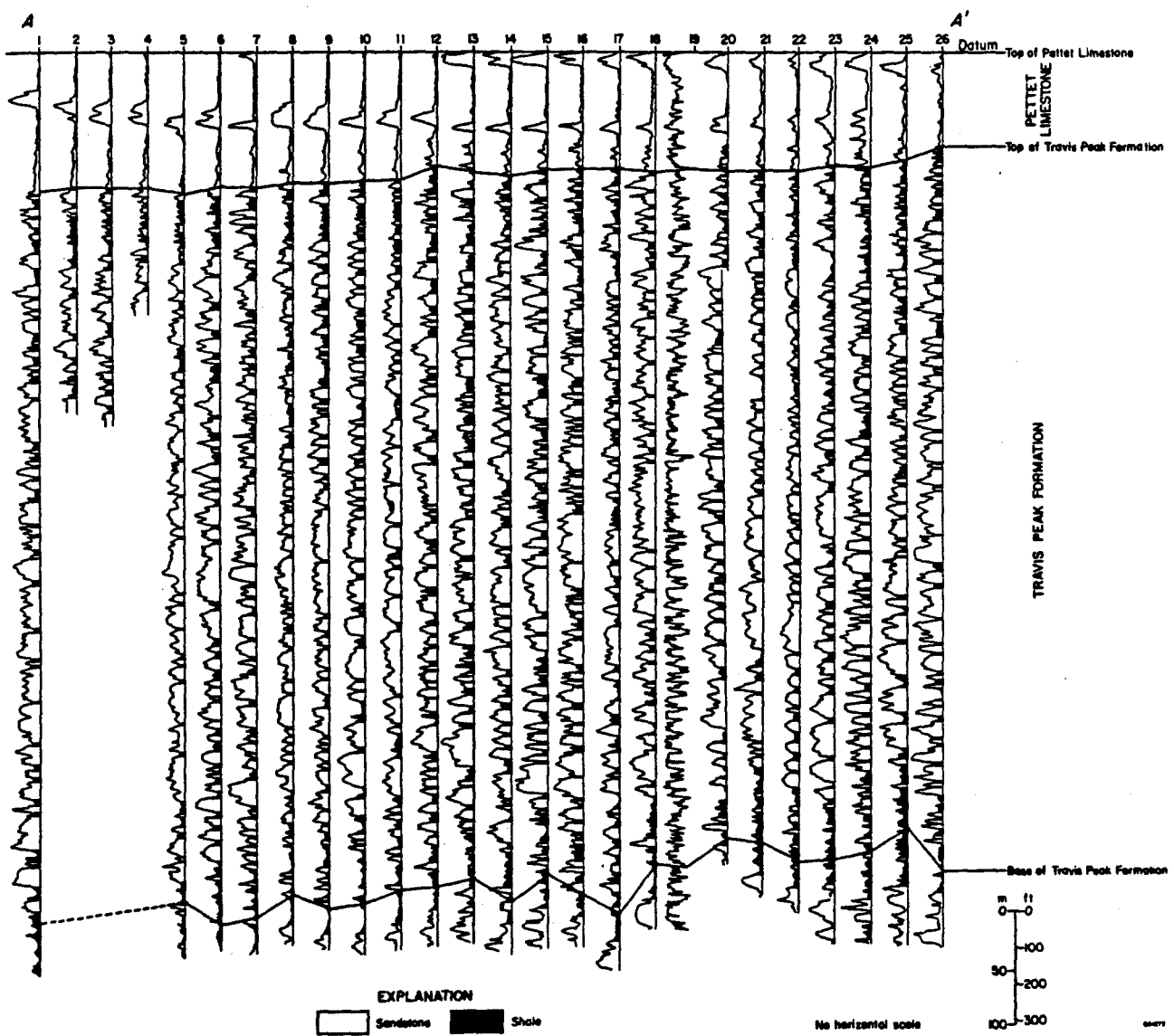


Figure 93. Dip-oriented cross-section A-A' of Travis Peak Formation in eastern Rusk County showing distribution of sandstone and mudstone (location map is figure 97).

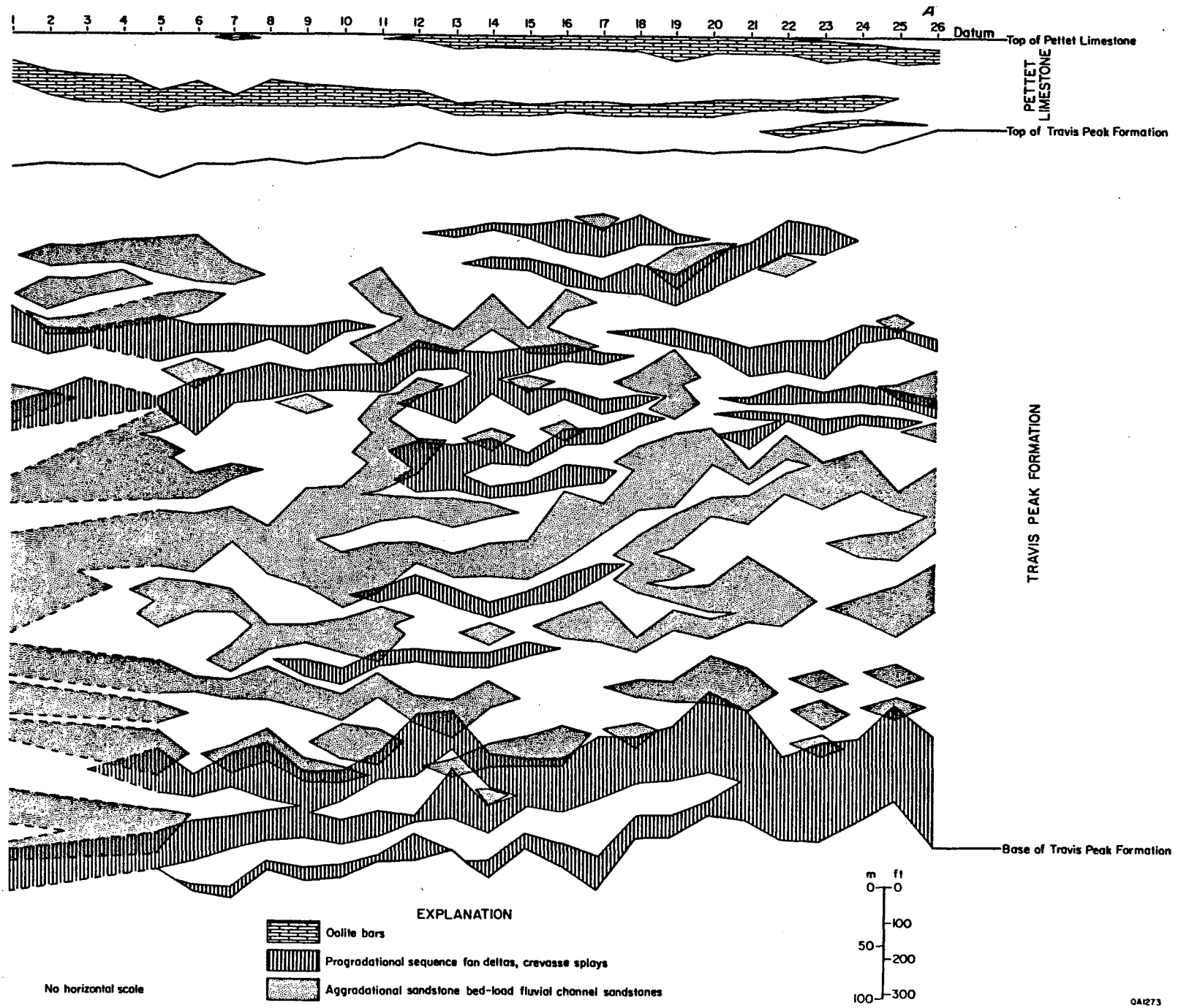


Figure 94. Dip-oriented cross section A-A' of Travis Peak Formation in eastern Rusk County showing depositional facies (location map is figure 97).

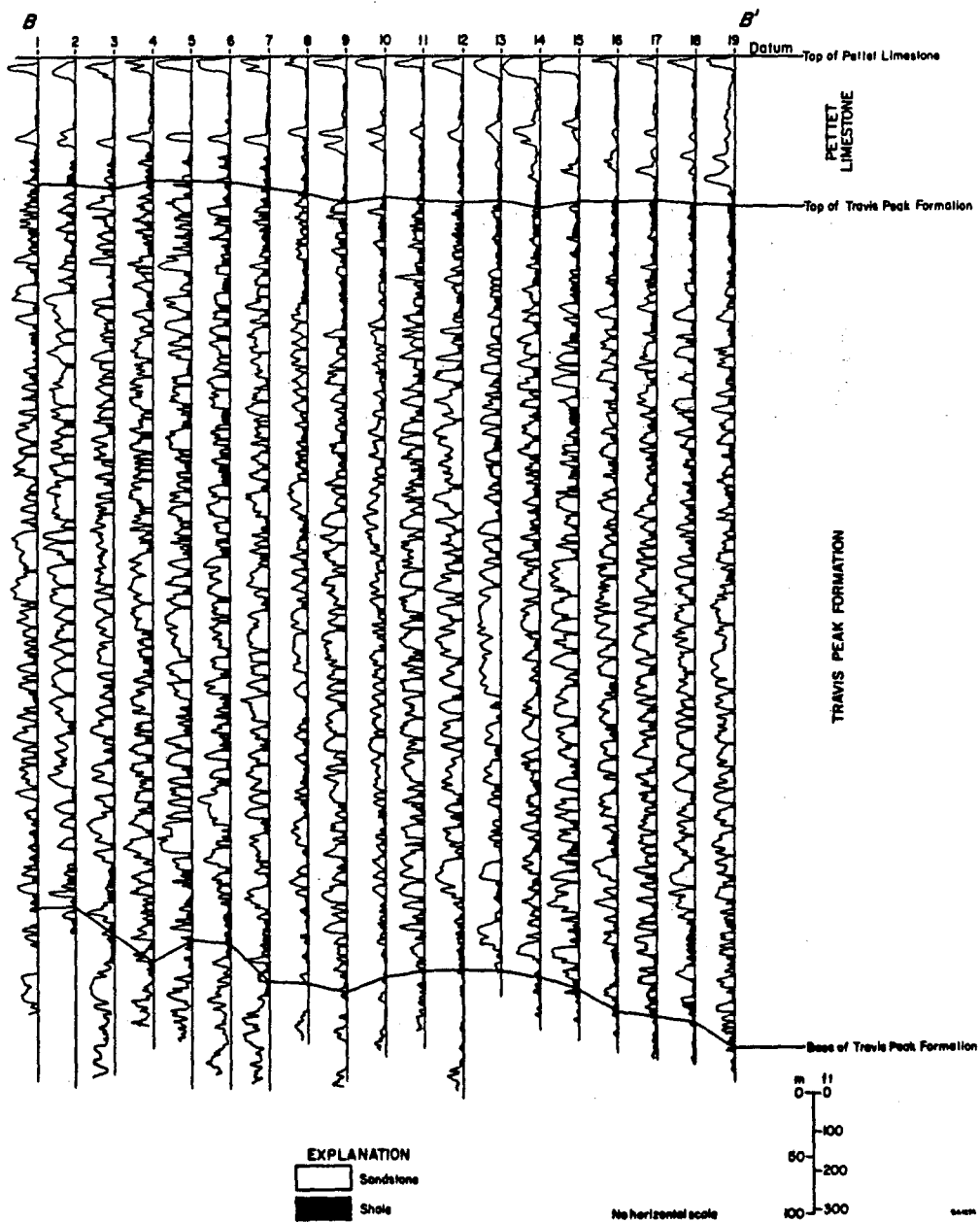


Figure 95. Strike-oriented cross section B-B' of Travis Peak Formation in western Panola and eastern Rusk Counties showing distribution of sandstone and mudstone (location map is figure 97).

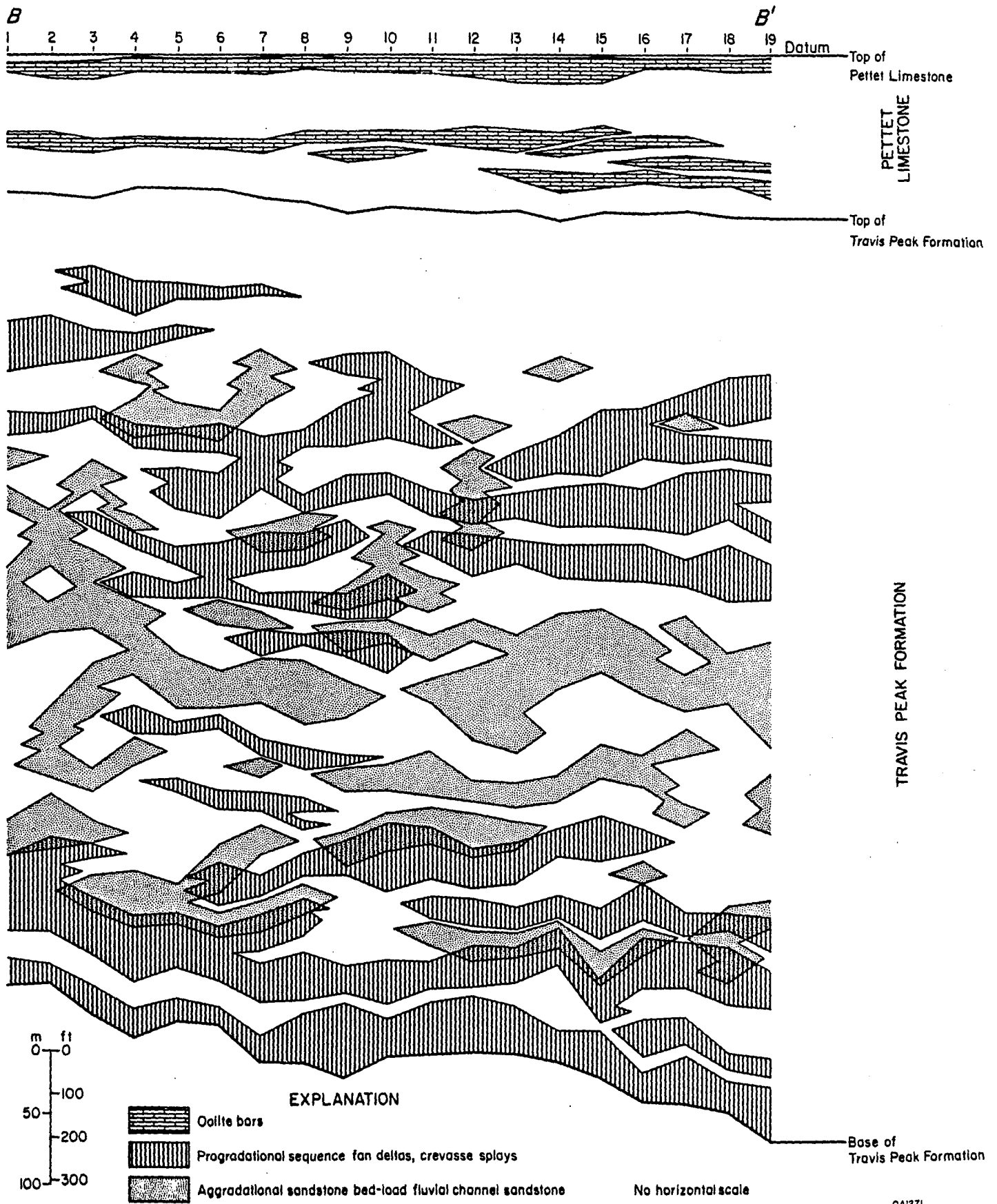


Figure 96. Strike-oriented cross section B-B' of Travis Peak Formation in western Panola and eastern Rusk Counties showing depositional facies (location map is figure 97).

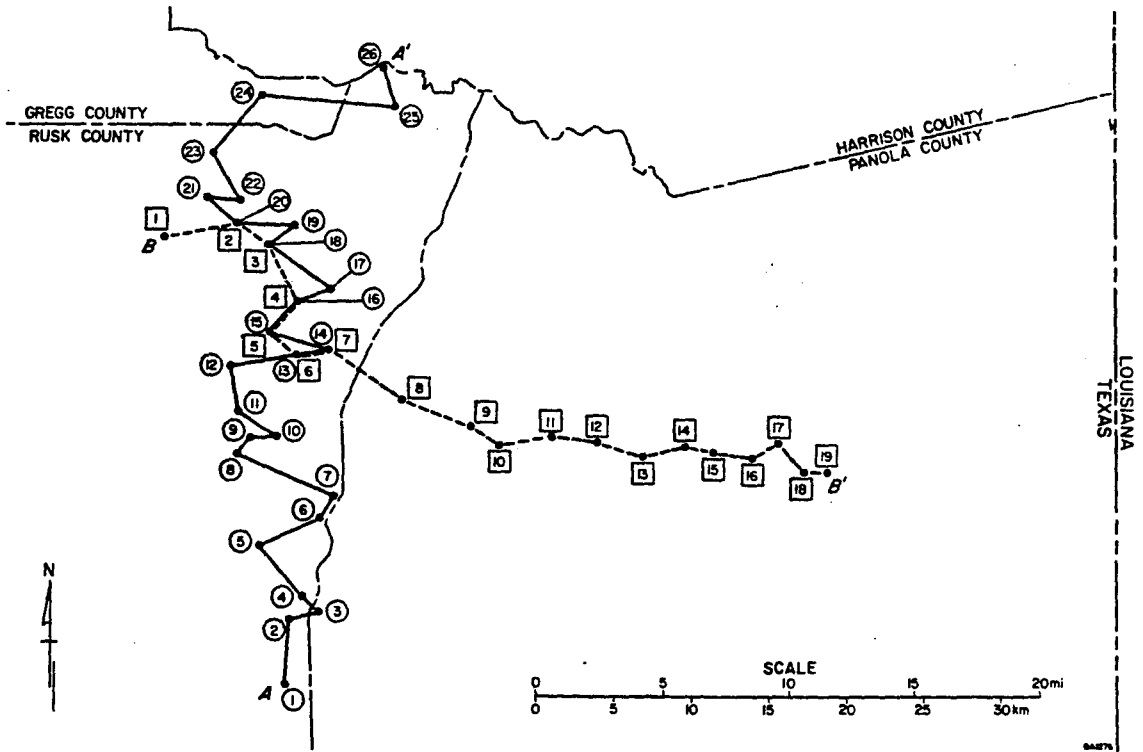


Figure 97. Location map for cross sections in figures 93 through 96.

indicate significant differential subsidence during the Early Cretaceous. During deposition of the Travis Peak-Pettet Formations, the area over the Sabine Uplift was subsiding at approximately the same rate as was the central part of the East Texas Basin. The Rusk County area was a relatively stable platform subsiding at a lesser rate. Whether this variation in rates of subsidence was due to basement tectonics or to salt tectonics is unknown at present.

Lower Progradational Sequence

The lateral continuity of sandbodies in the lower progradational sequence is illustrated in figures 94 and 96. The lower progradational deltaic sequence is 200 to 400 ft thick. Isolated well control indicates that this lower sequence thickens southward to over 700 ft in Nacogdoches County.

In a strike direction individual progradational lobes are continuous over approximately 30 mi. Lateral continuity of progradational lobes increases vertically with increasing thickness of individual lobes.

In a dip direction, the progradational sequences offlap older lobes in a southerly direction. Small, thin lobes occur at base and pinch out to the south. Younger lobes prograded over older lobes and thickened on the downdip (southern) side. Travis Peak deposition in Rusk and Panola Counties began when small delta lobes or fan deltas prograded across the area from north to south.

Middle Fluvial Facies

Fluvial sandbodies exhibit similar lateral variations in strike and dip direction, as do the previously described deltaic facies. Aggradational fluvial sand bodies in strike-oriented section B-B' (fig. 96) are less continuous laterally than sand bodies in the dip-oriented section A-A' (fig. 94). Length-to-width ratios for entire sand bodies average 250 to 1 and range from 40 to 500 to 1. In a dip direction aggradational sand bodies are locally continuous throughout the study area. Within the central fluvial sequence, sand-body continuity increases vertically. This vertical increase in sand body continuity is possibly due to a change from meandering streams

near the base of the fluvial facies to bed-load or braided streams at the top of the fluvial facies.

Upper Transitional Facies

The upper transitional facies of the Travis Peak is marked by a gradational contact with the overlying Pettet Formation. The upper transitional facies is characterized by thin progradational sequences near the base and abundant mudstone and many thin sandstone bodies near the top. Aggradational sandstone bodies greater than 50 ft thick are rare. Correlation of individual sandstone bodies was not generally possible because of their thinness and abundance.

Permeable oolite shoals in the Pettet Formation are readily correlated and may approximate time lines within the Pettet/Travis Peak interval (fig. 96). In a dip section (fig. 94) these oolite shoals climb stratigraphically to the south. Individual oolite shoals that occur near the base of the Pettet Formation in the north occur near the top in the south. Thus, individual oolite shoals indicate that the Pettet Formation overlapped the Travis Peak Formation from south to north. This is the expected stratigraphic relationship during relative rise of sea level; it results in deposition of a recessive facies tract of marine environments (Pettet) over transitional margin marine, strandplain, deltaic, or tidal flat environments in the upper transitional facies of the Travis Peak. If Pettet oolite shoals approximate time lines, then the Pettet is a downdip marine facies that is time-equivalent with updip marginal marine and eventually fluvial facies in the Travis Peak.

Travis Peak Fields and Structure

Travis Peak fields are not distributed uniformly over structural highs in the East Texas Basin. The inferred mechanisms for various uplifts and resultant structural closure are shown in figure 98 with the location of Travis Peak fields. Most Travis Peak fields and production are associated with the Sabine Uplift (Bethany, Carthage, Waskom, and Woodlawn) and with a ring of smaller structures (Whelan, Lansing, Willow Springs, Danville, Henderson, and Trawick) on the western rim of the uplift.

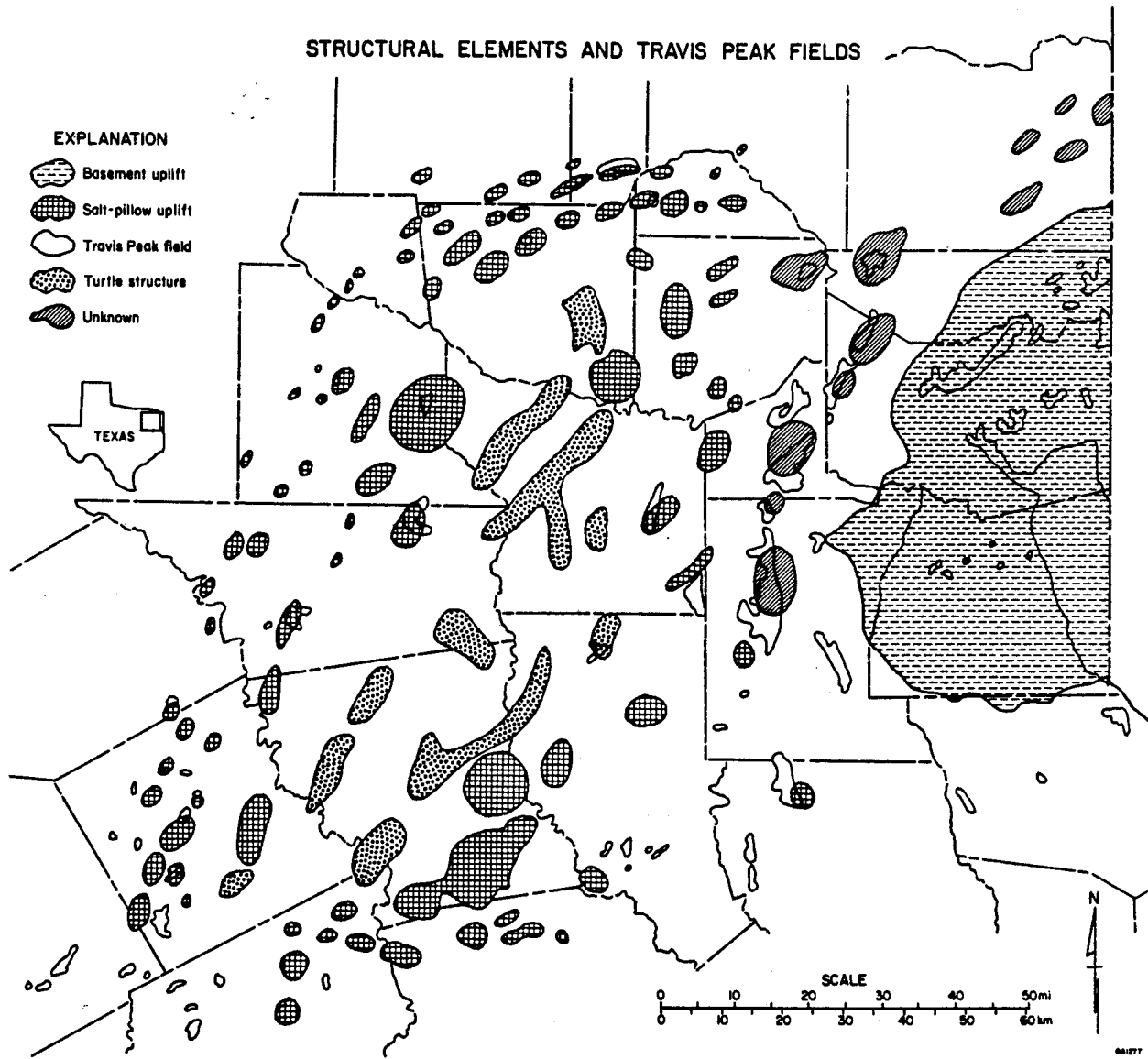


Figure 98. Map of Travis Peak fields and structural highs.

Few Travis Peak fields are located on structural highs over salt pillows and turtle-structure anticlines. Reasons for the absence of Travis Peak fields on such structures may include: (1) limited drilling has not adequately tested Travis Peak as a deep objective, and; (2) absence of significant post-Travis Peak salt flow in underlying salt pillows did not allow any mechanism for enhancing natural fractures in the Travis Peak.

In contrast to deep structural highs in the center of the East Texas Basin, the shallow depth of the Travis Peak over the Sabine Uplift has fostered a greater density of drilling and subsequently greater gas production. Movement and timing of the Sabine Uplift and related structures may have also contributed to the abundance of fields in the eastern part of the basin. Thickening of the Travis Peak over the Sabine Uplift and related structures suggests that movement of these structures post-dates Travis Peak deposition. This timing thus allows a mechanism for enhancing permeability of natural Travis Peak fractures by continued uplift and extension over the crest of these structures.

The genesis of the structural highs below Whelan, Lansing, Willow Springs, Danville, Henderson, and Trawick fields is problematic. These uplifts are similar in size and are on the same trend along an arcuate north-south band around the western flank of the Sabine Uplift. A single deep well (Western #1 Stevens) in Willow Spring Field penetrated Triassic Eagle Mills red beds without indicating Louann Salt. Thus, this uplift and possibly the other similar uplifts along the north-south trend cannot be due to salt flow. A basement uplift is the inferred origin of this group of structures; gravity data will help to verify this interpretation.

Recent Exploration Activity in the East Texas Basin

The Travis Peak Formation and the Cotton Valley Group are the major producers of gas in the East Texas Basin. Continued interest in the Travis Peak Formation is evidenced by the high level of exploratory drilling in the first half of 1983. The number of new Travis Peak discoveries in the first half of 1983 exceeded all other stratigraphic units except the Pettet Formation. Travis Peak discoveries include six new fields, six new pays, and eight long extensions of existing fields (fig. 99).

In the first six months of 1983, drilling activity in the East Texas Basin declined 17% from the pace set in the first six months of 1982 (fig. 100). New hole footage declined 24% over the same period. In the first half of 1983, 11 new oil fields and 16 new gas fields were discovered. The rate for wildcat successes was 20%.

Wildcat activity was concentrated on Lower Cretaceous and Jurassic targets including the Pettet Formation (Lower Cretaceous), Travis Peak Formation (Lower Cretaceous), Cotton Valley Group (Jurassic), and Smackover Formation (Jurassic) (fig. 101). Wildcat success was the greatest in the Pettet Formation, where there were 11 new field discoveries. Pettet drilling activity was concentrated in Rusk, Gregg, and Panola Counties. Prospective targets were permeable oolite shoals on subtle structure and in stratigraphic traps occurring around the western flank of the Sabine Uplift.

The Travis Peak Formation was the second most successful wildcat target, having six new gas field discoveries. Travis Peak drilling activity was the busiest in Rusk, Nacogdoches, eastern Panola, and western Cherokee Counties, Texas.

Three new field discoveries in the Cotton Valley were scattered around the East Texas Basin to the north (Bowie County), west (Anderson County), and east (Shelby County). Although no new fields were discovered in the Smackover Formation, good gas production was achieved by Prairie Production Company from an extension of Ginger Southeast Field.

An Eagle Mills (Triassic?) discovery by Cities Service at Frazier Creek in Cass County generated national attention. The well produced more than 900 barrels of oil per day and 1.4 MCF per day. However, within several days the well began producing large amounts of salt water and was plugged back for a small Cotton Valley oil completion.

Figure 101 summarizes Travis Peak wildcat activity thus far in 1983. The six new Travis Peak gas fields discovered in the first six months of 1983 include Redlands Northeast in Angelina County, Doyle Creek in Cherokee County, Laura Grace in Rusk County, Prairie Point in Limestone County, and two unnamed fields, one in Henderson County and one in Panola County. The Travis Peak Formation in the first half of 1983 also yielded five new gas pay

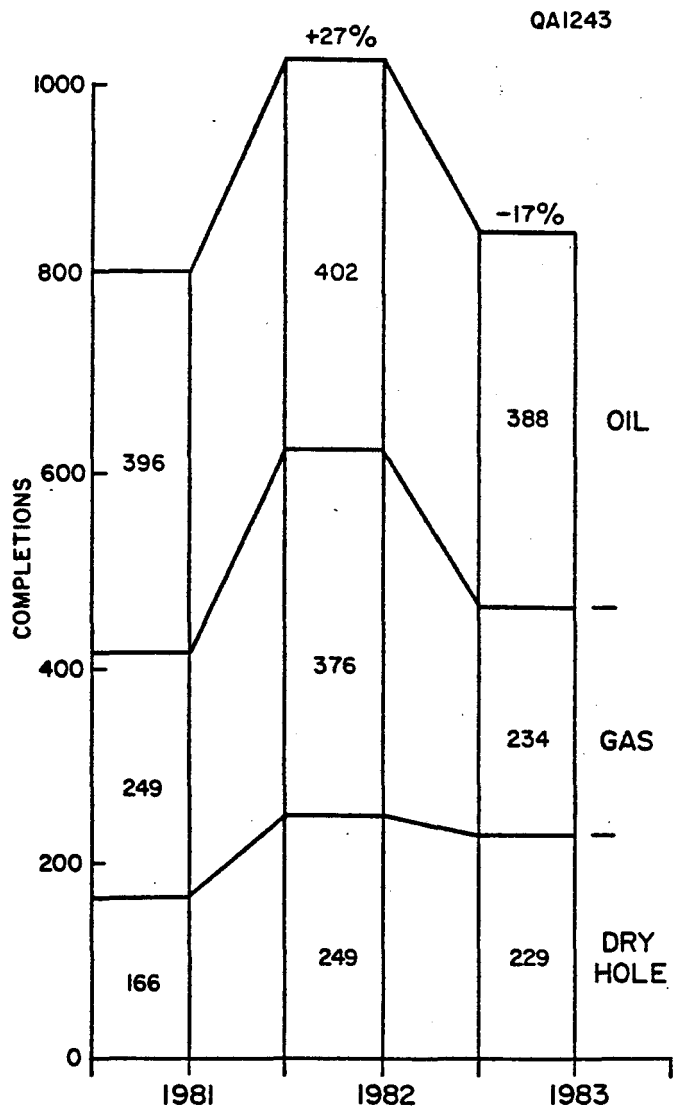


Figure 100. Number of wells drilled in first half of 1981, 1982, and 1983.

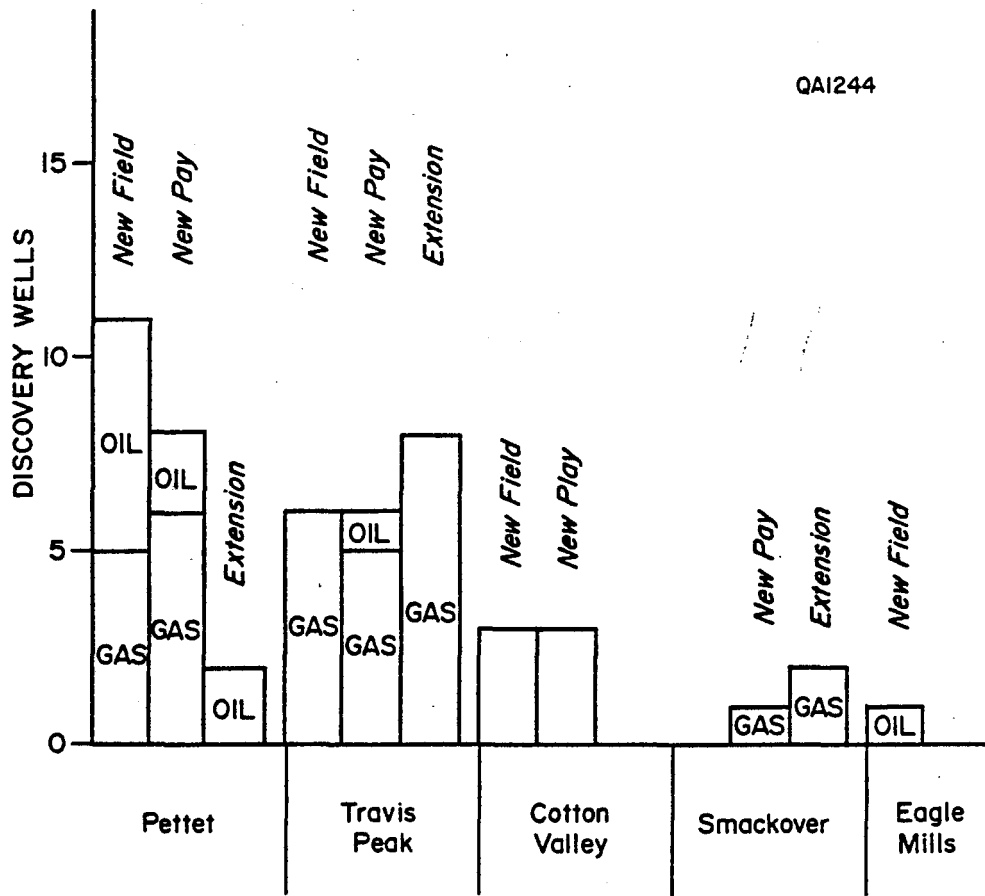


Figure 101. Number of new fields for Pettet, Travis Peak, Cotton Valley, Smackover, and Eagle Mills stratigraphic units.

discoveries, one new oil pay discovery, and eight extensions of producing field. Additional drilling in Gregg, Harrison, Marion, Nacogdoches, Panola, and Rusk Counties through September 1983 yielded two new fields in Rusk County, one in Marion, and two in Nacogdoches County. Three new pay discoveries were also completed in Rusk County.

HOSSTON (TRAVIS PEAK) FORMATION, SOUTH ARKANSAS AND NORTH LOUISIANA

Introduction

Since April 1983 a more intensive effort has been made to study the Hosston (Travis Peak) in north Louisiana and south Arkansas. The data base was expanded from 100 to 450 electric logs in Louisiana and 90 logs were purchased to cover south Arkansas. Most of these 540 electric logs penetrate the entire Hosston Formation and are fairly evenly distributed over the study area at a spacing of 4 to 6 mi. In addition, regional base maps were obtained from Geomap, Inc., for northeast Louisiana, south Arkansas, and south Mississippi, and reports of well completions and drilling activity are being received for this area from Petroleum Information, Corporation.

Emphasis to date has been on data acquisition, thorough literature review, and subsurface correlation of the Hosston Formation. With the electric log correlations essentially complete, an isopach map of the Sligo-Hosston interval and a structure map of the top of the Sligo Formation have been constructed. Future work will involve facies analysis of the Hosston Formation and should result in a series of lithofacies maps depicting the major facies tracts within this gas-productive unit.

Stratigraphy

The Travis Peak Formation was defined by Hill (1890) from surface exposures near Travis Peak post office in Travis County, Texas. The type section in Central Texas includes the Hensell Sand, the Cow Creek Limestone, and the Sycamore Sand (Hazzard, 1939; Forgotson, 1957), and is thus equivalent to the lower Glen Rose Formation in north Louisiana. The thick section of sandy strata conformably below the Glen Rose has come to be known as the "Travis Peak" in East Texas. In an effort to avoid this confusion of terms, Imlay (1940) introduced the name Hosston Formation for this thick sand section. Since this formation does not crop out in north Louisiana, a subsurface interval in the Dixie Oil Company, Dillon No. 92 well, located in

section 13, T21N R15W, Caddo Parish, Louisiana, was designated as the type section. The term Travis Peak is still used by industry in East Texas for this same stratigraphic interval but has been entirely replaced by the name Hosston Formation in Louisiana and Mississippi.

Hosston (Travis Peak) Formation

The Hosston Formation is in the Nuevo Leon Group of the Lower Cretaceous Coahuilan Series and represents the earliest Cretaceous sedimentary unit in the Gulf Coast region. It consists of a thick wedge of clastic sediment which prograded southward across East Texas, south Arkansas, and south Mississippi. Major deltaic depositional sites in Hosston time were located in East Texas and south Mississippi (fig. 102). North Louisiana appears to have been an interdeltic area where the Hosston Formation is thickest, but the percentage of sandstones in the formation is much less than it is to the east or west. An approximately dip-oriented stratigraphic section A-A' (fig. 103) illustrates how rapidly the sandy facies of the Hosston disappears basinward.

The Hosston Formation is a well-defined stratigraphic unit in north Louisiana. It conformably overlies the Jurassic Cotton Valley Formation and its top grades upward through a transition zone into the Sligo (Pettet) Formation. The Cotton Valley is entirely marine in Louisiana (Dickinson, 1968) and it is capped by a relatively thin, but widespread, lagoonal limestone facies consisting of interbedded argillaceous limestones and dark-gray shales called the Knowles Limestone (Mann and Thomas, 1964). The Knowles Limestone becomes silty to the north in Arkansas and eventually disappears due to this facies change, or to erosional truncation, for the Hosston oversteps the eroded edge of the Cotton Valley Formation near the basin rim in southern Arkansas. In the updip area there is a basal conglomerate within the Hosston which serves as a useful marker bed in Arkansas and portions of north Louisiana.

To the south in Louisiana, the Knowles Limestone terminates downdip against a reef or barrier bar that extends along an arcuate line from the northeast corner of Sabine Parish to northern Caldwell Parish. As indicated in stratigraphic section A-A' (fig. 103), it appears that

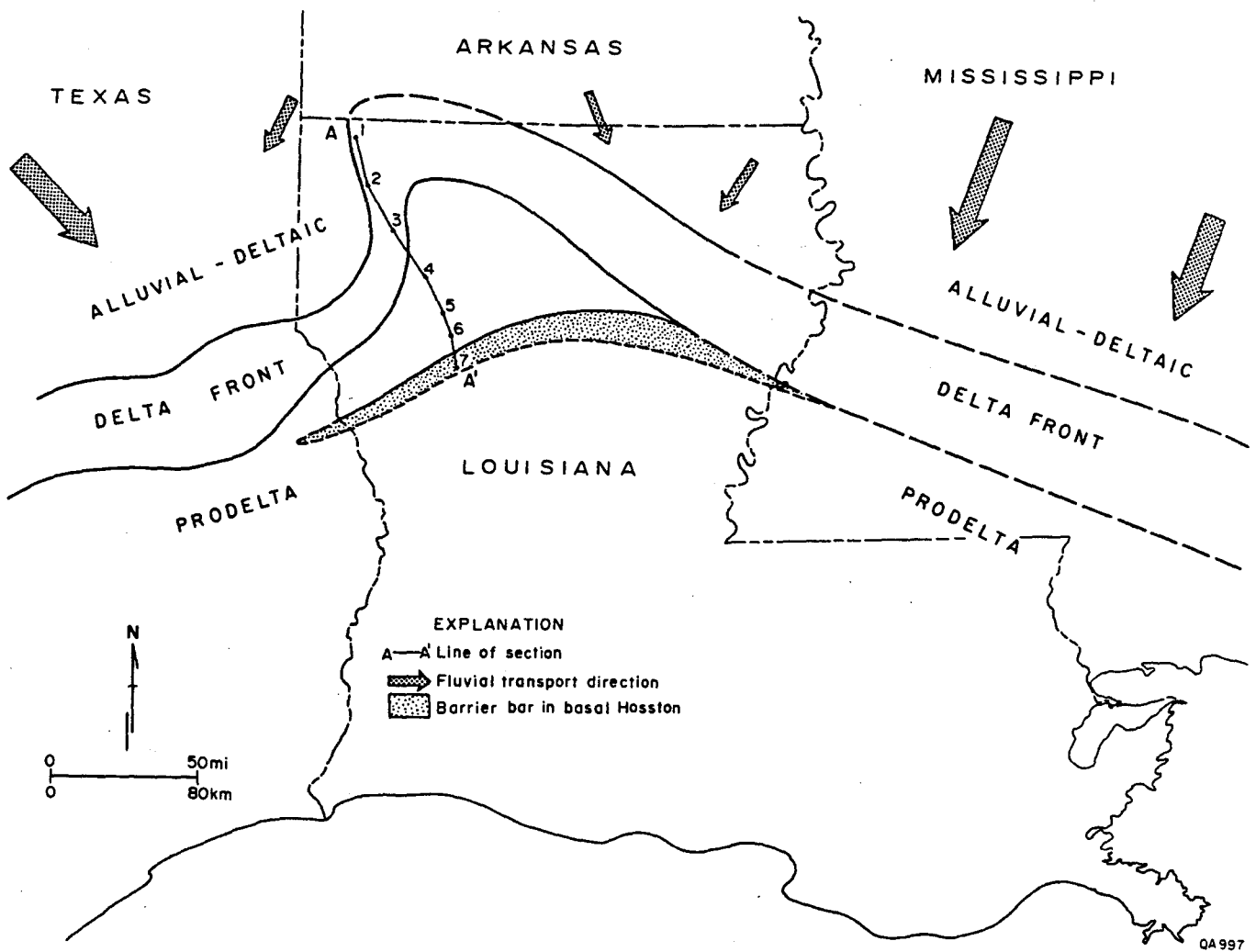


Figure 102. Map showing the major facies tracts of the Hosston (Travis Peak) Formation which incorporates data from Bushaw (1968) on East Texas and Nunnally and Fowler (1954) on south Mississippi.

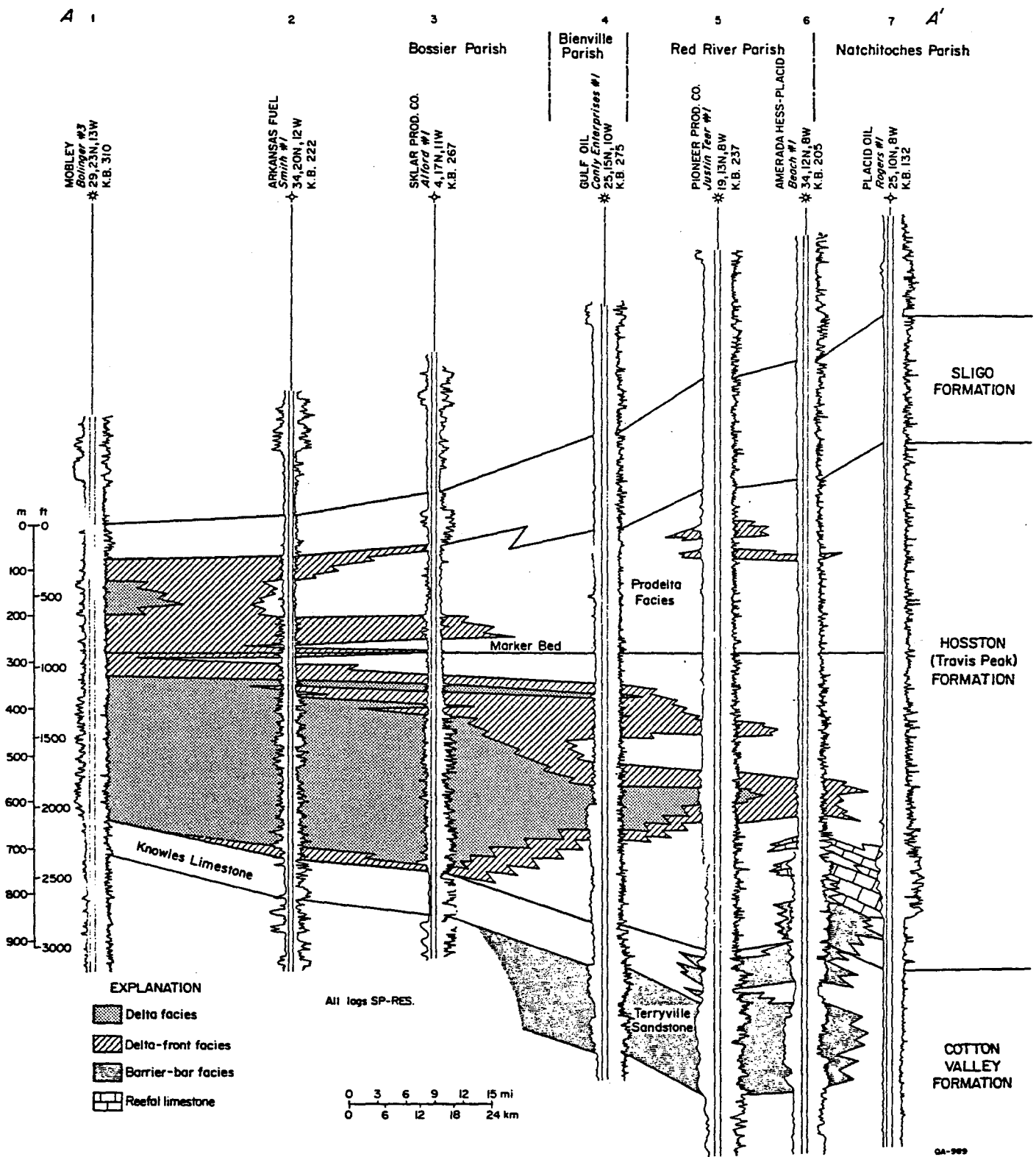


Figure 103. Stratigraphic section A-A' showing the various facies within the Hosston (Travis Peak) Formation and their relation to the adjacent formations. The line of section is shown on figures 102 and 104.

the Terryville barrier-bar complex in the upper Cotton Valley climbs stratigraphically up through the Knowles interval and into the lower Hosston Formation in Natchitoches Parish. Coleman and Coleman (1981) recognized this thick sandstone buildup above the Knowles Limestone in Winn Parish, but they have kept it in the Cotton Valley Formation by redefining the contact at a higher stratigraphic level above the Knowles. A lower Hosston reef occurs above and parallel to the bar sand (fig. 102). This reef, as much as 450 ft thick, appears to underlie Sabine, Natchitoches, Winn, and northern La Salle Parishes and extends an unknown distance downdip.

The Sligo Formation as defined by Imlay (1940) is a gray to brown shale containing lenses of sandstone and limestone capped by a persistent limy unit called the "three-finger limestone" by petroleum geologists. According to Forgotson (1957), the top of the Sligo appears to be an isochronous surface of regional extent, and it is therefore a widely used datum for mapping. The base of the Sligo Formation is placed at the lowest recognizable limestone in the Sligo-Hosston transition zone and this contact steps down stratigraphically basinward as the upper Hosston becomes more and more marine (fig. 103). In Natchitoches and Winn Parishes, the Hosston interval is totally marine and could be considered all Sligo Formation according to the above definition. To avoid this nomenclatural problem and to ensure consistent, correlatable top and bottom contacts, the Hosston and Sligo Formations were combined for mapping purposes. The isopach map, therefore, represents the entire Nuevo Leon Group.

The Hosston Formation in the type well in northern Caddo Parish is described as consisting of mainly gray and red shale with lenticular sandstones in the upper half, and dominantly gray fine-grained sandstones in the lower half of a 2,100-ft section (Imlay, 1940). In general, the Hosston becomes more sandy and continental to the northwest, north, and northeast and grades into a basinward-thickening marine section of gray shale with increasing carbonate content to the south (Cullom and others, 1962). Although facies analysis is just beginning, it is obvious that sandstones deposited in a great variety of depositional environments are present in the Hosston Formation at moderate drill depths, whereas in East Texas the

Hosston appears to contain predominantly fluvial sandstones in the middle part of the formation (Phase A, this report).

Sligo-Hosston Isopach Map

The published maps of the Hosston Formation are very generalized regional maps (Murray, 1952, 1961). More detailed maps have been made of the Hosston in the East Texas Basin (Bushaw, 1968; this report, Phase A) and in southern Arkansas (Imlay, 1940), but the comparable map for Louisiana covers only the northwest corner of the state (Granata, 1963). Even though the density of control points remains sparse in some areas, such as in southern Bienville Parish, there are now enough data available to map the Sligo-Hosston interval over most of north Louisiana. In spite of the wide-spaced control, the Sligo-Hosston isopach map shows some interesting features (fig. 104), the most obvious of which is the distortion in the pattern of regular basinward thickening caused by movement of the Jurassic Louann Salt.

The Sligo-Hosston interval thickens from less than 800 ft in southwest Arkansas to more than 4,800 ft in north-central Louisiana. The depositional strike appears to have been almost east-west in Arkansas, but it curved to the southeast in northeastern Louisiana. In northwest Louisiana the contours strike northeasterly. This arc in depositional strike is caused by a broad, shallow syncline, cited in Murray (1962) as the North Louisiana Syncline, whose axis extends from northern Caddo Parish to Winn Parish (fig. 105). It plunges to the southeast and it is along the deepest portion of this axis that the underlying salt was mobilized into salt stocks in Late Jurassic and Early Cretaceous time. In south Arkansas the 1,400 ft thickness contour forms a string of closures which represent salt anticlines (Bornhauser, 1958). Similar structures are known from drilling and seismic data to exist across the state line in Louisiana, although they are poorly defined on the isopach map. Rosenkrans and Marr (1967) dated the formation of these salt anticlines as the end of Smackover time (Late Jurassic). In Louisiana these salt ridges, or swells, turn more southeasterly and appear to parallel the basin rim as indicated by the edge of the Louann Salt (fig. 104).

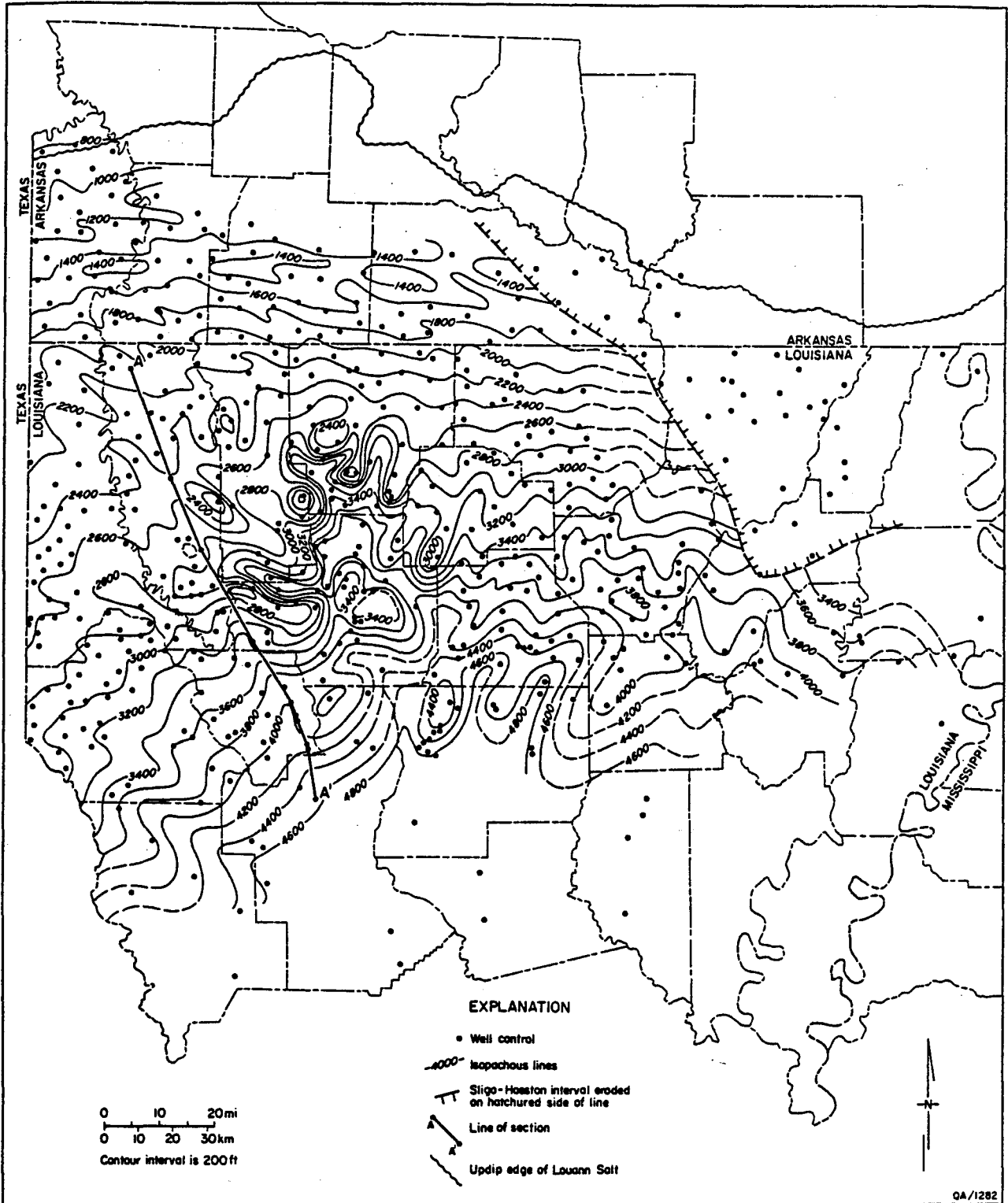


Figure 104. Isopach map of the combined Sligo and Hosston (Travis Peak) Formations.

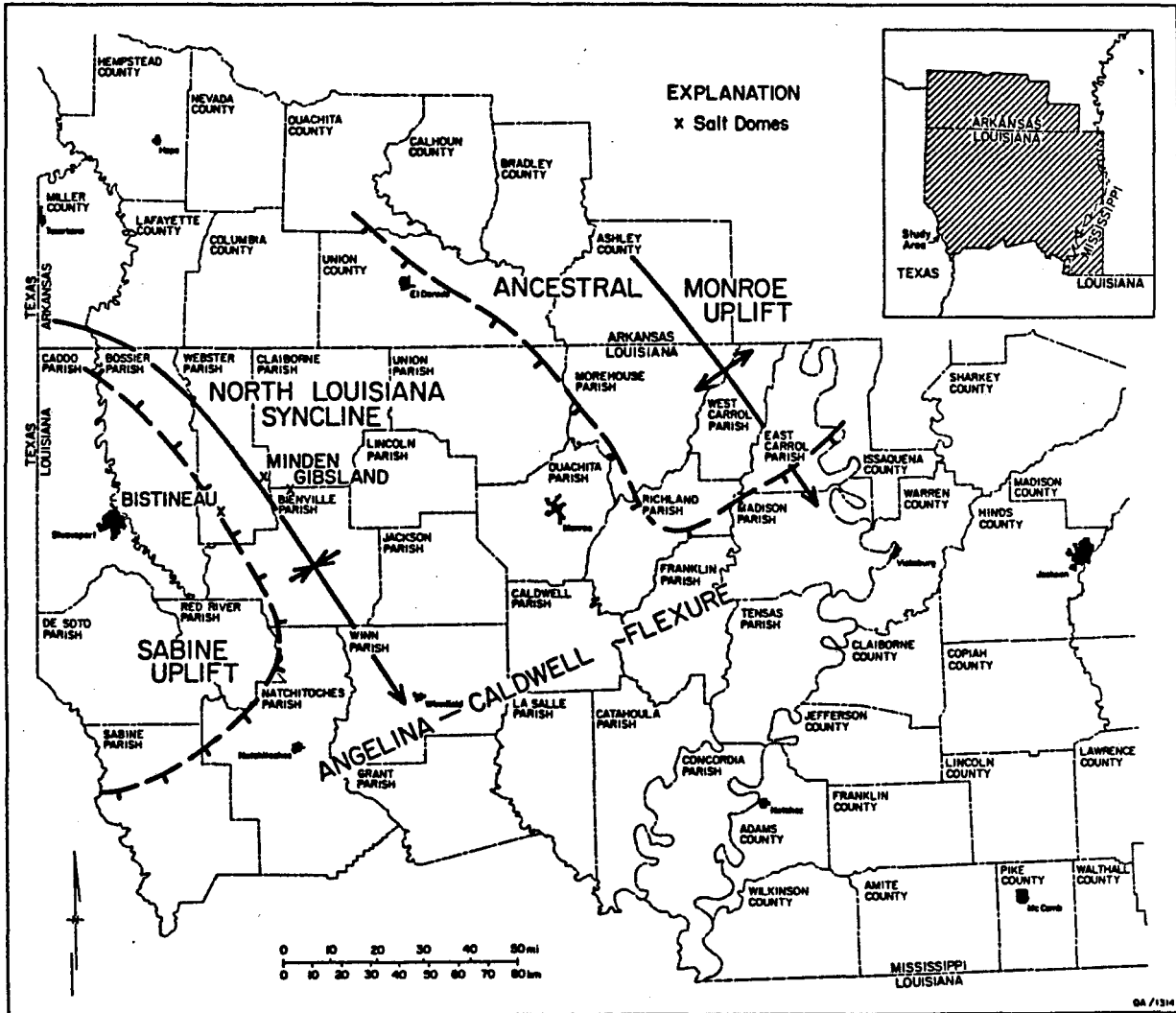


Figure 105. Index map of north Louisiana and southwest Arkansas showing the political subdivisions and the major tectonic elements of the region.

The regular pattern of linear thickening and thinning of the Hosston Formation in Webster and Bossier Parishes suggests that early salt anticlines also developed down slope within the North Louisiana Syncline contemporaneous with Hosston deposition. Broader and shallower "swells" occur farther to the southwest in DeSoto and Sabine Parishes. All of these subparallel Sligo-Hosston thins were an expression of early lateral salt movement in response to early sedimentary loading. The salt anticlines in the North Louisiana Syncline appear to have become segmented into distinct salt pillows in response to deeper burial. In the deepest part of the syncline, some of the salt pillows "burst," forming salt diapirs. As the salt escaped from the pillows these positive structures became basins due to the withdrawal of the salt. The Sligo-Hosston isopach map shows that some of the salt-withdrawal basins were well developed in Hosston time, or earlier, in central Winn Parish and northern Bienville Parish (fig. 104).

Structure

The major basement-controlled tectonic elements in south Arkansas and north Louisiana are the Monroe and Sabine Uplifts, which are separated by the North Louisiana Syncline (fig. 105). There is little or no evidence of the Sabine Uplift as a separate positive element in Lower Cretaceous time. The Monroe Uplift was probably slowly rising throughout Early Cretaceous time and the North Louisiana Syncline was accentuated by salt movement, possibly as early as the Late Jurassic. The structures which influenced Hosston deposition and formed the present oil and gas traps are all related to halokinesis, as defined by Trusheim (1960). The mobilization of the Louann Salt has produced non-piercement structures such as salt anticlines, salt pillows, and turtle structures, and piercement structures called salt stocks, diapirs, or salt domes.

Sligo Structure Map

The structure map (fig. 106) was drawn using the top of the Sligo Formation as a datum. This datum is a distinctive and widely used mapping horizon that shows the present structures

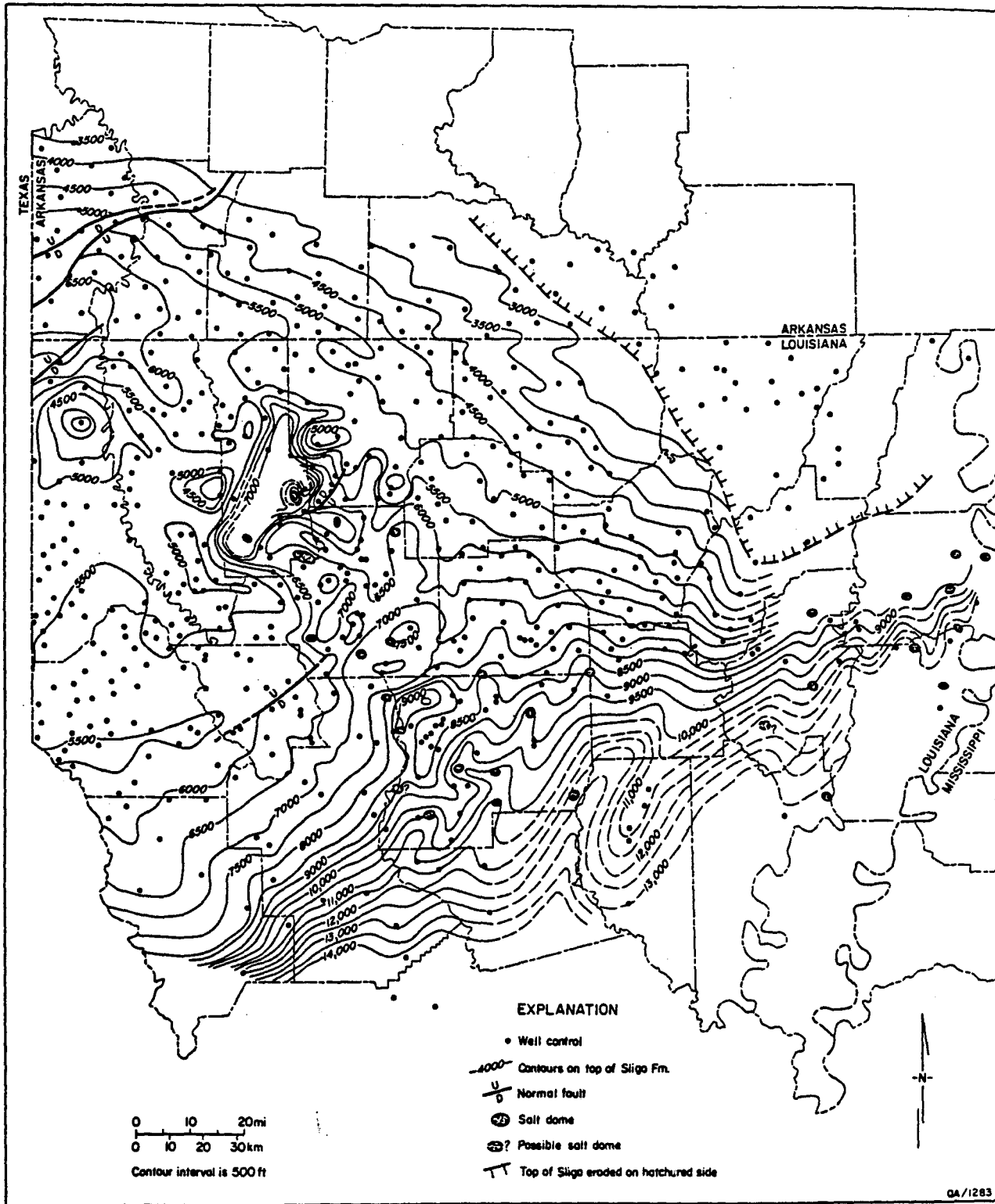


Figure 106. Structure-contour map on the top of the Sligo Formation.

extremely accurately. The widely spaced control points used for this study do not allow the detailed mapping that is possible if all the available Sligo well control were used. The purpose of this generalized structure map is to show the major structural features and to allow a comparison with the Sligo-Hosston isopach map, which also serves as a paleo-structure map. Some idea of the growth history of the salt structures can be gained by comparing these two maps.

The Monroe and Sabine Uplifts appear as one broad platform with a bend in it at the 5,500-ft contour (fig. 106). In mid-Cretaceous time, the Monroe Uplift was arched upward along a broad northwest-trending axis that plunged to the southeast. This arching accentuated the southwesterly dip into north-central Louisiana and caused erosion of Early Cretaceous and Jurassic strata from the crest of the uplift. The Monroe-Sabine platform is bordered to the south-southeast by the Angelina-Caldwell flexure, where the rate of dip increases from 30 to 100 ft/mi on the platform to 250 ft/mi in the flexure.

The North Louisiana Syncline remains a rather ill-defined string of salt withdrawal basins that cross the platform in a northwest direction parallel to the axis of the mid-Cretaceous Monroe Uplift. The greatest structural relief is found around the large Minden salt withdrawal basin in Webster Parish, where there is over 2,000 ft of structural relief on the top of the Sligo across the western rim of the basin. Salt pillows that surround the Minden basin have structural closures ranging from several hundred feet to over 1,000 ft at the Sligo horizon. The Minden basin was not recognizable in Sligo-Hosston time (fig. 104) because it apparently formed at a later date when salt was withdrawn into the Minden and Bistineau salt domes. The three salt pillows west of the basin also appear to have grown since Hosston time but have failed to form diapirs (fig. 106).

There appears to have been a progressive development of salt structures which migrated up the axis of the North Louisiana Syncline through time. One of the earliest documented salt domes is the Gibsland dome, which was a salt anticline or pillow in Cotton Valley time (Kupfer and others, 1976), but which became a deep salt-withdrawal basin in Hosston time (fig. 104).

The ring of salt pillows surrounding the Gibsland dome in northern Bienville Parish (fig. 104) may be an exceptionally good example of Sannemann's (1968) salt stock family. If the German examples are used as a model, the Gibsland dome would be the mother stock with younger daughter pillows and stocks surrounding it. The salt structures grow centrifugally away from the central primary stock. The radiating wave of younger salt structures is initiated and propagated by the withdrawal of salt into the central diapir. The subsequent downbuilding of the overburden into the rim syncline around the mother stock causes lateral pressure to be exerted outward, which pushed up new daughter salt pillows along the axes of pre-existing salt ridges. The semicircle of salt pillows on the west side of the Minden basin appears to be a further manifestation of this centrifugal process. If these pillows are connected with other known salt structures, it appears that they form another, larger and younger ring around the Gibsland dome. The salt domes farther south in Winn Parish apparently belong to a separate, deeper, and probably older salt stock family, but drilling to date is insufficient to decipher the older growth histories of these domes.

Several large northeast-striking normal faults with displacements of up to several hundred feet are shown on the Sligo structure map (fig. 106). It is postulated that the common northeast orientation is due to northwest-southeast tension generated by the migration of salt down the present dip to the southeast. This tension has been accentuated by the progressive development of salt domes from the southeast toward the northwest. The large, shallow basinal feature centered in DeSoto Parish is possibly due to post-Hosston movement of a relatively thin salt layer into the east-trending anticlinal structure crossing the south half of the parish.

Summary

Essentially all the structural deformation allowing the accumulation of oil and gas is due to salt tectonics. The Sligo-Hosston isopach map has indicated some genetic relations among salt structures that were not previously recognized. It appears that the earliest salt structures to form were salt anticlines or swells that grew at fairly regular intervals down the paleo-slope,

which was to the southwest in Jurassic time. The axes of these structures were parallel to the basin rim, as indicated by the updip edge of the Louann Salt. The salt anticlines that were downwarped into the deepest part of the North Louisiana Syncline formed salt pillows, some of which proceeded to the diapir stage. The earliest diapirs were probably in Winn Parish; their development moved up the synclinal axis through time as the depth of burial increased and as the deeper salt withdrawals triggered new vertical salt growth. A similar pattern of salt structure development from deeper to shallower depths has been documented in the East Texas Basin (Seni and Jackson, 1983).

According to Woodbury and others (1980), 38 percent of the presently known hydrocarbons in the East Texas and North Louisiana Basins are associated with salt structures, and of this, 98 percent are over non-piercement salt pillows and turtle structures. Therefore, the application of a more refined genetic model for the development of these salt structures should be of value in predicting the location, type, and relative ages of the deeper structures in Winn Parish and elsewhere.

CORCORAN AND COZZETTE SANDSTONES, PICEANCE CREEK BASIN

Introduction

Phase A of this report indicates that the Corcoran and Cozzette Sandstones of the Piceance Creek Basin meet GRI requirements for research objectives with extrapolation potential and with the opportunity to foster new resource development. Planning for coring, logging, and testing operations arranged cooperatively with well operators requires that interpretation of genetic depositional units be made on a timely basis for areas where new drilling is anticipated. Such areas primarily are within Shire Gulch and Plateau Fields in Mesa County, Colorado. Thus, work reported here emphasizes the latter fields as an appropriate starting point wherein closely spaced well control was used to interpret lateral facies variations. Regional facies delineation, as outlined under Phase B of contract activities, has proceeded at a slower pace but at a level adequate to ensure that interpretations made for Shire Gulch - Plateau reservoirs are consistent with regional depositional patterns.

Methodology

At the start of Phase B studies, well log coverage was upgraded to approximately one log suite per section where logs were available from commercial sources; more densely spaced coverage was obtained in Shire Gulch and Plateau Fields. An electrical log and a porosity log (usually neutron-density) were obtained wherever the Corcoran-Cozzette was penetrated. Newly released logs were monitored during the period of budget constraint and are now being acquired for recently developed areas throughout the Piceance Creek Basin; many of these wells are Dakota Sandstone tests that provide full coverage of the gradational base of the Corcoran Sandstone. A complete set of completion cards for the southern Piceance Creek Basin was obtained from the Petroleum Information Corporation and new operator activity continues to be monitored through the daily Rocky Mountain Regional Report, Four Corners Intermountain Edition, also purchased from the Petroleum Information Corporation. Base maps

at a scale of 1" = 4,000 ft were obtained for use in detailed mapping and in tracking operator activity. New wells with log data available and future wells of interest to the GRI research program are located on these relatively large-scale maps.

In preparation for generating a comprehensive set of regional cross sections in the southern Piceance Creek Basin, well locations and formations penetrated have been checked and coded on the 1" = 4,000 ft base map. Data from Petroleum Information Corporation have been compared to data in the files of the Colorado Oil and Gas Conservation Commission and missing or incorrect data were noted. Many wells do not penetrate all of the Corcoran Sandstone, and despite optimum location, these wells cannot be effectively used on regional cross sections. Validation of the base data is being done by the Colorado Geological Survey and will continue into the early part of the next contract year. Progress of this work was significantly affected by budget constraints, but has been completed for the central part of the Corcoran-Cozzette producing trend from T7S to T11S and R91W to R99W. Access by the Colorado Geological Survey to the files of the Colorado Oil and Gas Conservation Commission has provided data on existing core, on water analyses from Corcoran-Cozzette producing zones, and has yielded copies of conventional core analyses. Much of these data will be utilized in upcoming contract work during which diagenesis, resource distribution, and responses to stimulation will be analyzed.

Analysis of Potential Piggyback Locations

CER Corporation provided data on potential piggyback well locations that were evaluated using existing well control. Although no such operations were engaged in by GRI during this contract period, several cross sections illustrating facies differences across parts of Plateau Field were prepared and were provided to GRI and to CER Corporation. One result of these investigations over limited areas is that the number of zones perforated, the initial potential flow, and the magnitude of the hydraulic fracture treatment given one or more perforated zones can vary widely between wells only 1 mi apart and drilled by the same operator (fig. 107).

Actual neutron-density log crossover is limited to approximately 3 ft in the Bevans No. 1-29 and 9 ft in the Trahern No. 1-20 (fig. 107); it appears that perforated zones in the Trahern well were selected primarily on the basis of near-crossover on the neutron and density logs, or perhaps on the basis of experience with other wells. From completion of the Trahern well in 1977 to completion of the Bevans well in 1980 there was a shift toward a much smaller hydraulic fracture treatment over a smaller perforated interval, but the initial potential flow showed the opposite tendency (fig. 107). The amounts of initial water production, if any, in these wells were not reported by Petroleum Information Corporation.

Differences in the results achieved in drilling and completing these two wells are a function of variability in the resource (gas saturation, permeability, porosity), in the response of the logs (how well can prospective zones be defined), and in the completion practices adopted by the operator. The latter depends heavily upon the past experience of personnel completing the well, but the former are directly amenable to study as part of geologic resource characterization and of log interpretation analysis.

Regional Depositional Patterns

Mapping net sandstone in combination with log facies analysis offers a means of understanding and defining the depositional systems of a stratigraphic unit. Net sandstone in the Corcoran, Cozzette, and Rollins Sandstones was calculated for approximately 200 wells in the southern Piceance Creek Basin using gamma-ray (GR) logs. A pilot study of closely spaced wells in the Shire Gulch - Plateau Field area showed variation of up to 30 API units for the shaliest part of the Mancos Shale tongue between the Rollins and Cozzette Sandstones. This implied non-uniform calibration between logging tools, therefore an absolute API value for sandstone compared to shale was not established; instead, net sandstone was counted as sandstone exceeding 50 percent of the difference between the shale reading noted above and the minimum gamma-ray reading in sandstone of the Corcoran or Cozzette on each log. The lower half to two-thirds of the Corcoran and Cozzette Sandstones typically shows an upward-

ADOLPH COORS COMPANY
Bevans 1-29
 29-10S-96W
 elev. 5723 KB

ADOLPH COORS COMPANY
Trahern 1-20
 20-10S-96W
 elev. 5554 KB

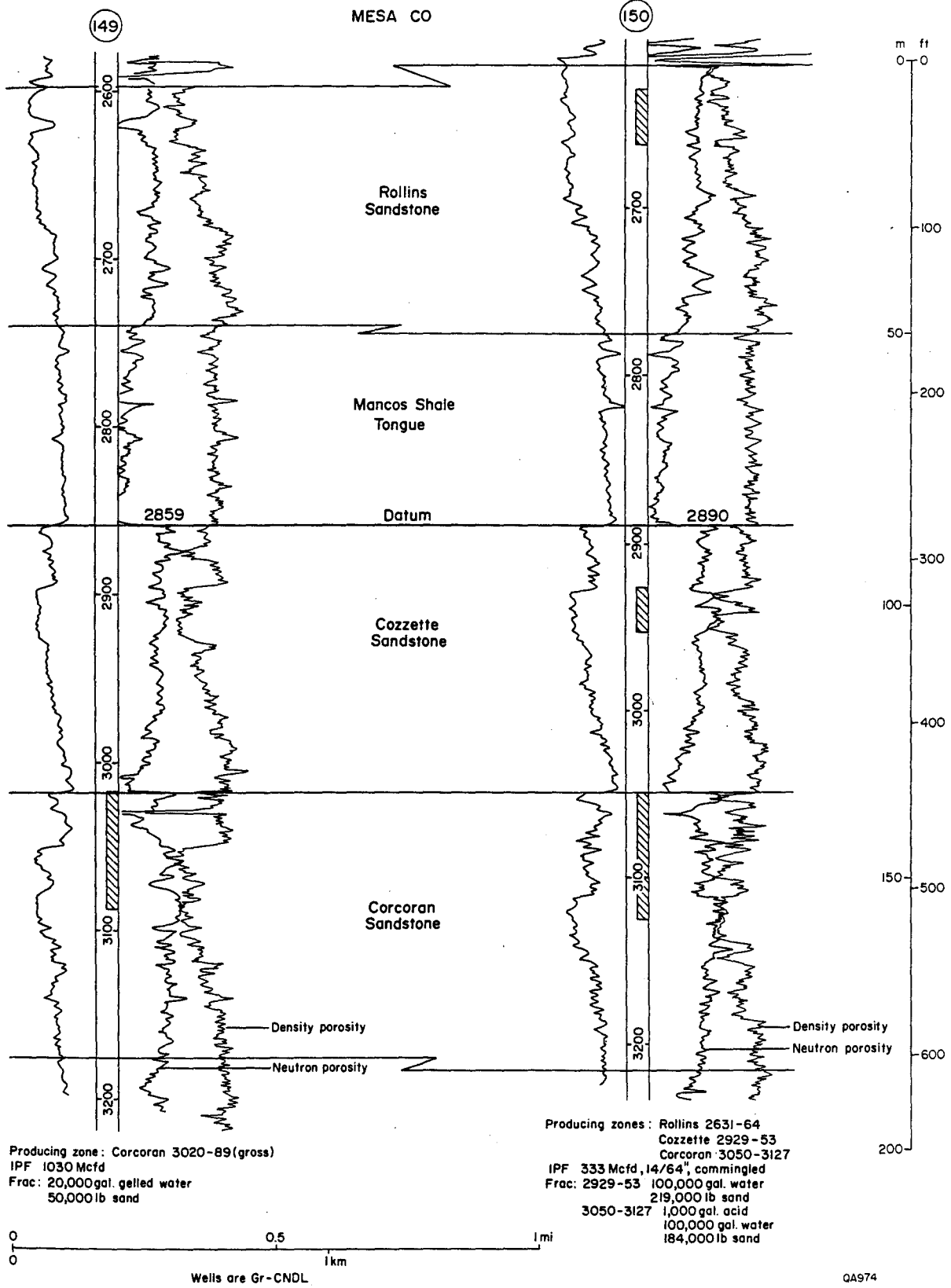


Figure 107. Logs, perforation and production data for two wells in adjacent sections of Plateau Field.

coarsening progradational log pattern sometimes capped by a blocky, aggradational log pattern. This is overlain by a more variable interval of shale, sandstone, and thin (2 to 4 ft) coal beds (fig. 107). Net sandstone was tabulated separately for the upward-coarsening lower sequence and the remaining upper part of the formation within the Corcoran and Cozzette Sandstones and for the Rollins Sandstone as a whole.

Corcoran Sandstone

Net sand in the Corcoran Sandstone as a whole was mapped across the southern half of the Piceance Creek Basin. A thick net-sandstone trend extends from T10S R97W northeastward toward T6S R93-94W (fig. 108). Data are unevenly distributed across the map area, in part because of topographic restrictions on drilling, and because some wells penetrate only the Cozzette or only part of the Corcoran. The northeast trend of thick net sandstone probably represents upper and lower shoreface and barrier sediments of the Corcoran shoreline deposited during the Middle Iles - Palisade regression defined by Zapp and Cobban (1960). This orientation is consistent with previous work by Warner (1964) and, in the eastern part of the basin, by Collins (1976).

Thick net sandstone trending northwest occurs in the northwest corner of T10S R98W extending into T9S R99W (fig. 108). This dip-oriented trend may represent fluvial input to the marginal marine system. Probable fluvial sandstones with blocky, aggradational GR-log character in Shire Gulch Field, described later in this report, occur in T9S R97W. In T9S R90W, anomalously thick sandstone in the Corcoran in one well may represent localized marine bar development with a possible source to the northeast; acquisition of additional well control in Divide Creek Field will help to evaluate this explanation. Data from the vicinity of T11S R90W (fig. 108) show more than 20 ft of net sandstone extending a greater distance downdip than in any area to the west in the basin. Such a net-sandstone distribution along the eastern margin of the Piceance Creek Basin would be consistent with a major Campanian delta to the northeast, along the Colorado-Wyoming border (Weimer, 1970), and a postulated north to south longshore drift along the western margin of the Cretaceous Seaway (Kent, 1968).

247

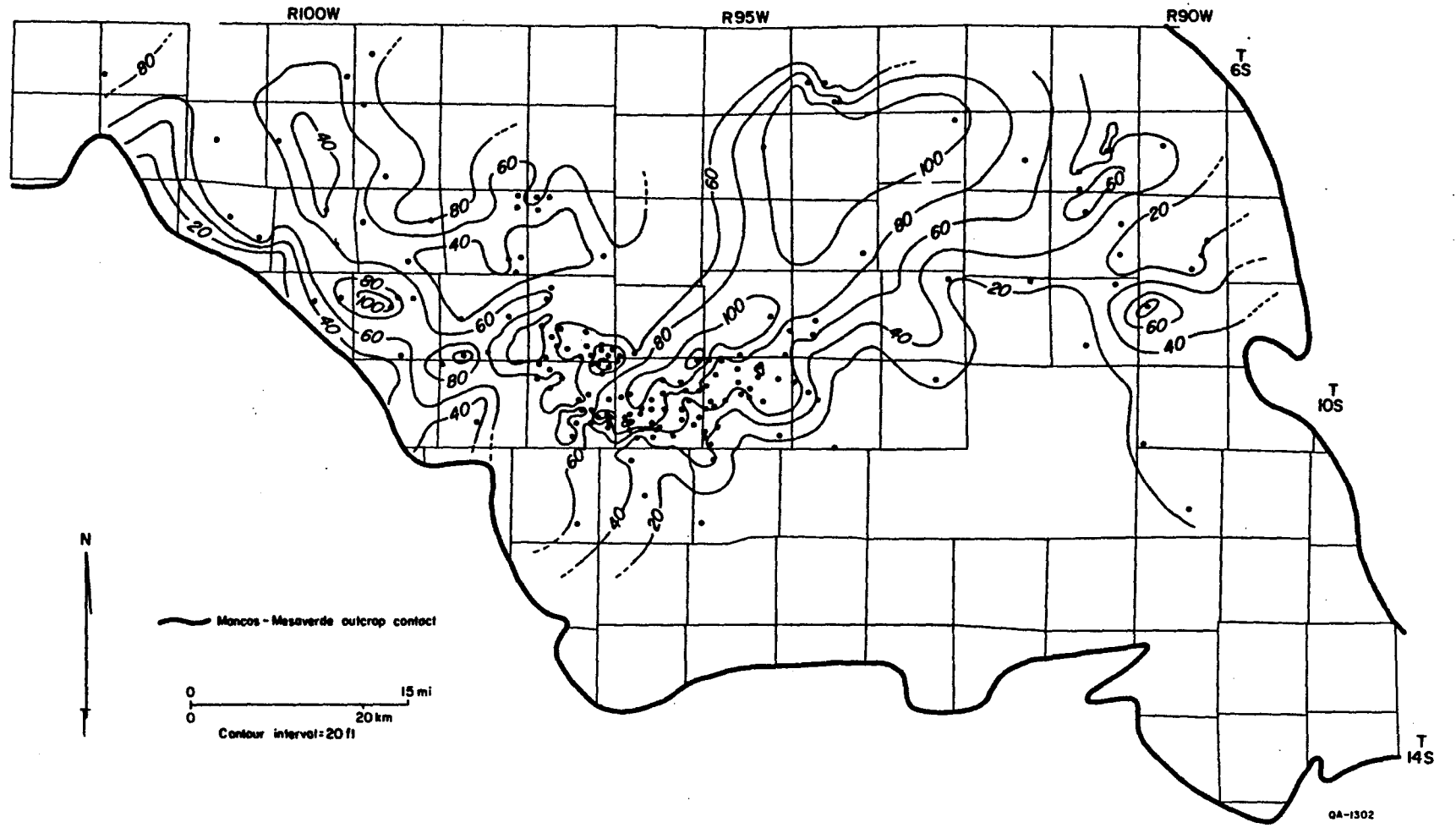


Figure 108. Total net sand in the Corcoran Sandstone, southern Piceance Creek Basin. Mesaverde-Mancos contact from Tweto (1979).

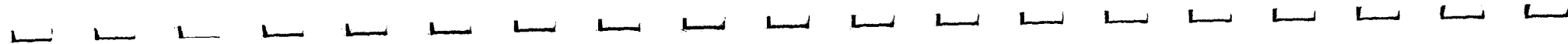
Corcoran-Cozzette Coal Distribution

Thin coal beds in the upper Corcoran Sandstone and the upper Cozzette Sandstone are present northwest of a line from T6S R93W to T10S R97W (fig. 109). Maximum total thickness of coal reaches 24 ft in the Corcoran and 10 ft in the Cozzette. Up to five individual coal beds may be present, and are recognizable on logs by high resistivity, low gamma-ray count, high apparent density, neutron, and sonic porosity, and washout on the caliper log. Corcoran coals are found farther to the southeast than Cozzette coals, thus indicating possible greater Corcoran progradation into the Cretaceous Seaway, which is consistent with the distribution of aggradational log patterns (fig. 52).

Correlation of these 2- to 4-ft-thick coals is possible only locally over distances less than 1 to 1.5 mi. These coals are highly lenticular and the total number and aggregate thickness may change significantly between adjacent wells. Given these limitations and the irregular distribution of data clustered in few existing fields, an isopach of a given coal may not provide distinct dip or strike orientations useful in depositional systems interpretations. Other researchers have, however, counted the total number of coals in each well in an area, and these data have yielded interpretable patterns (W. Ayers, personal communication, 1983). This approach will be utilized in Shire Gulch Field (T9S R97W) (fig. 109) once additional well control has been acquired.

Shire Gulch - Plateau Fields

Shire Gulch and Plateau Fields are the largest producers of gas from the Corcoran and Cozzette Sandstones (table 4), and have a cumulative production of 9.8 Bcf through January 1, 1982 (Colorado Oil and Gas Conservation Commission, 1981a). Depositional systems studies were initiated in these fields because they are sites of potential piggyback operations and because they contain the greatest density of well control in the southern Piceance Creek Basin.



249

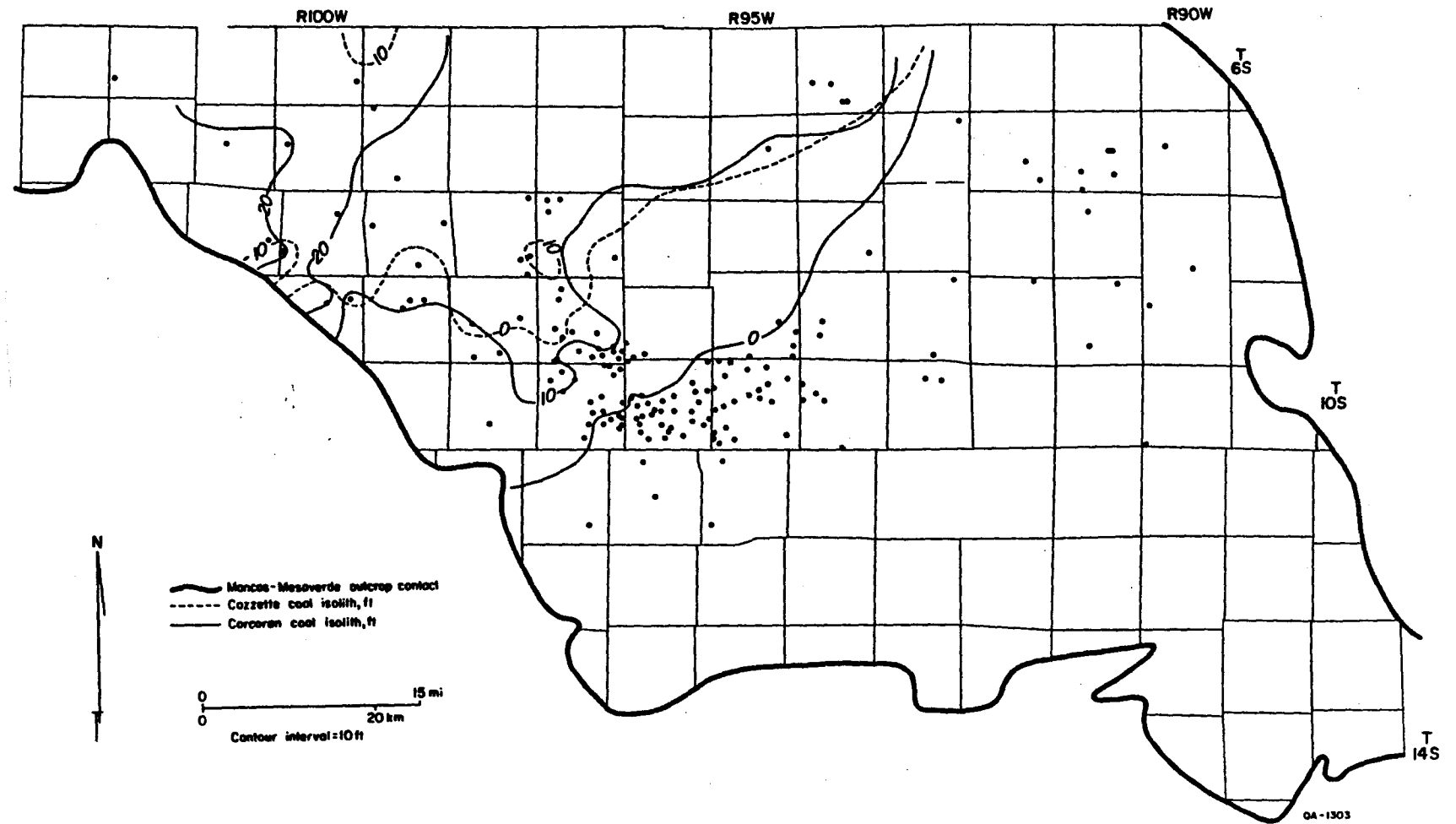


Figure 109. Generalized coal isoliths for the Corcoran and Cozzette Sandstones, southern Piceance Creek Basin. Mesaverde-Mancos contact from Tweto (1979).

Facies Delineation

Throughout Shire Gulch and Plateau Fields, the Corcoran and Cozzette Sandstones were divided into upper and lower operational units for mapping of net sandstone. The lower part of each sandstone shows a well-defined, upward-coarsening progradational GR-log pattern, which for the Corcoran represents the transition from several thousand feet of Mancos Shale deposition to deposition of marginal marine and continental facies of the Mesaverde Group. The upward-coarsening sequence in the lower Cozzette follows a minor marine incursion at the end of Corcoran deposition and essentially repeats the depositional pattern of the lower Corcoran. Sandstones showing blocky, aggradational GR-log patterns sometimes cap the lower units of the Corcoran and the Cozzette. The upper unit of the Corcoran and Cozzette may contain blocky, aggradational sandstones, upward-coarsening sandstones, or interbedded shale, sandstone, and thin coals. The distribution of these lithologies is dependent upon position in the facies tract. Lithofacies of the Corcoran and Cozzette Sandstones can be illustrated using a series of dip-oriented cross sections displaying seven GR-log facies in Shire Gulch and Plateau Fields (figs. 110 and 111; table 20). These cross sections (figs. 112 through 116) may be examined in conjunction with net sandstone maps to define genetic facies and interpret depositional systems. All cross sections are hung on a laterally persistent marker horizon (bentonite?) in the Mancos Shale tongue and lower Rollins Sandstone.

Lower Corcoran

Net lower Corcoran sandstone more than 30 ft thick forms a well-defined linear northeast trend and builds up to a maximum of 85 ft of sandstone in section 1, T10S R96W (fig. 117). The trend of net sandstone more than 60 ft thick covers only small areas and cannot be continued to the northeast due to lack of well control. Net sandstone less than 50 ft thick tends to cut across the northeast trend in sections 23 and 24, T10S R97W. All cross sections (figs. 112 through 116) show a transition toward the southeast from an upward-coarsening sequence along the trend of high net sandstone to dominantly shale with an erratic to serrate log pattern due to

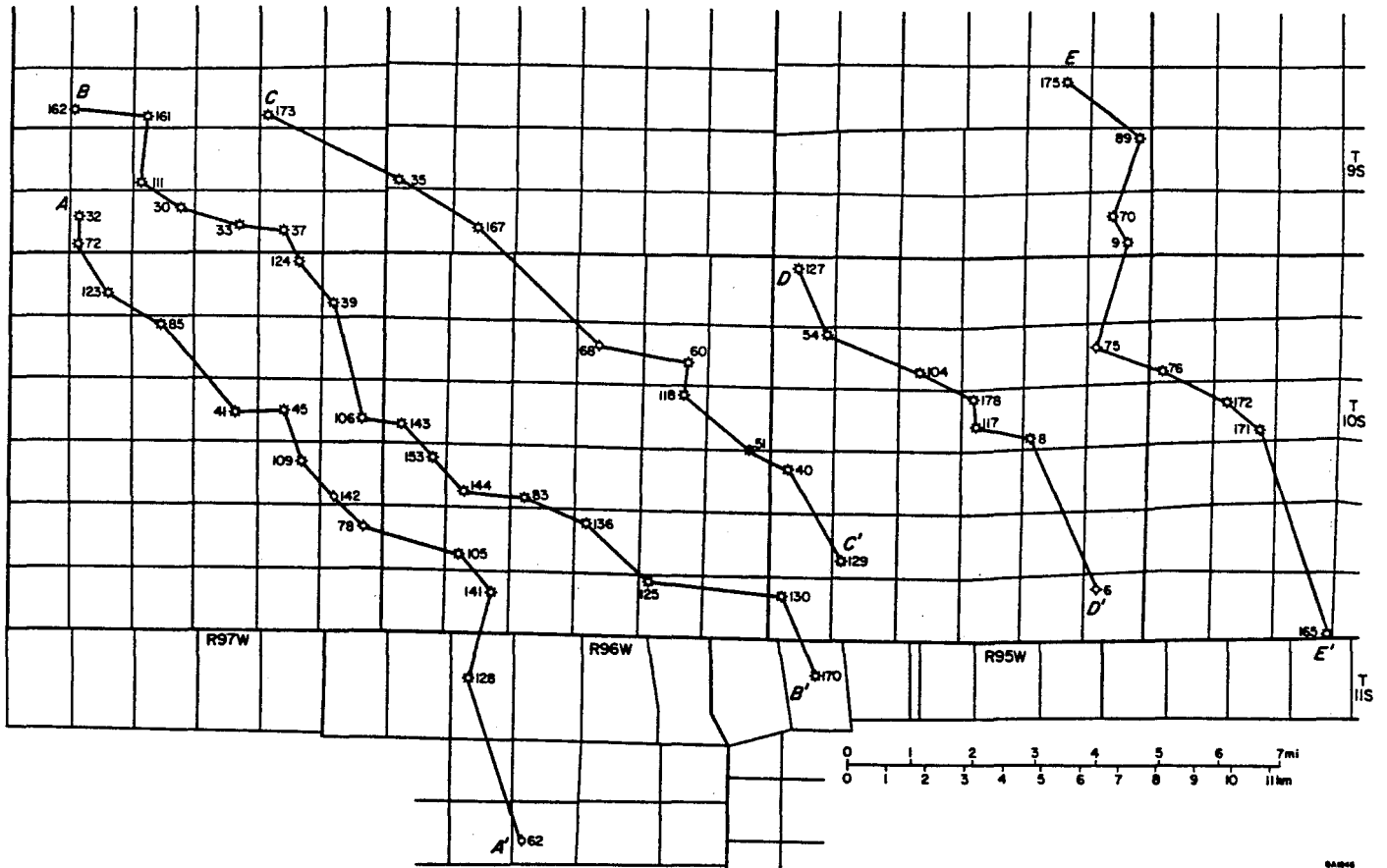
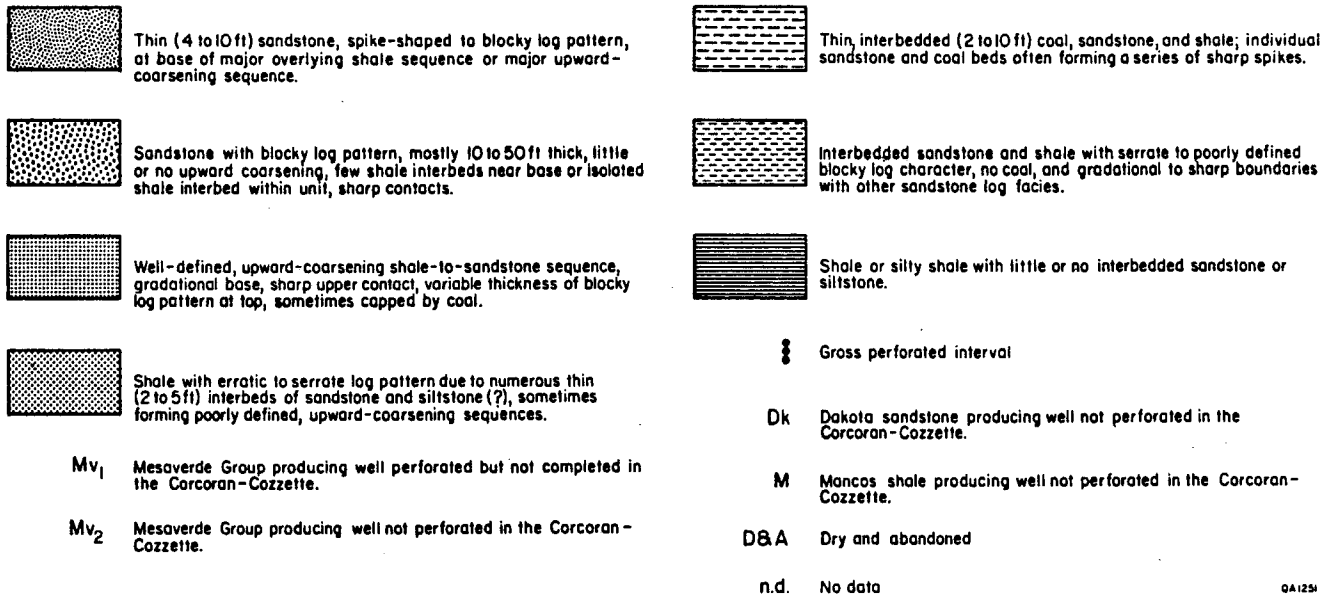


Figure 110. Index to cross sections through Shire Gulch and Plateau Fields; numbered wells are identified in table 1.

CORCORAN-COZZETTE GAMMA-RAY LOG FACIES



QA1251

Figure 111. Explanation of log facies and producing interval codes used in gamma-ray log cross sections of Shire Gulch and Plateau Fields.

Table 20. List of wells utilized in cross sections A-A' through E-E' of the Corcoran-Cozzette in the Shire Gulch - Plateau Field area.

<u>Number</u>	<u>Well</u>
6	Exxon Company, Old Man Mtn., #2
8	Teton Energy, Walck #14-3
9	Teton Energy, Sparks #36-4
30	Koch Exploration, Horseshoe Canyon #4
32	Alta Energy, Federal #32-1
33	Koch Exploration, Horseshoe Canyon #5
35	Pacific Natural Gas, Shire Gulch #14-30-3
37	Pacific Natural Gas, Shire Gulch #23-35
39	Martin Oil, Federal #1-3
40	Flying Diamond, Wallace Currier #19-2
41	Coors Energy, Nichols #1-15CM
45	Coors Energy, Nichols #1-14CM
51	Flying Diamond, Nichols #13-1
54	A. Coors, Acco-Meador #1-24
60	Gasco, Gasco-Walker #1
62	Kenai Oil and Gas, Bull Basin Fed. #15-3
68	Flying Diamond, Federal #10-1
70	Carter & Carter, Plateau Creek Ranch #1
72	Texaco, Haffelmire-Gov't #1
75	Pan American, Walck #1
76	Teton Energy, Anderson #7-3
78	Atlantic and Apache, Windger Flats #1
83	Coors Energy, Currier #4-21
85	Norris Oil, Federal #19-1
89	Exxon Company, Gunderson #1
104	Flying Diamond, Big Creek #9-1
105	A. Coors, Wilson #2-29
106	Coors Energy, Wolverton #1-13
109	A. Coors, Nichols #1-23
111	Koch Exploration, Horseshoe Canyon #3
117	Apache Corp, Young #1-15
123	Texaco, Roberts Canyon #1
124	Pacific Natural Gas, Shire Gulch #31-2
125	Mountain Fuel, Bull Basin Fed. #1-35
127	Exxon Company, Rodgers-Fed. #1
128	Coors Energy, Boruch #1-4
129	Coors Energy, Nichols #1-29
130	Norris Oil, Currier #31-2
136	Hammonds & Blanco, U.S. Moran #27-1
141	A. Coors, Wood #2-32
142	A. Coors, ACCO-Meadows #1-42-2
143	A. Coors, Nystrom #2-18
144	A. Coors, Shepard #3-20
153	A. Coors, Feters #2-19
161	Koch Exploration, Horseshoe Canyon #1-21
162	Koch Exploration, Horseshoe Canyon #1-20
165	Exxon Company, Old Man Mtn., #1
167	Chandler, Plateau Creek #11-32

Table 20. (continued)

<u>Number</u>	<u>Well</u>
170	Coors Energy, Swetland #1-5
171	Beartooth Oil & Gas, Colorado Land #2
172	Beartooth Oil & Gas, Colorado Land #1
173	Alta Energy, Alta #23-1
175	Exxon Company, C.H. Four #1
178	Teton Energy, Colorado Water #15-2

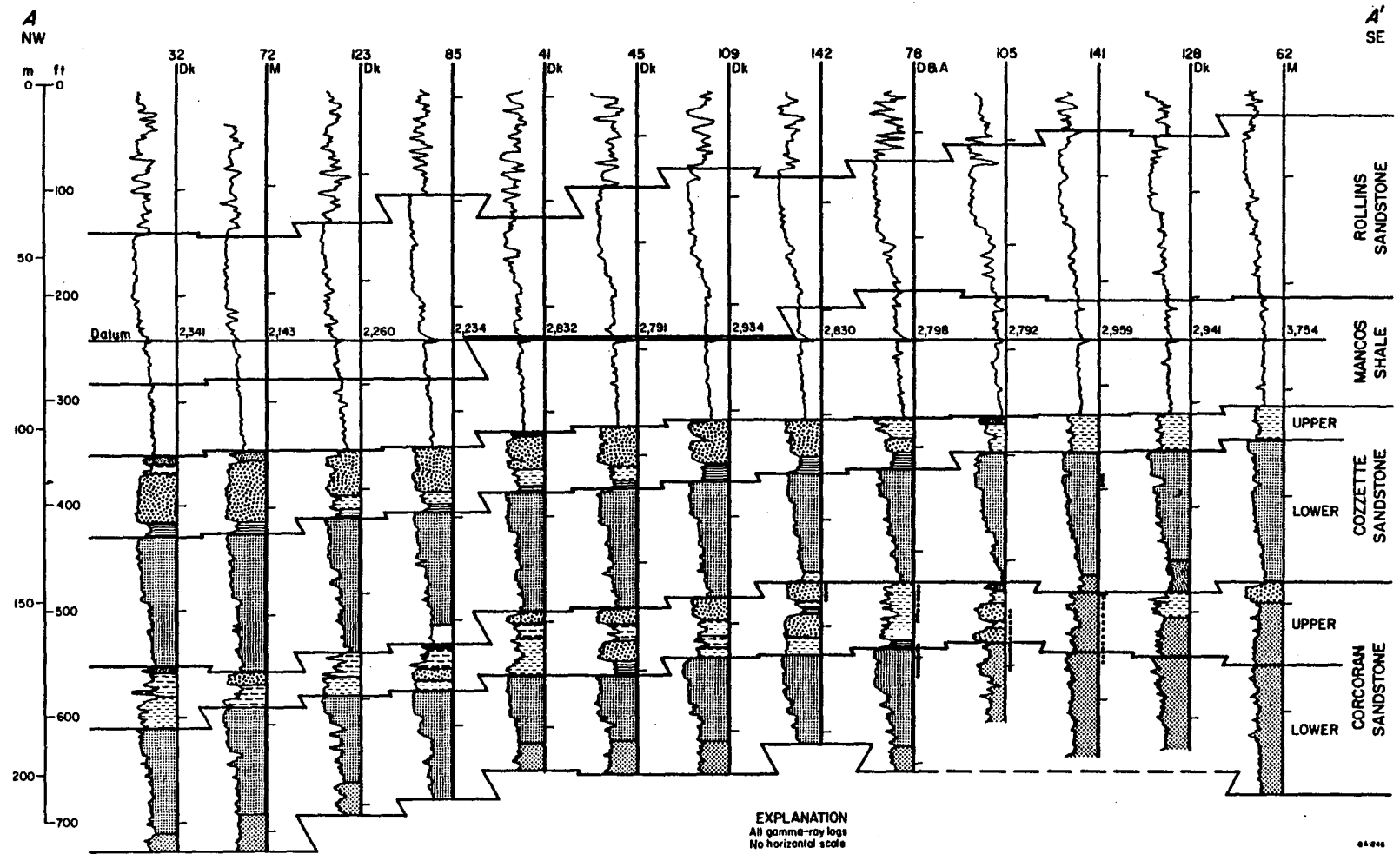


Figure 112. Cross section A-A', Shire Gulch and Plateau Fields.

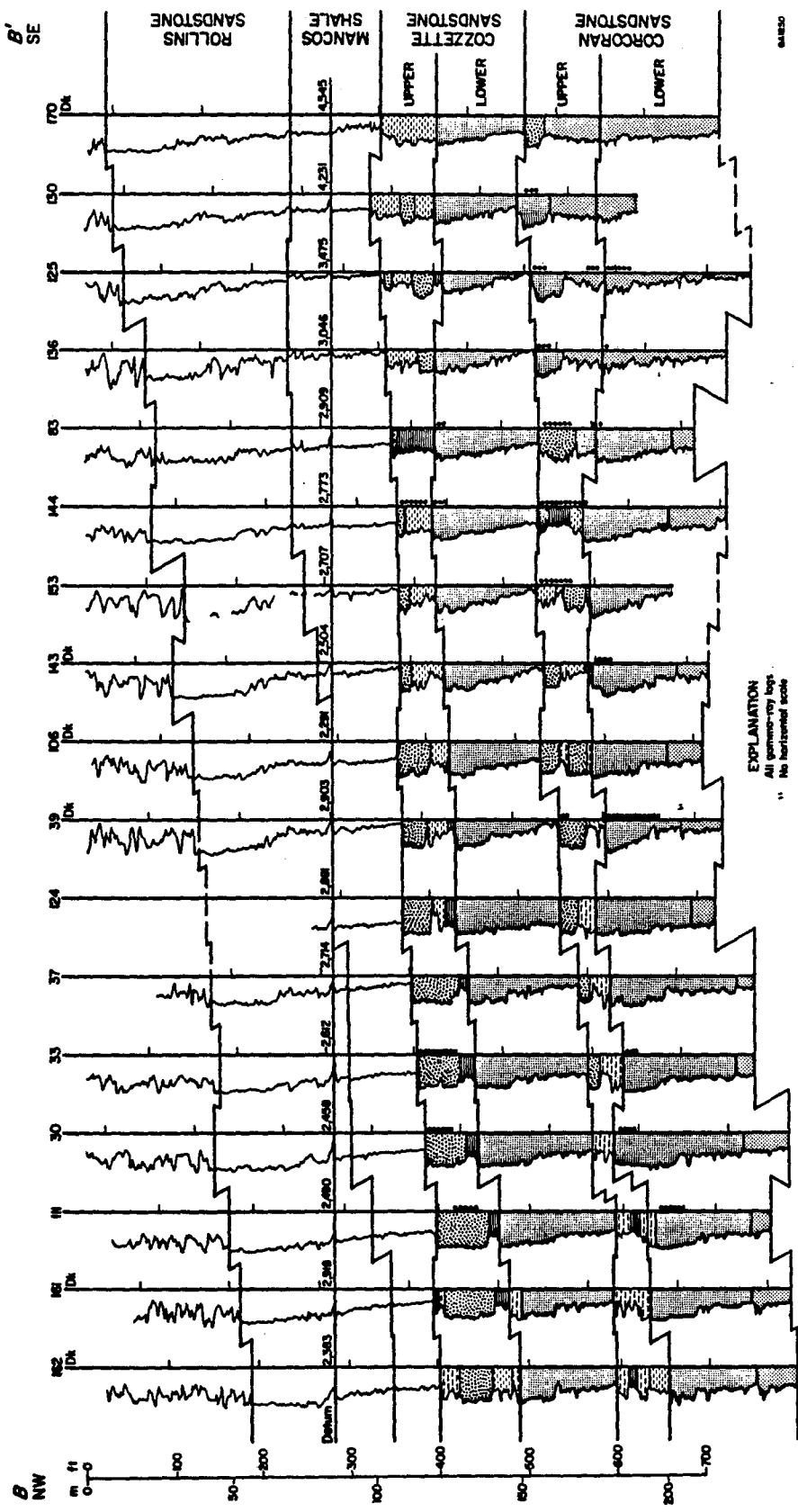


Figure 113. Cross section B-B', Shire Gulch and Plateau Fields.

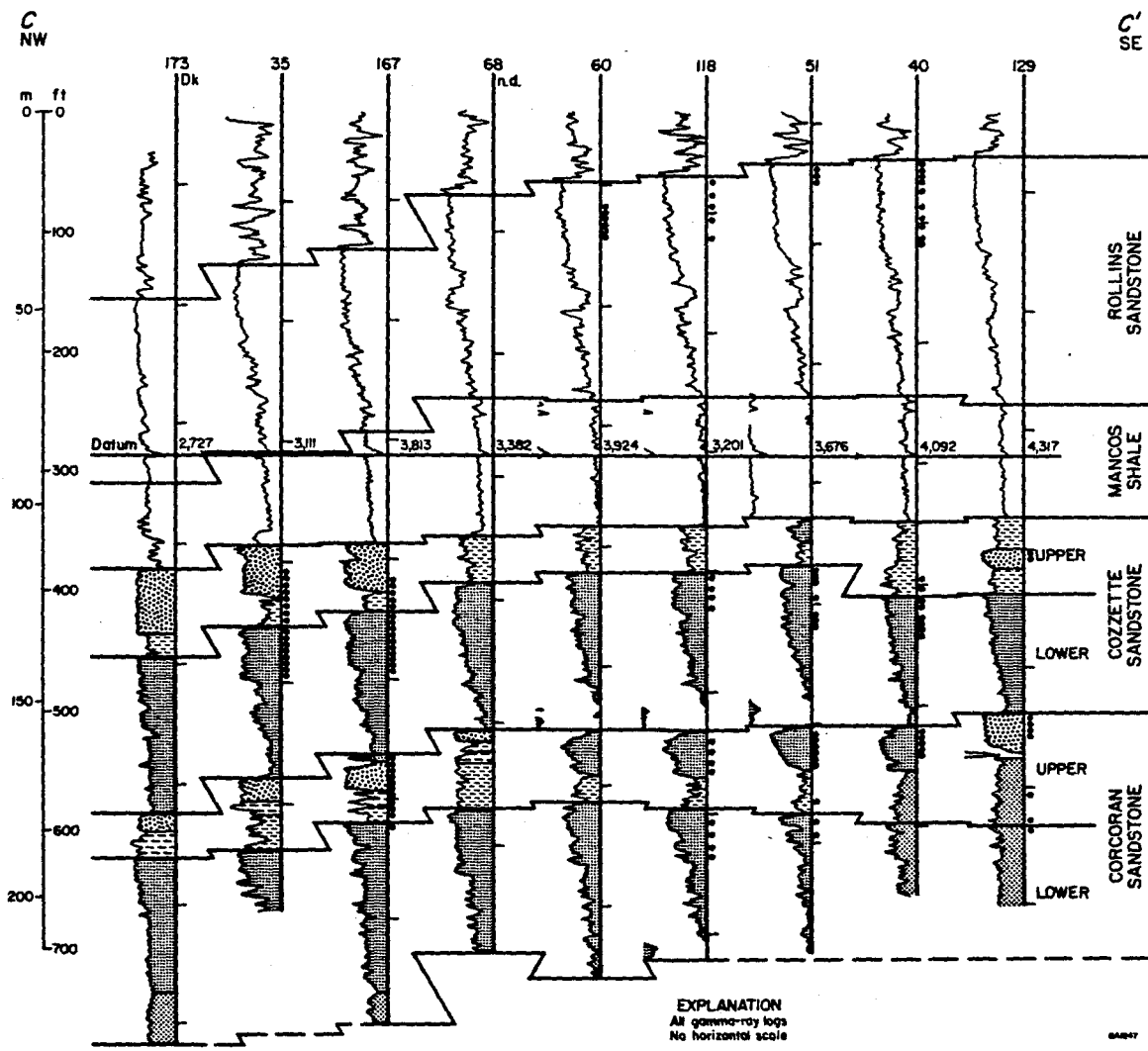


Figure 114. Cross section C-C', Shire Gulch and Plateau Fields.

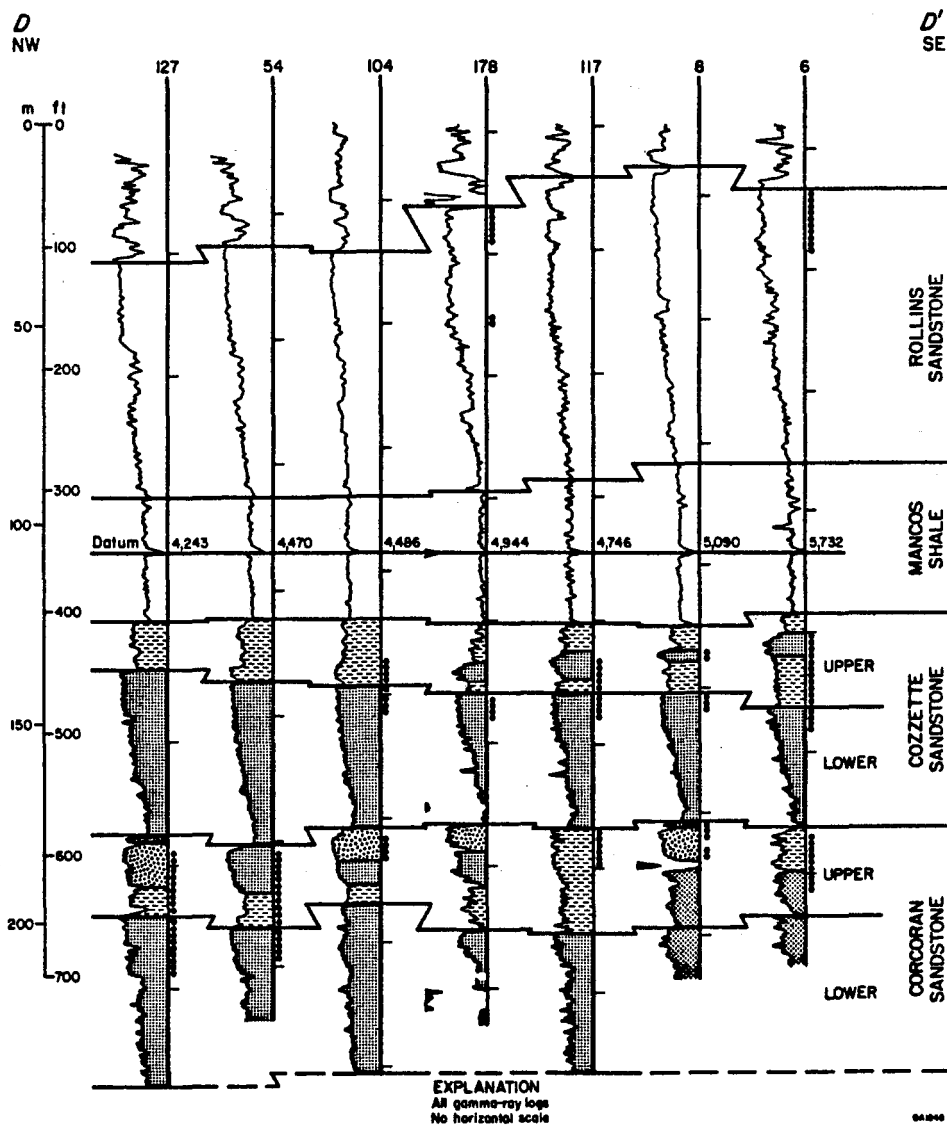


Figure 115. Cross section D-D', Plateau Field.

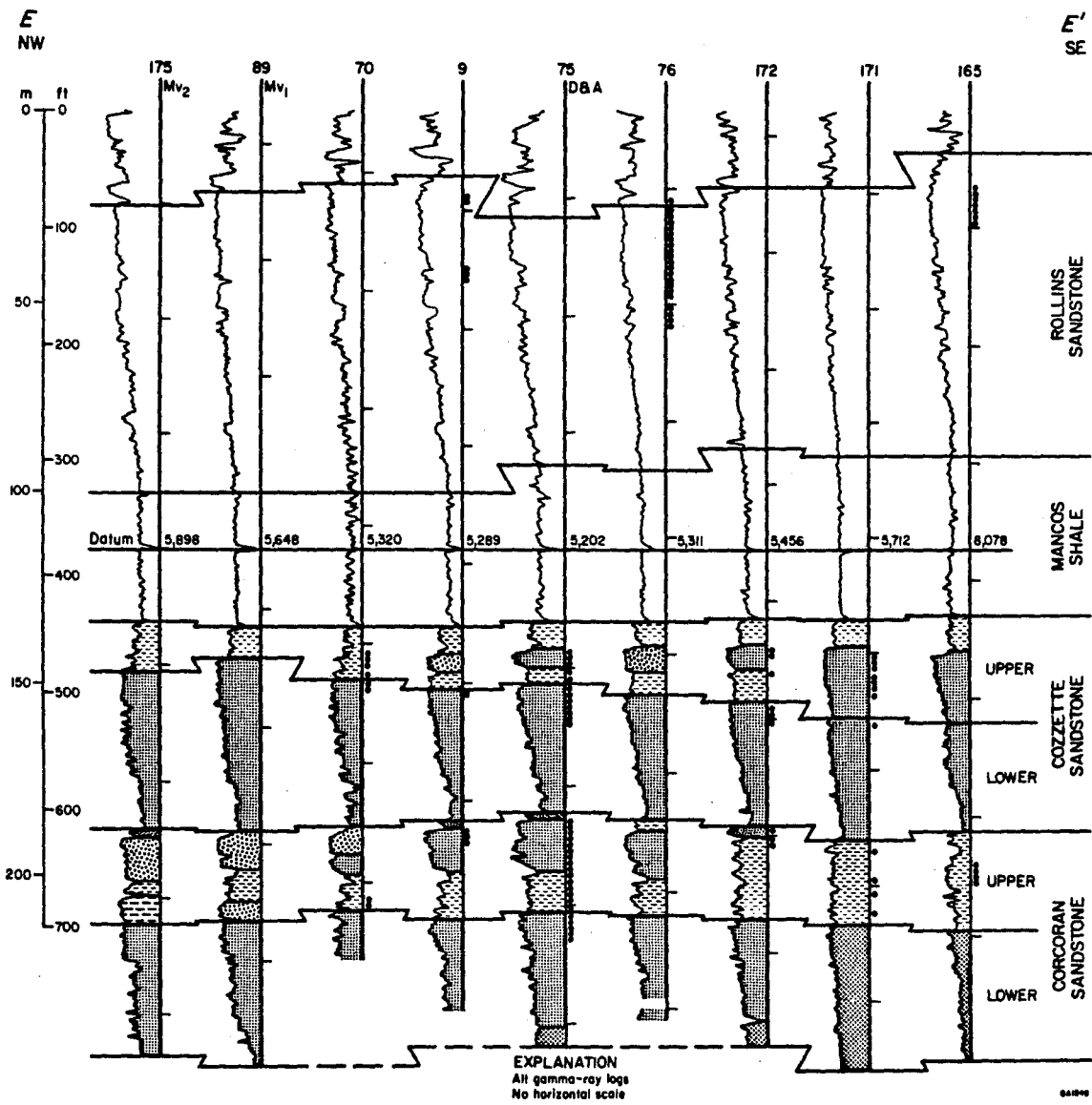


Figure 116. Cross section E-E', Plateau Field.

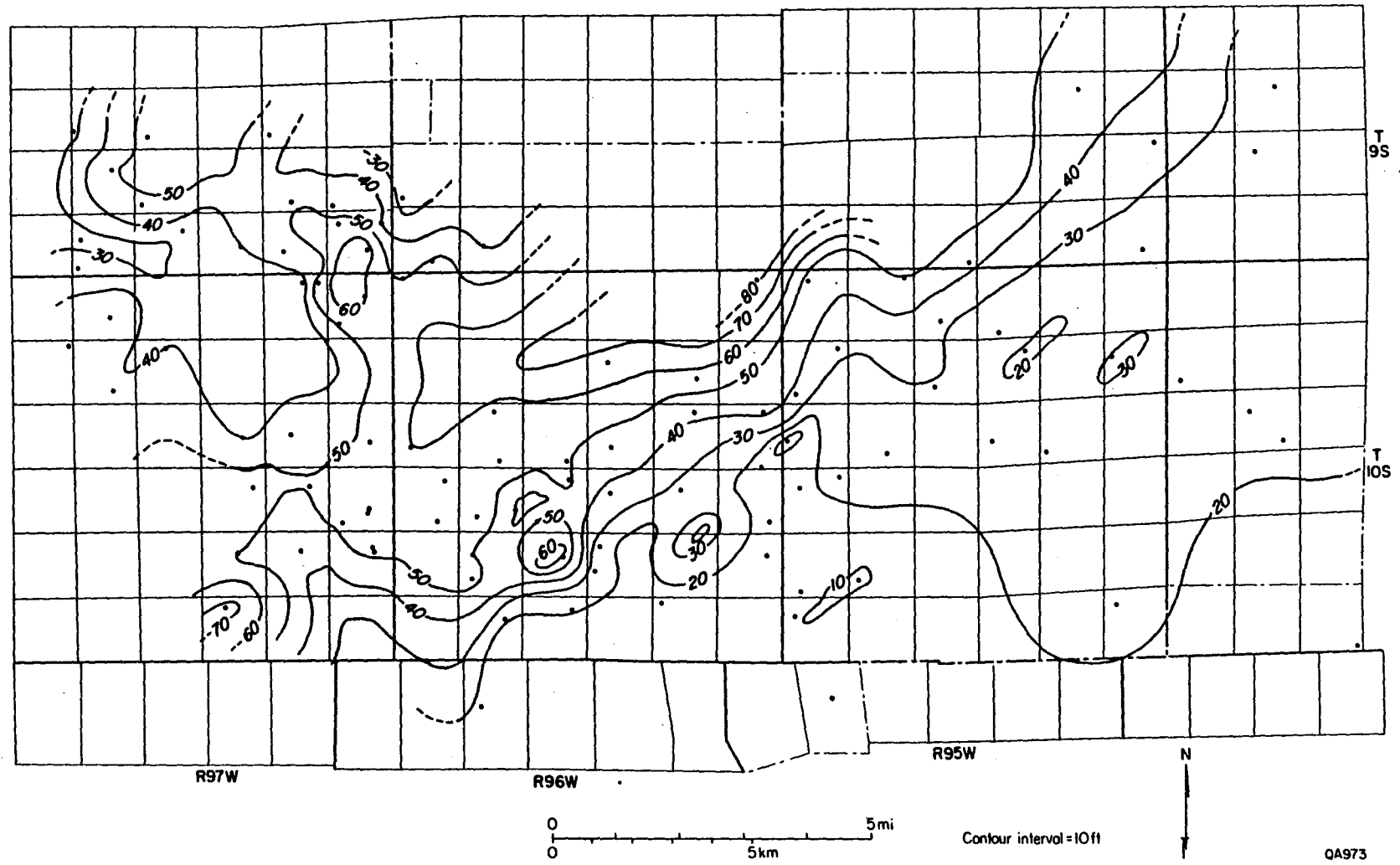


Figure 117. Net sandstone in the lower Corcoran Sandstone, Shire Gulch and Plateau Fields.

sandstone and siltstone(?) interbeds. This transition is especially clear between wells 144 and 170, cross section B-B' (fig. 113).

The GR-log patterns and net sand distribution of the lower Corcoran suggest that it represents upper and lower shoreface to possible foreshore deposition. Shoreface sequences may be associated with the delta front of wave-dominated deltas as well as with barrier island and strandplain systems (Fisher and Brown, 1972); therefore lateral and vertical facies associations must be used to distinguish these depositional systems (Balsley, 1980).

Upper Corcoran

Limited areas of net sandstone greater than 40 ft thick occur coincident with or (mostly) downdip of the maximum net sandstone trend in the lower Corcoran (fig. 118). Within T10S R95W, net sandstone greater than 40 ft thick occurs entirely seaward of maximum lower Corcoran net sandstone, and sandstones are most frequently upward-coarsening to blocky in log pattern (wells 40 and 129, fig. 114; wells 104, 178, 117, and 8; fig. 115). The lower Corcoran in the latter township is mostly interbedded shale and sandstone with poorly defined upward-coarsening sequences in some wells. The downdip upper Corcoran may also represent shoreface deposits and possibly an emergent foreshore, as in the lower Corcoran, or a nearly emergent marine bar. The sinuous nature of net sandstone distribution from the northeast corner of the map area to the southeast corner of T10S R95W is an indication of a strike-fed system.

Other areas of net sandstone exceeding 40 ft in thickness occur updip in Shire Gulch Field within southeastern T9S R97W and northeastern T10S R97W (fig. 118). The pattern of net sandstone distribution over a relatively small area in these townships does not aid interpretation of the depositional origin of these sandstones, but their blocky log character, association with coal-bearing sequences (wells 33, 37, and 124; fig. 113), and lenticular nature (compare wells 30 and 33; fig. 113) suggest that they may represent distributary channels. Substantial additional well control is available in parts of T9-10S R97W, and future use of additional well data may better define a channel pattern. However, the width of individual lenticular channel fills in the Blackhawk Formation within the Mesaverde Group of Utah ranges from 800 to 2,000 ft (Balsley,

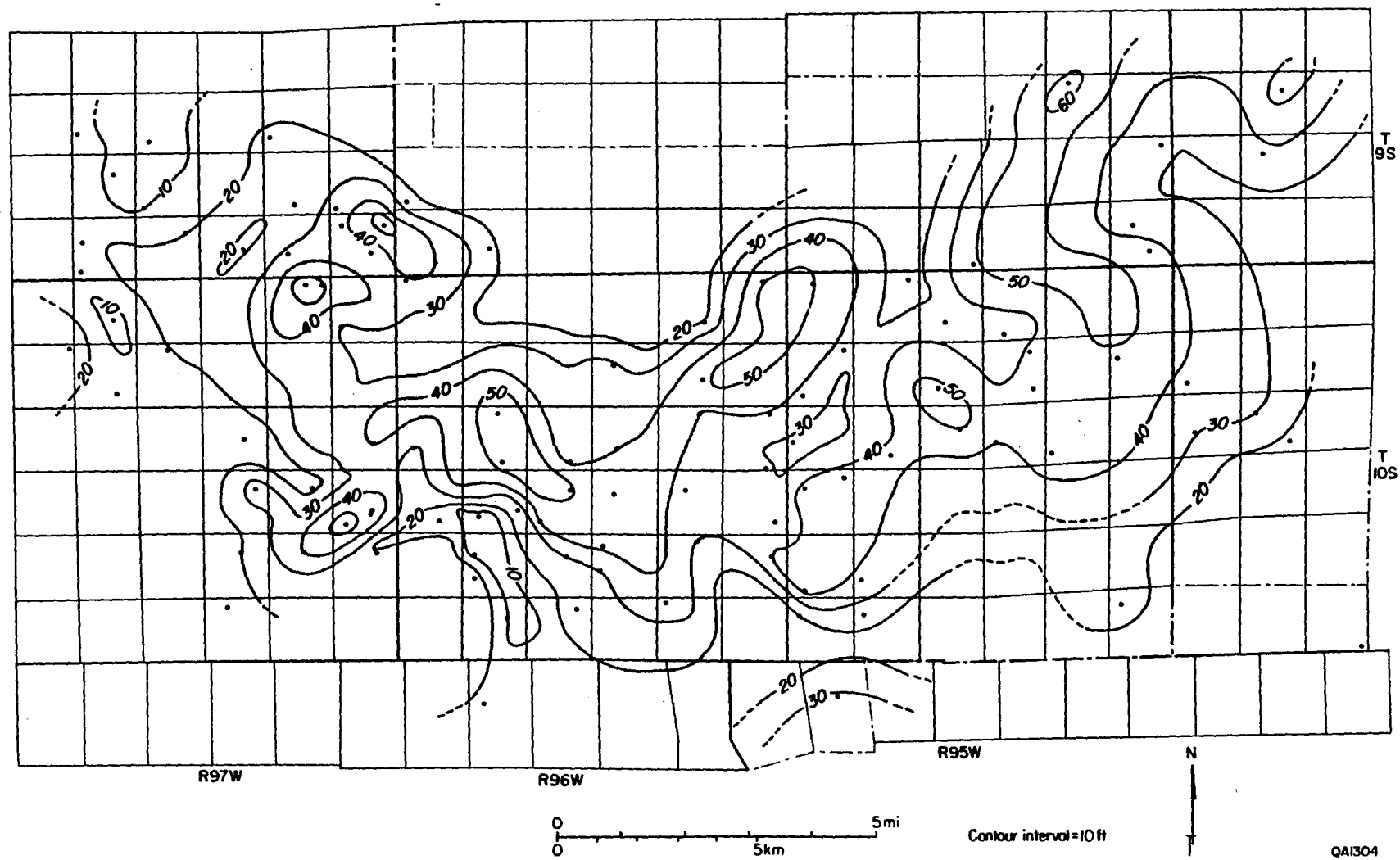


Figure 118. Net sandstone in the upper Corcoran Sandstone, Shire Gulch and Plateau Fields.

1980). Such sand bodies may therefore occur between the most dense available well control, and similar but not identical sandstones may be miscorrelated as the same unit when in reality more than one channel sandstone exists laterally in the same stratigraphic position.

Lower Cozzette

Maximum net sandstone in the lower Cozzette, as in the lower Corcoran, follows a northeast trend and includes more areally extensive thick net sandstone than in any other subdivision of the Corcoran and Cozzette Sandstones (fig. 119). A thick, rapidly upward-coarsening sequence with blocky sand at the top characterizes the thickest areas of lower Cozzette net sandstone, as in well 141 (fig. 112), wells 127 and 54 (fig. 115), and wells 175 and 89 (fig. 116). More sand-rich middle and lower sections of the lower Cozzette characterize all these wells and indicate an abundant sediment supply to areas of shoreface development.

Updip of the maximum net sandstone trend, in the western half of the map area, isolated maxima of net sandstone of 60 to 70 ft suggest less laterally continuous sand deposition in the lower and middle sections of the stratigraphic unit. A relatively thick, blocky sandstone with a sharp to somewhat upward-coarsening base occurs at the top of the unit (well 167; fig. 114). Laterally this upper sandstone in the lower Cozzette thins or contains a greater proportion of shaly sandstone (wells 39 and 37; fig. 113), probably due to local variations in sediment supply.

Upper Cozzette

Net sandstone greater than 40 ft thick in the upper Cozzette is distributed unequally in the southeast and northwest parts of the map area (fig. 120). Upward-coarsening to slightly upward-coarsening and blocky sandstone sequences and shale comprise the upper Cozzette to the southeast (wells 75, 76, 172, 171, and 165; fig. 116). These wells suggest continuation of the shoreface buildup from the lower Cozzette (wells 172 and 165) and possibly marine bar development. In the northwest part of the map area, net sandstone from 40 to over 60 ft thick consists predominantly of a single blocky unit with sharp upper and lower contacts (wells 32 and 72, fig. 112; wells 162, 161, 111, and 30; fig. 113) which may represent distributary-mouth bar deposition as part of a small deltaic complex behind a barrier island.

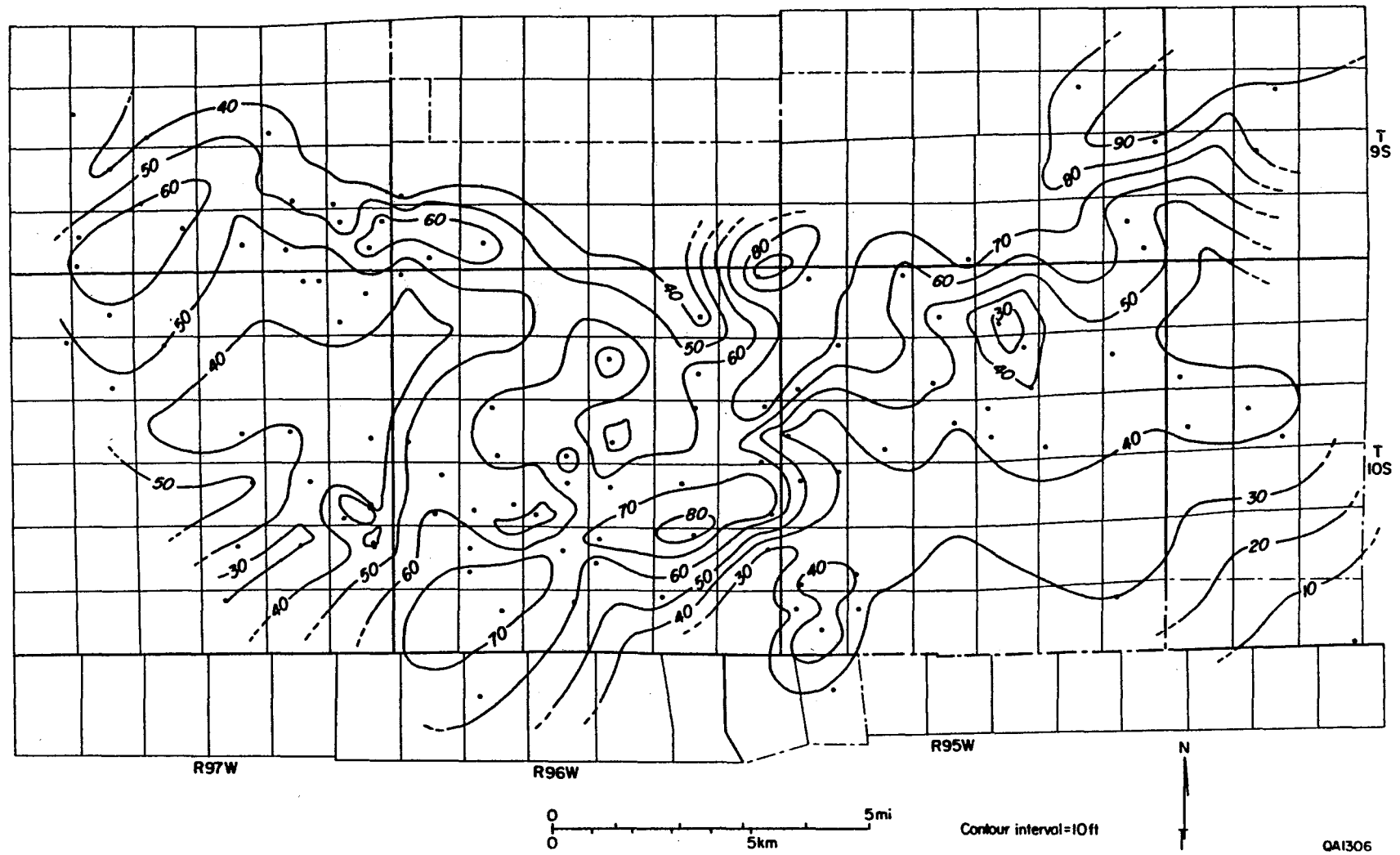


Figure 119. Net sandstone in the lower Cozzette Sandstone, Shire Gulch and Plateau Fields.

Discussion

Regional studies of sedimentation in the Cretaceous Seaway place a major point of repetitive deltaic deposition along the Colorado-Wyoming border centered approximately 130 mi north to northeast of Plateau Field (Weimer, 1970; Asquith, 1974). Regressive shorelines of the Campanian lower and middle Iles Formation, equivalent in part to the Corcoran and Cozzette Sandstones, trend northeastward through the Piceance Creek Basin (Zapp and Cobban, 1960). The distribution of total net sandstone in the Corcoran (fig. 108) and the orientation of the zero coal isoliths in the Corcoran and the Cozzette (fig. 109) support a northeastward shoreline trend during deposition of these sandstones in the southern part of the basin. Within Shire Gulch and Plateau Fields, net sandstone mapping of the lower parts of the Corcoran and Cozzette sharply define shoreface sequences with decreasing sand content and a transition into the marine Mancos Shale to the southeast (figs. 117, 119 and 42). The Corcoran and Cozzette Sandstones therefore separated open marine conditions toward the base of each unit from coal-forming environments at the top. This same cycle was repeated once again above the Cozzette with deposition of a tongue of Mancos Shale overlain by the Rollins Sandstone, the youngest marginal marine sandstone preceding continental deposition of the overlying Mesaverde Group. A major coal-bearing interval, the Cameo Coal Zone, immediately overlies the Rollins Sandstone.

Thus, in a regional setting marginal to a major deltaic depocenter and within the context of overall shoreline progradation, a barrier or strandplain origin for the Corcoran and Cozzette Sandstones fits regional strike-elongate sandstone geometries and vertical sequences of GR-log facies. Barrier and strandplain depositional systems may exist lateral to, or actually as part of, wave-dominated delta systems; the distinction between barrier and strandplain is dependent upon the presence of a lagoonal facies (Fisher and Brown, 1972). Barrier and strandplain systems are not mutually exclusive, however, and may exist in close lateral juxtaposition, dependent on the degree of development of landward bay and lagoonal facies along strike (McCubbin, 1982). The Corcoran and Cozzette Sandstones are interpreted to represent barrier

deposition primarily in the lower units of each sandstone. Major facies present are lower to upper shoreface and foreshore.

Although sediment may have moved several hundred miles along strike from a major prograding delta, it is also likely that coastal plain streams fed smaller deltas within bays and lagoons, and that these deltas may have locally filled the back-barrier environments and prograded to the open shoreline. The vertical and lateral variability of the upper Corcoran and upper Cozzette Sandstones in Shire Gulch and Plateau Fields suggests that such small deltas were present in addition to a bay-lagoon facies. Shales and silty or sandy shales probably were deposited in open, brackish water whereas interbedded sandstones, coal, and shale represent deltaic bay-lagoon filling. Sandstones with log patterns that are blocky or have slightly upward-coarsening bases may represent distributary-mouth bars (wells 32 southeast through 142, fig. 112), possibly overlain by distributary channel sandstones where more than one depositional sequence seems to be present (wells 123, 41, 45, and 109, fig. 112).

Important steps remain to clarify several of the above inferences; more complete interpretations are not possible at present because budget constraints affected data acquisition over a significant portion of the Phase B contract period. With the acquisition of additional well logs in Shire Gulch - Plateau Fields, the upper parts of the Corcoran and the Cozzette must be examined in detail to define the geometry of deltaic framework sandstones and define the sandstone platforms that supported peat accumulation. A depositional model, presented by Ferm and others (1971), of Carboniferous delta-plain and barrier environments of northeastern Kentucky, wherein back-barrier coals were formed, has potential application in the southern Piceance Creek Basin. The lateral continuity of upper Cozzette and Corcoran Sandstones may be limited for facies such as distributary channels, and may need to be categorized separately from laterally persistent shoreface sandstones when comparing gas production to lateral reservoir extent. Identification of wells by the Colorado Geological Survey that penetrate the entire Corcoran-Cozzette outside the Shire Gulch - Plateau Field will allow retrieval of well data from the files of the Colorado Oil and Gas Conservation Commission that are not available

from commercial services. These files are presently being utilized to identify existing core and to locate core analyses that have been submitted by operators. These data, reviewed together with core to be taken by GRI, with log-pattern distribution maps, and with other types of detailed facies distribution studies, will help delineate specific, productive facies and characterize reservoir quality within each sandstone. However, because data are not evenly distributed over the study area it must be ensured that inferred depositional patterns are not overly influenced by lack of data in some areas or by high concentrations of data in few fields.

Production-Facies Relationships

Geological characterization of the Corcoran-Cozzette gas resource requires analysis of gas productivity by stratigraphic unit, by facies within that unit, and by trapping mechanism. Future study of initial or long-term production trends may be hampered by the distribution of perforations in a single well among two or among all three units in the Corcoran-Cozzette-Rollins sequence. Reservoir pressures in these units are such that production is commingled in many wells; however, 60 wells in the southern Piceance Creek Basin have been identified that are completed only in the Corcoran (46 wells), the Cozzette (12 wells), or the Rollins (2 wells). Logs of these wells will be examined to make further subdivisions according to facies, and production data will be compiled by facies distribution as analysis of depositional systems proceeds.

A preliminary examination of producing interval versus stratigraphic unit in Shire Gulch and Plateau Fields shows that perforated intervals in 34 wells are mostly within the upper Corcoran (44%) and subequally within the lower Corcoran (20%), lower Cozzette (20%), and upper Cozzette (16%). Total gross perforated interval in these wells is 2,105 ft, not including any perforations in the Rollins Sandstone. The productive upper Corcoran is often an upward-coarsening sequence in the downdip (southeastern) parts of this area and is not associated with interbedded coal. Fluvial or deltaic upper Corcoran in a positionally updip position in Shire Gulch Field has not been tested in many wells in favor of deeper objectives.

The Corcoran Sandstone appears to be more productive than the Cozzette Sandstone on the basis of these simple initial reviews of productive unit and perforated interval. More complete studies in relation to facies are part of the next phase of geologic tight gas sandstone studies within which production history and productive area are related to genetic facies, reservoir geometry, and trends of mineralogy and diagenesis.

RESERVOIR ANALYSIS

Introduction

Permeability, porosity, and water saturation are important parameters for accurate estimates of gas resources and reserves as well as for geological studies. Porosity and water saturation were determined from well logs for the Corcoran and Cozzette Sandstones, and permeability was determined using flow potential tests for the Travis Peak Formation.

To confirm the methodology used in well log interpretations, calculated porosity and water saturation were compared with results from foot-by-foot core measurements from the Corcoran and Cozzette Sandstones in the Koch Exploration, Horseshoe Canyon no. 1-21 well. The methodology used here in determining porosity and water saturation may be applied to the same formation in other areas.

The methodology of using flow potential tests was implemented in this work to determine formation permeability because pressure drawdown/buildup test data are not normally available from public records. Permeability distribution was estimated from flow potential test data from the Travis Peak Formation in Lansing North Field, Harrison County, Texas.

Corcoran and Cozzette Sandstones

Porosity Logs Interpretations

Porosity may be derived from the interpretation of density, neutron, and acoustic logs. All these logs respond not only to porosity, but also to lithology and to fluid in the pore space of the formation. These logs may be interpreted individually or two or three logs may be analyzed simultaneously. The results of analyzing two or three logs simultaneously are always better than the results of interpreting each log individually (Dresser Atlas, 1975).

The assumption of a given grain density (or lithology) for a formation is critical in interpreting density logs (Kukul and others, 1983). However, in the situation where there are two known major minerals in a formation, porosity and grain density (or lithology) may be

derived by using two or three porosity logs simultaneously. If the rock is more complex, the grain density (or lithology) derived from interpretation of two logs (neutron and density) may be less accurate or reliable than is desirable, but porosity remains accurate (Dresser Atlas, 1975). Thus far, it has been assumed that the formation is shale-free. For shaly sands, a shale correction using the gamma-ray log should be made prior to any porosity interpretations. A hydrocarbon correction is also necessary for a reservoir containing hydrocarbons, but may be made later.

Methodology

Since the well logs used in this study were surveyed by Dresser Atlas, the methodology and charts (or correlations) developed by Dresser Atlas (1975) have been adopted. The overall methodology to derive porosity is described by a flow chart (fig. 121). It is common to analyze neutron and density logs simultaneously, as shown in the left column of the figure, in which porosity as well as grain density may be simultaneously determined by cross-plotting techniques. For purposes of comparison, porosity calculations (right column in fig. 121) may also be derived from neutron and density logs with known grain density (or lithology) from a core sample. This approach is dependent upon having a core sample available.

Porosity unit and density/lithology relationship.--Neutron porosity is normally based on limestone units; however, other lithological porosity units, such as sandstone or dolomite, may also be recorded. The relationship among limestone, dolomite, and sandstone porosity units provides the basis for conversion of neutron porosity units from one type to another (Dresser Atlas, 1975, fig. 6-4, compensated neutron lithology effect, p. 6-5).

Density porosity is normally based on grain density of 2.65 gm/cc (sandstone) or 2.68 gm/cc (sandstone-limestone). With knowledge of grain density, density porosity may be accurately calculated from an equation (Dresser Atlas, 1975), such as

$$\phi_d = \frac{\rho_{ma} - \rho_b}{\rho_{ma} - \rho_f} \quad (1)$$

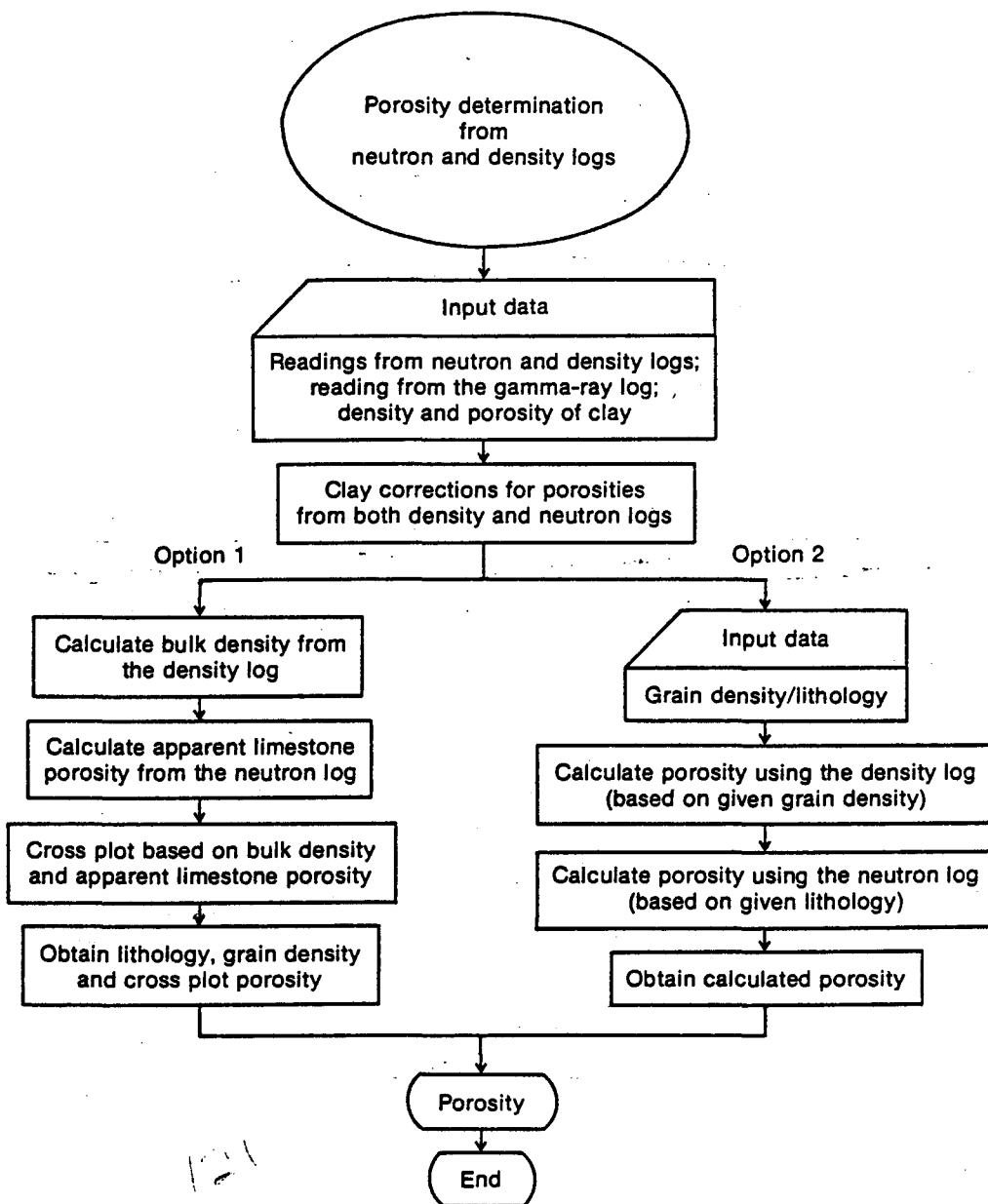


Figure 121. Flow chart showing procedures to determine porosity from well log analysis.

where ϕ_d = density derived porosity, fraction
 ρ_{ma} = matrix or grain density, gm/cc
 ρ_b = formation bulk density from density log, gm/cc
 ρ_f = density of drilling fluid, gm/cc

In cross-plotting techniques, bulk density from density porosity with shale correction (if any) is required. By rearranging the above equation, the bulk density of the formation can be calculated from a known density porosity and a given grain density, such as

$$\rho_b = \phi_d \rho_f - \rho_{ma} (\phi_d - 1) \quad (2)$$

From the effect of lithology/grain density in density and neutron logging calculations, it is revealed that higher grain density used in the porosity calculations will lead to higher apparent density porosity and lower apparent neutron porosity, and vice versa. Thus, porosities determined from those two logs will tend to compensate each other with grain density (or lithology) effect when analyzing two logs simultaneously.

Porosity corrections for shale effect.--Due to the presence of shale in the formation, the determination of shale content for correction of porosity is essential. Shale content, or more appropriately clay content, is related to gamma-ray index. Gamma-ray index (IGR), or relative gamma-ray deflection, is established by observing a clean sand deflection and shale base line such as (Dresser Atlas, 1975):

$$IGR = \frac{GR \text{ (at specific zone)} - GR \text{ (clean sand)}}{GR \text{ (shale)} - GR \text{ (clean sand)}} \quad (3)$$

where GR = gamma ray reading, API units.

With a given gamma-ray index, clay content or volume of clay may be obtained (Dresser Atlas, 1975, fig. 6-1, clay content from Gamma Ray Index, p. 6-2). Shale corrections can then be made by using shale correction charts (Dresser Atlas, 1975, chart 7, Densilog porosity and shale correction, and chart 8, Neutron Shale Correction).

Neutron-density crossplot technique.--A neutron log (compensated) and a density log are required by cross-plotting techniques in which the general type of solutions for three basic lithologies, such as sandstone, limestone, and dolomite, are shown (fig. 122). When data from a sandstone and a limestone formation are plotted, the points should fall along the sandstone and the limestone lines in the crossplot (fig. 122), respectively. The equivalent is true for dolomite. For a limy dolomite, the points will fall between the limestone and the dolomite lines. It is necessary to know if a sandstone-limestone, a limestone-dolomite, or a dolomite-sandstone rock composes the formation, because a point could fall between the limestone and the dolomite lines for a sandstone-dolomite rock. Porosity may be determined by joining the equivalent porosity points on two known lithology lines to construct a porosity scale.

If significant amounts of gas are present in the invaded zone surrounding the wellbore, the points on figure 122 will be shifted to the lower left corner of the figure. In this case, corrections for hydrocarbon density variation are required (Dresser Atlas, 1975, chart 20, Estimation of porosity in hydrocarbon zones with Neutron and Densilog).

Porosity calculations from neutron-density logs with known grain density.--Foot-by-foot grain (or matrix) density is not normally available; when available, grain density data become valuable for comparing porosity.

With a given density of drilling fluid, the porosity may be estimated (eq.(1)) by knowing bulk density from the density log and grain density from the core measurement. Equivalent procedures may be applied to obtain porosity from the neutron log (Dresser Atlas, 1975, fig. 6-4, Compensated neutron lithology effect, p. 6-5). Given both density and neutron porosities, lithology-corrected porosity may be obtained (Dresser Atlas, 1975, chart 20, Estimation of porosity in hydrocarbon zones with Neutron and Densilog).

Input Data

To calculate formation porosity from density and neutron logs using the methodology described above, the data required are summarized as follows:

**POROSITY & LITHOLOGY DETERMINATION FROM
DENSILOG & COMPENSATED NEUTRON LOG ($\rho_f = 1.0 \text{ gm/cm}^3$)**

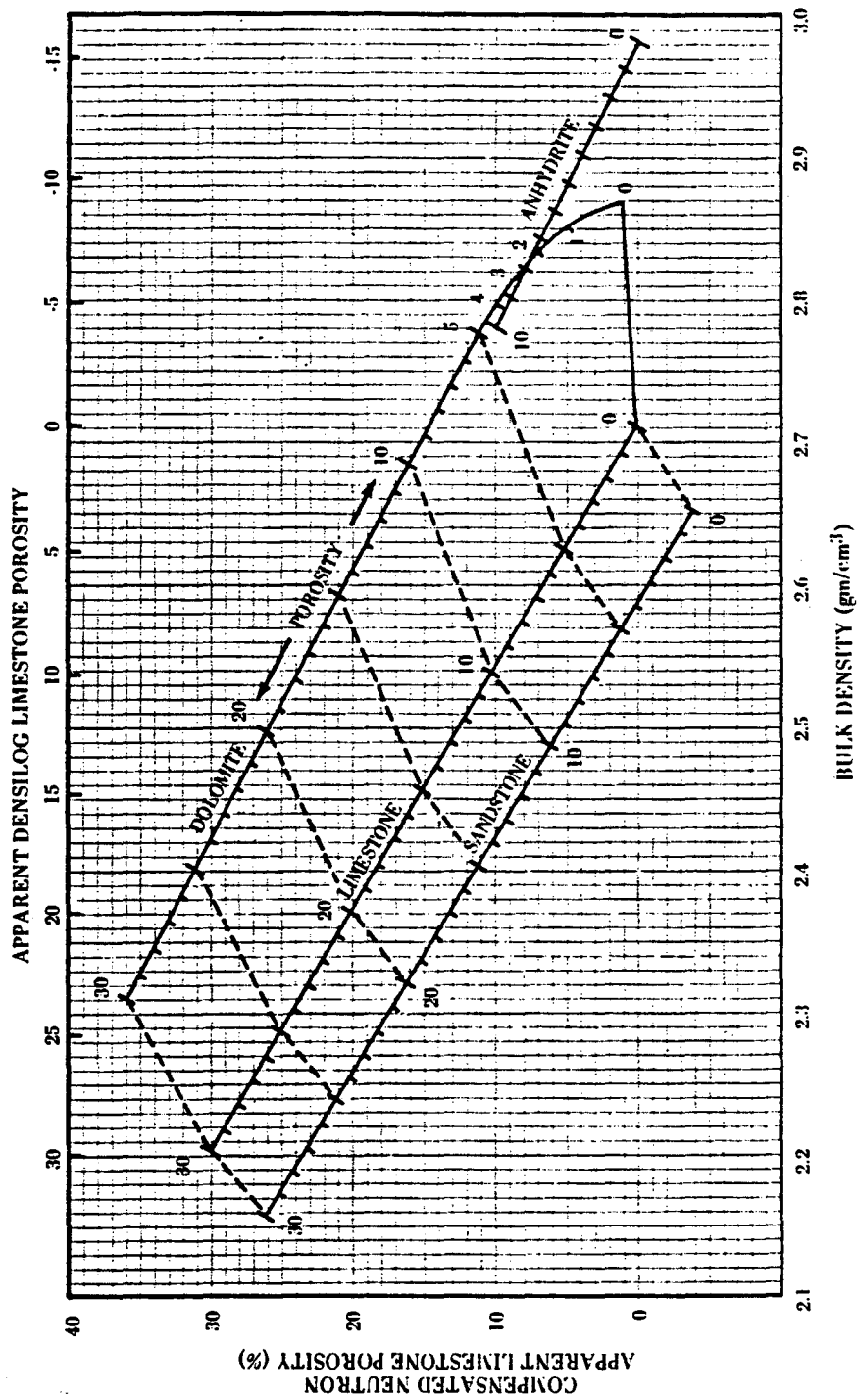


Figure 122. Porosity and lithology determination from density and compensated neutron logs. From Dresser Atlas (1975).

- (1) bulk density or porosity reading from density log at zone of interest (with grain density used),
- (2) porosity reading from neutron log at zone of interest (with lithology used in log),
- (3) gamma ray reading at zone of interest,
- (4) neutron porosity of adjacent shale,
- (5) density porosity (or bulk density) of adjacent shale,
- (6) gamma-ray reading in shale zone,
- (7) gamma-ray reading in clean sand, and
- (8) grain density from core analysis.

Results and Discussion

Based on the methodology described in the previous section, porosities determined (table 21) for the Cozzette Sandstone in the Koch Exploration, Horseshoe Canyon no. 1-21 well, Shire Gulch field, Mesa County, Colorado, were obtained from two logs (neutron and density logs) used together, and two logs analyzed separately. Using crossplot techniques, grain density and porosity were also simultaneously determined by assuming two known minerals in the formation, i.e., sandstone and limestone. The results of calculated porosities have been compared with these from core measurements by plotting:

- (1) core porosity versus calculated porosity from neutron-density crossplot (with no grain density information),
- (2) core porosity versus calculated porosity from neutron-density logs (based on core grain density information),
- (3) core porosity versus calculated porosity from density log (based on calculated grain density),
- (4) core porosity versus calculated porosity from density log (based on core grain density),
- (5) core porosity versus calculated porosity from neutron log (based on calculated grain density), and
- (6) core porosity versus calculated porosity from neutron log (based on core grain density).

Table 21. Porosities from log analysis and from core measurements for the Cozzette Sandstone in Koch Exploration, Horseshoe Canyon no. 1-21.

Sample number	Log depth (ft)	Density porosity reading ($\rho_m=2.68 \text{ g/cm}^3$) (gm/cm ³)	Neutron porosity reading (sandstone) (%)	Gamma reading (API)	Bulk density (with shale correction) (%)	Neutron porosity limestone (with shale correction) (%)	Cross-plot grain density (%)	Cross-plot porosity (%)	Core grain density (gm/cm ³)	Core porosity (%)	Calculated density-neutron porosity (based on core grain density) (%)
2, 3	3,040-3,042	16.5	18.0	81	2.423	9.5	2.648	13.4	2.640	13.35	12.8
4, 5	3,042-3,044	15.5	17.5	75	2.445	10.3	2.660	13.2	2.650	12.75	12.2
6, 7	3,044-3,046	15.0	17.5	70	2.441	11.2	2.670	13.5	2.650	12.90	12.5
8, 9	3,046-3,048	15.5	18.0	65	2.426	12.5	2.670	14.7	2.650	12.80	13.5
10, 11	3,048-3,050	13.5	16.5	70	2.462	10.3	2.675	12.6	2.645	7.55	11.3
12, 13	3,050-3,052	12.0	19.0	73	2.490	12.0	2.700	12.3	2.645	11.00	10.3
14, 15	3,052-3,054	13.5	18.5	73	2.466	11.0	2.680	12.7	2.650	11.50	11.5
16, 17	3,054-3,056	13.5	18.0	75	2.466	11.5	2.680	13.0	2.650	10.25	11.5
18, 19	3,056-3,058	12.5	17.5	71	2.481	12.0	2.700	12.6	2.650	11.15	11.0
20, 21	3,058-3,060	15.0	16.0	80	2.436	7.8	2.630	11.6	2.650	11.35	12.1
22, 23	3,060-3,062	16.5	14.5	65	2.411	9.2	2.640	13.5	2.650	13.15	13.5
24, 25	3,062-3,064	16.0	16.0	75	2.425	9.0	2.645	12.9	2.650	12.10	12.8
26, 27	3,064-3,066	12.8	17.0	75	2.478	10.0	2.680	11.5	2.650	8.70	10.6
28, 29	3,066-3,068	13.0	15.0	67	2.473	9.2	2.660	11.5	2.650	11.25	10.7

277

Table 21 (continued)

Sample number	Log depth (ft)	Density porosity reading ($\rho_m=2.68 \text{ g/cm}^3$) (gm/cm ³)	Neutron-porosity reading (sandstone) (%)	Gamma reading (API)	Bulk density (with shale correction) (%)	Neutron porosity limestone (with shale correction) (%)	Cross-plot grain density (%)	Cross-plot porosity (%)	Core grain density (gm/cm ³)	Core porosity (%)	Calculated density-neutron porosity (based on core grain density) (%)
30, 31	3,068-3,070	14.2	16.0	67	2.448	10.2	2.660	13.0	2.640	10.95	11.9
32, 33	3,070-3,072	14.6	15.0	65	2.445	9.8	2.660	12.8	2.655	10.80	12.0
34, 35	3,072-3,074	11.0	15.5	63	2.504	10.5	2.690	11.0	2.690	9.20	10.4
36, 37	3,074-3,076	6.5	15.5	62	2.576	10.5	2.730	9.0	2.685	6.10	7.5
38, 39	3,076-3,078	10.5	16.0	67	2.515	10.2	2.700	11.0	2.650	10.95	9.0
278 40, 41	3,078-3,080	12.0	18.5	75	2.495	11.3	2.700	11.9	2.655	10.35	10.0
42, 43	3,080-3,082	5.5	21.0	95	2.625	10.0	2.750	8.0	2.670	8.25	4.7
44, 45	3,082-3,084	12.5	18.1	80	2.490	9.8	2.680	11.3	2.650	10.20	10.0
46, 47	3,084-3,086	13.0	18.5	85	2.485	9.3	2.675	11.4	2.655	11.20	10.2
48, 49	3,086-3,088	13.2	15.8	77	2.475	8.5	2.670	11.2	2.670	9.30	11.0
50, 51	3,088-3,090	13.7	15.1	75	2.462	9.8	2.665	12.3	2.680	11.90	12.2
52, 53	3,090-3,092	13.5	15.5	80	2.470	7.3	2.650	11.0	2.680	12.35	11.2
54, 55	3,092-3,094	13.5	18.0	82	2.470	9.8	2.670	12.0	2.680	12.30	11.8
56, 57	3,094-3,096	12.5	18.8	85	2.495	9.5	2.680	11.0	2.690	12.90	11.0
61, 62	3,116-3,118	14.5	17.5	79	2.453	10.0	2.665	12.6	2.65	12.3	11.9

Table 21 (continued)

Sample number	Log depth (ft)	Density porosity reading ($\rho_m=2.68 \text{ g/cm}^3$) (gm/cm ³)	Neutron-porosity reading (sandstone) (%)	Gamma reading (API)	Bulk density (with shale correction) (%)	Neutron porosity limestone (with shale correction) (%)	Cross-plot grain density (%)	Cross-plot porosity (%)	Core grain density (gm/cm ³)	Core porosity (%)	Calculated density-neutron porosity (based on core grain density) (%)
63, 64	3,118-3,120	11.5	18.1	79	2.504	10.5	2.69	11.2	2.645	9.05	13.0
65, 66	3,120-3,122	13.0	22.0	70	2.468	16.7	2.72	15.5	2.66	11.85	17.3
67, 68	3,122-3,124	21.0	19.0	60	2.331	14.7	2.645	18.8	2.675	11.1	18.0
69, 70	3,124-3,126	14.5	17.0	60	2.438	12.7	2.70	12.0	2.655	11.65	13.1
71, 72	3,126-3,128	14.5	17.4	61	2.438	13.1	2.71	14.6	2.66	10.45	13.5
279 73, 74	3,128-3,130	14.5	17.0	65	2.440	11.8	2.67	14.0	2.66	11.15	14.2
75, 76	3,130-3,132	13.5	16.1	67	2.462	10.0	2.67	12.5	2.65	11.85	11.5
77, 78	3,132-3,134	12.1	17.5	81	2.502	9.2	2.68	11.0	2.655	10.9	9.7
79, 80	3,134-3,136	11.0	18.0	81	2.519	9.7	2.695	10.5	2.65	7.8	9.0
81, 82	3,136-3,138	11.5	20.5	90	2.520	10.5	2.70	10.8	2.665	8.35	9.5
83, 84	3,138-3,140	11.8	21.0	90	2.515	10.7	2.70	11.0	2.645	10.6	9.0
85, 86	3,140-3,142	14.0	19.0	80	2.462	11.0	2.68	13.0	2.64	7.7	11.2
87, 88	3,142-3,144	15.4	18.0	79	2.440	10.2	2.665	13.3	2.665	12.8	13.0
89, 90	3,144-3,146	14.9	19.8	79	2.446	11.9	2.68	13.8	2.665	14.4	13.0
91, 92	3,146-3,148	13.8	18.5	80	2.465	10.5	2.68	12.5	2.68	12.5	12.4

Table 21 (continued)

Sample number	Log depth (ft)	Density porosity reading ($\rho_m=2.68 \text{ g/cm}^3$) (gm/cm ³)	Neutron-porosity reading (sandstone) (%)	Gamma reading (API)	Bulk density (with shale correction) (%)	Neutron porosity limestone (with shale correction) (%)	Cross-plot grain density (%)	Cross-plot porosity (%)	Core grain density (gm/cm ³)	Core porosity (%)	Calculated density-neutron porosity (based on core grain density) (%)
93, 94	3,148-3,150	12.5	18.0	80	2.487	10.0	2.685	11.7	2.685	13.1	11.2
95, 96	3,150-3,152	9.5	17.5	80	2.541	9.8	2.71	9.6	2.695	8.6	9.1
97, 98	3,152-3,154	13.0	20.5	80	2.478	12.7	2.695	13.1	2.675	13.2	12.0
99, 100	3,154-3,156	14.5	21.5	78	2.453	13.7	2.695	14.5	2.67	12.95	13.2
101, 102	3,156-3,158	10.0	19.5	95	7.8	8.5	2.70	9.0	2.66	14.35	7.6
103, 104	3,158-3,160	7.5	19.5	88	6.2	10.2	2.73	9.2	2.695	5.15	7.6
105, 106	3,160-3,162	10.0	17.5	80	9.2	9.7	2.70	10.0	2.705	6.9	10.5
107, 108	3,162-3,164	10.0	16.0	80	8.8	8.0	2.69	9.2	2.68	10.35	8.6
109, 110	3,164-3,166	8.5	17.5	125	-	-	-	-	2.69	8.75	-
112, 113	3,266-3,268	16.8	13.1	72	16.3	7.0	2.62	13.0	2.655	12.15	13.2
114, 115	3,268-3,270	14.0	14.0	83	13.7	5.5	2.63	11.0	2.66	11.85	11.2
116, 117	3,270-3,272	17.5	14.5	70	17.0	8.5	2.625	14.0	2.655	12.3	15.0
18, 119	3,274-3,274	17.5	14.2	58	17.4	10.0	2.63	15.0	2.655	13.35	15.5
20, 121	3,274-3,276	17.5	14.2	58	17.4	10.0	2.63	15.0	2.655	10.0	15.5

Table 21 (continued)

Sample number	Log depth (ft)	Density porosity reading ($\rho_m=2.68 \text{ g/cm}^3$) (gm/cm ³)	Neutron-porosity reading (sandstone) (%)	Gamma reading (API)	Bulk density (with shale correction) (%)	Neutron porosity limestone (with shale correction) (%)	Cross-plot grain density (%)	Cross-plot porosity (%)	Core grain density (gm/cm ³)	Core porosity (%)	Calculated density-neutron porosity (based on core grain density) (%)
122, 123	3,276-3,278	15.8	13.3	58	15.7	9.1	2.64	14.0	2.65	12.1	13.3
124, 125	3,278-3,280	16.0	13.0	58	15.9	8.8	2.64	13.5	2.65	11.75	13.2
126, 127	3,280-3,282	16.0	13.0	58	15.9	8.8	2.64	13.5	2.655	11.25	13.4
128, 129	3,282-3,284	15.0	12.5	58	14.9	8.3	2.645	12.8	2.65	13.2	12.3
281 130, 131	3,284-3,286	15.4	13.2	60	15.2	8.9	2.645	13.2	2.655	11.85	13.0
132, 133	3,286-3,288	15.5	13.3	60	15.3	9.0	2.645	13.5	2.65	12.4	13.0
134, 135	3,288-3,290	16.0	12.3	65	15.7	7.3	2.63	13.0	2.655	11.4	13.0
136, 137	3,290-3,292	15.2	13.0	72	2.436	6.7	2.64	12.0	2.65	10.7	11.9
138, 139	3,292-3,294	13.2	14.0	74	2.470	7.0	2.65	11.0	2.675	10.25	11.0
140, 141	3,294-3,296	11.6	16.7	78	2.507	8.8	2.67	10.0	2.665	9.4	9.6
142, 143	3,296-3,298	13.0	15.0	70	2.470	9.0	2.665	11.8	2.66	11.25	11.0
144, 145	3,298-3,300	17.0	14.0	75	2.408	7.0	2.62	13.0	2.675	10.25	13.7
146, 147	3,300-3,302	14.5	15.5	74	2.450	8.6	2.65	12.2	2.67	10.65	12.2
148, 149	3,302-3,304	14.7	15.4	74	2.448	8.7	2.65	12.2	2.675	10.95	12.2

Table 21 (continued)

Sample number	Log depth (ft)	Density porosity reading ($\rho_m=2.68 \text{ g/cm}^3$) (gm/cm ³)	Neutron porosity reading (sandstone) (%)	Gamma reading (API)	Bulk density (with shale correction) (%)	Neutron porosity limestone (with shale correction) (%)	Cross-plot grain density (%)	Cross-plot porosity (%)	Core grain density (gm/cm ³)	Core porosity (%)	Calculated density-neutron porosity (based on core grain density) (%)
150, 151	3,304-3,306	13.9	15.4	72	2.458	9.0	2.66	12.3	2.685	10.75	12.2
152, 153	3,306-3,308	13.8	14.5	73	2.462	7.8	2.65	11.5	2.69	11.6	11.8
154, 155	3,308-3,310	11.0	16.5	74	2.512	9.5	2.69	10.5	2.685	9.9	10.0
156, 157	3,310-3,312	12.5	16.0	78	2.487	8.3	2.665	11.0	2.675	12.25	10.4
158, 159	3,312-3,314	15.7	15.6	77	2.431	8.2	2.645	13.0	2.685	11.85	13.4
160, 161	3,314-3,316	15.6	15.6	74	2.431	8.5	2.645	12.8	2.70	11.5	14.2
162, 163	3,316-3,318	14.5	16.0	78	2.453	8.2	2.65	12.0	2.715	11.5	13.6
164, 165	3,318-3,320	14.8	17.2	80	2.452	9.2	2.66	12.4	2.69	12.35	12.7
166, 167	3,320-3,322	13.5	16.5	80	2.470	8.6	2.665	11.5	2.715	11.8	12.2

When core porosities are compared with porosities derived from analyzing density and neutron logs individually, porosities based on core grain densities are always closer to porosity actually measured in core than to porosities derived on the basis of calculated grain densities. In addition, density log-derived porosities are always closer to core porosity than are neutron log-derived porosities.

In a plot of core porosity versus calculated porosity from the neutron-density crossplot (fig. 123), the data points are scattered around the line of unity that represents perfect agreement between calculated and measured values. In this plot, it is shown that porosities calculated by crossplotting average approximately 1.8 percent higher than core-measured porosity. The agreement between calculated porosity and core porosity was apparently improved if core grain density was used in porosity determinations (fig. 124). The average difference in porosity then becomes approximately 1 percent.

Water Saturation Determination

Water saturation of a formation may be determined either by the Archie equation or by the ratio method; the Archie equation (Archie, 1942) was used in this study. The resistivity of formation water must be known in order to use this equation. Two methods, based on apparent formation water resistivity or on spontaneous potential, may be used to derive formation water resistivity; the spontaneous potential (SP) method has been used in this work.

Methodology

Archie equation.--Water saturation (S_w) of a formation may be calculated by the Archie (1942) formula, such as

$$S_w = \sqrt{\frac{FR_w}{R_t}} \quad (4)$$

where F = formation factor = $\frac{a}{\phi_m}$
 ϕ = porosity
 a = tortuosity factor

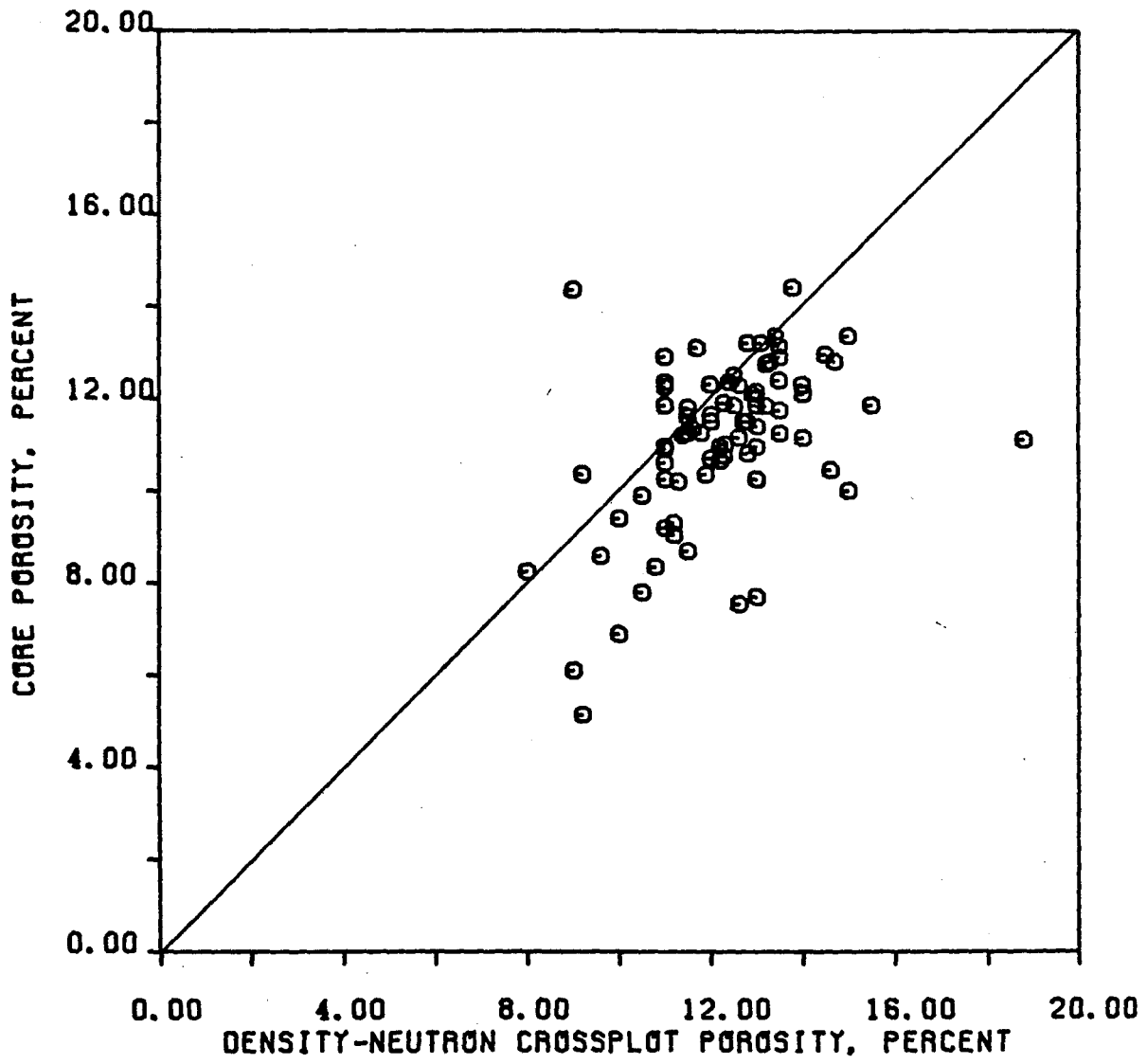


Figure 123. Correlation between core porosity and cross-plot porosity for the Cozzette Sandstone in Koch Exploration, Horseshoe Canyon no. 1-21.

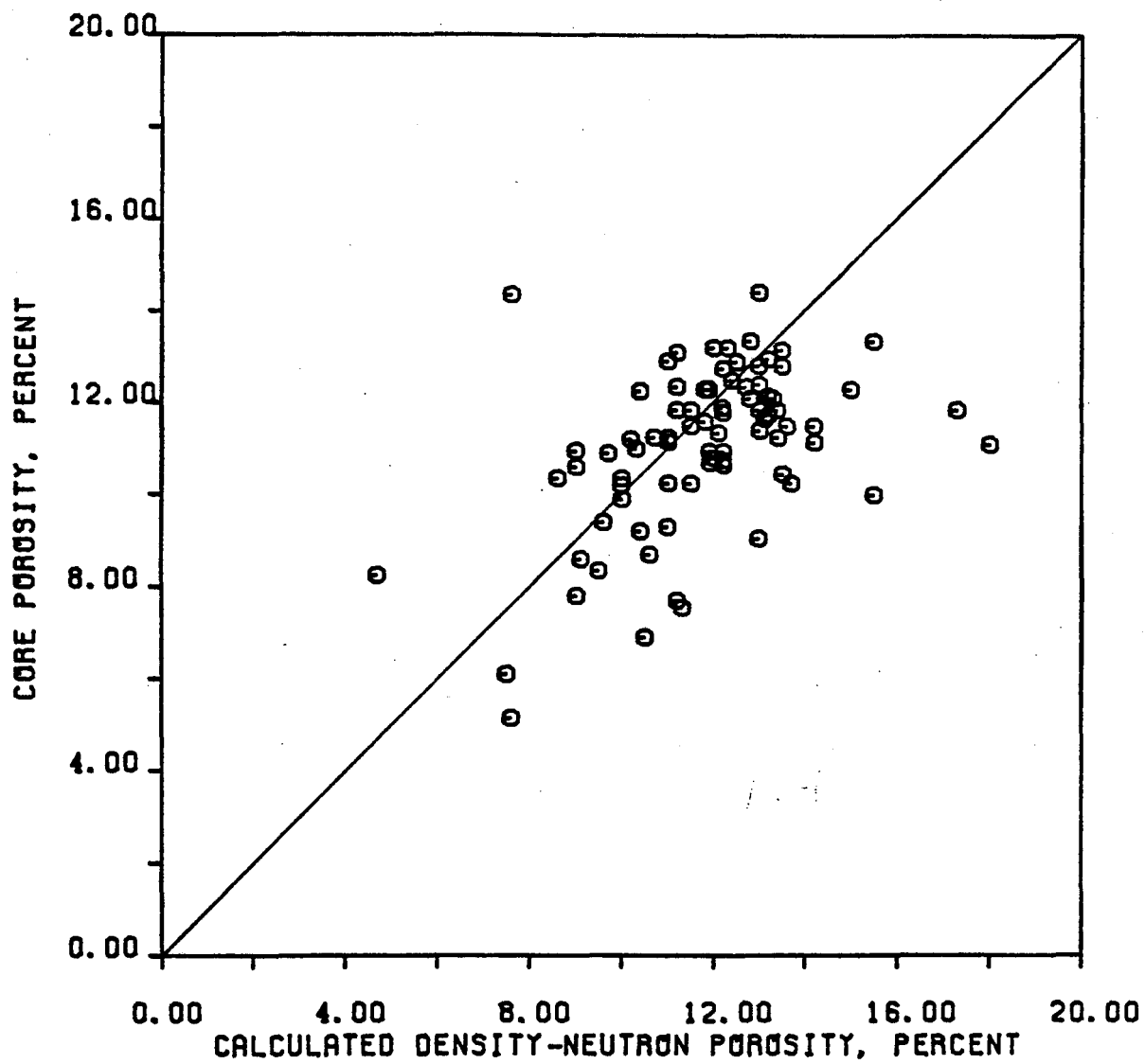


Figure 124. Correlation between core porosity and neutron-density porosity using core grain density for the Cozzette Sandstone in Koch Exploration, Horseshoe Canyon no. 1-21.

m = cementation exponent

R_w = resistivity of formation water at formation temperature

R_t = true resistivity of formation

The tortuosity factor (a) and cementation exponent (m) are constants that depend that upon the lithology of the formation; the porosity (ϕ) used in the above equation may be either from core measurement or from well log analysis. The only unknown present is the resistivity of formation water (R_w), which may be estimated by using the SP method.

Spontaneous potential (SP) method.--Resistivity of formation water (R_w) may be calculated from the SP curve. The SP reading from a formation must be corrected to the static SP (SSP) before it can be used to determine R_w , but for a thick bed the correction factor is close to 1 (Dresser Atlas, 1975; chart 3, SP correction). In this case, SP is the same as SSP and no correction is required.

Once the value of SSP is determined, the ratio of equivalent resistivity of mud filtrate and equivalent resistivity of formation water (R_{mfe}/R_{we}) may be obtained by using the following correction:

$$\frac{R_{mfe}}{R_{we}} = -10 \frac{-SSP}{K} \quad (5)$$

where $K = 60 + (0.133 * T_f)$

T_f = formation temperature, °F

Equivalent resistivity of mud filtrate (R_{mfe}) may be calculated from resistivity of mud filtrate:

$$R_{mfe} = \frac{(146 * R_{mf} - 5)}{(337 * R_{mf} + 77)} \quad (6)$$

if R_{mf} (at 75°F) < 0.1

or

$$R_{mfe} = 0.85 * R_{mf} \quad (7)$$

$$\text{if } R_{mf} \text{ (at } 75^{\circ}\text{F)} > 0.1$$

$$\text{where } R_{mf} \text{ (at } 75^{\circ}\text{F)} = \frac{R_{mf} * (T + 6.77)}{81.77} \quad (8)$$

T = temperature at which R_{mf} is measured, °F

By using the results obtained from eq. (5) for R_{mfe}/R_{we} , and R_{mfe} from eq. (6) or (7), the value of equivalent water resistivity may be estimated:

$$R_{we} = \frac{R_{mfe}}{(R_{mfe}/R_{we})} \quad (9)$$

Water resistivity may then be calculated by using equivalent water resistivity:

$$R_w \text{ (at } 75^{\circ}\text{F)} = \frac{(77 * R_{we} + 5)}{(146 - 377 * R_{we})} \quad (10)$$

$$\text{if } R_{we} < 0.12$$

or

$$R_w \text{ (at } 75^{\circ}\text{F)} = -[0.58 - 10^{(0.69 * R_{we} - 0.24)}] \quad (11)$$

$$\text{if } R_{we} > 0.12$$

Finally, water resistivity at formation temperature may be determined by:

$$R_w \text{ (at formation temperature)} = \frac{R_w \text{ (at } 75^{\circ}\text{F)} * 81.77}{(T_f + 6.77)} \quad (12)$$

where T_f = formation temperature, °F

Input Data

The data required for determination of water saturation within a given zone of interest are:

- (1) porosity,
- (2) resistivity of the formation,
- (3) SP reading,
- (4) formation temperature, and
- (5) resistivity of mud filtrate and temperature measured.

Results and Discussion

Using the methodology described above, water saturation was calculated for the Corcoran and Cozzette Sandstones in the Koch Exploration, Horseshoe Canyon no. 1-21 well in Shire Gulch Field. When a tortuosity factor of 0.62 and cementation exponent of 2.15 (Humble formula) were chosen in obtaining formation factor, water saturation was estimated (table 22) based on both core porosity and crossplot porosity. Well log derived water saturations based on core porosities are close to those from core measurements (fig. 125), whereas water saturation values based on crossplotting techniques are lower than those from core measurements (fig. 126) because crossplot porosities are higher than core porosities.

Other values for tortuosity factor (1.45) and cementation exponent (1.54) were used to obtain a formation factor (Carothers, 1968) that was also used to calculate water saturation. Even though this set of coefficients was derived for a sandstone rock, water saturation calculated using these coefficients is not as good as the values derived from the previous data set. We suggest that in order to get good results, the tortuosity factor and cementation exponent should be derived using available core information. This work will be done in the near future.

Travis Peak Formation

Permeability Determinations

Reservoir analysis including only permeability determinations for the Travis Peak Formation has been done within this research phase. Permeability is preferably calculated on the basis of transient pressure analysis using data from pressure buildup/drawdown tests

Table 22. Water saturations from log analysis and from core measurements for the Cozzette Sandstone in Koch Exploration, Horseshoe Canyon no. 1-21.

Sample number	Log depth (ft)	Core porosity (%)	Crossplot porosity (%)	Formation resistivity (Ω -m)	SP (mV)	Calculated water resistivity (Ω -m)	Calculated water saturation (%) (based on core porosity)		Calculated water saturation (%) (based on crossplot porosity)		Measured water saturation (%)
							a=0.62 m=2.15	a=1.45 m=1.54	a=0.62 m=2.15	a=1.45 m=1.54	
2, 3	3,040-42	13.35	13.4	25	-5	0.0868	40.42	33.45	40.26	33.35	61.30
4, 5	3,042-44	12.75	13.2	21	-5	0.0868	46.34	37.81	44.64	36.81	63.05
6, 7	3,044-46	12.9	13.5	20	-5	0.0868	46.89	38.40	44.65	37.07	57.85
8, 9	3,046-48	12.8	14.7	20.5	-6	0.0843	46.02	37.60	39.66	33.80	57.15
10, 11	3,048-50	7.55	12.6	20.5	-8	0.0797	78.93	54.89	45.51	37.00	76.20
12, 13	3,050-52	11.0	12.3	20.5	-8	0.0796	52.64	41.06	46.68	37.67	62.40
14, 15	3,052-54	11.5	12.7	21	-8	0.0796	49.58	39.20	44.56	36.32	62.35
16, 17	3,054-56	10.25	13.0	22	-8	0.0796	54.82	41.85	42.46	34.85	73.35
18, 19	3,056-58	11.15	12.6	25	-8	0.0796	46.97	36.79	41.19	33.49	65.35
20, 21	3,058-60	11.35	11.6	28	-8	0.0796	43.55	34.29	42.54	33.72	56.40
22, 23	3,060-62	13.15	13.5	34	-8	0.0796	33.73	27.79	32.79	27.23	44.25
24, 25	3,062-64	12.1	12.9	33	-8.5	0.0785	37.19	29.86	34.71	28.43	47.25
26, 27	3,064-66	8.7	11.5	30	-9	0.0774	55.21	40.09	40.9	32.34	46.85
28, 29	3,066-68	11.25	11.5	31	-9	0.0774	41.20	32.36	40.24	31.82	44.65
30, 31	3,068-70	10.95	13.0	35	-9	0.0774	39.92	31.09	33.19	27.24	44.85
32, 33	3,070-72	10.8	12.8	36	-9.5	0.0763	39.66	30.77	33.04	26.99	41.50
34, 35	3,072-74	9.2	11.0	43	-10	0.0753	42.83	31.64	35.35	27.57	62.60
36, 37	3,074-76	6.1	9.0	40	-10	0.0753	69.08	45.01	45.47	33.36	63.65
38, 39	3,076-78	10.95	11.0	33	-10	0.0753	40.55	31.58	40.35	31.47	48.20
40, 41	3,078-80	10.35	11.9	28	-10	0.0753	46.77	35.81	40.25	32.16	48.20
42, 43	3,080-82	8.25	8.0	26	-10	0.0753	61.93	44.25	64.02	45.31	58.55
44, 45	3,082-84	10.2	11.3	27	-9.5	0.0762	48.67	37.10	43.59	34.29	55.15

Table 22. (continued)

Sample number	Log depth (ft)	Core porosity (%)	Crossplot porosity (%)	Formation resistivity (Ω -m)	SP (mV)	Calculated water resistivity (Ω -m)	Calculated water saturation (%) (based on core porosity)		Calculated water saturation (%) (based on crossplot porosity)		Measured water saturation (%)
							a=0.62 m=2.15	a=1.45 m=1.54	a=0.62 m=2.15	a=1.45 m=1.54	
46, 47	3,084-86	11.2	11.4	29	-9.5	0.0762	42.47	33.31	41.67	32.86	49.40
48, 49	3,086-88	9.3	11.2	30	-9.5	0.0762	50.99	37.79	41.75	32.75	41.15
50, 51	3,088-90	11.9	12.3	29	-8	0.0793	40.59	32.43	39.17	31.62	42.90
52, 53	3,090-92	12.35	11.0	28	-9	0.0772	39.16	31.65	44.35	34.60	52.65
54, 55	3,092-94	12.3	12.0	24	-9.5	0.0761	42.18	34.04	43.32	34.70	50.80
56, 57	3,094-96	12.9	11.0	19	-10	0.0751	44.75	36.64	53.11	41.42	53.35
61, 62	3,116-18	12.3	12.6	22	-9	0.0769	44.29	35.74	43.16	35.09	60.85
63, 64	3,118-20	9.05	11.2	22	-8	0.0790	59.26	44.20	49.65	38.94	62.70
65, 66	3,120-22	11.85	15.5	27	-8	0.0789	42.15	33.63	31.58	27.35	68.05
67, 68	3,122-24	11.1	18.8	31	-7	0.0811	42.79	33.47	24.28	22.31	67.45
69, 70	3,124-26	11.65	12.0	31	-7	0.0812	40.64	32.26	39.37	31.54	52.80
71, 72	3,126-28	10.45	14.6	30	-6	0.0835	47.09	36.16	32.87	27.95	59.25
73, 74	3,128-30	11.15	14.0	26	-7	0.0811	46.49	36.42	36.40	30.56	47.55
75, 76	3,130-32	11.85	12.5	23	-7	0.0811	46.30	36.95	43.72	35.46	51.60
77, 78	3,132-34	10.9	11.0	20	-7	0.0811	54.32	42.25	53.79	41.96	54.55
79, 80	3,134-36	7.8	10.5	16	-7	0.0811	87.03	61.13	63.22	48.62	68.95
81, 82	3,136-38	8.35	10.8	14	-7	0.0811	86.46	62.01	65.57	50.86	77.95
83, 84	3,138-40	10.6	11.0	12	-6	0.0833	73.24	56.48	70.38	54.90	76.45
85, 86	3,140-42	7.7	13.0	13	-4	0.0883	100.00	71.47	58.17	47.75	77.75
87, 88	3,142-44	12.8	13.3	14	-4	0.0883	57.00	46.56	54.70	45.21	69.80
89, 90	3,144-46	14.4	13.8	14	-5	0.0857	49.47	41.90	51.79	43.29	49.40
91, 92	3,146-48	12.5	12.5	15	-5	0.0857	55.65	45.13	55.65	45.13	68.80

Table 22. (continued)

Sample number	Log depth (ft)	Core porosity (%)	Crossplot porosity (%)	Formation resistivity (Ω -m)	SP (mV)	Calculated water resistivity (Ω -m)	Calculated water saturation (%) (based on core porosity)		Calculated water saturation (%) (based on crossplot porosity)		Measured water saturation (%)
							a=0.62 m=2.15	a=1.45 m=1.54	a=0.62 m=2.15	a=1.45 m=1.54	
93, 94	3,148-50	13.1	11.7	16	-7	0.0809	49.78	40.95	56.21	44.68	69.55
95, 96	3,150-52	8.6	9.6	15	-8	0.0787	79.72	57.68	70.83	53.00	79.75
97, 98	3,152-54	13.2	13.1	14	-7	0.0809	52.78	43.53	53.22	43.78	65.30
99, 100	3,154-56	12.95	14.5	15	-8	0.0787	51.34	42.09	45.46	38.58	70.00
101, 102	3,156-58	14.35	9.0	18	-8	0.0787	41.97	35.50	69.30	50.85	70.20
103, 104	3,158-60	5.15	9.2	20	-9	0.0765	100.00	73.10	63.31	46.76	86.65
105, 106	3,160-62	6.9	10.0	25	-9	0.0765	77.14	52.20	51.77	39.22	78.35
107, 108	3,162-64	10.35	9.2	30	-10	0.0745	44.94	34.41	51.01	37.68	56.50
112, 113	3,266-68	12.15	13.0	28	-11	0.0718	38.44	30.91	35.74	29.34	46.95
114, 115	3,268-70	11.85	11.0	26	-11	0.0718	40.98	32.70	44.39	34.62	44.10
116, 117	3,270-72	12.3	14.0	28	-11	0.0717	37.91	30.59	32.98	27.69	47.05
118, 119	3,272-74	13.35	15.0	29	-11	0.0717	34.11	28.22	30.09	25.80	37.35
120, 121	3,274-76	10.0	15.0	29	-11	0.0717	46.53	35.26	30.09	25.80	37.25
122, 123	3,276-78	12.1	14.6	28	-11	0.0716	38.90	31.16	31.51	26.79	48.25
124, 125	3,278-80	11.75	13.5	27	-11	0.0716	40.52	32.25	34.90	28.98	37.70
126, 127	3,280-82	11.25	13.5	28	-12	0.0699	41.20	32.36	33.86	28.12	44.60
128, 129	3,282-84	13.2	12.8	29	-11	0.0716	34.50	28.45	35.66	29.13	40.35
130, 131	3,284-86	11.85	13.2	30	-12	0.0698	37.61	30.01	33.49	27.62	36.70
132, 133	3,286-88	12.4	13.5	30	-12	0.0698	35.82	28.98	32.69	27.15	34.60
134, 135	3,288-90	11.4	13.0	30	-12	0.0698	39.21	30.92	34.05	27.95	56.15
136, 137	3,290-92	10.7	12.0	30	-12	0.0698	41.97	32.47	37.11	29.72	38.15
138, 139	3,292-94	10.25	11.0	29	-12	0.0698	44.71	34.13	41.44	32.33	42.45

Table 22. (continued)

Sample number	Log depth (ft)	Core porosity (%)	Crossplot porosity (%)	Formation resistivity (Ω -m)	SP (mV)	Calculated water resistivity (Ω -m)	Calculated water saturation (%) (based on core porosity)		Calculated water saturation (%) (based on crossplot porosity)		Measured water saturation (%)
							a=0.62 m=2.15	a=1.45 m=1.54	a=0.62 m=2.15	a=1.45 m=1.54	
140, 141	3,294-96	9.4	10.0	28	-12	0.0698	49.94	37.13	46.72	35.40	67.00
142, 143	3,296-98	11.25	11.8	28	-12	0.0698	41.17	32.33	39.11	31.17	31.55
144, 145	3,298-300	10.25	13.0	29	-11	0.0715	45.25	34.54	35.05	28.77	35.90
146, 147	3,300-02	10.65	12.2	28	-11	0.0715	44.19	34.13	38.19	30.74	41.15
148, 149	3,302-04	10.95	12.2	28	-11	0.0715	42.89	33.41	38.19	30.74	37.80
150, 151	3,304-06	10.75	12.3	27	-11	0.0715	44.56	34.51	38.55	31.11	42.45
152, 153	3,306-08	11.6	11.5	26	-11	0.0714	41.81	33.14	42.20	33.37	37.25
154, 155	3,308-10	9.9	10.5	25	-11	0.0714	50.56	38.19	47.46	36.50	67.75
156, 157	3,310-12	12.25	11.0	24	-11	0.0714	41.04	33.08	46.07	35.94	36.15
158, 159	3,312-14	11.85	13.0	25	-11	0.0714	41.67	33.25	37.72	30.96	38.65
160, 161	3,314-16	11.5	12.8	23	-11	0.0714	44.87	35.48	39.99	32.67	43.70
162, 163	3,316-18	11.5	12.0	22	-11	0.0714	45.88	36.27	43.82	35.10	32.75
164, 165	3,318-20	12.35	12.4	20	-11	0.0714	44.56	36.01	44.37	35.90	46.95
166, 167	3,320-22	11.8	11.5	19	-11	0.0714	48.02	38.27	49.36	39.03	60.15

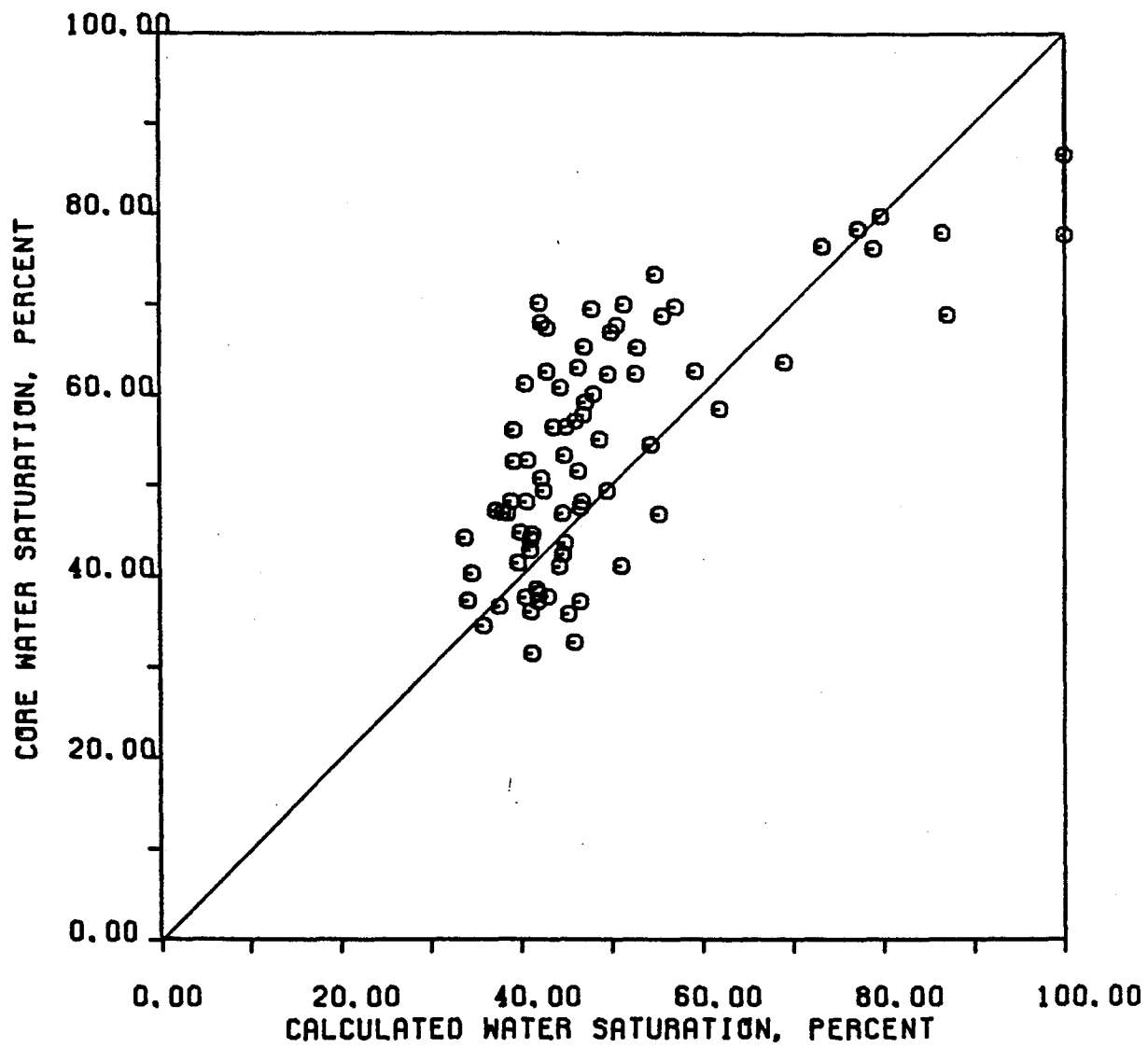


Figure 125. Correlation between core water saturation and calculated water saturation (based on core porosity) for the Cozzette Sandstone in Koch Exploration, Horseshoe Canyon no. 1-21.

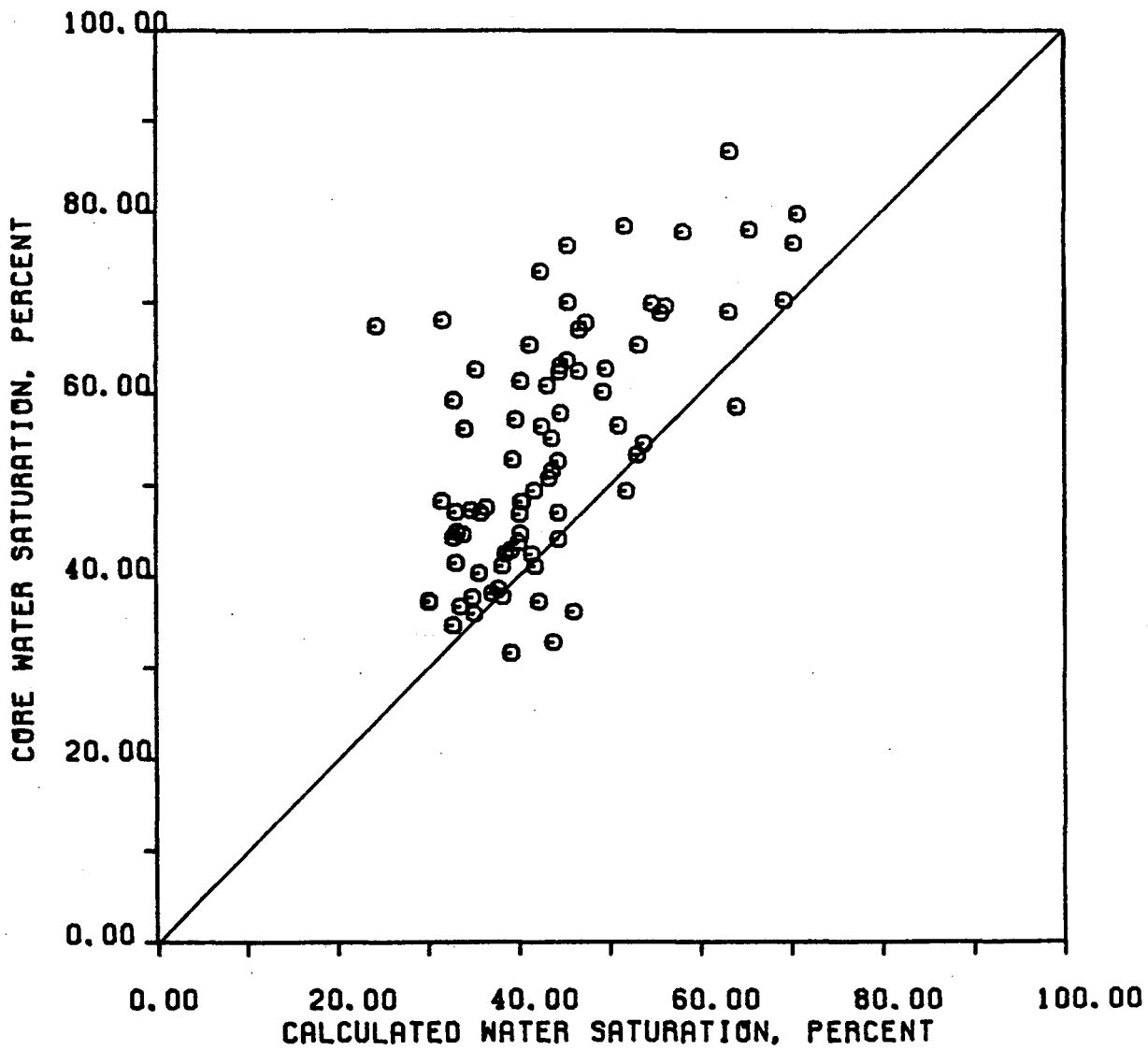


Figure 126. Correlation between core water saturation and calculated water saturation (based on cross-plot porosity) for the Cozzette Sandstone in Koch Exploration, Horseshoe Canyon no. 1-21.

(Earlougher, 1977; Matthews and Russell, 1967), but may be approximated from conventional core measurements with extrapolation to in-situ conditions (Jones and Owens, 1979). Special core analysis under conditions of restored water saturation, overburden pressure, and pore pressure may give the most realistic direct measurements of reservoir permeability; however, these types of data are not usually available from public records.

Formation permeability may be estimated from flow potential tests or back-pressure tests, obtained from a low-permeability reservoir prior to stimulation (Lee, 1980). In Texas, operators are required to file data from gas-well back-pressure tests with the Railroad Commission of Texas. These data are available as public information, therefore, this work focused on how formation permeability may be estimated using back-pressure test data.

Mathematically, the analytical solution for the gas flow equation of non-linearity is unavailable. However, the slightly compressible fluid flow solution can be applied to the gas flow equation by analogy. Thus, there are three analytical solutions for the gas flow equation; that is, the pressure equation, the pressure-squared equation, and the pseudo-pressure equation, depending on the range of reservoir pressure and the fluid properties (Aziz and others, 1976).

Lee (1980) used the pressure equation and the pressure-squared equation to calculate formation permeability for pressures greater than 3,000 psi and less than 2,000 psi, respectively. There was no discussion of the pseudopressure equation, which can be used at all pressure levels.

The purposes of this study on permeability determinations are (1) to use the pseudo-pressure equation in addition to the pressure and the pressure-squared equations to calculate formation permeability using back-pressure test data, and (2) to determine the permeability distribution in a small part of the Travis Peak Formation.

Methodology

Working Equations.--Permeability is calculated using one of the following equations depending on the pressure range in the reservoir:

(1) pseudo-pressure equation--for all pressure ranges

$$k = \frac{712 qT}{h[m(p_i)-m(p_w)]} \left[\ln \left(\frac{2.634 \times 10^{-4} kt}{\mu_i C_{gi} \phi \gamma_w^2} \right) + 0.80907 \right] \quad (13)$$

where real gas pseudopressure, $m(p)$, and pressure, p , are related by the following equation

$$m(p) = 2 \int_0^p \frac{p}{\mu z} dp \quad (14)$$

k = permeability, md

q = flow rate, Mcf/D

T = reservoir temperature, °R

h = formation thickness, ft

p_i = initial reservoir pressure, psi

p_w = pressure at wellbore, psi

t = time, hrs

μ_i = gas viscosity at initial reservoir conditions, cp

C_{gi} = gas compressibility at initial reservoir conditions, psi⁻¹

ϕ = porosity, dimensionless

γ_w = wellbore radius, ft

z = gas deviation factor, dimensionless

(2) pressure equation--for pressure greater than 3,000 psi

$$k = \frac{356 qT \mu_i z_i}{h(p_i - p_w) p_i} \left[\ln \left(\frac{2.634 \times 10^{-4} kt}{\mu_i C_{gi} \phi \gamma_w^2} \right) + 0.80907 \right] \quad (15)$$

(3) pressure-squared equation--for pressure less than 2,000 psi

$$k = \frac{712 qT \mu_i z_i}{h(p_i^2 - p_w^2)} \left[\ln \left(\frac{2.634 \times 10^{-4} kt}{\mu_i C_{gi} \phi \gamma_w^2} \right) + 0.80907 \right] \quad (16)$$

Eq. (15) and eq. (16), which have been used by Lee (1980), are special cases of eq. (13): In other words, eq. (13) is a generalized equation to calculate permeability.

Solution Technique.--Since these three working equations are implicit to the permeability, k , that is, permeability appears in both sides of the equality, an iterative technique must be used in the calculation process. In the iterative technique, the permeability term in the right-hand side of the equation can be assigned an assumed value in the first iteration. The permeability obtained from the first iteration will be used for the permeability term in the right-hand side of the equation to calculate the permeability for the second iteration. This process will continue until permeabilities calculated in two successive iterations are sufficiently close.

Computations of Real Gas Pseudopressure.--The pseudopressure equation (eq. 13) includes a real gas pseudopressure function which is defined in eq. (14) as an integral. With prepared graphical or tabular data, the computation of the real gas pseudopressure function generally can be performed by trapezoidal's or Simpson's rule. However, to compute the function effectively, least-square polynomial curve fits for $\frac{P}{\mu z}$ as a function of pressure for specified gas gravity and reservoir temperature were obtained. Then, real gas pseudopressure could also be expressed by a polynomial function which was achieved by integrating the polynomial curves of $\frac{P}{\mu z}$ as a function of pressure.

Input Data

The input data required to calculate permeability should include all variables or parameters in the right-hand side of eq. (13), eq. (15), or eq. (16). However, gas deviation factor (or z -factor), viscosity, and gas compressibility, which may or may not be given from laboratory analysis, can also be determined from experimental correlations by knowing gas compositions (or specific gas gravity), temperature, and pressure. Thus, the data required for permeability calculations in this study are:

- (1) net pay,
- (2) gas porosity,

- (3) wellbore radius,
- (4) initial reservoir pressure,
- (5) tested flow rate,
- (6) duration of flow test,
- (7) flowing bottom-hole pressure at end of test,
- (8) formation temperature,
- (9) specific gas gravity, and
- (10) gas deviation factor, viscosity and gas compressibility (optional).

The above data (except gas porosity) can be found on the form for reporting gas well back-pressure tests required by the Railroad Commission of Texas. Gas porosity data may be obtained from core sample measurements and/or estimated from well log analysis. In the absence of gas porosity data, reasonable assumed values might be used in the calculations if calculated permeability is not very sensitive to the given gas porosity. Sensitivity and error analyses for these purposes are discussed in a forthcoming section.

From the data shown in applications for tight formation designations submitted to the Railroad Commission of Texas, the assumed formation and gas properties (table 23), which were used by Lee (1980) as a typical example for the Cotton Valley Formation, may be also a representative example for the Travis Peak Formation. Based on the data shown (table 23), studies were made to investigate how gas porosity affects the results of the calculated permeability. The calculated permeability is 0.0113 md where gas porosity is 0.045 (table 23). With gas porosities in the range of 2% to 10%, the calculated permeabilities range from 0.0127 to 0.01002 md (fig. 127). Gas porosity in the Travis Peak Formation of Texas typically ranges from 3% to 9% (from applications for tight formation designations submitted to the Railroad Commission of Texas). If gas porosity of 6% is used in all cases, the expected maximum error in calculated permeability will be 10%. The in-situ permeability in a tight sand gas is generally less than 0.1. Therefore, the error of 0.01 md (10% of 0.1 md) in calculated permeability from an error introduced in the gas porosity term is insignificant in resource estimation and in

Table 23. Reservoir properties and flow test data (from Lee, 1980).

Gas specific gravity = 0.65

Reservoir temperature = 265° F

Initial reservoir pressure = 5200 psi

Gas porosity = 0.045

Wellbore radius = 0.333 ft

Net pay = 50 ft

Gas deviation factor at initial reservoir condition = 0.983

Gas compressibility at initial reservoir condition = 1×10^{-4} psi⁻¹

Gas viscosity at initial reservoir condition = 0.0328 cp

Gas formation volume factor at initial reservoir condition = 0.691 RB/Mscf

Well spacing = 320 acres

Flow rate = 100 Mcf/D

Flow time = 6 hr

Flowing bottom-hole pressure = 3,000 psi

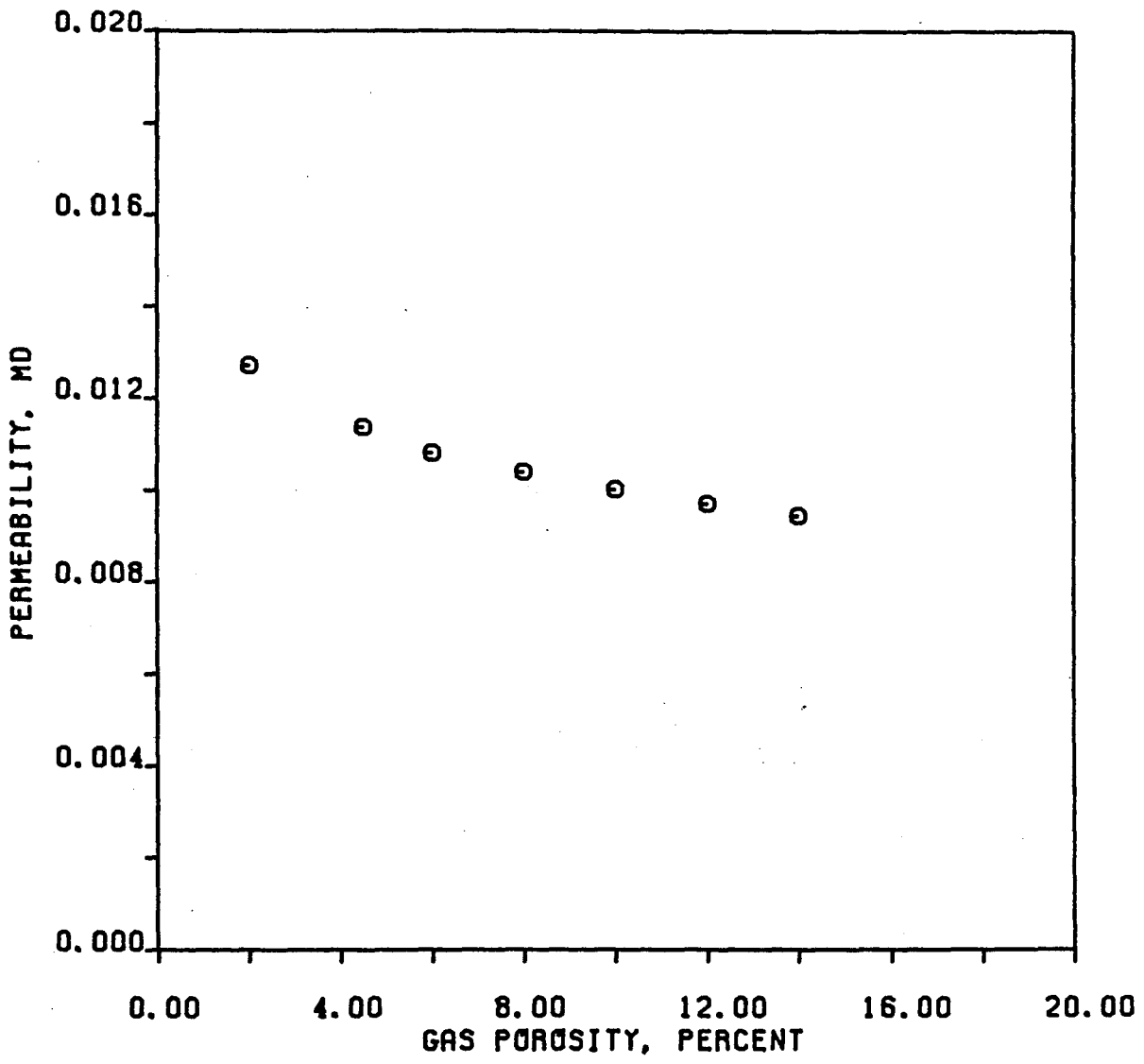


Figure 127. Sensitivity of calculated permeability to varying gas porosity.

geological studies. These estimations and studies involve other assumptions and other statistical data that will have similar, and possibly larger, sources of error associated with them.

Results and Discussion

The pseudopressure equation (eq. (13)), pressure equation (eq. (15)), and pressure-squared equation (eq. (16)) are basically applied in permeability determinations for gas wells, not only using data from back-pressure tests, but also using data from pressure buildup/drawdown tests. Only one pressure value in each test run, excluding the initial pressure, is required to calculate permeability using data from back-pressure tests, while two or more pressure values are required to use pressure buildup/drawdown test data. In the former case, as described in the previous section, an iterative process must be adopted to determine permeability. In the latter case, the plot of pseudopressure (or pressure or pressure-squared) vs. flow time in special coordinates is necessary to obtain the slope of the line to calculate formation permeability. Because fewer data are used, the precision of permeability determined from using back-pressure test data is not expected to be as good as from the use of buildup/drawdown test data.

Sample calculations to determine permeability using data obtained from gas well back-pressure test data were compared with those derived from a pressure buildup/drawdown test for the same well. Permeabilities calculated (table 24) from equations 13, 15, and 16 were obtained for several wells regardless of the pressure level. The permeabilities (table 24) derived from pressure-buildup test data were extracted from applications for tight formation designations submitted to the Railroad Commission of Texas. Results from pressure-buildup tests are close to those from back-pressure tests using the pressure equation (eq. (15)), because the equivalent pressure equation was used by the applicant to analyze the pressure-buildup test. The agreements in permeability calculated from pressure-buildup and from back-pressure tests are good enough for resource estimation and geological studies.

For the same set of back-pressure test data, permeabilities calculated from the pressure equation are higher than those computed from the pressure-squared equation; results from the pseudopressure equation fall between the two.

Table 24. Comparison of permeabilities calculated from transient-pressure analysis and back-pressure test.

Field name	Well name	Calculated permeability, md	
		Transient-pressure analysis	Back-pressure test
Swanson Landing	Carl Jones Lou-Tex #3	0.0825	0.11040
Appleby, N.	E. A. Blount G.U. #1	0.0131	0.00434
Appleby, N.	Max Hart #2	0.0133	0.01189
Appleby, N.	D. H. Newman G.U. #1	0.0060	0.00802
Kendrick	T. J. Kendrick #1	0.0270	0.02942
White Oak Creek	Temple-Eastex G.U. #1	0.0330	1.16560
White Oak Creek	Temple-Eastex G.U. #1	0.0015	0.00133
Wildcat	George H. Henderson #1	0.0100	0.07243

Based on the pseudopressure equation, permeability distributions for the Travis Peak Formation in the Lansing North Field, Harrison County, Texas, are shown in figure 128; a list of wells corresponding to well numbers in figure 128 is shown (table 25). Permeability distributions in the Lansing North Field (fig. 128) range from a high of 1.5327 md to a low of 0.0015 md; the mean is 0.2426 md; standard deviation is 0.438 md; median is 0.12 md. Gas porosity of 6% was assumed for all wells because porosity calculations for the area are incomplete.

The calculated permeability is only as accurate as the available information for input data and assumptions for the equation used. Some assumptions involved obtaining analytical solutions from simplified gas flow equations, such as a logarithm approximation to an exponential function, are also potential sources of errors (Earlougher, 1977). Calculated permeability will be too high if a formation near the wellbore was stimulated by acidified or/and fractured treatment, which is related to the skin effect of the wellbore and is not considered in the working equations. It is quite likely that a tight-sand formation has been stimulated prior to back-pressure testing. On the other hand, the derived permeability will be too low if the perforated interval, which is shown in the back-pressure test information sheets, is used instead of an effective production thickness. The determination of an effective production thickness, which has not been done in this study, may be conducted from well log analysis if required logs are available. However, the accuracy of calculated permeability will be improved in future studies if more required data are available and more sophisticated working equations are used.

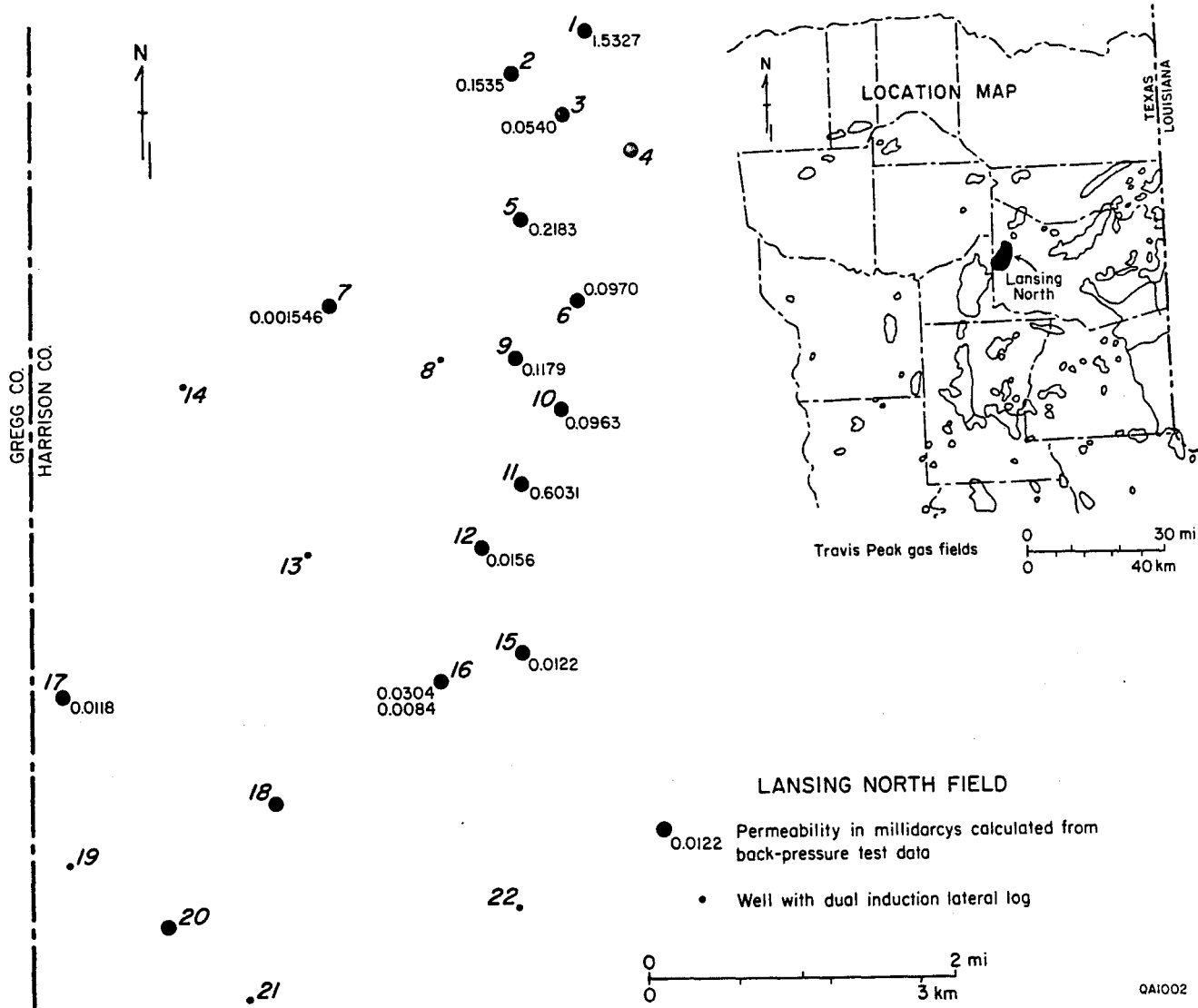


Figure 128. Permeability distribution in the Travis Peak Formation for Lansing North Field, Harrison County, Texas.

Table 25. Well names and numbers shown on figure 128.

<u>Well number</u>	<u>Well</u>
1	Estate 1 Birdsong
2	Clemco 1 Clements
3	Estate 2 Williams
4	Estate 1 Williams
5	Estate 1 Feist
6	Estate 1 Pitts
7	Estate 1 Taylor
8	Estate 2 Keasler
9	Estate 1 Keasler
10	Estate 2 Taylor
11	Estate 1 Suggs
12	Eubank and Bishop 1 Te Caro Wood
13	Clemco 2 Clements
14	Cook 1 Bussey
15	Eubank 1 Black-Clark
16	Eubank 1 Ing Heirs
17	Clemco 3 Clements
18	Eubank 1 Huffman
19	Key 1 Skipper
20	Key 1 Smelley
21	Key 1-A Zahn
22	Riddle 1 Grisgsby

DISCUSSION AND CONCLUSIONS: PHASE B

Results of Phase B studies brought additional verification of the geological interpretations made during the study of six stratigraphic units (Phase A) and during the national survey of blanket-geometry tight gas sandstones (Finley, 1982). The three-part division of the Travis Peak Formation has been shown to be applicable in preliminary studies of selected fields producing gas from the Travis Peak. In Whelan Field, the middle braided fluvial section of the Travis Peak shows good lateral continuity of sand bodies over 1 to 3 mi. These sandstones are probably best classified as of broadly lenticular to blanket geometry, and would not present the fracturing problems that a truly lenticular sand would cause. The effectiveness of shale barriers between zones of interest may be of concern, however, because interbedded shales in the sand-rich Travis Peak vary from less than 10 ft up to 30 ft between major sandstone bodies. Vertical fracture growth out of the desired zone therefore becomes a potential problem.

The upper transitional facies of the Travis Peak is the perforated interval within much of the productive area of the formation, and this part of the formation is not tight in some areas (B. Brown, personal communication, 1983). The Railroad Commission of Texas (1983) recently sought to expedite designation of the Travis Peak as a tight gas sandstone in Commission Districts 5 and 6 by excluding the upper 200 ft of the Travis Peak in 45 wells from the application pending before FERC. The specific depositional or diagenetic factors leading to improved permeability in the upper Travis Peak will be examined in the forthcoming phase of research.

Shire Gulch and Plateau Fields form the largest area of tight gas sand production from the Corcoran and Cozzette Sandstones. Because this area contains one to three wells per section over approximately three townships, it is ideal for defining the types of lateral changes that may occur within these stratigraphic units. The strike-parallel nature of the lower Corcoran and lower Cozzette are well-defined by net sandstone trends, and it is probably the lower, upward-coarsening sequence of the Corcoran that determines the northeast trend of thick net

sandstone in the entire Corcoran across the southern Piceance Creek Basin. It is unlikely, however, that the projection of the Corcoran-Cozzette trend to the northeast between Shire Gulch - Plateau and Rulison Fields will be confirmed by drilling in the near term. Rugged terrain and elevations on the order of 10,000 ft adversely affect the economics of the tight gas resource in the latter region.

The facies variability of the sandstones in association with shale and coal in the upper Corcoran and upper Cozzette must be evaluated using additional well data. Lateral changes in the number and thickness of coal beds are indicative of the variability that may occur where small deltas enter protected bay-lagoon environments. The associated framework sandstones may be of moderate areal extent (the delta front of a relatively small delta) or highly lenticular (a distributary channel sandstone). The distribution of stacked coals can be an indicator of local deltaic deposition or of sites of bay-lagoon organic accumulations, but the much lower density of well control northeast, north, and southwest of Shire Gulch Field will limit interpretation of the geometry of the coal-forming environments. For example, it is unlikely that strike-parallel geometries could be unequivocally defined for coals in Shire Gulch Field and surrounding areas even if they retain such geometry from a bay-lagoon origin. The data are too strongly influenced by the nearly equidimensional shape of the producing area. Finally, petrographic data may contribute to interpretation of depositional environments and will complement studies of framework sandstones; CBW Services (1983) reported finer grain sizes in more distal, marine parts of the Corcoran-Cozzette sequence, and the allogenic clay content of these distal sandstones must also be examined as part of future studies.

ACKNOWLEDGMENTS

This work was prepared for the Gas Research Institute under Contract No. 5082-211-0708, Robert J. Finley, Principal Investigator. Data collection was initiated under Contract No. GRI-BEG-SC-112-82 from the Gas Research Institute through CER Corporation, Robert J. Finley, Principal Investigator.

Additional data for formations in the Piceance Creek Basin were provided by CBW Services, Inc., and for formations in the Greater Green River Basin by Alan J. VerPloeg, Rodney H. De Bruin, Robert L. Oliver, and Michael L. Clark, Geological Survey of Wyoming. Mark J. Berlinger and Gay Nell T. Gutierrez served as project research assistants, with additional assistance by William A. Ambrose.

The manuscript was prepared by Dorothy C. Johnson, Jana J. McFarland, Phyllis J. Hopkins, Marcia J. Franklin, and Doris J. Tyler. Illustrations were prepared by John T. Ames, Jeff S. Horowitz, Margaret R. Day, and Richard M. Platt under the direction of Dan F. Scranton and Richard L. Dillon. Editorial review was by Amanda R. Masterson and Susann V. Doenges. The manuscript was reviewed by Walter B. Ayers, Jules R. DuBar, Colin M. Jones (Phase A), and Robert A. Morton (Phases A and B).

REFERENCES

- Anderman, G. G., 1956, Subsurface correlation in the Green River Basin, Wyoming, in Burk, C. A., ed., Symposium on Wyoming stratigraphy, part I, Subsurface stratigraphy of the pre-Niobrara formations in Wyoming: Wyoming Geological Association, 98 p. (Chart in pocket).
- Archie, G. E., 1942, The electrical resistivity log as an aid in determining some reservoir characteristics: *Petroleum Technology*, v. 5, p. 54-62.
- Asquith, D. O., 1974, Sedimentary models, cycles, and deltas, Upper Cretaceous, Wyoming: *American Association of Petroleum Geologists Bulletin*, v. 58, no. 11, p. 2274-2283.
- 1975, Petroleum potential of deeper Lewis and Mesaverde sandstones in the Red Desert, Washakie and Sand Wash Basin, Wyoming and Colorado, in Bolyard, D. W., ed., Deep drilling frontiers in the central Rocky Mountains: Rocky Mountain Association of Geologists, 1975 Symposium, p. 159-162.
- Aziz, K., Matter, L., Ko, S., and Brar, G. S., 1976, Use of pressure, pressure-squared or pseudo-pressure in the analysis of transient pressure drawdown data from gas wells: *Journal of Canadian Petroleum Technology*, v. 15, no. 2, p. 56-65.
- Balsley, J. K., 1980, Cretaceous wave-dominated delta systems: Book Cliffs, east-central Utah: a field guide: Amoco Production Company, 163 p.

Barlow, J. A., and Haun, J. D., 1966, Regional stratigraphy of Frontier Formation and relation to Salt Creek Field, Wyoming: American Association of Petroleum Geologists Bulletin, v. 50, no. 10, p. 2185-2196.

Blackstone, D. L., Jr., 1979, Geometry of the Prospect-Darby and La Barge faults at their junction with the La Barge Platform, Lincoln and Sublette Counties, Wyoming: Geological Survey of Wyoming, Report of Investigations No. 18, 34 p.

Bornhauser, Max, 1958, Gulf Coast tectonics: American Association of Petroleum Geologists Bulletin, v. 42, no. 2, p. 339-370.

Boyles, J. M., and Scott, A. J., 1982, A model for migrating shelf-bar sandstones in Upper Mancos Shale (Campanian) northwestern Colorado: American Association of Petroleum Geologists Bulletin, v. 66, no. 5, p. 491-508.

Burgess, J. D., 1970, Palynological correlation and interpretation of Frontier environment in central Wyoming, in Enyert, R. L., ed., Symposium on Wyoming sandstones: Wyoming Geological Association Guidebook, 22nd Annual Field Conference, p. 133-145.

Burke, K., and Dewey, J. F., 1973, Plume-generated triple junctions: key indicators in applying plate tectonics to old rocks: Journal of Geology, v. 81, p. 406-418.

Bushaw, D. J., 1968, Environmental synthesis of the East Texas Lower Cretaceous: Gulf Coast Association of Geological Societies Transactions, v. 18, p. 416-438.

- Caffey, K. C., 1978, Depositional environments of the Olmos, San Miguel, and Upson Formations (Upper Cretaceous), Rio Escondido Basin, Coahuila, Mexico: The University of Texas at Austin, Master's thesis, 86 p.
- Cardinal, D. F., and Stewart, W. W., eds., 1979, Wyoming oil and gas fields symposium, Greater Green River Basin: Wyoming Geological Association, 428 p.
- Carothers, J. E., 1968, A statistical study of the formation factor relation to porosity: *The Log Analyst*, v. 9, p. 38-52.
- CBW Services, Inc., 1983, A preliminary overview of the Corcoran, Cozzette, and Rollins Sands, Piceance Basin, Colorado: Report to the Bureau of Economic Geology, 36 p., plus exhibits.
- Coalson, E. B., 1979, Echo Springs Field, in Cardinal, D. F., and Stewart, W. W., eds., Wyoming oil and gas fields symposium, Greater Green River Basin: Wyoming Geological Association, p. 137.
- Cobban, W. A., and Reeside, J. B., Jr., 1952, Frontier Formation, Wyoming and adjacent areas: *American Association of Petroleum Geologists Bulletin*, v. 36, p. 1913-1961.
- Coleman, J. L., Jr., and Coleman, C. J., 1981, Stratigraphic, sedimentologic, and diagenetic framework for the Jurassic Cotton Valley Terryville massive sandstone complex, northern Louisiana: *Gulf Coast Association of Geological Societies Transactions*, v. 31, p. 71-79.

Collins, B. A., 1976, Coal deposits of the Carbondale, Grand Hogback, and southern Danforth Hills coal fields, eastern Piceance Basin, Colorado: Quarterly of the Colorado School of Mines, v. 71, no. 1, 138 p.

Colorado Oil and Gas Conservation Commission, 1980a, Cause no. NG-5, application by Coseka Resources (U.S.A.), Limited, for designation of the Mancos "B" Formation in parts of Garfield and Rio Blanco Counties, Colorado, as a tight gas sand.

_____ 1980b, Cause no. NG-6, application by Chandler and Associates, Inc., for designation of the Mancos "B" Formation in part of Rio Blanco County, Colorado, as a tight gas sand.

_____ 1980c, Cause no. NG-7, application by Chandler and Associates for designation of the Rollins, Cozzette, and Corcoran Sandstones in North Plateau Creek, Mesa County, Colorado, as tight gas sands.

_____ 1980d, Cause no. NG-12, application by Koch Industries, Inc., for designation of the Rollins, Cozzette, and Corcoran Formations in parts of Mesa and Garfield Counties, Colorado, as a tight gas sand.

_____ 1980e, Cause no. NG-14, application by Northwest Exploration Company for designation of the Mancos "B" Formation in part of Rio Blanco County, Colorado, as a tight gas sand.

_____ 1980f, Cause no. NG-15-1, application by American Resources Management Corporation for designation of the Mancos "B" Formation in parts of Garfield and Rio Blanco Counties, Colorado, as a tight gas sand.

————— 1980g, Cause no. NG-17, application by Dome Petroleum Corporation for designation of the Rollins, Cozzette, and Corcoran Formations in part of Garfield County, Colorado, as tight gas sands.

————— 1980h, Cause no. NG-14, application by Northwest Exploration Company for designation of the Mancos "B" Formation in part of Rio Blanco County, Colorado, as a tight gas sand.

————— 1980i, Cause no. NG-15-1, application by American Resources Management Corporation for designation of the Mancos "B" Formation in parts of Garfield and Rio Blanco Counties, Colorado, as a tight gas sand.

————— 1981a, Oil and gas statistics, 241 p.

————— 1981b, Cause no. NG-21, application by Northwest Exploration Company for designation of the Mesaverde Formation in part of Garfield County, Colorado, as a tight gas sand.

————— 1981c, Cause no. NG-26, application by Snyder Oil Co. for designation of the Mesaverde and Upper Mancos sands in parts of Garfield, Mesa, Pitkin, Gunnison, and Delta Counties, Colorado, as tight gas sands.

————— 1982a, Cause no. NG-27, application by Sun Oil for designation of the Mesaverde and Mancos Formations in part of Rio Blanco County, Colorado, as tight gas sands.

_____ 1982b, Cause no. NG-35, application by South Louisiana Production Co. for designation of the Mesaverde Formation in parts of Rio Blanco County, Colorado, as a tight gas sand.

Cullom, M., Granata, W., Gayer, S., Heffner, R., Pike, S., Herrmann, L., Meyertons, C., and Sigler, C., 1962, The basin frontiers and limits for exploration in the Cretaceous system of central Louisiana: Gulf Coast Association of Geological Societies Transactions, v. 12, p. 97-116.

De Chadenedes, J. F., 1975, Frontier deltas of the western Green River Basin, Wyoming, in Bolyard, D. W., ed., Symposium on deep drilling frontiers in the central Rocky Mountains: Rocky Mountain Association of Geologists, 1975 Symposium, p. 149-157.

Dickinson, K. A., 1968, Upper Jurassic stratigraphy of some adjacent parts of Texas, Louisiana, and Arkansas: U.S. Geological Survey Professional Paper 594-E, 25 p.

Doelger, M. J., 1979, Wamsutter Field, in Cardinal, D. F., and Steward, W. W., eds., Wyoming oil and gas fields symposium, Greater Green River Basin: Wyoming Geological Association, p. 402-403.

Dresser Atlas, 1975, Log interpretation fundamentals: Dresser Atlas Division, Dresser Industries, Inc., variously paginated.

Dunham, D. R., 1954, Big Foot Field, Frio County, Texas: Gulf Coast Association of Geological Societies Transactions, v. 4, p. 44-53.

Dunn, H. L., 1974, Geology of petroleum in the Piceance Creek Basin, northwestern Colorado, in Murray, D. K., ed., Energy resources of the Piceance Creek Basin, Colorado: Rocky Mountain Association of Geologists Guidebook, 25th Field Conference, p. 217-223.

Earlougher, R. C., Jr., 1977, Advances in well test analysis: Dallas Society of Petroleum Engineers of AIME, Monograph Series, no. 5.

Ferm, J. C., Horne, J. C., Swinchatt, J. P., and Whaley, P. W., 1971, Carboniferous depositional environments in northeastern Kentucky: Geological Society of Kentucky, Annual Spring Field Conference Guidebook, 30 p.

Finley, R. J., 1982, Geology and engineering characteristics of selected low-permeability gas sands, a survey: Report to CER Corporation and the Gas Research Institute by the Bureau of Economic Geology, The University of Texas at Austin, Contract No. GRI-BEG-SC-111-81, 329 p., plus addendum.

Finley, R. J., and Han, J. H., 1982, Analysis of low-permeability gas sands suitable for future research programs--Final report: Bureau of Economic Geology Contract No. GRI-BEG-SC-112-82, 19 p., plus appendix.

Fisher, W. L., and Brown, L. F., Jr., 1972, Clastic depositional systems--a genetic approach to facies analysis: The University of Texas at Austin, Bureau of Economic Geology, 211 p.

Flores, R. M., 1978, Barrier and back barrier environments of deposition of the Upper Cretaceous Almond Formation, Rock Springs Uplift, Wyoming: The Mountain Geologist, v. 15, no. 2, p. 57-65.

Forgotson, J. M., Jr., 1957, Stratigraphy of Comanchean Cretaceous Trinity Group: American Association of Petroleum Geologists Bulletin, v. 41, no. 10, p. 2328-2363.

Fouch, T. D., and Cashion, W. B., 1979, Distribution of rock types, lithologic groups, and depositional environments for some lower Tertiary and Upper and Lower Cretaceous, and Upper and Middle Jurassic rocks in the subsurface between Altamont oil field and San Arroyo gas field, northcentral to southeastern Uinta Basin, Utah: U.S. Geological Survey Open-File Report 79-365, 2 sheets.

Galloway, W. E., Hobday, D. K., and Magara, K., 1982, Frio Formation of Texas Gulf Coastal Plain: Depositional systems, structural framework and hydrocarbon distribution: American Association of Petroleum Geologists Bulletin, v. 66, no. 6, p. 649-688.

Gas Research Institute, 1982, GRI program plan for tight gas sand reservoirs, 16 p.

Gill, J. R., and Hail, W. J., Jr., 1975, Stratigraphic sections across Upper Cretaceous Manco Shale--Mesaverde Group boundary, eastern Utah and western Colorado: U.S. Geological Survey Oil and Gas Investigations Chart, OC-68, 1 sheet.

Gill, J. R., Merewether, F. A., and Cobban, W. A., 1970, Stratigraphy and nomenclature of some Upper Cretaceous and Lower Tertiary rocks in south-central Wyoming: U.S. Geological Survey Professional Paper no. 667, 53 p.

Glover, J. E., 1955, Olmos sand facies of southwest Texas: Gulf Coast Association of Geological Societies Transactions, v. 5, p. 135-144.

- _____ 1956, Sealing agents in the Olmos sands of southwest Texas (abs.): *Oil and Gas Journal*, v. 54, no. 53, p. 144.
- Goodell, H. G., 1962, The stratigraphy and petrology of the Frontier Formation of Wyoming, in Symposium on Early Cretaceous rocks of Wyoming and adjacent areas: Wyoming Geological Association Guidebook, 17th Annual Field Conference, p. 173-210.
- Granata, W. H., Jr., 1963, Cretaceous stratigraphy and structural development of the Sabine Uplift area, Texas and Louisiana, in Herrmann, L. A., ed., Report on selected North Louisiana and South Arkansas oil and gas fields and regional geology: Shreveport Geological Society Reference Volume 5, p. 50-95.
- Gries, R., 1983, Oil and gas prospecting beneath Precambrian of foreland thrust plates in Rocky Mountains: *American Association of Petroleum Geologists Bulletin*, v. 67, no. 1, p. 1-28.
- Gudim, C. J., 1956, Subsurface correlation along the eastern margin of the Great Divide and Washakie basins, Wyoming, in Burk, C. A., ed., Symposium on Wyoming stratigraphy, Part I, Subsurface stratigraphy of the pre-Niobrara Formations in Wyoming: Wyoming Geological Association, 98 p. (Chart in pocket).
- Hagar, R., and Petzet, G. A., 1982, Hefty wellhead prices spark drilling in U.S. tight gas sands: *Oil and Gas Journal*, v. 80, no. 17, p. 69-74.
- Hale, L. A., 1962, Frontier Formation--Coalville, Utah and nearby areas of Wyoming and Colorado, in Symposium on Early Cretaceous rocks of Wyoming and adjacent areas: Wyoming Geological Association Guidebook, 17th Annual Field Conference, p. 211-220.

- Hale, L. A., and Van de Graaff, F. R., 1964, Cretaceous stratigraphy and facies patterns, northeast Utah and adjacent areas, in Sabatka, E. F., ed., Geology and Mineral Resources of the Uinta Basin: Intermountain Association of Petroleum Geologists Guidebook, p. 115-138.
- Hansen, W. R., 1965, Geology of the Flaming Gorge area, Utah-Colorado-Wyoming: U.S. Geological Survey Professional Paper 490, 196 p.
- Haun, J. D., 1958, Early Upper Cretaceous stratigraphy, Powder River Basin, Wyoming, in Strickland, J., ed., Powder River Basin: Wyoming Geological Association Guidebook, 13th Annual Field Conference, p. 84-89.
- Haun, J. D., and Barlow, J. A., Jr., 1962, Lower Cretaceous stratigraphy of Wyoming, in Symposium on Early Cretaceous rocks of Wyoming and adjacent areas: Wyoming Geological Association Guidebook, 17th Annual Field Conference, p. 15-22.
- Hawkins, C. M., 1980, Barrier bar sands in the Second Frontier Formation, Green River Basin, Wyoming, in Harrison, A., ed., Stratigraphy of Wyoming: Wyoming Geological Association Guidebook, 31st Annual Field Conference, p. 155-161.
- Hazzard, R. T., 1939, Notes on the Comanche and pre-Comanche(?) Mesozoic formations of the Ark-La-Tex area--and a suggested correlation with northern Mexico: Shreveport Geological Society Guidebook No. 14, p. 155-189.
- Hill, R. T., 1890, A brief description of the Cretaceous rocks of Texas and their economic value: Texas Geological Survey, 1st Annual Report, p. 103-141.

Hunter, L. D., 1952, Frontier Formation along the eastern margin of the Big Horn Basin, Wyoming, in Spalding, R. W., and Wold, J. E., eds., Southern Big Horn Basin, Wyoming: Wyoming Geological Association Guidebook, 7th Annual Field Conference, p. 63-66.

Imlay, R. W., 1940, Lower Cretaceous and Jurassic formations of southern Arkansas and their oil and gas possibilities: Arkansas Resources and Development Commission, Division of Geology, Information Circular 12, 64 p. (reprinted 1974).

Jacka, A. D., 1965, Depositional dynamics of the Almond Formation, Rock Springs Uplift, Wyoming, in De Voto, R. H., Bitter, R. K., and Austin, A. C., eds., Sedimentation of Late Cretaceous and Tertiary outcrops, Rock Springs Uplift, Wyoming: Wyoming Geological Association Guidebook, 19th Annual Field Conference, p. 81-100.

Jackson, M. P. A., 1981, Tectonic environment during early infilling of the East Texas Basin, in Geology and geohydrology of the East Texas Basin, a report on the progress of nuclear waste isolation feasibility studies (1980): The University of Texas at Austin, Bureau of Economic Geology Geological Circular No. 81-7, p. 7-11.

————— 1982, Fault tectonics of the East Texas Basin: The University of Texas at Austin, Bureau of Economic Geology Geological Circular 82-4, 31 p.

Johnson, R. C., and Keighin, C. W., 1981, Cretaceous and Tertiary history and resources of the Piceance Creek Basin, western Colorado, in Epis, R. C., and Callender, J. F., eds., Western Slope Colorado: New Mexico Geological Society Guidebook, 32nd Annual Field Conference, p. 199-210.

Jones, F. O., and Owens, W. W., 1979, A laboratory study of low permeability gas sand: 1979 SPE Symposium on low permeability gas reservoirs, Paper SPE 7551.

Keefer, W. R., 1960, Progressive growth of anticlines during Late Cretaceous and Paleocene time in central Wyoming: U.S. Geological Survey Professional Paper 400-B, p. B233-B236.

————— 1969, Geology of petroleum in Wind River Basin, central Wyoming: American Association of Petroleum Geologists Bulletin, v. 53, no. 9, p. 1839-1865.

Kehle, R. O., 1971, Origin of the Gulf of Mexico: The University of Texas at Austin, unpublished manuscript, unpaginated.

Kellogg, H. E., 1977, Geology and petroleum of the Mancos "B" Formation, Douglas Creek Arch area, Colorado and Utah, in Veal, H. K., ed., Exploration Frontiers of the central and southern Rockies: Rocky Mountain Association of Geologists, 1977 Symposium, p. 167-179.

Kent, H. C., 1968, Biostratigraphy of Niobrara-equivalent part of Mancos shale (Cretaceous) in northwestern Colorado: American Association of Petroleum Geologists Bulletin, v. 52, no. 11, p. 2098-2115.

Knight, W. C., 1902, The petroleum fields of Wyoming III: Engineering and Mining Journal, v. 72, p. 720-724.

Kukal, G. C., Biddison, C. L., Hill, R. E., Monson, E. R., and Simons, K. E., 1983, Critical problems hindering accurate log interpretation of tight gas sand reservoirs, in

Proceedings, 1983 SPE/DOE Joint Symposium on Low Permeability Reservoirs, SPE/DOE Paper 11620, p. 181-190.

Kupfer, D. H., Crowe, C. T., and Hessenbruch, J. M., 1976, North Louisiana Basin and salt movements (halokinetics): Gulf Coast Association of Geological Societies Transactions, v. 26, p. 94-110.

Law, B. E., Spencer, C. W., and Bostik, N. H., 1980, Evaluation of organic matter, subsurface temperature and pressure with regard to gas generation in low-permeability Upper Cretaceous and Lower Tertiary sandstones in Pacific Creek area, Sublette and Sweetwater Counties, Wyoming: The Mountain Geologist, v. 17, no. 2, p. 23-35.

Lee, W. J., 1980, Estimation of permeability and stabilized rate from transient flow data in tight gas reservoir, in S. A. Holditch & Associates, Inc., Application for tight formation designations by Amoco: Railroad Commission of Texas, exhibit no. 22, Docket no. 6-78910.

Lewin and Associates, Inc., 1978, Enhanced recovery of unconventional gas, main report: v. 2, chapter 3, 92 p.

Lewis, J. L., 1965, Measured surface sections of the Almond Formation on the east flank of the Rock Springs Uplift, Sweetwater County, Wyoming, in De Voto, R. H., Bitter, R. K., and Austin, A. C., eds., Sedimentation of Late Cretaceous and Tertiary outcrops: Wyoming Geological Association Guidebook, 19th Annual Field Conference, p. 101-111.

Lorenz, J. C., 1982, Sedimentology of the Mesaverde Formation at Rifle Gap, Colorado and implication for gas-bearing intervals in the subsurface: Sandia National Laboratories, report no. SAND82-0604, 46 p.

————— 1983, Lateral variability in the Corcoran and Cozzette blanket sandstones and associated Mesaverde rocks, Piceance Creek Basin, northwestern Colorado: SPE/DOE Symposium on Low Permeability, no. 11608, p. 81-86.

Louisiana Office of Conservation, 1981, Docket no. NGPA 81-TF-7, application by Amerada Hess Corporation for designation of the Hosston Formation in parts of Winn, Bienville, Red River and Natchitoches Parishes, Louisiana, as a tight gas sand.

Love, J. D., 1948, Mesozoic stratigraphy of the Wind River Basin, central Wyoming, in Maebius, J. B., ed., Wind River Basin: Wyoming Geological Association Guidebook, 3rd Annual Field Conference, p. 96-111.

————— 1956, Cretaceous and Tertiary stratigraphy of the Jackson Hole area, northwestern Wyoming, in Berg, R. R., and Strickland, J. W., eds., Jackson Hole: Wyoming Geological Association Guidebook, 11th Annual Field Conference Guidebook, p. 76-94.

————— 1961, Definition of Green River, Great Divide and Washakie basins, southwestern Wyoming: American Association of Petroleum Geologists Bulletin, v. 45, no. 10, p. 1749-1755.

Love, J. D., Duncan, D. C., Bergquist, H. R., and Hose, R. K., 1948, Stratigraphic sections of Jurassic and Cretaceous rocks in the Jackson Hole area, northwestern Wyoming: Wyoming Geological Survey Bulletin 40, 48 p.

Love, J. D., McGrew, P. O., and Thomas, H. D., 1963, Relationship of latest Cretaceous and Tertiary deposition and deformation to oil and gas in Wyoming, in Childs, O. E., and Beebe, B. W., eds., Backbone of the Americas: American Association of Petroleum Geologists Memoir No. 2, p. 196-208.

Love, J. D., Tourtelot, H. A., Johnson, C. O., Thompson, R. M., Sharkey, H. H., and Zapp, A. D., 1947, Stratigraphic sections of Mesozoic rocks in central Wyoming: Wyoming Geological Survey Bulletin 38, 59 p.

Love, J. D., Weitz, J. L., and Hose, R. K., 1955, Geologic map of Wyoming: U.S. Geological Survey, scale 1:500,000, 1 sheet.

Luttrell, P. E., 1977, Carbonate facies distribution and diagenesis associated with volcanic cones--Anacacho Limestone (Upper Cretaceous) Elaine Field, Dimmit County, Texas, in Bebout, D. G. and Loucks, R. G., eds., Cretaceous carbonates of Texas and Mexico--applications to subsurface exploration: The University of Texas at Austin, Bureau of Economic Geology, Report of Investigations No. 89, p. 260-285.

Mann, C. J., and Thomas, W. A., 1964, Cotton Valley Group (Jurassic) nomenclature, Louisiana and Arkansas: Gulf Coast Association of Geological Societies Transactions, v. 14, p. 143-152.

————— 1968, The ancient Mississippi River: Gulf Coast Association of Geological Societies Transactions, v. 18, p. 187-204.

- Masters, J. A., 1952, The Frontier Formation of Wyoming, in Spalding, R. W., and Wold, J. S., eds., Southern Big Horn Basin, Wyoming: Wyoming Geological Association Guidebook, 7th Annual Field Conference, p. 58-62.
- Matthews, C. S., and Russell, D. G., 1967, Pressure buildup and flow tests in wells: Society of Petroleum Engineers of AIME, Monograph Series No. 1, 167 p.
- McCubbin, D. G., 1982, Barrier-island and strandplain facies, in Scholle, P. A., and Spearing, D., eds., Sandstone depositional environments: American Association of Petroleum Geologists, Memoir 31, p. 247-279.
- McCubbin, D. G., and Brady, M. J., 1969, Depositional environment of the Almond reservoirs, Patrick Draw field, Wyoming: *The Mountain Geologist*, v. 6, no. 1, p. 3-26.
- McDonald, R. E., 1973, Big Piney-La Barge producing complex, Sublette and Lincoln counties, Wyoming, in Schell, E. M., ed., Greater Green River Basin Symposium: Wyoming Geological Association Guidebook, 25th Annual Field Conference, p. 57-77.
- McGowen, M. K., and Harris, D. W., in press, Cotton Valley (Late Jurassic)--Hosston (Lower Cretaceous) depositional systems and their influence on salt tectonics in the East Texas Basin: The University of Texas at Austin, Bureau of Economic Geology.
- McPeck, L. A., 1981, Eastern Green River Basin: a developing giant gas supply from deep, overpressured Upper Cretaceous sandstone: American Association of Petroleum Geologists Bulletin, v. 65, no. 6, p. 1078-1098.

Merewether, E. A., Cobban, W. A., and Ryder, R. T., 1975, Lower Upper Cretaceous strata, Bighorn Basin, Wyoming and Montana, in Exum, F. A., and George, G. R., eds., Geology and mineral resources of the Big Horn Basin: Wyoming Geological Association Guidebook, 27th Annual Field Conference, p. 73-84.

Miller, D. N., and Ver Ploeg, A. J., 1980, Tight gas sand inventory of Wyoming: Wyoming Geological Survey DB-684, 20 p.

Miller, F. X., 1977, Biostratigraphic correlation of the Mesaverde Group in southwestern Wyoming and northwestern Colorado, in Veal, H. K., ed., Exploration frontiers of the central and southern Rockies: Rocky Mountain Association of Geologists, 1977 Symposium, p. 117-137.

Murray, D. K., and Haun, J. D., 1974, Introduction to the geology of the Piceance Creek Basin and vicinity, northwestern Colorado, in Murray, D. K., ed., Energy resources of the Piceance Creek Basin, Colorado: Rocky Mountain Association of Geologists Guidebook, 25th Field Conference, p. 29-39.

Murray, G. E., 1952, Volume of Mesozoic and Cenozoic sediments in central Gulf Coastal Plain, Part 3 of sedimentary volumes in Gulf Coastal Plain of United States: Geological Society of America Bulletin, v. 63, p. 1177-1192.

————— 1957, Geologic occurrence of hydrocarbons in Gulf Coastal Province of the United States: Gulf Coast Association of Geological Societies Transactions, v. 7, p. 253-299.

————— 1961, Geology of the Atlantic and Gulf Coastal Province of North America: Harper's Geoscience Series, 692 p.

Myers, R. C., 1977, Stratigraphy of the Frontier Formation (Upper Cretaceous) Kemmerer area, Lincoln County, Wyoming, in Heisey, E. L., Lawson, D. E., Norwood, E. R., Wach, P. H., and Hale, L. A., eds., Rocky Mountain Thrust Belt geology and resources: Wyoming Geological Association Guidebook, in conjunction with Montana Geological Society and Utah Geological Society, 29th Annual Field Conference, p. 271-311.

National Petroleum Council, 1980a, Unconventional gas source, Tight gas reservoirs, v. 5, part I, p. 1-222.

————— 1980b, Unconventional gas source, Tight gas reservoirs, v. 5, part II, p. 10-1 - 19-24.

Newman, H. E., III, 1981, The Upper Cretaceous and Lower Tertiary stratigraphy and natural gas potential of the Greater Green River Basin of Wyoming: U.S. Department of Energy, Bartlesville Energy Technology Center, DOE-BC-10003-20.

Noe, D. C., 1983, Storm-dominated shoreface deposits, Sego Sandstone (Campanian), Northwestern Colorado (abs.): American Association of Petroleum Geologists Bulletin, v. 67, no. 3, p. 526.

Pisasale, E. T., 1980, Surface and subsurface depositional systems in the Escondido Formation, Rio Grande Embayment, South Texas: The University of Texas at Austin, Master's thesis, 172 p.

Porter, K. W., and Weimer, R. J., 1982, Diagenetic sequence related to structural history and petroleum accumulation: Spindle Field, Colorado: American Association of Petroleum Geologists Bulletin, v. 66, no. 12, p. 2543-2560.

Quigley, M. D., 1965, Geologic history of Piceance Creek-Eagle Basins: American Association of Petroleum Geologists Bulletin, v. 49, no. 11, p. 1974-1996.

Railroad Commission of Texas, 1980, Annual Report, Oil and Gas Division, 700 p.

————— 1981a, Annual Report, Oil and Gas Division, 700 p.

————— 1981b, Docket no. 5-76,659, application by Texas Oil and Gas for designation of the Travis Peak Formation in Texas, RRC Districts 5 and 6, as a tight gas sand.

————— 1982, Annual Report, Oil and Gas Division.

————— 1983, Recommendation that the Travis Peak Formation be designated as a tight formation in Texas: Docket No. 5-76659, September 12, 1983, 3 p.

Reeside, J. B., Jr., 1955, Revised interpretation of the Cretaceous section on Vermilion Creek, Moffat County, Colorado, in Anderman, G. G., ed., Green River Basin: Wyoming Geological Association Guidebook, 10th Annual Field Conference, p. 85-88.

Reynolds, M. W., 1976, Influence of recurrent Laramide structural growth on sedimentation and petroleum accumulation, Lost Soldier area, Wyoming: American Association of Petroleum Geologists Bulletin, v. 60, no. 1, p. 12-33.

- Rice, D. D., and Shurr, G. W., 1980, Shallow, low-permeability reservoirs of northern Great Plains--assessment of their natural gas resources: American Association of Petroleum Geologists Bulletin, v. 64, no. 7, p. 969-987.
- Ritzma, H. R., 1964, Structural and stratigraphic development, Washakie and Sand Wash Basins, Wyoming and Colorado: American Association of Petroleum Geologists Bulletin, v. 48, no. 11, p. 1877.
- Rocky Mountain Association of Geologists, 1977, Subsurface cross sections of Colorado: Special Publication no. 2, 39 p., plus plates.
- Rosenkrans, R. R., and Marr, J. D., 1967, Modern seismic exploration of the Gulf Coast Smackover trend: Geophysics, v. 32, no. 2, p. 184-206.
- Sannemann, D., 1968, Salt-stock families in north-western Germany, in Diapirism and diapirs: American Association of Petroleum Geologists Memoir 8, p. 261-270.
- Seni, S. J., and Jackson, M. P. A., 1983, Evolution of salt structures, East Texas diapir province, part 2--patterns and rates of halokinesis: American Association of Petroleum Geologists Bulletin, v. 67, no. 8, p. 1245-1274.
- Seni, S. J., and Kreitler, C. W., 1981, Evolution of the East Texas Basin, in Geology and geohydrology of the East Texas Basin, a report on the progress of nuclear waste isolation feasibility studies (1980): The University of Texas at Austin, Bureau of Economic Geology, Geological Circular 81-7, p. 12-20.

Shipp, B. G., and Dunnewald, J. B., 1962, The Big Piney-La Barge Frontier gas field, Sublette and Lincoln counties, Wyoming, in Symposium on Early Cretaceous rocks of Wyoming and adjacent areas: Wyoming Geological Association Guidebook, 17th Annual Field Conference, p. 273-279.

Shreveport Geological Society, 1980, Report on selected oil and gas fields, north Louisiana and south Arkansas, Reference volume VI, 160 p.

Siemers, C. T., 1975, Paleoenvironmental analysis of the Upper Cretaceous Frontier Formation, northwestern Big Horn Basin, Wyoming, in Exum, F. A., and George, G. R., eds., Geology and mineral resources of the Big Horn Basin: Wyoming Geological Association Guidebook, 27th Annual Field Conference, p. 85-100.

Snedden, J. W., and Kersey, D. G., 1982, Depositional environments and gas production trends Olmos Sandstone, Upper Cretaceous Webb County, Texas: Gulf Coast Association of Geological Societies Transactions, v. 32, p. 497-518.

Spencer, A. B., 1965, Upper Cretaceous asphalt deposits of the Rio Grande Embayment: Corpus Christi Geological Society Guidebook, 67 p.

Spencer, C. W., 1983, Geologic aspects of tight gas reservoirs in the Rocky Mountain Region: SPE/DOE Symposium on Low Permeability, no. 11647, p. 399-408.

Spencer, C. W., Fouch, T. D., and Rice, D. D., 1977, Geological program to provide a characterization of tight, gas-bearing reservoirs in the Rocky Mountain Region: Proceedings 3rd ERDA Symposium on Enhanced Oil and Gas Recovery and Improved Drilling Methods, p. E-1/1 to E/1/15.

- Stancliffe, R., 1983, Vertically accreted foreshore to shoreface deposits of Sego Sandstone (Campanian), Northwest Colorado (abs.): American Association of Petroleum Geologists Bulletin, v. 67, no. 3, p. 55.
- Thomas, W. A., and Mann, C. J., 1966, Late Jurassic depositional environments, Louisiana and Arkansas: American Association of Petroleum Geologists Bulletin, v. 50, no. 1, p. 178-182.
- Thompson, R. M., Love, J. D., and Tourtelot, H. A., 1949, Stratigraphic sections of pre-Cody Upper Cretaceous rocks in central Wyoming: U.S. Geological Survey Oil and Gas Investigations Preliminary Chart 36.
- Tillman, R. W., and Almon, W. R., 1979, Diagenesis of Frontier Formation offshore bar sandstones, Spearhead Ranch Field, Wyoming, in Scholle, P.A., and Schluger, P. R., eds., Aspects of diagenesis: Society of Economic Paleontologists and Mineralogists, Special Publication No. 26, p. 337-378.
- Tonnson, J. J., 1980, The Frontier Formation in northwestern Wyoming and adjacent areas, in Harrison, A., ed., Stratigraphy of Wyoming: Wyoming Geological Association Guidebook, 31st Annual Field Conference, p. 173-184.
- Towse, D., 1952, Frontier Formation, southwest Powder River Basin, Wyoming: American Association of Petroleum Geologists Bulletin, v. 36, no. 10, p. 1962-2010.
- Trusheim, F., 1960, Mechanism of salt migration in northern Germany: American Association of Petroleum Geologists Bulletin, v. 44, no. 9, p. 1519-1540.

Tweto, Ogden, 1979, Geologic map of Colorado: U.S. Geological Survey, scale 1:500,000.

Tyler, T. F., 1978, Preliminary chart showing electric log correlation section A-A' of some Upper Cretaceous and Tertiary rocks, Washakie Basin, Wyoming: U.S. Geological Survey Open-File Report 78-703, 4 sheets.

————— 1980, Preliminary chart showing electric log correlation section H-H' of some Upper Cretaceous and Tertiary rocks, south end, Rock Springs Uplift, Washakie Basin, Wyoming: U.S. Geological Survey Open-File Report 80-1248, 3 sheets.

Van Houten, F. B., 1962, Frontier Formation, Bighorn Basin, Wyoming, in Symposium on Early Cretaceous rocks of Wyoming and adjacent areas: Wyoming Geological Association Guidebook, 17th Annual Field Conference, p. 221-231.

Veatch, A. C., 1906, Coal and oil in southern Uinta County, Wyoming: U.S. Geological Survey Bulletin 285, p. 331-356.

Ver Ploeg, A. J., and de Bruin, R. H., 1983, Discussion to accompany Mesaverde and Frontier cross sections: Geological Survey of Wyoming, report to The University of Texas at Austin, Bureau of Economic Geology, 23 p.

Wach, P. H., 1977, The Moxa Arch, an overthrust model?, in Heisey, E. L., and others, eds., Rocky Mountain Thrust Belt, Geology and Resources: Wyoming Geological Association Guidebook, 29th Annual Field Conference, p. 651-664.

Walper, J. L., 1977, Paleozoic tectonics of the southern margin of North America: Gulf Coast Association of Geological Societies Transactions, v. 27, p. 230-241.

- 1980, Tectonic evolution of the Gulf of Mexico, in Pilser, R. H., Jr., ed., The origin of the Gulf of Mexico and the early opening of the central North Atlantic Ocean: Louisiana State University, Symposium Proceedings p. 87-98.
- Warner, D. L., 1964, Mancos-Mesaverde (Upper Cretaceous) intertonguing relations southeast Piceance Basin, Colorado: American Association of Petroleum Geologists Bulletin, v. 48, no. 7, p. 1091-1107.
- Wegemann, C. H., 1911, The Salt Creek oil field, Wyoming: U.S. Geological Survey Bulletin 452, p. 37-83.
- Weimer, R. J., 1960, Upper Cretaceous stratigraphy, Rocky Mountain area: American Association of Petroleum Geologists Bulletin, v. 44, p. 1-20.
- 1962, Late Jurassic and Early Cretaceous correlations, south-central Wyoming and northwestern Colorado, in Symposium on Early Cretaceous rocks of Wyoming and adjacent areas: Wyoming Geological Association Guidebook, 17th Annual Field Conference, p. 124-130.
- 1965, Stratigraphy and petroleum occurrences, Almond and Lewis Formations (Upper Cretaceous), Wamsutter Arch, Wyoming, in Sedimentation of Late Cretaceous and Tertiary outcrops, Rock Springs Uplift, Wyoming: Wyoming Geological Association Guidebook, 19th Annual Field Conference, p. 65-80.
- 1970, Rates of deltaic sedimentation and intrabasin deformation, Upper Cretaceous of Rocky Mountain region, in Morgan, J. P., ed., Deltaic sedimentation modern and

ancient: Society of Economic Paleontologists and Mineralogists Special Publication 15, p. 270-292.

Weise, B. R., 1980, Wave-dominated delta systems of the Upper Cretaceous San Miguel Formation, Maverick Basin, South Texas: The University of Texas at Austin, Bureau of Economic Geology, Report of Investigations No. 107, 39 p.

Wellborn, R. E., 1981, Marianne Field--air drilling for gas, in Reid, S. G., and Miller, D. D., eds., Energy resources of Wyoming: Wyoming Geological Association Guidebook, 32nd Annual Field Conference, p. 109-117.

Winn, R. D., Jr., and Smithwick, M. E., 1980, Lower Frontier Formation, southwestern Wyoming--depositional controls on sandstone compositions and on diagenesis, in Harrison, A., ed., Stratigraphy of Wyoming: Wyoming Geological Association Guidebook, 31st Annual Field Conference, p. 137-153.

Wood, D. H., 1981, Structural effects of salt movement in the East Texas Basin, in Geology and geohydrology of the East Texas Basin, a report on the progress of nuclear waste isolation feasibility studies (1980): The University of Texas at Austin, Bureau of Economic Geology, Geological Circular 81-7, p. 7-11.

Wood, M. L., and Walper, J. L., 1974, The evolution of the interior western basins and the Gulf of Mexico: Gulf Coast Association of Geological Societies Transactions, v. 24, p. 31-41.

Woodbury, H. O., Murray, I. B., Jr., and Osborne, R. E., 1980, Diapirs and their relation to hydrocarbon accumulation, in Miall, A. D., ed., Facts and principles of world petroleum occurrence: Canadian Society of Petroleum Geologists, p. 119-142.

Wyoming Oil and Gas Conservation Commission, 1980, Docket no. 92-80, Cause no. 1, Application by Amoco Production Company for designation of the Mesaverde Group in parts of Sweetwater and Carbon Counties, Wyoming, as a tight gas sand.

————— 1981, Wyoming oil and gas statistics, Part I, 77 p.

Young, R. G., 1975, Lower Cretaceous rocks of northwestern Colorado and northeastern Utah, in Bolyard, D. W., ed., Symposium on deep drilling frontiers in the central Rocky Mountains: Rocky Mountain Association of Geologists Guidebook, p. 141-147.

Zapp, A. D., and Cobban, W. A., 1960, Some Late Cretaceous strandlines in northwestern Colorado and northeastern Utah: U.S. Geological Survey Professional Paper 400-B, p. B246-B249.